UNESCO-IHE
Institute for Water Education

# Physical model tests on new armour block Crablock for breakwaters to come to preliminary design guidance

Md. Salauddin

MSc Thesis WSE-HECEPD-15.04

April 2015

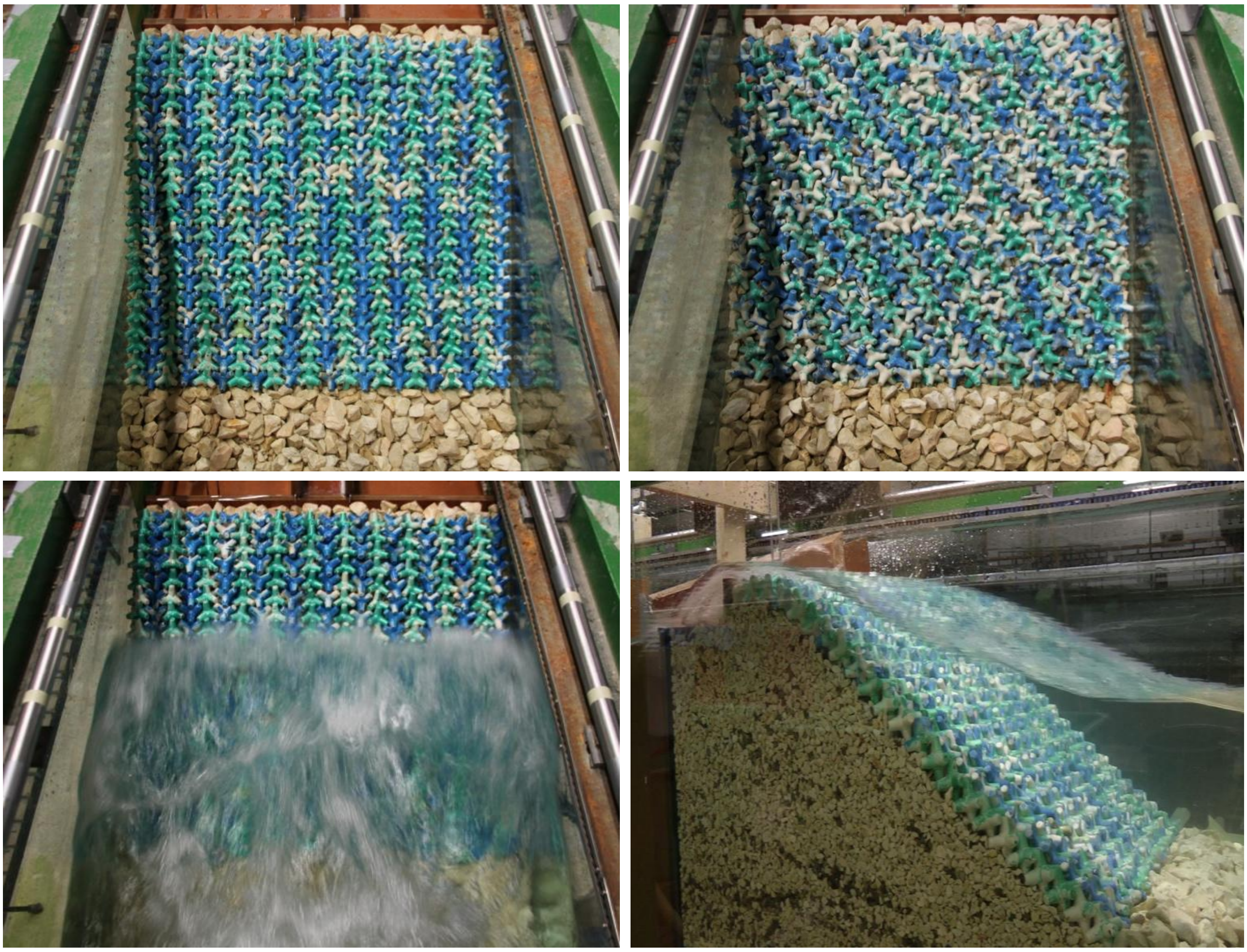

# Physical model tests on new armour block Crablock for breakwaters to come to preliminary design guidance

Master of Science Thesis
by
**Md. Salauddin**

Supervisor
**Prof. J.W. Van der Meer**

Mentor
**Dr. Ali Dastgheib**

Examination committee
**Prof. J.W. Van der Meer**
**Dr. Ali Dastgheib**
**Ir. Eelco Bijl**

This research is done for the partial fulfilment of requirements for the Master of Science degree at the UNESCO-IHE Institute for Water Education, Delft, the Netherlands

**Delft**
**April 2015**

# Abstract

In the design of rubble mound breakwaters, nowadays single layer systems using concrete armour units have become more common practice compared to conventional two layer systems. However, after the introduction of the accropode in eighties, a small number of single layer armour units have been developed over the years; for example core-loc, A-jack, xbloc, accropode-II, cubipod and core-loc II. Recently, a new concrete armour unit called crablock has been invented and applied as one layer system in one damaged breakwater at Al Fujeirah, UAE. In contrast to other existing monolayer units, the shape of this unit is symmetrical which allows placing both in uniform and random pattern. As the crablock unit is still under development, no design guidance exists yet for this concrete armour unit. To use crablock as monolayer system the preliminary design guidance on placement of crablock, stability and wave overtopping are required. This led the present research to investigate the placement pattern, packing density and wave overtopping over slope to come with first design guidance for the application of crablock. It should be mentioned that stability of the crablock against wave attack was also looked at, but that will be reported by Mr. André Broere, an MSc-student at Delft University of Technology.

The present research was based on a literature study, small scale dry placement tests and small scale hydraulic tests in a wave flume. Regarding to the review of literature studies on the existing single layer units and crablock, set up of dry placement tests and flume tests have been made for this experimental research. Dry placement tests as well as 2D wave flume tests were carried out at the Fluid Mechanics Laboratory of the Faculty of Civil Engineering and Geosciences at Delft University of Technology, Netherlands. Both placement and hydraulic tests were executed with the use of small units.

In total 14 independent placement test series were executed to investigate the placement pattern, placing grid and packing density of crablock. All the tests were performed on a 1:4/3 slope with the use of random and uniform placement in a rectangular as well as in a diamond shaped placing grid. Results of placement tests showed that uniform placement of crablock is achievable with the use of relatively small and smooth under layer in a rectangular placing grid. The performance of regular placement using a conventional under layer with size 1/10$^{th}$ to 1/15$^{th}$ of the size of the armour layer was not so satisfactory. Furthermore, it was found that uniform pattern was hardly reachable in a diamond-shaped grid with conventional under layer. However, irregular placement of crablock was certainly easier to construct and possible to place with higher accuracy compared to uniform placement in a diamond grid. It should be noted that all the tests using a conventional underlayer were performed without the fixation of first row due to the difficulties in placement with model crablock units. If this can be fixated by designing dedicated toe units (both in rotation and location) it may perform better. Still, the large underlayer makes it difficult to place uniformly. Finally, two preferred placing patterns appeared from the placement tests, a regular pattern in a rectangular grid using a relatively small under layer and a random pattern in a diamond grid using a conventional under layer.

For the determination of wave overtopping, altogether 14 different test series were performed in a wave flume. In this research, two constant spectral wave steepnesses ($s_{m-1,0}$) of 0.02 and 0.04 were tested together with two different orientations of units, two different placing grids and four different packing densities. The preferred placing patterns were constructed in a wave flume on a modelled breakwater cross-section in front of the sloping foreshore of 1:30. Each test series was comprised of number of sub tests for specific wave height and period. In each test series, wave heights and periods were continued to measure until the failure of armour slope. The armour layer was reconstructed prior to start of each test series.

The test results of 2D flume tests showed that wave overtopping over crablock slope did not vary much between the different test series with same wave steepness. Nevertheless, it was observed that wave overtopping is little bit higher for longer wave period that means for low steepness compared to short period. Based on test results, it was also found that overtopping behaviour does not really change with the change in packing density and also with different placement pattern of armour layer.

Regarding to the comparison of relative overtopping rate over crablock armour between test results and empirical prediction, it was found that that empirical equation with assuming roughness factor ($\gamma_f$) of 0.45 underestimate the measured wave overtopping over crablock. However, the comparison between the test results on overtopping percentages and estimation by EurOtop (2007) proved that percentage of waves overtopped over crablock can be well predicted by using empirical formula.

Furthermore, the measured wave overtopping over crablock slope was found slightly higher in comparison to CLASH (2004) results on other single layer units. This variation was mainly observed for the test results with low wave steepness $s_{m-1,0}$ = 0.02 ($s_{op}$ = 0.015) which was out of CLASH (2004) range ($s_{op}$ = 0.02, 0.035 and 0.05). Besides relatively low wave steepness, most of the tests on crablock were performed with relatively longer wave periods in comparison to CLASH (2004) which was also one of the triggering factor for higher overtopping over crablock slope compared to CLASH (2004). Moreover, the use of sloping foreshore (1:30) instead of horizontal one by CLASH (2004) might also influence the overtopping behaviour. The 1:30 slope changed the shape of the waves and the waves at the structure toe showed a clear increase in velocity of the wave crest (near or at breaking)

The resulting wave overtopping over crablock slope was also compared with the overtopping over xbloc slope measured by DMC (2003). From the comparison, it was found that wave overtopping over crablock is significantly lower compared to xbloc measurements by DMC (2003).

Based on the comparison of wave overtopping over different armour slope with and without Ursell parameter, it was recognised that use of the Ursell parameter may explain wave period differences in some cases, but introduces also unexpected differences.

Key words: Crablock, Overtopping, Placement pattern, Packing density, Single layer armour.

# Acknowledgements

First of all, i would like to remember almighty Allah for enabling me to complete my MSc research successfully. My sincere thanks go to all my family members for their continuous encouragement during my MSc studies at abroad.

I would like to show my deepest regards and gratitude to my supervisor, Professor J.W. Van der Meer, for his assistance throughout the research, for sharing his valuable experience and for helping me out from every single doubt. In my every step of dissertation, I always got his precise support and direction to go further step. It was a great opportunity for me to work under his supervision. During my whole thesis period, I have learnt so much from him. This thesis would not have been possible to complete without his guidance.

I am especially grateful to my mentor, Dr. Ali Dastgheib, who encouraged me to continue my research. I would like to thank him for introducing me such a nice and challenging topic to do my MSc research. From the beginning of my MSc study, he helped and supported me in difficult time.

Furthermore, I am grateful to all the lecturers of coastal engineering department at UNESO-IHE for sharing their knowledge, for providing us required tools and finally for making us able to face any difficulties in our working place.

I want to thank Mr. Andre Broere (MSc student TU) for his great co-operation during the flume tests, especially for last few tests. Furthermore, my sincere thanks go to Ir. H.J. Verhagen (TU Delft) for providing me all the facilities I needed at TU to complete a successful laboratory work. Also, I would like to place my appreciations to all the members of the support staff of the Hydraulics Laboratory at TU Delft for their assistance and advice during the experiments.

I would also like to thank my sponsor, NICHE-081 BGD project, for funding my MSc study at UNESCO-IHE. On this note, my special thanks go to all the members of NICHE-081 BGD project, for selecting me as an MSc student at UNSECO-IHE. Also, I would like to appreciate CUET (Chittagong University of Engineering and Technology) administration, for allowing me to pursue my MSc degree from abroad.

In addition, my cordial appreciations also go to AM Marine Works and CDR international for sponsoring the laboratory studies at Delft University of Technology. Special thanks go to Ir. Eelco Bijl (CDR Int.) for his valuable advices and guidance throughout the research.

Finally, my heartfelt appreciations go to everyone who contributed either directly or indirectly to this experimental research.

# Table of Contents

# List of Figures

# List of Tables

# Abbreviations

| | |
|---|---|
| 2D | Two Dimensional |
| CLASH | Crest Level Assessment of Coastal Structures by full scale monitoring and Hazard Analysis on permissible wave overtopping |
| CLI | Concrete Layer Innovations |
| DMC | Delta Marine Consultants |
| PD | Packing Density |
| SPM | Shore Protection Manual |

# List of Symbols

| Symbol | Meaning | Unit |
|---|---|---|
| $A$ | Surface area | $[m^2]$ |
| $A_c$ | Freeboard of armour | [m] |
| $d$ | Local water depth at structure | [m] |
| $D$ | Height of crablock model unit | [m] |
| $D_n$ | Nominal diameter | [m] |
| $D_x$ | Horizontal placement distance centre to centre | [m] |
| $D_y$ | Upslope placement distance centre to centre | [m] |
| $E(f)$ | Variance density | $[m^2/Hz]$ |
| $f$ | Frequency | [Hz] |
| $g$ | Gravitational acceleration | $[m/s^2]$ |
| $H_0$ | Design wave height | [m] |
| $H_{1/3}$ | Significant wave height determined from time series analysis as highest one third of wave heights | [m] |
| $H_{m0}$ | Significant wave height determined from spectra analysis | [m] |
| $K_d$ | Hudson stability coefficient | [-] |
| $L_t$ | Local wave length at structure derived from $T_p$ | [m] |
| $L_x$ | Horizontal length of the section | [m] |
| $L_y$ | Length up the slope of the section | [m] |
| $N_a$ | Number of armour units | [-] |
| $N_s$ | Stability number | [-] |
| $N_{ow}$ | Number of overtopping waves | [-] |
| $N_w$ | Number of incident waves | [-] |
| $N_x$ | Horizontal number of units in a section | [-] |
| $N_y$ | Number of horizontal rows | [-] |
| $P_{ov}$ | Percentage of overtopping waves | [-] |
| $q$ | Mean wave overtopping discharge per m width | $[m^3/s$ per m] |
| $R_c$ | Crest freeboard | [m] |
| $S_{op}$ | Fictitious wave steepness for peak period, $s_{op} = (2\pi H_{m0}/gT_p^2)$ | [-] |
| $s_{m-1,0}$ | Fictitious wave steepness for average spectral period, $s_{m-1,0} = (2\pi H_{m0}/gT_{m-1}^2)$ | [-] |
| $T_m$ | Average wave period calculated from time series analysis | [s] |
| $T_{m-1,0}$ | Average spectral wave period defined from spectral analysis by $m_{-1}/m_0$ | [s] |
| $T_p$ | Spectral peak wave period | [s] |

| | | |
|---|---|---|
| $W$ | Weight of individual armour stone | [kg] |
| $W_{50}$ | Weight of a unit with a diameter $D_{n50}$ | [kg] |
| $\Delta$ | Relative density | [-] |
| $\rho_s$ | Mass density of armour stone | [kg/m$^3$] |
| $\alpha$ | Angle between overall slope and structure | [°] |
| $\gamma_b$ | Influence factor for a berm | [-] |
| $\gamma_f$ | Influence factor for roughness elements on a slope | [-] |
| $\gamma_\beta$ | Influence factor for oblique wave attack | [-] |
| $\gamma_v$ | Influence factor for a vertical wall on a slope | [-] |
| $\xi_{m-1,0}$ | Breaker parameter | [-] |
| $\phi$ | Nominal packing density | [per $D_n^2$] |

# CHAPTER 1

# Introduction

**The present chapter is an overall introduction to the research project. It assists the reader to understand the purpose of this study and how it contributes to the design of rubble mound breakwaters with a new armour unit, the Crablock. Firstly, section 1.1 provides an overview on single layer concrete armour units. Next, section 1.2 describes the background of the research. It discusses about the development of Crablock as single layer armour system on a rubble mound breakwater. Section 1.3 defines the research problem. Then, section 1.4 gives the objectives of this research. The research questions in line with research objectives are also described in this section. Section 1.5 examines the importance of this study to our existing knowledge. Further, section 1.6 focuses on the scope of this research. Section 1.7 presents an overview of research methodology followed in this study. The introductory section ends with providing an outline of this experimental research.**

## 1.1. Overview

Breakwaters are expensive coastal structures generally applied for harbours and similar structures along coasts to protect the beaches, dunes from the action of waves, currents and also to stop siltation in the approach channel (SPM, 1984). Rubble mound breakwaters have been mostly applied by designers among several types of breakwaters. A rubble mound breakwater is usually made with the use of rock armour or concrete armour in double layer systems or in single layer systems. In the design of rubble mound breakwaters, nowadays one layer systems using concrete armour units have become more common practice compared to conventional two layer systems.

The 1950s saw an upsurge interest in developing and using concrete armour for rubble mound breakwaters. As a consequence after 1950s a large variety of concrete armour units has been invented by different consultants in different countries. As the theme of this research is based on single layer concrete armour units thus only monolayer system are discussed in this paper. The one layer concrete armour units have been developed as both pattern placed block and randomly oriented block. For example Cob in 1969, Seabee in 1978, Shed in 1982 and Diahitis in 1998 were invented as uniformly placed monolayer armour units (Bettington, et al., 2011). These are hollow blocks and placement of these blocks under water seems rather difficult therefore application is limited to only above low water (Muttray and Reedijk, 2009, Reedijk, et al., 2003, Vanhoutte, 2009). The details on application and properties of these units are not well known. They are also more compared with placed block revetments, as applied on dikes, then with common rubble mound breakwater armour.

| Single layer concrete armour | Shape |
| --- | --- |
| Name: Cube (Single layer cube) | 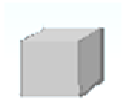 |
| Name: Cob<br>Place and Year of Invention: Uk, 1969<br>Placement Pattern: Regular | 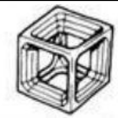 |
| Name: Seabee<br>Place and Year of Invention: Australia, 1978<br>Placement Pattern: Regular | 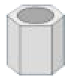 |
| Name: Accropode<br>Place and Year of Invention: France, 1980<br>Placement Pattern: Random |  |
| Name: Shed<br>Place and Year of Invention: UK, 1982<br>Placement Pattern: Regular |  |
| Name: Core-loc<br>Place and Year of Invention: UK, 1995<br>Placement Pattern: Random | 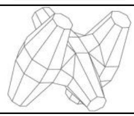 |
| Name: A-Jack<br>Place and Year of Invention: USA, 1998<br>Placement Pattern: Random |  |
| Name: Diahitis<br>Place and Year of Invention: USA, 1998<br>Placement Pattern: Regular | 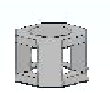 |
| Name: Xbloc<br>Place and Year of Invention: Netherlands, 2003<br>Placement Pattern: Random |  |
| Name: Accropode II<br>Place and Year of Invention: France, 2004<br>Placement Pattern: Random | 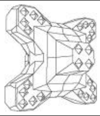 |
| Name: Cubipod<br>Place and Year of Invention: Spain, 2005<br>Placement Pattern: Random |  |
| Name: Core-loc II<br>Place and Year of Invention: UK, 2006<br>Placement Pattern: Random |  |
| Name: Crablock<br>Place and Year of Invention: UAE, 2007<br>Placement Pattern: Both Random and Regular | 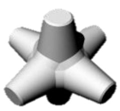 |

**Figure 1.1** Development of single layer concrete armour units [Source: (DMC, nd, Hendrikse, 2014, Vanhoutte, 2009)]

In the eighties Sogreah introduced first randomly placed one layer concrete armour unit is known as accropode (CLI, 2011a). After the introduction of accropode it has been applied more than 200 breakwaters (CLI, 2011b).

Next to accropode in the mid 1990s, another randomly oriented one layer concrete armour unit was invented by U.S. Army corps of Engineers (CLI, 2012): the core-loc. Melby, et al. (1994) argued that core-loc provides higher stability with good interlocking and low cost solution compared to other existing irregularly oriented armour units. However CIRIA, et al. (2007) warned that although in comparison to accropode the hydraulic stability of core-loc armour unit looks superior,the structural integrity of core-loc might be lower than the accropode armour block.

The development of single layer concrete was then followed by the invention of other randomly oriented one layer units, A-Jack in 1998 by Armortec, xbloc in 2003 by Delta Marine Consultants, accropode II in 2004 by Sogreah again followed by core-loc II in 2006 (DMC, nd).

Furthermore, in 2005 cubipod was developed as one layer randomly placed unit to improve the low hydraulic stability of cubes with keeping advantages of high structural strength and easier placement (Vanhoutte, 2009). Recently, a new concrete armour unit crablock has been invented in UAE and applied as repair in one damaged rubble mound breakwater as monolayer system. The overview of the development of one layer concrete armour is presented in **Figure 1.1**.

The main reasons behind the popularity of single layer systems are its characteristics like high interlocking, large structural stability and cost efficiency. Van der Meer (1999) investigated that due to high interlocking properties monolayer armour units can better sustain under higher wave heights compared to conventional double layer armour units. In addition to the stability of structures, a randomly placed one layer armour system provides better economic solution compared to conventional two layer system (Bakker, et al., 2003, Muttray, et al., 2003, Van Gent, et al., 1999). Furthermore, additional maintenance in a conventional two layer system compared to one layer system can be reduced with the use of appropriate design of single layer armour (Muttray and Reedijk, 2009).

On the other hand, failure of one layer systems shows much more fragile characteristics compared to double layer systems (Besley and Denechere, 2010, CIRIA, et al., 2007, Medina and Gómez-Martín, 2012, Van der Meer, 1999). Therefore, in comparison to traditional two layer armour system design of rubble mound breakwaters, using one layer armour system requires additional safety factors due to its failure mechanism (Medina and Gómez-Martín, 2012). Also, in order to keep the breakwaters away from repair works, extra safety is required in the design of one layer armour systems compared to conventional double layer system (Jensen, nd). Furthermore, the use of one layer armour system might increase the rate of overtopping discharge (Bruce, et al., 2009, EurOtop, 2007). As well as, according to Van Gent, et al. (1999) the different factors like placement pattern, allowable levels of damage and failure systems of armour layer should be treated with care for the application of monolayer system.

Therefore, it is necessary to understand the behaviour of one layer systems in order to use this system properly in the design of rubble mound breakwater.

## 1.2. Background of this research

The east coast of peninsula in Al Fujeirah was severely attacked by the Cyclone Gonu in 2007. By the catastrophic action of cyclone Gonu, major damage has been observed in many breakwaters in that area (Hendrikse, 2014, Phelp, et al., 2012). For example, **Figure 1.2** shows how it moved large concrete armour units and how the cyclone caused significant damage to rock armoured structures.

The Al Masaood harbour located in Dibba Al Fujeirah, UAE; was one of the harbours attacked by the Cyclone Gonu resulting damages in the breakwaters of the harbour (Phelp, et al., 2012). Therefore, in the repair works of the breakwaters at Al Masaood harbour, a new concrete armour unit has been applied in single layer armour system (CSIR, 2009). This new concrete armour unit is known as crablock which has been introduced by the owner of Al Masaood harbour.

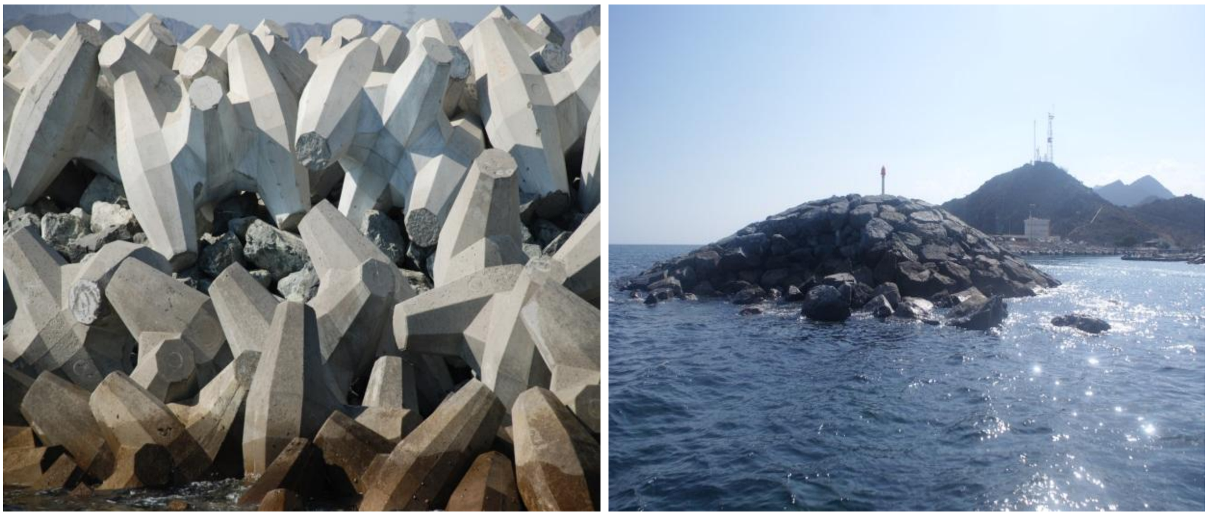

Movements of concrete armour units    Catastrophic damage of rock armour units

**Figure 1.2** Consequences of cyclone on breakwaters in Al Fujeirah [Source:Hendrikse (2014)]

Behind the development of this new armour block the main objectives of founder were to establish concrete armour unit containing the following properties (Hendrikse and Heijboer, 2014):

- one layer concrete armour unit
- high interlocking
- should have large hydraulic stability and sufficient structural strength
- can be placed in both random and uniform pattern
- symmetrical in shape to fit perfectly
- simple and speedy placement
- can be placed by excavator only without using wire-crane
- no necessity of drivers to place under water
- can be handled and stocked easily
- easy to cast and efficient use of concrete
- should be capable to reduce wave overtopping

The shape of this new armour block looks a little bit different from the other existing single layer armour units. **Figure 1.3** shows the top view and isometric view of crablock armour unit. The shape of most commonly used monolayer armour blocks like accropode, core-loc and xbloc are not symmetrical as crablock. The symmetrical shape of crablock allows placement both in random and regular pattern in a single layer system.

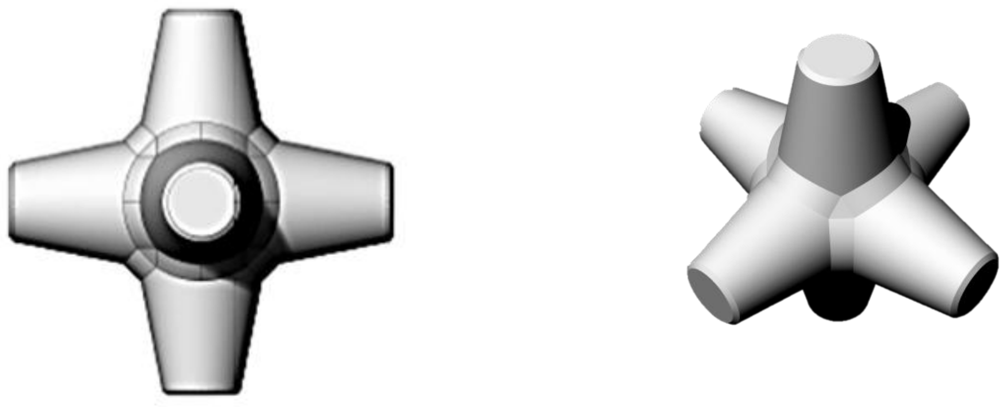

Top View of Crablock　　　　　　　　　　Isometric View of Crablock

**Figure 1.3** Crablock-a new single layer concrete armour unit [Source: Hendrikse (2014)]

As the crablock unit is still under development, no design guidance exists yet for this concrete armour unit. This led the present research to go forward to establish preliminary design guidance for the crablock armour unit. Therefore, small scale physical model testing was performed in this study to come with preliminary design guidance for the crablock armour block. Furthermore, from scientific point of view, it would also be interesting to observe the performance of single layer armour units in regular placement pattern as the current single-layer units are all placed randomly.

# 1.3. Problem description

**Figure 1.4** Crablock armour units as monolayer system in breakwaters at Al Fujeirah [Source: Hendrikse (2014)]

Recently, crablock has been developed as new single layer concrete armour block in Al Fujeirah, UAE. It has been already applied in the repair works of the breakwaters at Al Masaood harbour in Al Fujeirah, UAE (CSIR, 2009). **Figure 1.4** presents the first trial project of crablock armour unit as one layer armour system in breakwaters at Al Fujeirah, UAE. The picture indicates clearly that the early development of the crablock was a little more slender. The design has changed a little since.

In order to be able to use crablock as a single-layer system on rubble mound breakwaters, preliminary design guidance is required on the placement of crablock, hydraulic stability and waves overtopping the structure. Few physical model testing were performed on this new armour block by CSIR at South Africa. However, none of the research determined the stability number and wave overtopping discharge for the design of crablock armour unit. Furthermore, the placement pattern and packing density of this block have not been found in any research. Therefore, based on the available literature, no design guidance exists for this new single layer block compared to other existing one layer units.

## 1.4. Research objectives and questions

The overall objective of this MSc study is to come up with preliminary design guidance for the application of crablock as a single layer armour unit, based on physical model testing. The research has been carried out with the purpose to fulfil the following specific objectives:

- To examine the placement patterns of crablock armour units as a single layer armour system
- To investigate the packing density of the crablock armour units
- To analyse the wave overtopping over crablock slopes
- To compare the test results on wave overtopping with empirical prediction and also with other single layer units

In order to achieve the mentioned research objectives the following research questions were considered:

- Which placement techniques perform better for crablock units?
- What is the suitable packing density for this new single layer armour unit?
- What is the wave overtopping discharge and percentage of overtopping waves over crablock slopes?
- To what extend measured wave overtopping differ with empirical prediction and other single layer units?

It should be noted that the actual physical model investigation was performed in cooperation with André Broere, an MSc-student at Delft University of Technology. His main task of the research is to investigate the stability of the crablock against wave attack. It is for this reason that stability of crablock is not a topic for the present thesis.

## 1.5. Contributions

This research focuses on the experimental study of the crablock unit. The importance of this research to the existing knowledge can be pointed out as following:

- Implementation of uniformly placed single layer concrete armour system in the design of rubble mound breakwaters
- Assists to select proper placement techniques for the placement of crablock units
- Provides a comparison of wave overtopping over crablock with other existing single layer units
- Helps the designer to use as the preliminary guidelines in the design of rubble mound breakwaters using crablock armour units
- A basis for further research on the crablock units

## 1.6. Scope of the study

To come up with preliminary design guidance on crablock, Prof. Van der Meer was approached by AM Marine Works Ltd. and CDR International. Then a research project named crablock research has been developed by UNESCO-IHE. The whole research project is being carried out by number of researchers focussing on different parts. At first, Bonfantini (2014) did a theoretical study on the placement of crablock, possible hydraulic tests and similarities of crablock with other single layer units like accropode and xbloc. This experimental research is a part of crablock research focussing mainly on some specific issues. The scope of this thesis is limited to dry placement tests, set up of flume tests and performing flume tests with the analysis of waves overtopping. The performance of wave flume tests was done together with Mr. Andre Broere from TU Delft. However, this research will mainly concentrate on the analysis of wave overtopping over crablock slope. In **Figure 1.5**, an overview of crablock research together with scope of this thesis is presented.

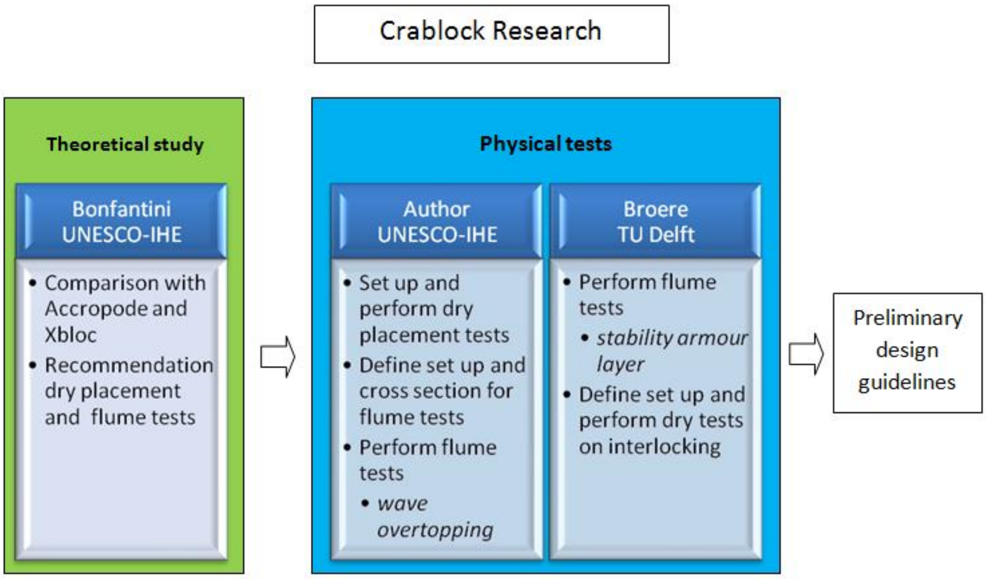


**Figure 1.5** Overview of crablock research

## 1.7. Research methodology

The methodology adopted in this research is discussed in this section presenting all the steps forward to achieve the research objectives. The overview of research methodology structure is presented by a flowchart in **Figure 1.6**.

At first, a literature study has been performed on different monolayer armour units. Also, the theoretical study on crablock armour units by (Bonfantini, 2014) was critically reviewed. Regarding to the review of literature studies on the existing single layer units, the governing environmental and structural parameters were identified for the design of breakwater using crablock units. After the governing design parameters were determined, the experimental set up been done to perform the small scale dry placement tests as well as hydraulic tests in a 2D wave flume.

The data collections of this research were done by performing dry placement tests and small scale hydraulic tests. The horizontal and upslope placement distance were collected as raw data during the placement tests. Also, for each individual test photographs have been captured to describe the tests visually. In this research, Microsoft Excel tools were used to process and to study the observed data of dry placement tests. The test results of dry placement tests were utilized to finalize the test programme for wave flume tests. At the time of 2D flume tests necessary data was collected for the determination of wave overtopping over crablock armour slopes. In case of wave flume tests, Matlab and Microsoft Excel tools have been used for the data processing and interpreting of results.

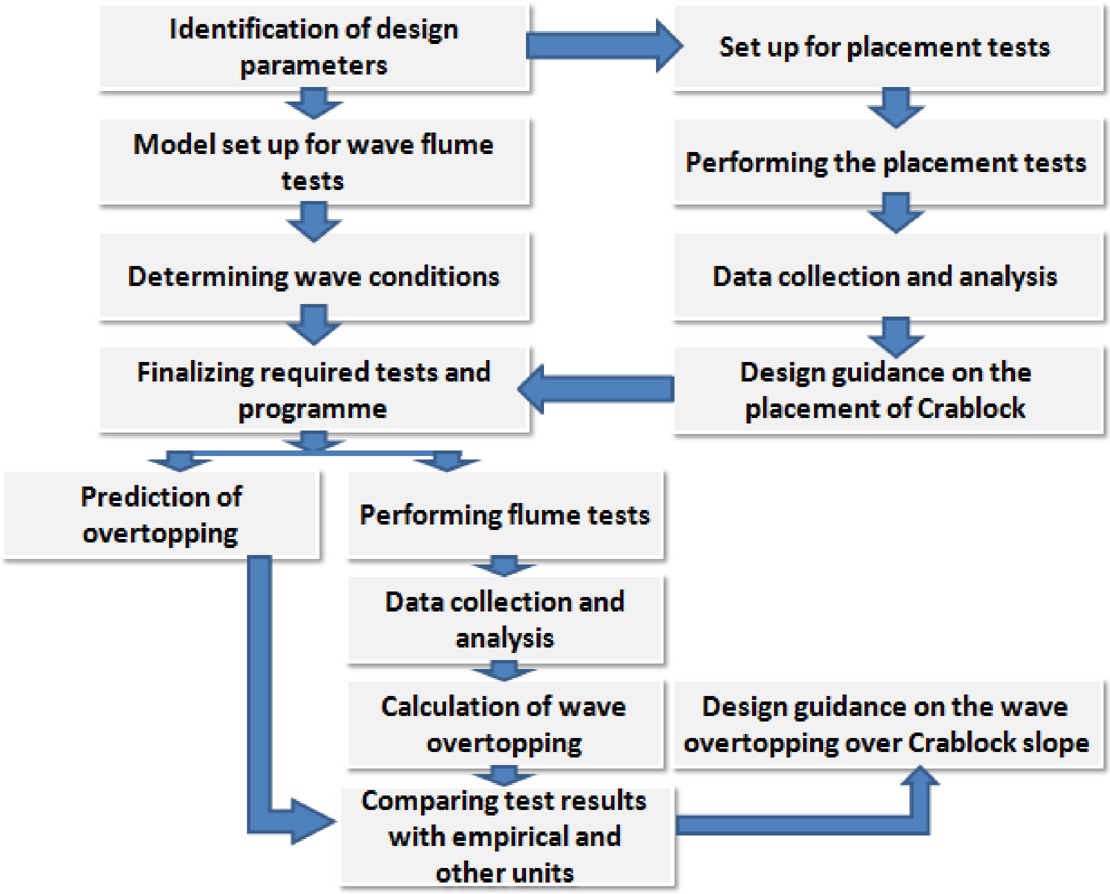


**Figure 1.6** Overview of research methodology

Finally, the preliminary design guidance in line with placement pattern and wave overtopping is set for the application of crablock armour units as single layer armour.

## 1.8. Research outline

CHAPTER 1 gives a brief overview of the study and states the objectives and justifications of research project. Also, it describes the research methods used to achieve the objectives of this research. After this introductory chapter, CHAPTER 2 is designed to present a general review of the available literature on different methodologies applied related to research area. This chapter is also intended to focus on the theoretical background of this experimental research. CHAPTER 3 provides the full picture of each individual dry placement tests where it treats issues like objectives of placement tests, set up of dry placement tests, description of each test series based on visual inspection, results analysis and discussions of each individual test series, etc. In CHAPTER 4, the complete set up of the performed wave flume experiment is discussed. In this chapter, the reader is introduced with testing equipments, test programme, testing procedure, etc of the hydraulic tests performed in this experimental research. The result analysis of 2D wave flume tests together with discussion for each individual test series are revealed in CHAPTER 5. The chapter ends by presenting a comparison between the test results on wave overtopping with empirical prediction and also with other units. In the end, the research is concluded in CHAPTER 6 and recommendations for investigations are highlighted.

# CHAPTER 2

# Theoretical Background

**The first step of the research methodology is the literature study, performed for this research. The literature with respect to stability of armour layer, overtopping of waves and placement of single layer armour and their relevance to this research is discussed mainly in this chapter. This chapter defines and reviews some of the important parameters used in this study based on the literature review. At first the previous studies on the stability of single layer armour is discussed. In the next section wave overtopping over armour slopes is treated. The final section reviews the different terms related with placement of single layer armour units, more specifically on the placement of crablock armour units.**

## 2.1. Previous studies

A lot of research has been done with respect to different concrete armour units as single layer armour. The researchers applied different techniques in order to examine the hydraulic stability, wave overtopping and placement patterns of different single layer armour units. To understand the method background and to develop research methodology an extensive literature review has been conducted in line with stability, overtopping and placement pattern of different armour units. However, the determination of hydraulic stability of the crablock armour is not included in this research. Therefore, the terminology associated with stability of single layer is not discussed in details. The crablock armour unit has a bulky shape like xbloc, accropode, accropode II (R) and core-loc II. Thus, in the literature review of this research, focus is paid on available studies on these blocks and available literature is reviewed critically. Others randomly placed single layer armour units like slender block A-Jack and core-loc are not investigated in detail.

Since crablock has been developed in recent years, very few studies have been conducted about the crablock armour layer. In 2009 CSIR performed some experimental studies on the hydraulic stability of crablock armour units. CSIR (2009) conducted 2D flume tests with the use of a typical cross-section in order to investigate the stability of the crablock unit for both regularly and irregularly oriented placement methods. The 2D flume tests were performed in a scale of 1:60 with the use crablock armour units in a slope of 1:1.5. The test results of that research showed that crablock armour units can sustain under certain wave heights.

Based on the available literature on existing single layer armour units and information on crablock units, Bonfantini (2014) performed an extensive theoretical research on the crablock mono layer armour blocks. The study compared crablock armour unit with two most commonly used single layer armour units accropode and xbloc. Furthermore, the main design parameters for the design of crablock armour layer were identified and discussed. In that academic research, the probable placement tests, placement grid and placement pattern of crablock were also proposed. Moreover, for the determination of hydraulic stability of crablock and wave overtopping over crablock slope, the 2D wave flume tests were also recommended in that study.

## 2.2. Stability of single layer armour

After the invention of the accropode concrete unit in the eighties, an upsurge of interest has been found in single layer system. There have been a large number of studies devoted to the specialized topic of stability of single layer armour. However, in the determination of the stability of armour units, different techniques have been applied for different single layer system. The most common way to determine the stability of armour block for rubble mound breakwater is finding the stability number by using Van der Meer stability formula or establishing design Hudson stability factor.

To identify the stability of amour units on rubble mound breakwaters, Hudson proposed the following formula (**Equation 2.1**) derived from the wide-ranging small scale tests (SPM, 1984). This stability formula is well known as Hudson stability formula. The design stability coefficients $K_D$ in this formula is normally differed with the shape of armour units (SPM, 1984).

$$W = \frac{\rho_s \cdot {H_0}^3}{K_D \cdot \Delta^3 \cdot cot\alpha} \tag{2.1}$$

The above formula can be reformed in the form of stability number, see in **Equation 2.2**. The stability number is very often used for indicating the stability of concrete armour units.

$$N_s = \frac{H_0}{\Delta D_n} = \sqrt[3]{K_D . cot \propto} \tag{2.2}$$

Where,
W = Weight of armour unit [kg]
$\rho_s$ = Density of armour unit [kg/m$^3$]
$H_0$ = Design wave height at structure [m]
$\Delta$ = Relative density of armour unit [-]
$D_n$ = Nominal diameter of armour unit [m]
$K_D$ = Stability coefficient [-]
$\propto$ = Angle of structure slope [°]
$N_s$ = Stability number [-]

Although the Hudson formula is popular because of its simplicity, it does not consider some important parameters like the wave period and the effect of random waves (Van der Meer, 1987a). Based on very extensive small scale tests, Van der Meer (1987a) developed new design formula to determine the stability of rubble mound structures removing the limitations of Hudson formula. For instance, the effect of the wave period, shape of the spectrum, grading of armour, number of waves, permeability of the core, surf-similarity parameter which are not taken into account in Hudson formula, have been included in this new design formula, see details in "Stability of Breakwater Armour Layers- Design Formula by Van der Meer (1987a)". This new design formula is now being most widely used for defining the stability of armour on a rubble mound breakwater.

In the determination of stability of armour block different ways of observing damage of armour block has been applied by researchers. Van der Meer (1988) determined the stability of accropode for the design of rubble mound breakwaters. In order to develop stability formula for artificial concrete armour block like accropode a new definition of damage with respect to number of actual displaced units was introduced in that study. Furthermore, the research recommended avoiding taking design stability value at start of damage for the monolayer unit accropode since the failure is very close to start of damage. Although several tests have also been conducted to determine the hydraulic stability of core-loc, there are very few data existing in literature (Bonfantini, 2014). In 1999 Van der Meer compared the design stability number for core-loc armour block using same definition of damage as accropode.

The same way of observing damage criteria like the accropode and core-loc has also been observed for the xbloc concrete armour unit. In 2003 the concrete armour unit xbloc was developed by delta marine consultants (DMC) in the Netherlands. A large number of tests, both 2D and 3D tests, were performed on this block. The hydraulic stability and overtopping performance of this block are available in its own web site. Bakker, et al. (2005) demonstrated the results of a number of hydraulic model tests to present the hydraulic performance of xbloc armour unit. The research proposed design stability number for xbloc by using relative damage levels as like as accropode and core-loc. Besides Van der Meer stability number the experiment also determined Hudson stability coefficient for the design of xbloc using the relationship between surf similarity parameter and stability parameter.

In contrast to the use of relative damage level by counting displaced armour block researcher also used other damage criteria to evaluate stability of single layer armour block. A-Jack was introduced as monolayer system after the application of accropode and core-loc in the design of rubble mound breakwater. LeBaron (1999) determined the hydraulic stability of breakwater armoured with A-Jack single layer units. Instead of relative damage level the research applied three damage categories to evaluate the hydraulic stability of the A-Jack block.

The development of single layer armour blocks continued with the introduction of the cubipod armour block. Opposed to using the well-known method of damage observation by counting displaced armour units or by determining the profile of the armour slope, Gómez-Martín and Medina (2006) introduced a new method called Virtual net method to determine the damage of the cubipod armour block. Furthermore, the research concluded that the use of the usual method of measuring damage of armour is not appropriate for uniformly shaped armour units. Also, in 2007 Gómez-Martín and Medina determined the Hudson stability coefficients by using the Virtual net method in order to examine the hydraulic stability of the cubipod armour block.

Furthermore, CSIR (2009) performed hydraulic tests on the crablock and compared pictures captured before and after every test to examine the stability of the armour units. The authors used software to investigate the displacement of the crablock armour units by the armour track method. Although Hudson stability coefficients were found, the research recommended avoiding the use of it for uniformly placed armour unit. The study showed that the crablock unit show satisfactory performance under the testing wave conditions up to 4m considering minor settlement and rocking. No tests were performed until failure of the structure; therefore no design parameters could be derived.

## 2.3. Definition of wave overtopping

In the design of coastal structures like sea defences to protect coastal flooding, coastal protections to minimize coastal erosion and breakwaters at harbours to ensure safe navigation and mooring of vessels; overtopping of waves is considered as one of the prime concern (EurOtop, 2007). Overtopping of waves mainly occur due to the low crest height in comparison to wave run-up levels of the utmost waves (TAW, 2002). In that case crest freeboard or free crest height ($R_c$) is determined by the difference in elevation between height of the crest and the still water level, see **Figure 2.1**. In general, wave overtopping is expressed by the term mean discharge per linear metre of width, q in terms of $m^3$/s per m or in l/s per m (EurOtop, 2007).

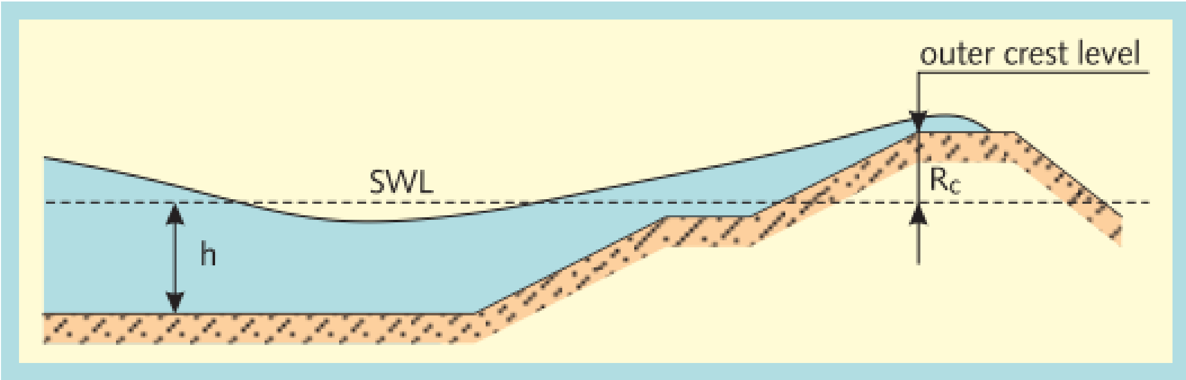


**Figure 2.1** Crest freeboard for wave overtopping [Source: TAW (2002)]

Besides crest freeboard and wave height at the structure, some research showed that wave steepness have also influence on the amount of wave overtopping. Van der Meer and Janssen (1995) provided a new formula on wave overtopping, including the wave steepness and the slope angle of the structure. The ratio between wave height and wave length is termed as wave steepness (EurOtop, 2007) . Wave steepness is sometimes recognised as one of the influencing factor on wave overtopping (DMC, 2003). However, it is mainly wave period which impacts on overtopping (EurOtop, 2007). In the determination of wave overtopping over accropode armour slope, Van der Meer (1987b) investigated that longer wave periods give higher overtopping rates compared to short wave periods.

## 2.4. Prediction of wave overtopping

Based on the available wave conditions and water levels, various methods have been prescribed in EurOtop (2007) to predict the overtopping of waves; Analytical method, Empirical methods, PC-Overtopping and Neural network tools from CLASH database, Numerical methods and finally Physical models. In this research, empirical methods have been used to estimate wave overtopping over one layer Crablock slopes, which have been checked with small scale 2D flume tests in this research. Therefore, others methods are not dealt with in details further in this study, see details in chapter 4 of EurOtop (2007).

### 2.4.1. Empirical methods

#### 2.4.1.1 Wave overtopping discharge

For the simplicity in determination, mean overtopping discharge (q) is very often used and expressed in terms of basic empirical equations of overtopping (EurOtop, 2007). EurOtop (2007) describes empirical equations in details for the approximation of overtopping over rubble mound slopes. For the prediction of wave overtopping of dikes, Van der Meer and Janssen (1995) introduced new conceptual design formulae for both breaking and non-breaking waves. In that research, estimation of overtopping of waves is expressed in terms of mean overtopping discharge, crest freeboard, slope angle, breaker parameter and the influence factors. These formulas are being widely used in the determination of wave overtopping and also explained further in TAW (2002) and in EurOtop (2007).

The general formula used for the estimation of wave overtopping discharge over coastal structure is (EurOtop, 2007),

$$\frac{q}{\sqrt{gH_{m0}^3}} = a\exp(-b\frac{R_c}{H_{m0}}) \quad (2.3)$$

Where,

$\frac{q}{\sqrt{gH_{m0}^3}}$ = Dimensionless overtopping discharge [-]

$\frac{R_c}{H_{m0}}$ = Dimensionless relative crest freeboard [-]

a and b are the coefficients in terms of the wave height, slope angle, breaker parameter and the influence factors.

The complete general formulae to estimate wave overtopping discharge over slopping coastal structures by EurOtop (2007) for both probabilistic and deterministic design are listed in the following equations.

*For Probabilistic Design*

Based on the mean prediction the following formulas (**Equation 2.4 and 2.5**) for the probabilistic design have been presented in EurOtop (2007).

— for breaking waves

$$\frac{q}{\sqrt{gH_{m0}^3}} = \frac{0.067}{\sqrt{\tan\alpha}} \cdot \gamma_b \cdot \xi_{m-1,0} \cdot \exp\left(-4.75\frac{R_c}{\xi_{m-1,0} \cdot H_{m0} \cdot \gamma_b \cdot \gamma_f \cdot \gamma_\beta \cdot \gamma_v}\right) \quad (2.4)$$

— and for non-breaking waves maximum value of

$$\frac{q}{\sqrt{gH_{m0}^3}} = 0.2 \cdot \exp(-2.6\frac{R_c}{H_{m0} \cdot \gamma_f \cdot \gamma_\beta}) \quad (2.5)$$

*For Deterministic Design*

For the deterministic design a more conservative approach has been proposed by EurOtop (2007). In that case one standard deviation has been recommended to add with mean overtopping rate, see in **Equation 2.6 and 2.7**.

— for breaking waves

$$\frac{q}{\sqrt{gH_{m0}^3}} = \frac{0.067}{\sqrt{\tan\alpha}} \cdot \gamma_b \cdot \xi_{m-1,0} \cdot \exp\left(-4.3\frac{R_c}{\xi_{m-1,0} \cdot H_{m0} \cdot \gamma_b \cdot \gamma_f \cdot \gamma_\beta \cdot \gamma_v}\right) \quad (2.6)$$

— and for non-breaking waves maximum value of

$$\frac{q}{\sqrt{gH_{m0}^3}} = 0.2 \cdot \exp(-2.3\frac{R_c}{H_{m0} \cdot \gamma_f \cdot \gamma_\beta}) \quad (2.7)$$

Where,

$q$ = Mean wave overtopping discharge [m3/s per m]

$g$ = Gravitational acceleration [m/s$^2$]

$H_{m0}$ = Significant wave height [m]

$\alpha$ = Angle between overall slope and structure [°]

$\gamma_b$ = Influence factor for a berm [-]
$\gamma_f$ = Influence factor for roughness elements on a slope [-]
$\gamma_\beta$ = Influence factor for oblique wave attack [-]
$\gamma_v$ = Influence factor for a vertical wall on a slope [-]
$\xi_{m-1,0}$ = Breaker parameter = $\frac{tan\alpha}{\sqrt{s_{m-1,0}}}$

In many cases rubble mound structures have been built with armour slope of around 1:1.5 for example single layer rubble mound breakwater with 1:1.5 or 1:1.33. Generally the steep smooth slope increases the probability of having largest overtopping (EurOtop, 2007). Therefore, in the determination of mean overtopping discharge for rubble mound breakwaters the maximum value of overtopping equations are recommended by EurOtop (2007). That means the equations (**Equation 2.5 and 2.7**) for non breaking waves in both probabilistic and deterministic design should be used for the single layer rubble mound structures following the approach by EurOtop (2007); Eqn. 6.6 and 6.5 in EurOtop (2007).

**New Empirical Equation**
Recently, Van der Meer and Bruce (2014) concluded that empirical formulas provided by EurOtop (2007), **Equation 2.4** for breaking waves as well as **Equation 2.5** for non-breaking waves over-estimate wave overtopping for slopping structures with very low or zero crest height. Furthermore, Van der Meer and Bruce (2014) recommended following formulas (**Equation 2.8 & 2.9**) to predict wave overtopping on slopping structures with zero and positive crest height.

- for breaking waves

$$\frac{q}{\sqrt{gH_{m0}^3}} = \frac{0.023}{\sqrt{\tan\alpha}} \cdot \gamma_b \cdot \xi_{m-1,0} \cdot \exp\left[-\left(2.7\frac{R_c}{\xi_{m-1,0} \cdot H_{m0} \cdot \gamma_b \cdot \gamma_f \cdot \gamma_\beta \cdot \gamma_v}\right)^{1.3}\right] \quad (2.8)$$

- and for non-breaking waves maximum value of

$$\frac{q}{\sqrt{gH_{m0}^3}} = 0.09 \cdot \exp\left[-\left(1.5\frac{R_c}{H_{m0} \cdot \gamma_f \cdot \gamma_\beta}\right)^{1.3}\right] \quad (2.9)$$

Furthermore, Van der Meer and Bruce (2014) illustrated new formula for the design of wave overtopping over smooth slopping structures of slope angles steeper than 1:2 with non-breaking conditions. The formula (**Equation 2.10)** prescribed in that research is as follows,

$$\frac{q}{\sqrt{gH_{m0}^3}} = a \cdot \exp\left[-\left(b\frac{R_c}{H_{m0}}\right)^{1.3}\right] \quad (2.10)$$

Where, coefficients a and b are mentioned by researchers as following,

$a = 0.09 - 0.01\,(2 - \cot\alpha)^{2.1}$, for $\cot\alpha \leq 2$ and: $a = 0.09$ for $\cot\alpha > 2$
$b = 1.5 + 0.42\,(2 - \cot\alpha)^{1.5}$, with a maximum of b = 2.35 and: $b = 1.5$ for $\cot\alpha > 2$

**Roughness factor**
In order to compute the average overtopping rate for rubble mound structures by above mentioned empirical formulas, individual roughness factors with respect to different types of armour layer are also available in Table 6.2 of EurOtop (2007); see **Table 2.1**. **Table 2.1** has been derived from the outputs of CLASH project on overtopping (EurOtop, 2007). From the table it is observed that monolayer armour units like accropode, core-loc and xbloc have more or less same roughness factors($\gamma_f$). Thus, to predict the

overtopping of waves over single layer crablock one of the roughness factor from these three can be assumed as the roughness factor for crablock.

**Table 2.1** Roughness factors ($\gamma_f$) for rubble mound structures in a slope of 1 in 1.5 [Source: EurOtop (2007), Tab. 6.2]

| Type of armour layer | $\gamma_f$ |
|---|---|
| Smooth impermeable surface | 1.00 |
| Rocks (1 layer, impermeable core) | 0.60 |
| Rocks (1 layer, permeable core) | 0.45 |
| Rocks (2 layers, impermeable core) | 0.55 |
| Rocks (2 layers, permeable core) | 0.40 |
| Cubes (1 layer, random positioning) | 0.50 |
| Cubes (2 layers, random positioning) | 0.47 |
| Antifers | 0.47 |
| HARO'S | 0.47 |
| Accropode™ | 0.46 |
| Xbloc® | 0.45 |
| CORE-LOC® | 0.44 |
| Tetrapods | 0.38 |
| *Dolose* | 0.43 |

#### 2.4.1.2 Percentage of overtopping waves

The percentage of waves overtopping the crest of the rubble mound breakwater can also be predicted using the empirical equations provided by EurOtop (2007). In the estimation of percentage of overtopping waves armour freeboard ($A_c$) introduced instead of crest freeboard ($R_c$), see **Figure 2.2**. By knowing the nominal diameter of the armour unit, significant wave height and armour freeboard, the number or the percentage of overtopping waves can be approximated as following the approach (**Equation 2.11**) by EurOtop (2007).

$$P_{ov} = \frac{N_{ow}}{N_w} = \exp[-(\frac{A_c \times D_n}{0.19 \times {H_{m0}}^2})^{1.4}] \qquad (2.11)$$

In which,
$H_{m0}$ = Significant wave height [m]
$D_n$ = Nominal diameter of armour block [m]
$A_c$ = Freeboard of armour [m]
$N_{ow}$ = Number of overtopping waves [-]
$N_w$ = Number of incident waves [-]
$P_{ov}$ = Percentage of overtopping waves [%]

### 2.4.2. CLASH database

To approximate wave overtopping for an extensive variety of coastal structures, a standard design tool has been generated in the European research project CLASH (Van Der Meer, et al., 2005). CLASH database is an international database freely available on internet for wave overtopping over coastal structures. The database is comprised of more than 10,000 tests from 163 independent test series which is formatted in Excel containing a matrix of 31 columns for 31 parameters and more than 10,000 rows (Steendam, et al., 2004). The overtopping discharges for all kind of coastal structures are available in the database, for example **Figure 2.3** presents the dimensionless overtopping discharge with respect to the relative crest freeboard for all the CLASH tests.

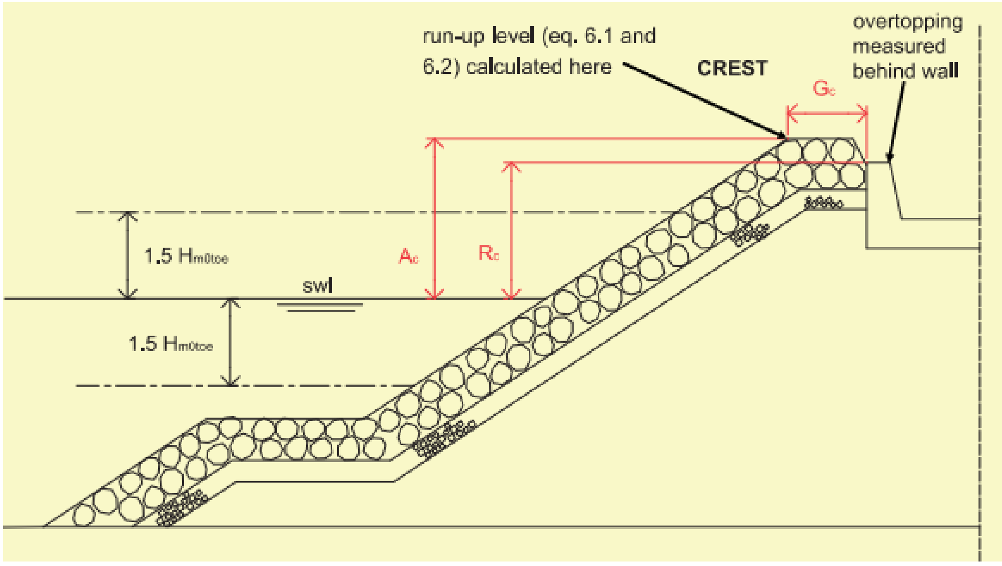


**Figure 2.2** Run-up level and location for overtopping differ [Source: EurOtop (2007)]

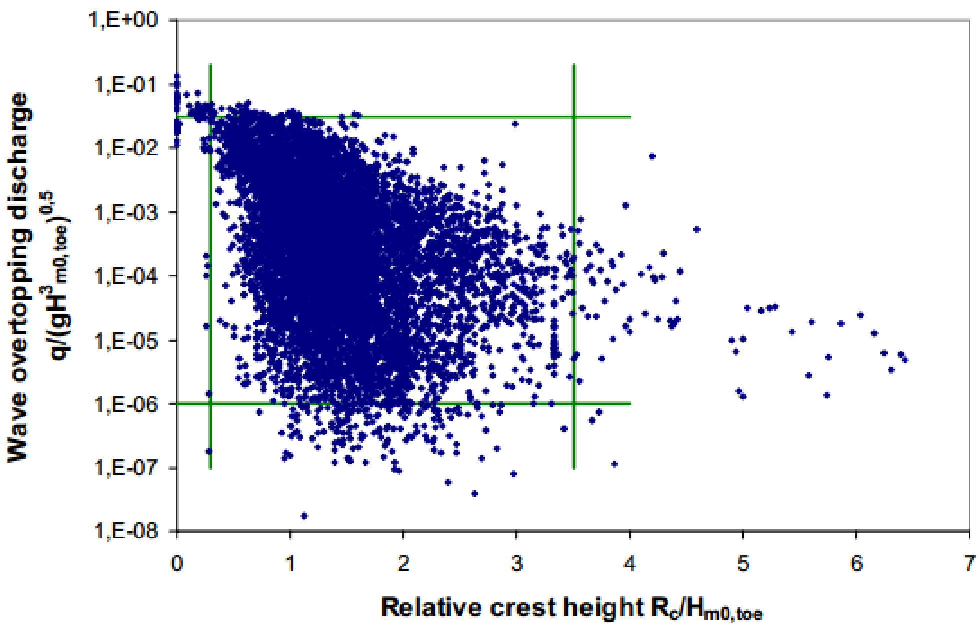


**Figure 2.3** Relative crest freeboard against relative wave overtopping for all tests [Source: Steendam, et al. (2004)]

### 2.4.3. Physical modelling

Analytical or theoretical methods to predict overtopping of waves have not been generated very well. Therefore, EurOtop (2007) recommended small scale wave flume tests to generate empirical equations of overtopping estimation. Prototype situation can be scaled to a physical model by the use of small scale model testing (Van Buchem, 2009). Furthermore, experimental model testing is often applied where the coastal structures are designed using single layer concrete armour units and overtopping is an important criterion (Wolters, et al., 2009). Also, with the use of small scale hydraulic tests in a wave flume, wave overtopping can be determined in terms of overtopping volume, number of waves, wave-overtopping velocities and depths (EurOtop, 2007). Small scale physical model tests were performed in this experimental research in order to determine wave overtopping over crablock slope.

## 2.5. Placement of armour blocks

### 2.5.1. Introduction

In general, the placement of single layer concrete armour units is difficult and challenging in real-life situations. The precision and speed of the placement might be affected by the harsh conditions and by deep water (Muttray and Reedijk, 2009). The placement of monolayer randomly placed armour units like accropode and core-loc are complicated (Bakker, et al., 2003). However, in order to ensure a firm armour cover with excellent interlocking capacity the placement of armour blocks has to be precise (Oever, 2006). The good placement of armour units ensures the stability of single layer armour system (Muttray, et al., 2005). Further, Frens (2007) mentioned that the stability of armour layer is effected by the placement technique. In addition to hydraulic stability of armour layers, the structural integrity of armour units are also influenced by the placement of monolayer armour blocks (Muttray, et al., 2005). Therefore, in order to make sure a good interlocked armour layer with high hydraulic stability, immense concentration should be paid in the placement of concrete elements. It should be noted that the symmetrical shape of crablock makes the unit different from other existing single layer units. The placement of crablock armour units is therefore also assumed different compared to other single layer blocks.

### 2.5.2. Placement grid

Generally, the single layer armour units are placed in a predefined grid position. The designed grid plays a significant role to place the armour units properly and to ensure proper interlocking between the units. The deviation of units from the designed position might influence the interlocking capacity of the armour layer. Therefore, to place the armour units accurately, placement grids should be well designed in line with reality. The horizontal and upslope placement distance are the main design parameters to design a placement grid. At present, there is no specific design guidance about the placement of crablock armour units. Nevertheless, different factors governing the placement of crablock can still be determined from the theoretical study. Based on the theoretical study on the placement pattern of existing single layer blocks, Bonfantini (2014) proposed an outline for the placement grid of crablock.

CSIR (2009) performed 2D wave flume tests using crablock armour blocks and argued that the grid placement distance $0.71\times$ D in horizontal direction and $0.57\times$ D in vertical direction provided the best placement pattern for randomly oriented crablock armour units. In that research, D was referred to as height of crablock armour unit. Based on this study, Bonfantini (2014) designed a standard rectangular grid with possible theoretical placement of crablock units, see **Figure 2.4**. The achievable packing density observed with this standard rectangular grid is $0.71/\mathrm{D_n}^2$, $D_n$ is the nominal diameter of crablock.

Moreover, the armour units can also be placed in a diamond shaped grid pattern. For example, Oever (2006) designed a diamond shaped grid to place the xbloc armour units. For the placement of crablock units Bonfantini (2014) suggested a diamond shaped grid pattern. In that study Bonfantini (2014) thought that crablock can be placed in a diamond-shaped grid with the minimum horizontal distance 0.6 D and the minimum upslope distance 0.5 D, D is the height of crablock unit. From the horizontal and upslope placement distances the packing density was proposed to $0.94/\mathrm{D_n}^2$ by researcher. **Figure 2.5** shows the planned diamond shaped grid with possible theoretical placement of crablock units by Bonfantini (2014).

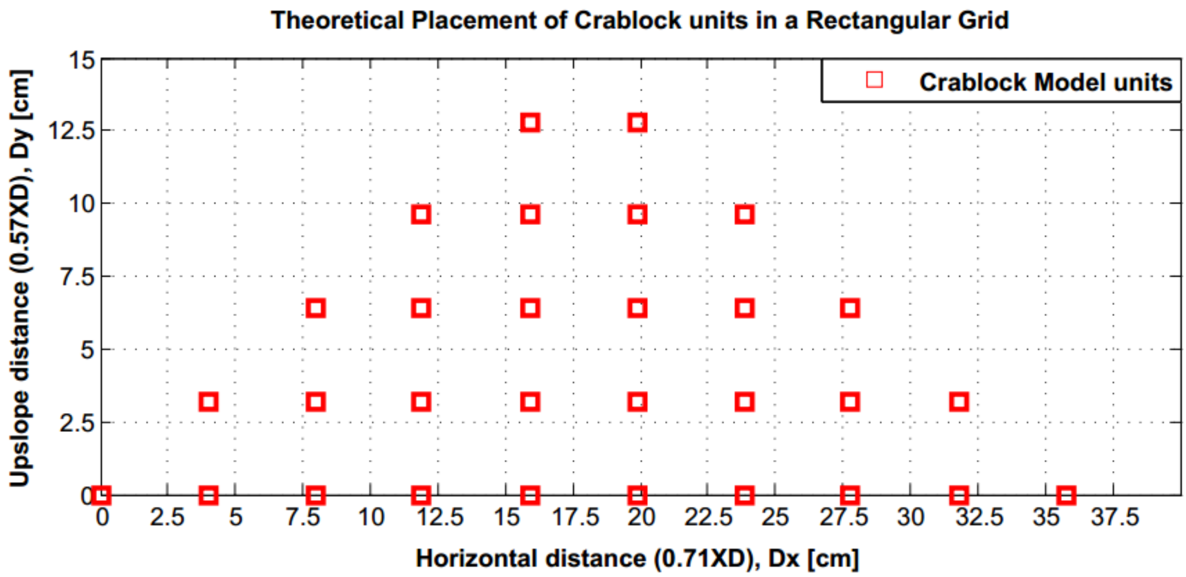


**Figure 2.4** Plan of a theoretically designed rectangular grid ($D_x = 0.71D$, $D_y = 0.57D$ and $PD = 0.71/D_n^2$) [Source: Bonfantini (2014)]

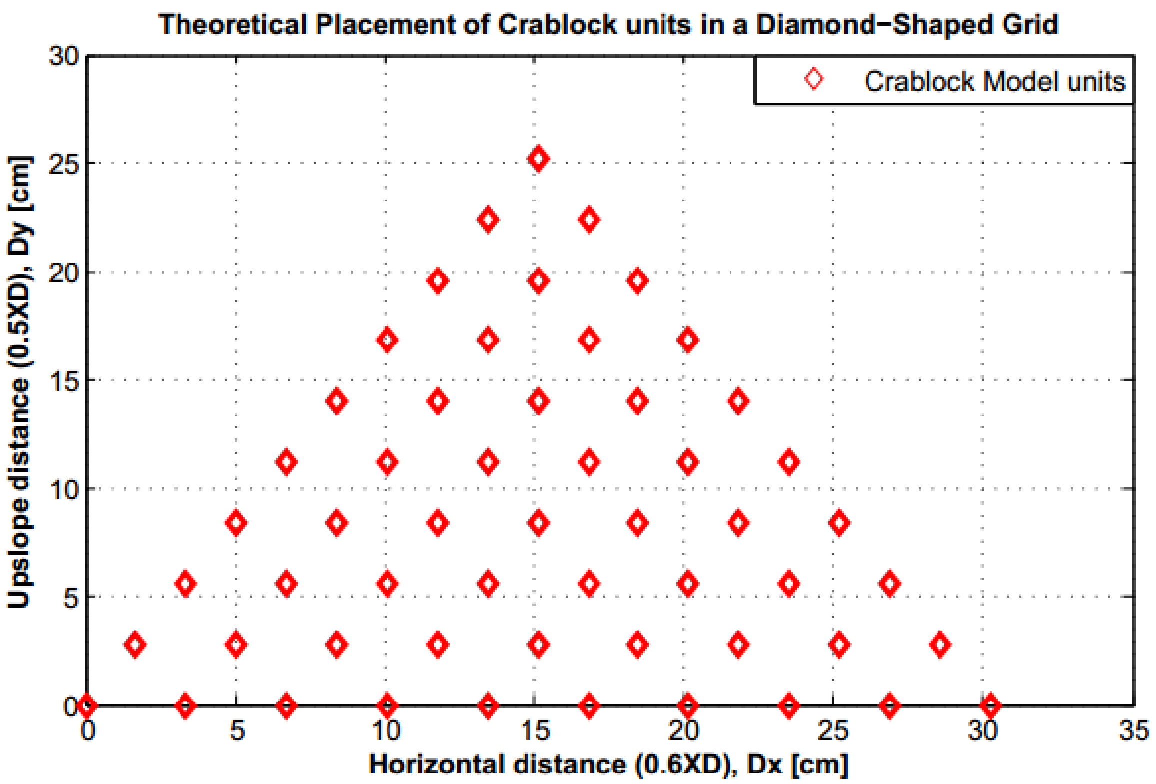


**Figure 2.5** Plan of a theoretically designed diamond grid ($D_x = 0.60D$, $D_y = 0.50D$ and $PD = 0.94/D_n^2$) [Source: Bonfantini (2014)]

### 2.5.3. Placement pattern

The hydraulic stability of an armour layer greatly depends on the interlocking capacity of armour units which is shaped by the quality of the placement pattern (Oever, 2006). Single layer concrete armour units can be placed as randomly oriented or as uniformly oriented. The orientation of armour units are predefined with a certain regular pattern for uniformly oriented blocks while orientation of armour units are irregular for randomly oriented blocks (Bakker, et al., 2005).

Generally, the placement of armour units with random orientation is relatively easier under water compared to strict orientation of units for uniform placement. Nevertheless, it should be noted that some blocks (like accropode) get their high interlocking by random placement and cannot be placed regular. The regular placement of armour block is aesthetically attractive and for the symmetrical blocks like crablock might be more stable in comparison to irregular placement. Phelp, et al. (2012) argued that crablock armour units with uniform orientations provides compact interlocked between the units. Hendrikse and Heijboer (2014) believed that crablock armour units can be placed with uniform orientation in both rectangular and diamond shaped grid, see **Figure 2.6**. In **Figure 2.7**, an example of randomly placed crablock armour units is presented.

Rectangular grid

Diamond -Shaped grid

**Figure 2.6** Uniform placement of crablock [Source: Hendrikse and Heijboer (2014)]

**Figure 2.7** Random placement of crablock [Source: Hendrikse and Heijboer (2014)]

### 2.5.4. Placement equipments

The proper selection of construction equipments certainly dictates the speed of the armour construction. The progress of construction of whole project is limited by the placement of armour (Muttray, et al., 2005). Generally, crawler crane and hydraulic excavators are applied for the placement of the armour units in a breakwater. In most of the cases single layer concrete armour units are positioned with a sling using a crawler crane or hydraulic excavator. For instance, to place accropode, core-loc and xbloc different sling methods have been applied. Similar to other units, crablock armour units can also be placed with use of crawler crane attached with sling, see **Figure 2.8**. However, Hendrikse and Heijboer (2014) believed that crablock armour units should be placed simply by an excavator with specialised clamp, instead of a wire-crane.

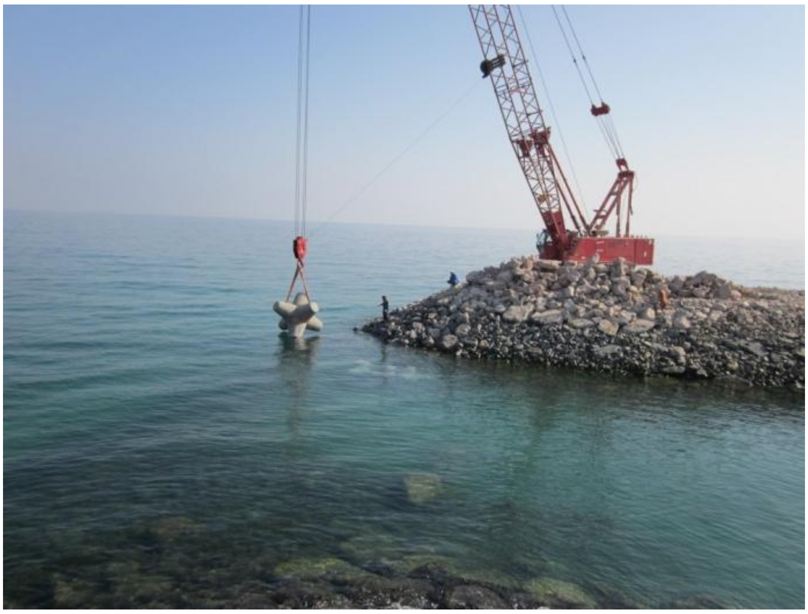

**Figure 2.8** Placement of crablock using crawler crane attached with sling [Source: Hendrikse (2014)]

In the placement of armour units using a crawler crane, it can be operated either from a barge or from the crest of the breakwater (Oever, 2006). The placement of armour units using crawler cranes are relatively slow in operation but good alternative for the large placement distance with heavy armour units (Bonfantini, 2014). Instead of a crawler crane, excavators are also used to locate armour units according to the predefined grid position. An excavator indeed ensures good operating speed and low cost in comparison to crawler crane for the placement of relatively smaller armour units. The minor lifting capacity of armour units, lower operating costs and high placing speed are the main distinguish features of hydraulic excavators in comparison to crawler cranes (Oever, 2006). However, with the use of an excavator, only small armour blocks can be lifted swiftly. In order to place large concrete armour blocks, relatively large hydraulic excavators with high lifting capacity should be used. These large excavators become more available and can be furthermore constructed for specific construction sites.

## 2.6. Packing density

Packing density is considered as main parameter for an armour cover which governs the interlocking capacity (Oever, 2006). The higher hydraulic stability as well as good interlocking capacity can be achieved by higher packing density (Bakker, et al., 2005, Oever, 2006). Packing density is very often defined as the number of units placed per square meter (Nik Mohd Kamel, 2007) or by the number of units placed per square nominal diameter (Van der Meer, 1999). The definition of packing density indicates that higher packing density means high volume of concrete. From the comparison of different concrete armour layers by Van der Meer (1999), it is seen that concrete armours with lower packing density indicates less volume of concrete. Therefore, design packing density considering both economic and safety is very important to know properly for the design of breakwater.

Packing density of armour layer can be determined by calculating the total number of units on a certain surface (Oever, 2006). The formula provided by Oever (2006) is following:

$$\text{PD} = \frac{(N_x - 1)(N_y - 1)}{L_x L_y} \tag{2.12}$$

Where,

$PD$ = packing density per square meter
$N_x$ = horizontal number of units
$N_y$ = number of horizontal rows
$L_x$ = horizontal length of the section in m and
$L_y$ = length up the slope along the slope in m

The packing density of an armour layer can also be evaluated by using the spacing in horizontal and upslope direction (DMC, 2003). DMC (2003) used the following formula (**Equation 2.13**) to calculate packing density of xbloc. However, by using this approach the local packing density cannot be determined the for the units placed in first row and for the units which do not have any units to its left; for instance in **Figure 2.9**, for units M1 and M3 the local packing density is not possible to calculate by this approach. After the determination of all possible local packing densities, the average packing density of the armour layer is the mean of all local packing densities.

$$\text{PD} = \frac{1}{D_x \times D_y} \tag{2.13}$$

In which,

$PD$ = packing density [units/m$^2$]
$D_x$ = horizontal placement distance from centre to centre [m]
$D_y$ = Upslope placement distance from centre to centre [m]

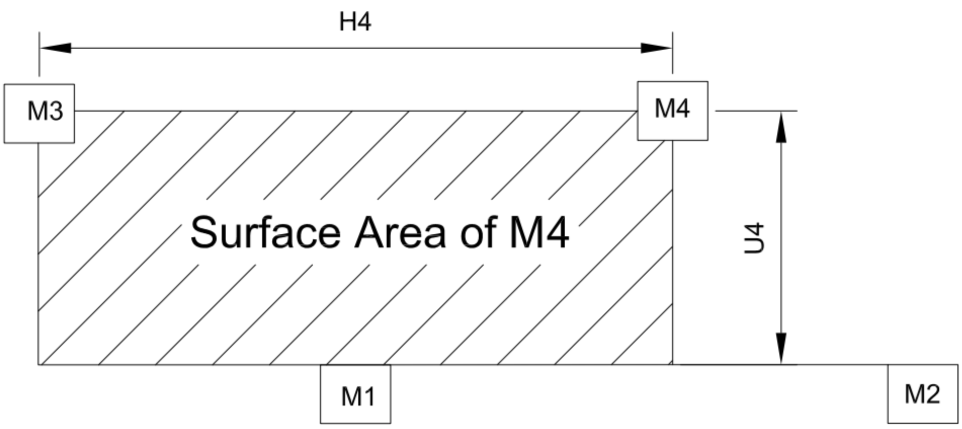


**Figure 2.9** Surface area of single unit [Source: Oever (2006)]

As mentioned earlier, the term packing density also can be elaborated by the number of armour units placed per square nominal diameter. Van der Meer (1999) used the following formula (**Equation 2.14**) to define the packing density in terms of nominal diameter of armour units.

$$\frac{N_a}{A} = \frac{\phi}{{D_n}^2} \tag{2.14}$$

In which,
$N_a$ = Number of armour units
$A$ = Surface area
$\phi$ = Packing density and
$D_n$ = Nominal diameter of armour unit

**CHAPTER 3**

# Dry Placement Tests

**In the previous chapter the theoretical placement grid and probable placement patterns of the Crablock unit have been discussed together with other issues. This chapter mainly focuses on the aim, approach, set up of placement tests and analysis of test results. In first section the objectives of the dry placement tests and approach followed in this research are treated. Section 3.2 describes the set up for dry placement tests reviewing the test facilities, set up, test programme and procedures followed to perform the tests. Further section presents a full description of the each individual test and also provides the analysis performed for each test. Moreover, the conclusions with respect to the visual description and analysis of each test are also described in that section. Finally, the chapter ends by providing a summary of all test results with associated discussions.**

## 3.1. Objectives and approach

The main purpose of the dry placement tests was to examine the possible placement methods for the crablock, to identify the possible associated packing density with good interlocking capacity and to verify the suggested theoretical packing density of crablock armour units. Moreover, the dry tests have been performed in order to establish the relation between horizontal and upslope placement distance of crablock armour units.

Bonfantini (2014) proposed an outline of four placement test series for placing crablock armour units as a single layer system. The recommended dry placement tests by Bonfantini (2014) consisted of standard rectangular grid as well as diamond-shaped grid with both uniform and random orientation of units in a certain packing density, see **Figure 2.4** and **Figure 2.5** . However, in the present research fourteen different test series were performed in order to achieve the above mentioned objectives. The reason for choosing fourteen different test series instead of four tests by Bonfantini (2014) was to have a good idea about the lower and upper limit of placement density of crablock armour units. In order to establish a reliable dataset, three repetition tests have been performed for each test series thus in total 42 tests were performed on the placement of crablock. The dry test series number one, five and eight have been conducted to verify the suggested theoretical packing density of crablock as proposed by Bonfantini (2014). In addition to these tests, a series of tests were executed with lower and higher theoretical packing densities. This variation in packing density has been done in order to find a range where the packing density would fit for crablock armour units.

The model units in the dry tests could be placed by using mini cranes or using a sling technique. However, all the units were placed only by hand due to the limited facilities and easier in placement. During the placement of units by hand, all the units were placed according to specific placement methods considering the real situation, see details in **section 3.2.5**. In this research, the maximum 10 units have been placed in one row for each individual test. Therefore, in total 30 units were used for one test in a rectangular grid and 55 units in a diamond-shaped grid. Similar to the placement tests on xbloc by Oever (2006), the position of crablock units has been determined by calculating X and Y-coordinates. The deviation of the units from the designed position and packing density were computed by using the position of units.

## 3.2. Set up for placement tests

This section is designed to describe the set up for performing the dry placement tests on crablock armour units. The test facilities used for the dry tests together with the model set up, test programme, testing procedure and methods followed to place crablock placement are discussed in this section.

### 3.2.1. Test facilities

The placement tests were carried out the Fluid Mechanics Laboratory of the Faculty of Civil Engineering and Geosciences at Delft University of Technology, Netherlands. The small scale dry tests were performed above a wooden table. A model breakwater was constructed on top of the table. The measurements were done by using measurement tap and by visual observation.

### 3.2.2. Model set up

**Profile of model breakwater**

A wooden frame with a thin wooden surface was used to make the core of the breakwater. The slope of the wooden frame was kept as 1 in 4/3 in order to ensure more interlocking between the units. The slope of the frame was also comprised of side walls to utilize the full width of the slope.

A rock underlayer was constructed on the top of the wooden frame and toe. Furthermore, the toe of the breakwater was made by wood. The height of the wooden toe which is not so significant for the placement tests was kept as 4 cm.

The profile of the model breakwater in order to perform the dry placement tests on crablock armour units is presented in **Figure 3.1**. Most of the tests have been conducted using relatively large frame. However, another relatively smaller frame was used to do the tests with smaller underlayer, see **Figure 3.1**.

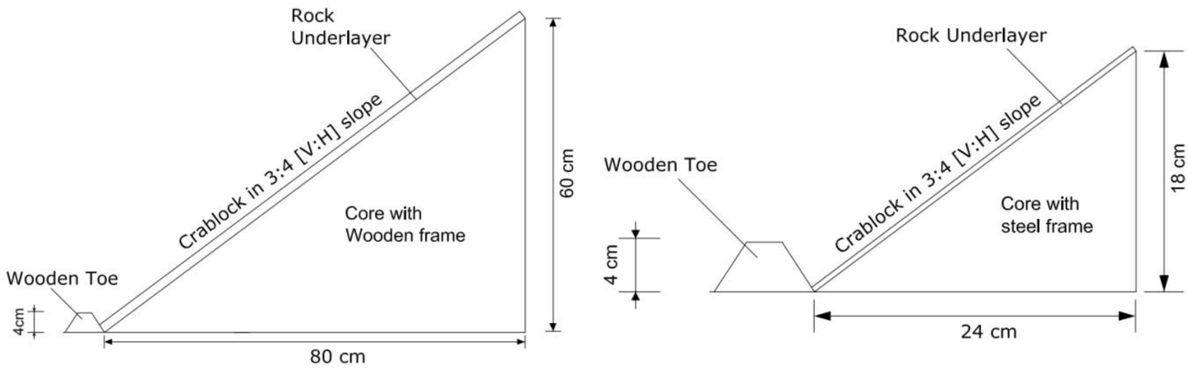


Large frame used for tests 1-11 Small frame used for tests 12-14

**Figure 3.1** Profile of the breakwater for placement tests

### Model units

The placement tests were performed using small scale crablock units with an average weight of 0.0637 kg and nominal diameter of around 0.03m. The mass density of this crablock unit was found to be 2364 kg/m3 in a range of concrete density. The different properties of the crablock model units are listed in **Table 3.1**. The resulting relative density of the model unit is very close to the relative density of the armour units in prototype situation. Furthermore, a picture of model crablock units is attached in **Figure 3.2**.

**Table 3.1** Properties of crablock model units

| Height [m] | Mass [kg] | Mass Density [kg/m$^3$] | Nominal Diameter $D_n$ [m] | Relative Density $\Delta$ [-] |
|---|---|---|---|---|
| 0.056 | 0.0637 | 2364 | 0.02999 | 1.36 |

**Figure 3.2** Model crablock units

### Underlayer

The property of the underlayer was very important to perform the placement tests on the crablock armour units. At first as a normal procedure a conventional underlayer of one-tenth of the weight of the crablock armour units has been considered for the placement tests, see in 4.4. The mass of under layer units used in the dry tests was in the range of 0.003-0.009 kg resulting 11 to 16 mm of nominal diameter.

However, by using this underlayer, regular placement of crablock was hard to achieve. Therefore, in order to observe the possibility of uniform placement of crablock units, a smaller under layer was used to place the armour units in a regular pattern. The smaller underlayer used to perform the dry tests was in the range of 7 to 11 mm of nominal diameter, having a mass in the range of 0.001-0.004 kg.. **Figure 3.3** shows the image of under layers used to perform dry tests.

Conventional (large) Under layer

Small Underlayer

**Figure 3.3** Picture of under layer

### 3.2.3. Test programme

The test programme in order to perform the dry tests on the placement of crablock is presented in **Table 3.2**. In this research, the following fourteen placement test series were performed to familiar the placement pattern of crablock as single layer system. The first eleven tests were executed with the use of large under layer whereas the last three placement tests were conducted using relatively small underlayer material.

**Table 3.2** Test programme for dry placement tests

| Test Series No. | Placement Grid | Orientation | Underlayer | Horizontal Distance | Upslope Distance | Designed PD (per $D_n^2$) |
|---|---|---|---|---|---|---|
| 1 | Rectangular | Uniform | 11 to 16 mm | 0.71 D | 0.57 D | $0.71/D_n^2$ |
| 2 | Rectangular | Uniform | 11 to 16 mm | 0.65 D | 0.60 D | $0.74/D_n^2$ |
| 3 | Rectangular | Uniform | 11 to 16 mm | 0.75 D | 0.65 D | $0.59/D_n^2$ |
| 4 | Rectangular | Uniform | 11 to 16 mm | 0.80 D | 0.60 D | $0.60/D_n^2$ |
| 5 | Diamond-shaped | Uniform | 11 to 16 mm | 0.60 D | 0.50 D | $0.96/D_n^2$ |
| 6 | Diamond-shaped | Uniform | 11 to 16 mm | 0.70 D | 0.60 D | $0.68/D_n^2$ |
| 7 | Diamond-shaped | Uniform | 11 to 16 mm | 0.80 D | 0.65 D | $0.55/D_n^2$ |
| 8 | Rectangular | Random | 11 to 16 mm | 0.71 D | 0.57 D | $0.71/D_n^2$ |
| 9 | Rectangular | Random | 11 to 16 mm | 0.65 D | 0.60 D | $0.74/D_n^2$ |
| 10 | Rectangular | Random | 11 to 16 mm | 0.75 D | 0.65 D | $0.59/D_n^2$ |
| 11 | Diamond-shaped | Random | 11 to 16 mm | 0.70 D | 0.60 D | $0.68/D_n^2$ |
| 12 | Rectangular | Uniform | 7 to 11 mm | 0.71 D | 0.57 D | $0.71/D_n^2$ |
| 13 | Rectangular | Uniform | 7 to 11 mm | 0.65 D | 0.60 D | $0.74/D_n^2$ |
| 14 | Rectangular | Uniform | 7 to 11 mm | 0.75 D | 0.65 D | $0.59/D_n^2$ |

### 3.2.4. Testing procedure

In this laboratory study, all the placement tests were performed only above water. At the start of the test, rock underlayer was placed on top of the wooden frame. Afterwards, crablock units started to place as single layer armour according to the designed placing grid and placement pattern. All the units were placed only by hand. At first, the armour units in the first row were positioned by pointing crablock units in the designed grid position. After that, the units have been set in the higher upslope maintaining rectangular pattern in a rectangular grid and diamond pattern in a diamond-shaped grid. After the placement of all the units photographs were taken to describe the placement of crablock visually. Then the grid coordinates of each individual unit in both horizontal and upslope direction were measured with care. At the time of measurement all the raw data were collected and then processed in excel. All the test series have been performed three times to get a more reliable and larger dataset.

### 3.2.5. Placement of a single crablock unit

The placement of the armour units in the first row is significantly important as it also dictates the accuracy of placing of other units in the upslope. The spacing in horizontal direction is the main criterion to locate the armour units in the first row. In both rectangular and diamond-shaped grid, all the units in the first row were placed with three points pointing downwards. However, units in the upslope were positioned with one point pointing downward. For the placement of units in a rectangular grid with uniform rotation, units in the first row were simply placed with two opposing directions. To get random placement, units were only placed according to designed grid position without keeping any specific orientation with neighbouring units. As stated earlier that, for a rectangular grid, units in the upslope were put maintaining rectangular grid position and in case of a diamond shaped grid, units in the upslope were placed in between two units of previous row.

## 3.3. Description of tests

In this section, the objective of each particular test is discussed with a small introduction to each test. Moreover, all the specific test series are described based on the experience of placement tests and visual point of view. In the visual description, the picture of only one sub test from each test series are provided here. To get more information about all the test series including subtests, see **Appendix A**. At the end, a small conclusion has been provided for each individual test regarding to only experience of placing and visual inspection.

### 3.3.1. Test 1: Rectangular grid with uniform placement (Designed PD = $0.71/D_n^2$)

**Introduction**

This placement test has been performed in a rectangular grid with the uniform orientation of crablock model units. The main aim of this specific test was to verify the theoretical packing density of crablock.The horizontal placement distances and upslope placement distances in the grid were kept same as observed in preliminary tests by CSIR (2009) and recommended by Bonfantini (2014), $D_x = 0.71 \times D$ and $D_y = 0.57 \times D$ with a nominal packing density of $0.71/D_n^2$. The considered rectangular grid with possible theoretical placement of crablock units is presented in **Figure 3.4.**

**Experience of placing and visual inspection**

A picture of the placement test number one in test series one (Test 1.1) is presented in **Figure 3.5**. From the visual inspection, it is observed that some of the units have uniform orientation whereas some of the units could not be placed with intended regular orientation. For instance, in the picture the yellow line together with red dots shows that not all the units have same orientations also not even in the same line. However, the units indicated by blue line are maintained similar orientations in a column. Furthermore, it is remarkably inspected from the photograph that all the units are interlocked with surrounding units.

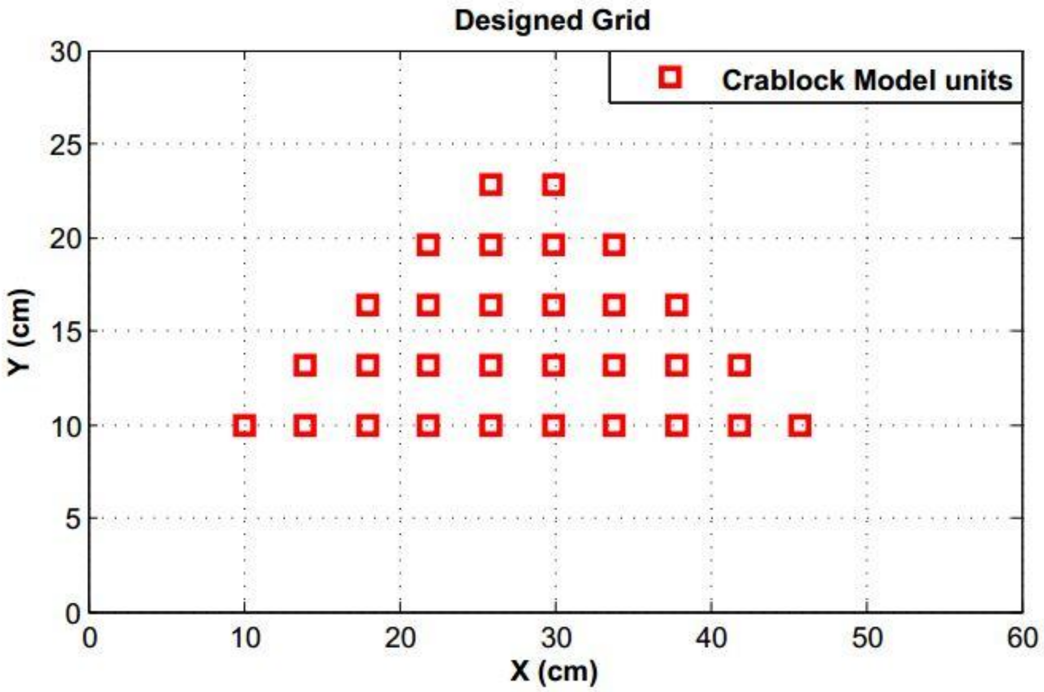


**Figure 3.4** Plan of designed rectangular grid with uniform placement ($D_x = 0.71D$, $D_y = 0.57D$ and $PD = 0.71/D_n^2$)

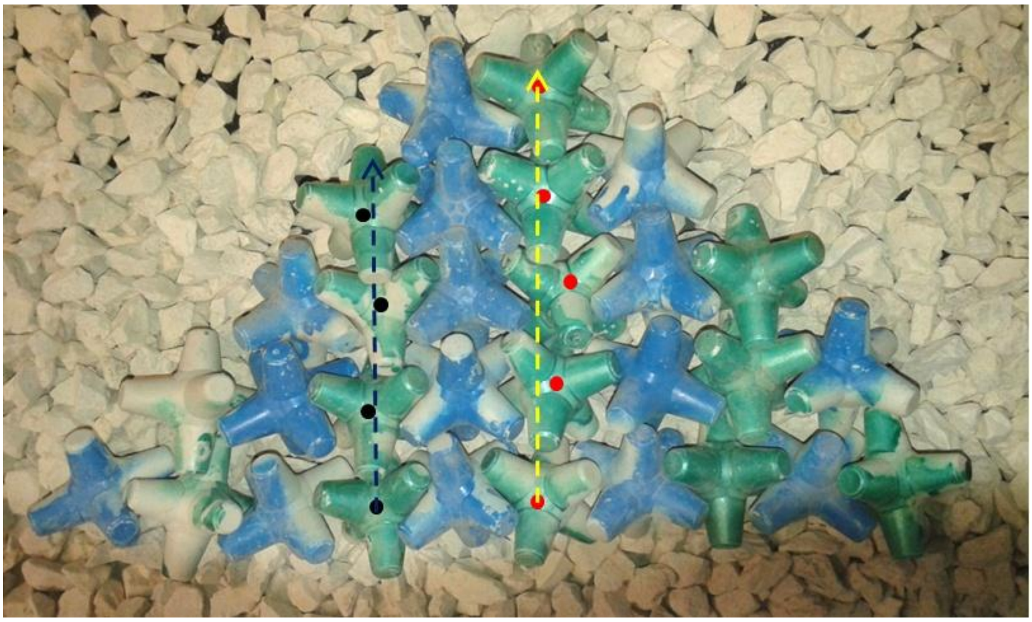

**Figure 3.5** Picture of placement test number one in test series one (Test 1.1)

## Conclusion

In general, in this test all the units were touched with other units that mean no loose units were observed which indicates the good quality of interlocking of armour units. However, from the experience of placing and visual inspection it was found that by using conventional underlayer it is hardly possible to place all the units with keeping regular orientation of units. Therefore, in reality the uniform placement of crablock armour units with the use of large underlayer might be difficult using this designed grid.

### 3.3.2. Test 2: Rectangular grid with uniform placement (Designed PD = $0.74/D_n^2$)

**Introduction**

The specific objective of this test was to check the placement of crablock units in a narrow rectangular grid. This placement test has been performed in a rectangular grid with the uniform orientation of crablock model units. The spacing in horizontal direction was fixed to $D_x = 0.65 \times D$ and the spacing in upslope direction was assumed $D_y = 0.60 \times D$ with a nominal packing density of $0.74/D_n^2$. A top view of the designed rectangular grid with is shown in **Figure 3.6**.

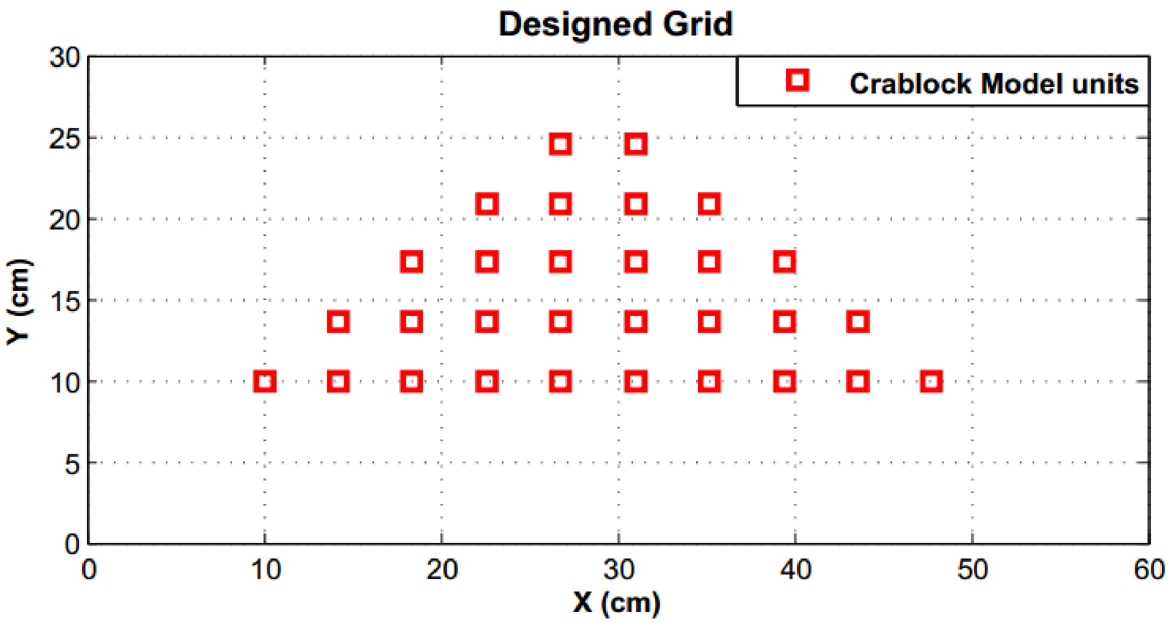


**Figure 3.6** Plan of designed rectangular grid with uniform placement ($D_x = 0.65D$, $D_y = 0.60D$ and PD = $0.74/D_n^2$)

**Experience of placing and visual inspection**

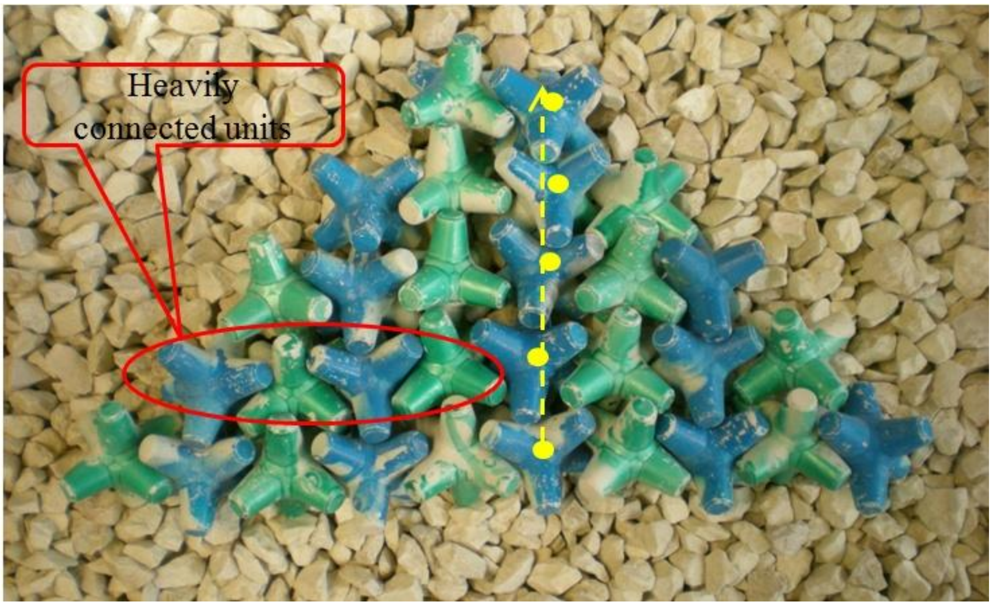


**Figure 3.7** Picture of placement test number one in test series two (Test 2.1)

To describe the placement test visually a picture of placement test number one in test series two (Test 2.1) is enclosed in **Figure 3.7**. In this image, it is seen that all the units are highly connected with each others that means no loose units were remarked in this test. However, based on the visual inspection it is clearly noticeable that a proper uniform pattern could not be obtained in this rectangular grid that means all the units do not have uniform orientations. For example, the yellow line in combination with dots in the following image indicate that all the units in that particular column is not in the same line and also shows that units in the subsequent row do not have similar orientations.

### Conclusion

In overall, as no loose units were observed in this grid thus it might be possible to achieve a highly interlocked armour layer. However, the main objective of this test was to get a proper uniform shaped which could not be achieved with the use of conventional underlayer. Therefore, in order to achieve good regular pattern of crablock this grid is not recommended using with large underlayer.

### 3.3.3. Test 3: Rectangular grid with uniform placement (Designed PD = $0.59/D_n^2$)

### Introduction

As similar as placement test one and two, this test was also conducted in a rectangular grid with the uniform orientation of crablock model units. The test has been performed to observe the placement pattern of crablock units in a relatively wider rectangular grid compared to previous two test series. The standard rectangular grid with assumed placement distances is shown in **Figure 3.8**.

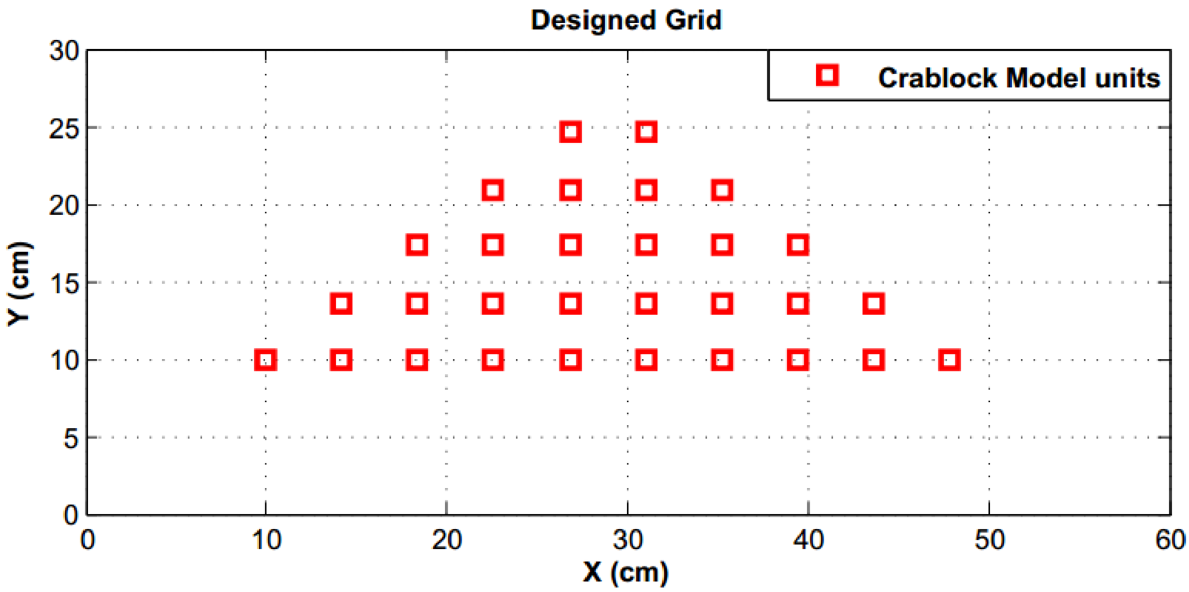


**Figure 3.8** Plan of designed rectangular grid with uniform placement ($D_x = 0.75D$, $D_y = 0.65D$ and PD = $0.59/D_n^2$)

### Experience of placing and visual inspection

**Figure 3.9** shows visual observation of placement test number two in test series three (Test 3.2). By the visual inspection, it is detected that uniform rectangular pattern could not be obtained as wanted in this planned grid. To cite an example, the red dots in the following photograph are indicating the armour units are not having regular orientation. Furthermore, few of the units are loosely interacted with neighbouring units whereas some units are closely interlocked with surrounding units such as units pointed out by yellow dots are loose units. It is recognised from the image that some of the units could not be placed regarding to the designed position in the column and row. For instance, the black dotted line in together with dots is drawn in the picture to show the misplaced units.

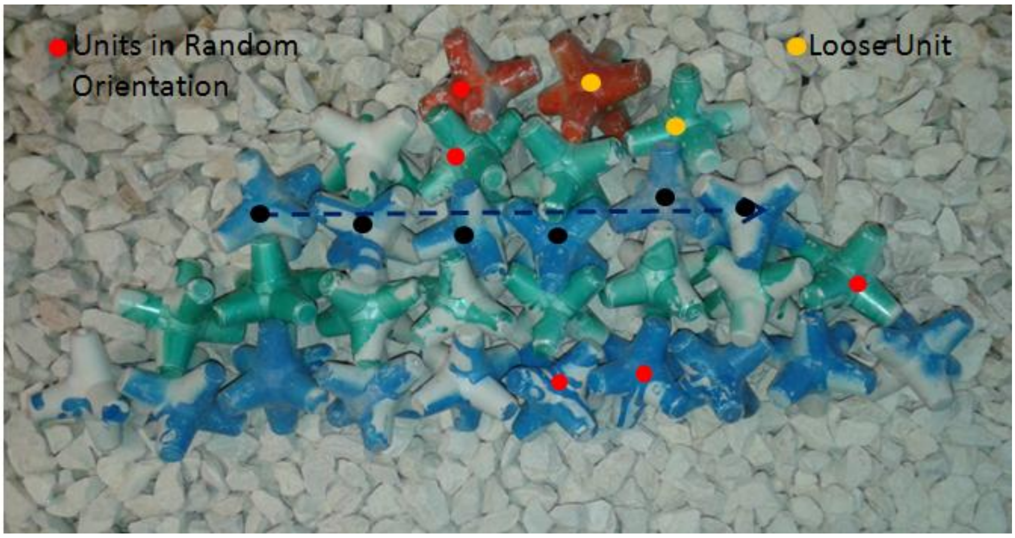


**Figure 3.9** Picture of placement test number two in test series three (Test 3.2)

### Conclusion

In conclusion, by using this standard rectangular grid crablock units can be placed in more or less defined position. But the placement test showed that some units are not really interlocked with surrounding units (low packing density) which might affect the hydraulic stability of armour layer. Moreover, the uniform pattern was also not obtainable by this designed grid. Therefore, for the regularly oriented crablock armour, this rectangular grid with large underlayer is not suggested to use.

## 3.3.4. Test 4: Rectangular grid with uniform placement (Designed PD = 0.60/$D_n^2$)

### Introduction

The objective of this test was to examine the performance of uniformly placed crablock armour units in a wide rectangular grid. **Figure 3.10** shows the planned rectangular grid with possible theoretical placement of crablock units.

### Experience of placing and visual inspection

The placement of crablock in this planned grid can be inspected visually from the picture printed in **Figure 3.11**. From the visual observation, it is noted that this designed grid is quite large for the placement of crablock. During the experiment, the placement of units in this wide grid was found extremely difficult as the units moved from the placing position because of loose connection with surrounding units, like yellow line and black dots in the picture display that units moved from their defined position in the row. As a consequence, a lot of loose units with small gaps between the units in the armour layer were examined during the tests which might cause settlements of the armour layer. For instance, small gaps in the armour layer can be detected very easily from the above image of the placement test. Furthermore, it was also remarked that despite having a wide grid all the units do not have regular orientation, such as red line in the photograph shows the units having quite random orientation in a column.

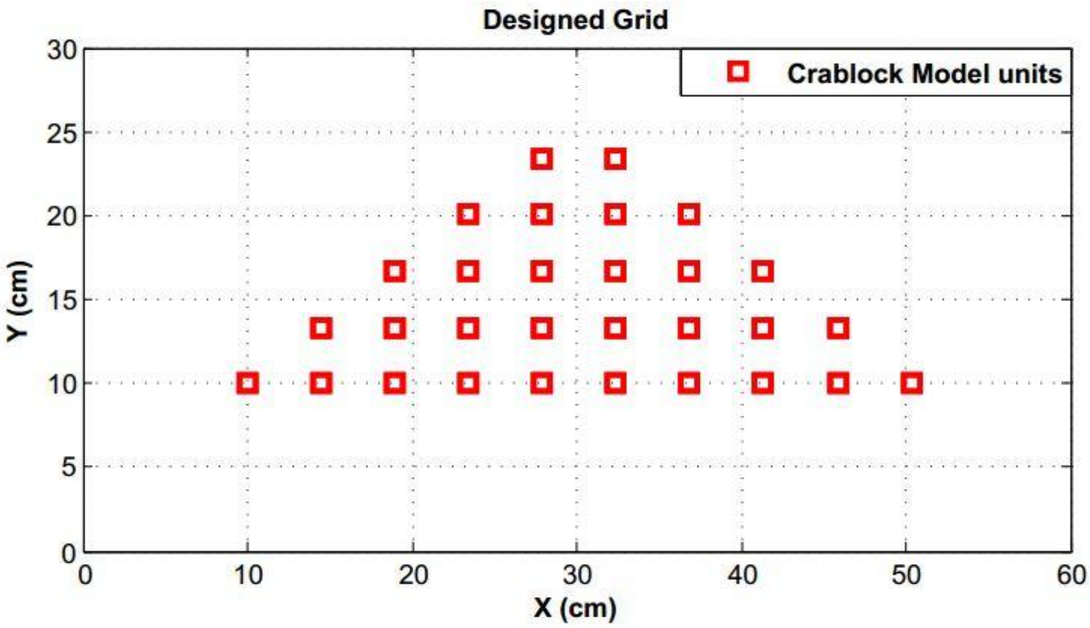


**Figure 3.10** Plan of designed rectangular grid with uniform placement ($D_x$ = 0.80D, $D_y$ = 0.60D and PD = $0.60/D_n^2$)

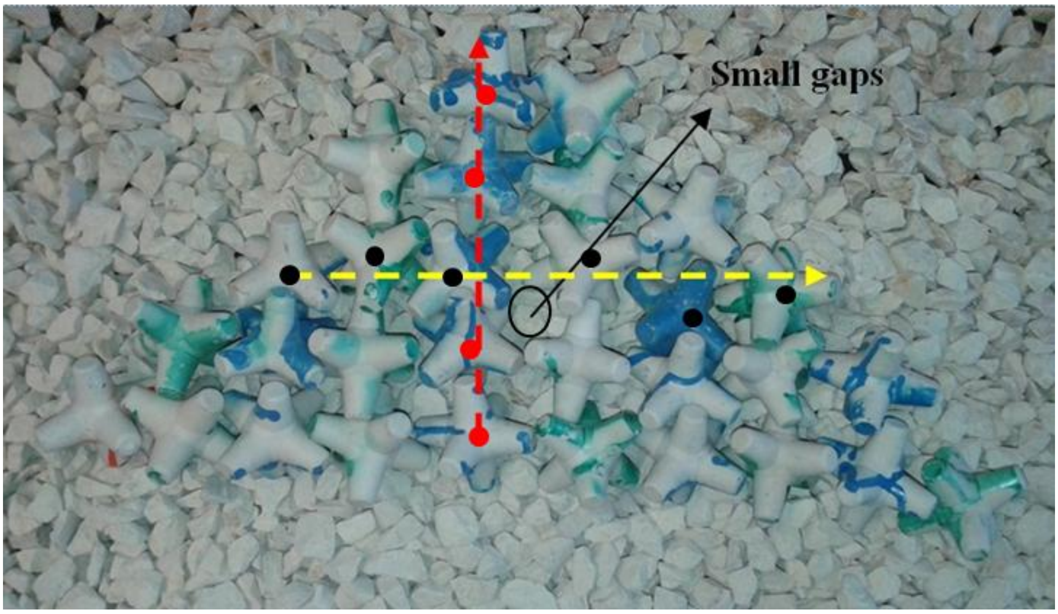


**Figure 3.11** Picture of placement test number two in test series four (Test 4.2)

## Conclusion

To conclude, in this test almost all the units were loose units that means units were not interacted with neighbouring units. In the design of single armour layer, loose units are not accepted as it decreases the quality of interlocking between units. Moreover, a uniform pattern of armour layer could not be obtained using this designed grid and underlayer. Hence, the placement of crablock using this particular rectangular grid is not recommended in real situations.

### 3.3.5. Test 5: Diamond-shaped grid with uniform placement (Designed PD = $0.96/D_n^2$)

**Introduction**

The particular objective of this placement test was to verify the placement pattern of crablock units in a diamond shaped grid with the uniform orientation of units. By theoretical study on diamond shaped grid for xbloc and shape of crablock armour units Bonfantini (2014) recommended horizontal placement distance $D_x = 0.60 \times D$ and upslope placement distance as $D_y = 0.50 \times D$ where D is the height of the crablock model unit. It should be noted that Bonfantini (2014) proposed a nominal packing density of $0.94/D_n^2$ for this designed grid, however regarding to calculated nominal diameter of model units packing density was found $0.96/D_n^2$. This small deviation mainly happened due to the variation of nominal diameter of crablock units assumed by Bonfantini (2014) with calculated diameter by density tests in this research. **Figure 3.12** presents the planned diamond shaped grid with possible theoretical placement of crablock units.

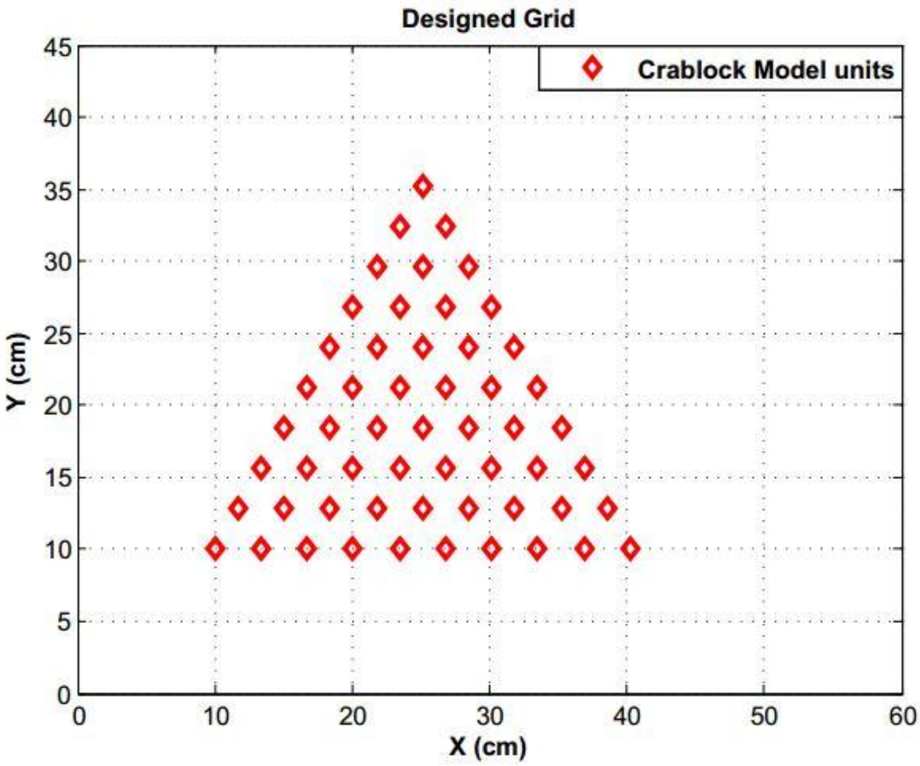


**Figure 3.12** Plan of designed diamond grid with uniform placement ($D_x = 0.6D$, $D_y = 0.5D$ and PD = $0.96/D_n^2$)

**Experience of placing and visual inspection**

During this specific test, it was highly recognised that model units are not possible to place uniformly according to the specific designed grid position. The theoretically designed grid with recommended placement distances was very small to place the units in position. **Figure 3.13** shows the visual observation of placement test number two in test series five (Test 5.2). From the visual inspection, it is seen that some of the units are not entirely interacted with other units. Moreover, most of the units misplaced from their planned grid position with loosing the diamond pattern, such as in the picture yellow line together with red dots indicate that some of the units could not be placed maintaining diamond pattern. Further, some of the units do not have the uniform orientation.

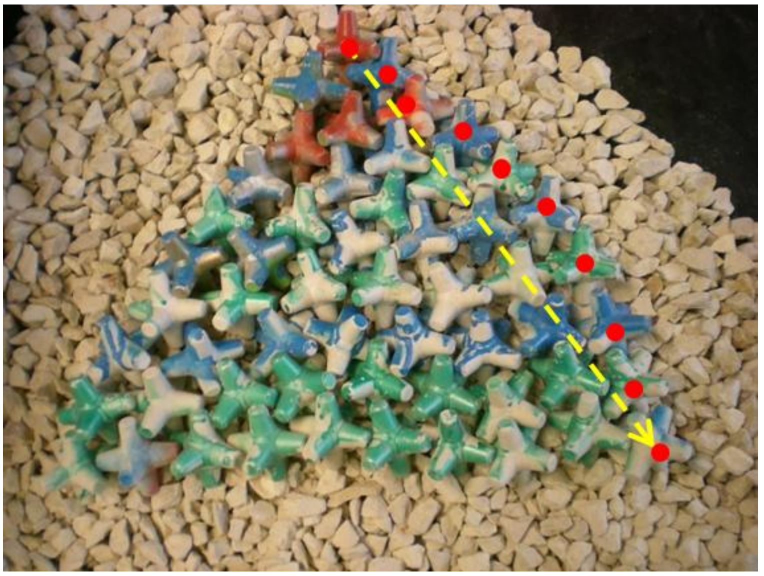

**Figure 3.13** Picture of placement test two in test series five (Test 5.2)

**Conclusion**

To sum up, the quality of the placement was observed extremely worse during the tests both in terms of placing grid and orientation of units. This placement test clearly indicates that crablock model armour units cannot be placed in this designed diamond shaped grid with regular orientation of units. Thus, this theoretically designed diamond shaped grid with uniform placement pattern is hardly possible using conventional underlayer and without fixation of first row by dedicated toe units (both rotation and location).

### 3.3.6. Test 6: Diamond-shaped grid with uniform placement (Designed PD = $0.68/D_n^2$)

**Introduction**

The aim of this test was to find the possibility of uniform placement of crablock units in a diamond shaped grid with horizontal placement distance of 0.70 times the height of crablock and upslope placement distance assumed 0.60 times the height of crablock model unit. The theoretically designed diamond shaped grid for this particular test is printed in **Figure 3.14**.

**Experience of placing and visual inspection**

The picture of the placement test number two in test series six (6.2) is attached in **Figure 3.15**. The image says that a proper uniform placement pattern could not be achieved in this test even though units are interlocked with surrounding units. All the units were placed with regular rotation according to the designed grid position. But, it is remarkably noted from the image that some of the units do not have uniform orientation. Moreover, some of the units are not in the same line with neighbouring units of same row. The model units in the row indicated by red dots in the following photograph do not have uniform orientation and also are not in the same line.

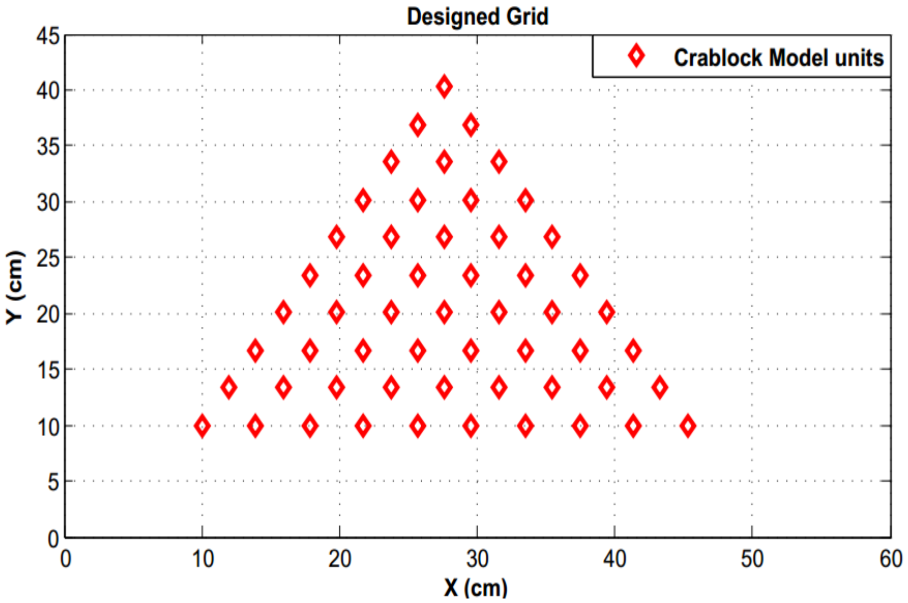


**Figure 3.14** Plan of designed diamond grid with uniform placement ($D_x = 0.7D$, $D_y = 0.6D$ and $PD = 0.68/D_n^2$)

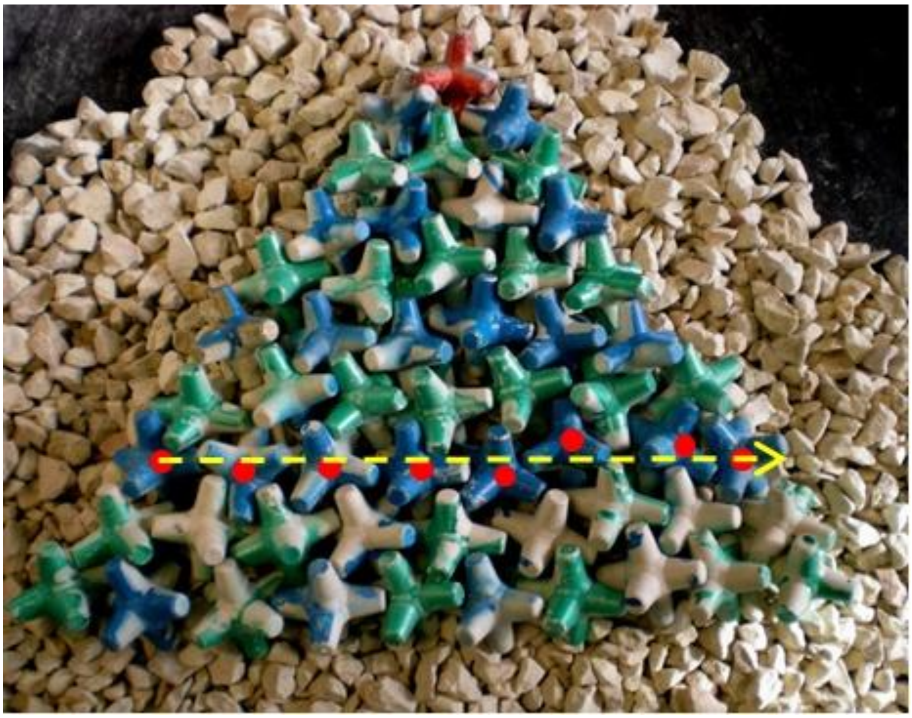

**Figure 3.15** Picture of placement test number two in test series six (Test 6.2)

## Conclusion

As a conclusion, placement tests showed that more or less good interlocked armour layer can be achieved with the placement of crablock in this designed grid. However, the rotation of units becomes random after the placement which points toward the incapability of uniform placement of crablock in a diamond shaped pattern with conventional large underlayer. It should be noted that focus should be paid on the first row and if this can be fixated (both in rotation and location) it may be better to place. Still, the large underlayer makes it difficult to place uniformly.

### 3.3.7. Test 7: Diamond-shaped grid with uniform placement (Designed PD = $0.55/D_n^2$)

**Introduction**

This test was also carried out in a diamond shaped grid with uniform rotation like previous test. However, the horizontal and upslope placement distance was changed to check the packing density of crablock armour units. Based on the assumed horizontal and upslope placement distance ($D_x$=0.80D and $D_y$=0.65D), a diamond shaped grid has been designed, see **Figure 3.16**.

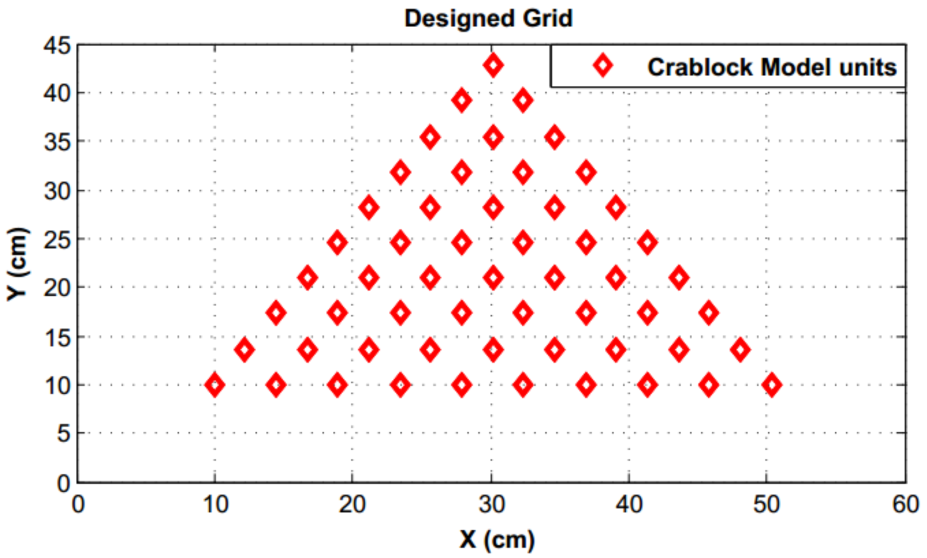


**Figure 3.16** Plan of designed diamond grid with uniform placement ($D_x$ = 0.80D, $D_y$ = 0.65D and PD = $0.55/D_n^2$)

**Experience of placing and visual inspection**

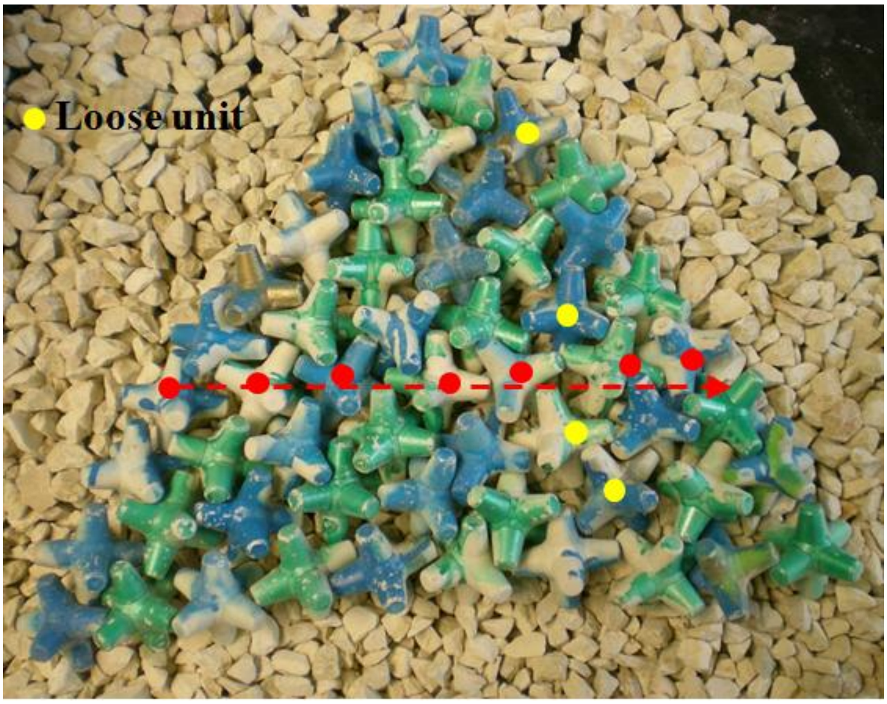


**Figure 3.17** Picture of placement test number two in test series seven (Test 7.2)

A visual inspection of placement test number two in test series seven (Test 7.2) is described in **Figure 3.17**. By visual observation, it is examined that the designed grid is relatively large and some units are not well interacted with other units, see **Figure 3.17**. Therefore, the interlocking capacity of armour layer is threatening due to the presence of loose armour units. Furthermore, it seems that most of the units are randomly oriented. Also, few units lost their position from the position in the designed row. For example, the model units pinpointed by red dots should have been positioned in the red line. It clearly shows that how the units from that particular row misplaced from their predefined position.

### Conclusion

In conclusion, at the time of placement tests a lot of loose units observed with this designed grid. These loose units are not allowable in practice as it increases the probability of settlement of armour layer. Also, the uniform diamond shaped pattern could not be obtained in this test. Therefore, this designed grid with regular rotation of units is not applicable for the placement of crablock using conventional underlayer. As mentioned earlier, focus should be paid on the first row and if this can be fixated it might perform better.

## 3.3.8. Test 8: Rectangular grid with random placement (Designed PD = $0.71/D_n^2$)

### Introduction

The purpose of this test was to verify the recommended theoretical packing density by Bonfantini (2014) in a rectangular grid with random orientation of units. Similar to the placement test one, this test was also performed in a same rectangular grid and also with same nominal packing density, only the orientations of the units were random for this test, see **Figure 3.4**.

### Experience of placing and visual inspection

The placement of units with random orientation was relatively easier and quick in comparison to previous all tests with uniform orientation. A photograph of placement test number three in test series eight (Test 8.3) is printed in **Figure 3.18**, to describe the test from visual observation. Based on visual inspection and experience of placing, it was inspected that all the units were more or less interacted with nearby units that means no loose units were observed in this placement test. However, the photograph (**Figure 3.18**) says that some units misplaced from their defined position in the vertical line (column) and horizontal line (row). For instance, the red line in the following image is indicating the straight column line and red dots are showing the position of units supposed to be that line. This observation clearly illustrates that most of the units in that particular column has moved from their designed position. Therefore, the accuracy of the placement of units might be less using this designed grid.

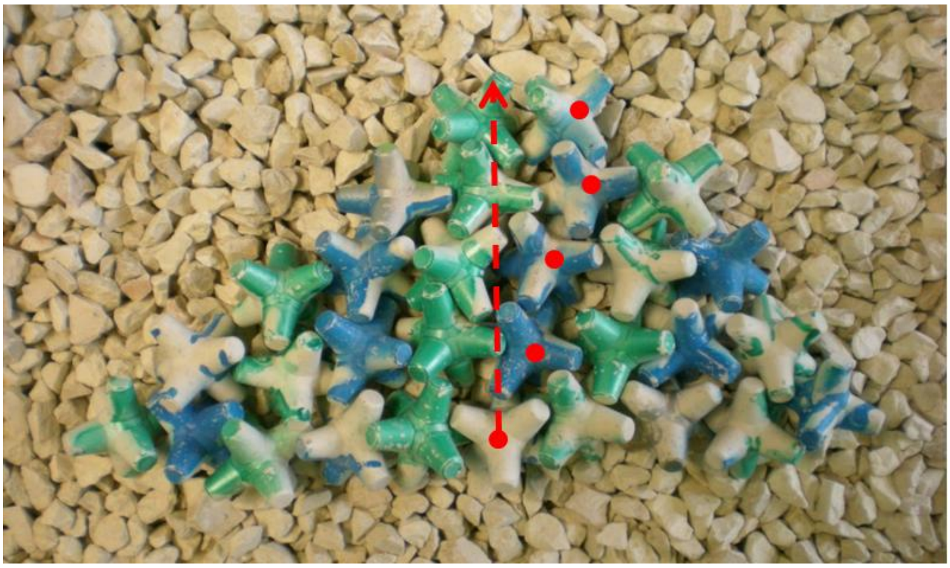

**Figure 3.18** Picture of placement test number three in test series eight (Test 8.3)

### Conclusion

To summarize, with the use of this designed grid it is possible to obtain an armour layer without having any loose units. However, this test gives an indication that with the use of random orientation of units the accuracy of placement of units in predefined position is lower than uniform placement in a same rectangular standard grid.

### 3.3.9. Test 9: Rectangular grid with random placement (Designed PD = $0.74/D_n^2$)

### Introduction

This particular test was carried out to monitor the performance of randomly oriented crablock armour units in a narrow rectangular grid. The same packing density as well as placement grid as used in the placement test series two, has been used in this test; see **Figure 3.6**. The only difference was that the orientations of the unit were random in this experiment.

### Experience of placing and visual inspection

A picture of placement test number one in test series nine (Test 9.1) is presented in **Figure 3.19**, to describe the test from visual point of view. It is observed that all the units are closely touched with surrounding units. However, it is seen that higher in the upslope, all the units could not be placed in line with previous units in the same column, for example, see marked units by red dots in **Figure 3.19**. The units out of place indicate that the suggested horizontal distance might be too small to come to the desired placing grid.

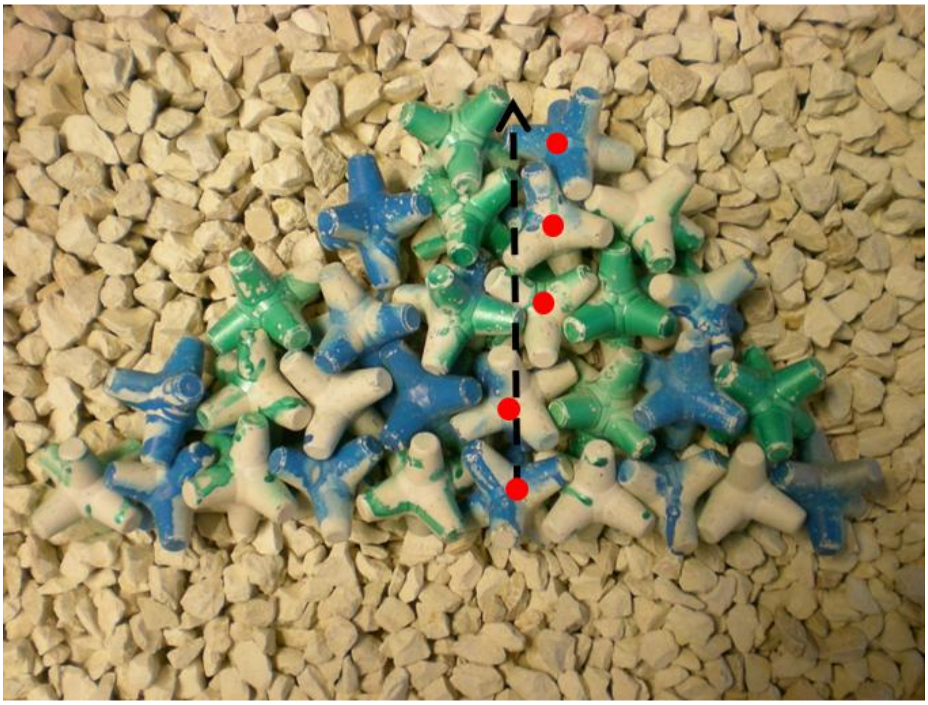

**Figure 3.19** Picture of placement test number one in test series nine (Test 9.1)

### Conclusion

In general, with this designed grid, it is quite tough to place the units randomly according to the desired grid position of individual units. The proposed grid was too narrow to place the crablock armour units in random pattern which might also effects the interlocking capacity of armour layer. Therefore, it is recommended to enlarge the placement distances in order to use have a good designed grid for the random placement of units.

### 3.3.10. Test 10: Rectangular grid with random placement (Designed PD = $0.59/D_n^2$)

**Introduction**

To investigate the random placement of crablock in a relatively wide rectangular grid this specific test was performed. In this test, the designed placement grid and designed packing density was exactly same as in the placement test series three, see **Figure 3.4**. The only difference was that the orientations of crablock model units were random for this test.

**Experience of placing and visual inspection**

**Figure 3.20** Picture of placement test number two in test series ten (Test 10.2)

In this experiment, it was remarkably noticed that the placement of crablock in random orientation is easy to place in dry condition. A picture describing the visual observation of placement test number two in test series ten (Test 10.2) is attached in **Figure 3.20**. The visual inspection gives an indication that all the units are still connected with surrounding units even though this designed grid is quite large compared to previous tests with random placement. Moreover, regarding to visual assessment, it is observed that most of the units have approximately maintained their position at the predefined row and column. While it should be noted that the exact position of armour units cannot be determined from this picture.

**Conclusion**

In this test, no loose units were observed even though all the units were not highly touched with surrounding units. Moreover, the designed spacing in horizontal and upslope direction was good enough to place the armour units according to the planned grid position. Thus, this designed grid can be applied for the placement of crablock with random orientation of units.

### 3.3.11. Test 11: Diamond-shaped grid with random placement (Designed PD = $0.68/D_n^2$)

**Introduction**

This test was designed to observe the placement pattern of randomly oriented crablock armour units in a diamond shaped grid. The designed placement grid and packing density used in this test was as same as in the placement test six, see **Figure 3.14.** However, the orientations of the units were random for this test instead of uniform.

### Experience of placing and visual inspection

In **Figure 3.21**, a picture of placement test number three in test series eleven (Test 11.3) is provided to describe the test visually. Founded on visual study, it is importantly marked that all the units are well interacted with other units. Indeed, this interlocking capacity of armour layer ensures the stability of armour layer and reduces the settlement of armour layer. Besides, it is identified that most of the units have maintained their position in the predefined horizontal and vertical line.

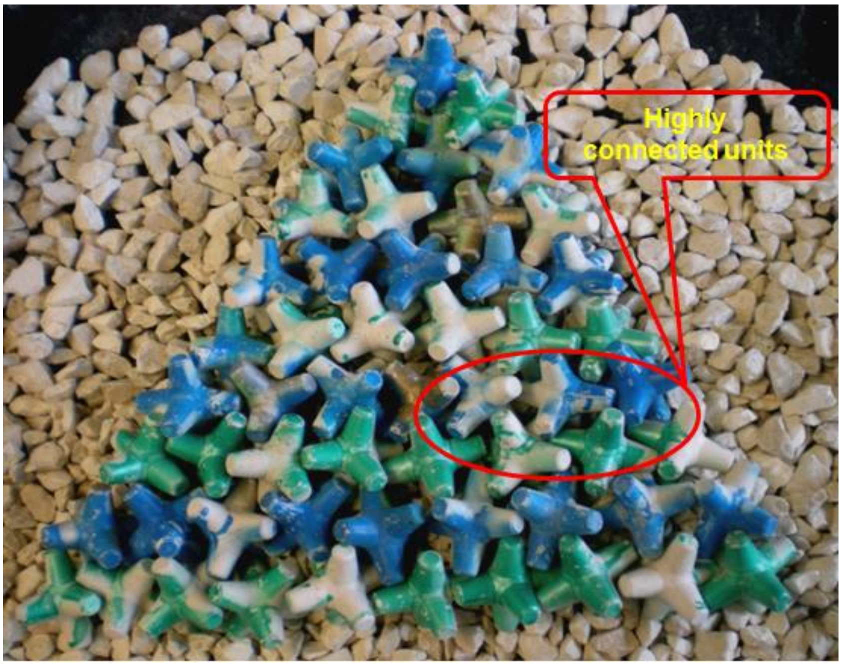


**Figure 3.21** Picture of placement test number three test series eleven (Test 11.3)

### Conclusion

In overall, placement test showed that all the units are vastly connected with each others. In reality, the good quality of interlocking capacity of armour ensures the high hydraulic stability of armour layer. Therefore, it is possible to use this designed grid with random orientations of crablock units in order to have an excellent interlocked armour layer.

## 3.3.12. Test 12: Rectangular grid with uniform placement (Designed PD = $0.71/D_n^2$)

### Introduction

The specific aim of this test was to examine the uniform placement pattern of crablock armour units in a smaller under layer. In this experiment, the horizontal and upslope placement distance were used as same as the placement test series one and eight, see **Figure 3.22**. However, in this experiment under layer was relatively small in size compared to previous tests. Also, the test was performed using a smaller model frame compared to other tests using large underlayer.

### Experience of placing and visual inspection

At the time of placement of units, it was noticed that uniform placement of armour units in a smaller under layer is relatively easy. Also, during the tests it was examined that even though almost all the units could be placed according to their design horizontal spacing but suggested upslope distance was quite short for most of the units. Based on the visual inspection, it is detected that a proper uniform pattern of crablock was achieved in this test, see **Figure 3.23**. To cite an example, units indicated by the red dots in the following picture reveals that all the units in that specific vertical line have same orientation and also position of almost all the units are in the line. Moreover, it is also identified that all the armour units are attached with neighbouring units which ensures good interlocking of armour layer.

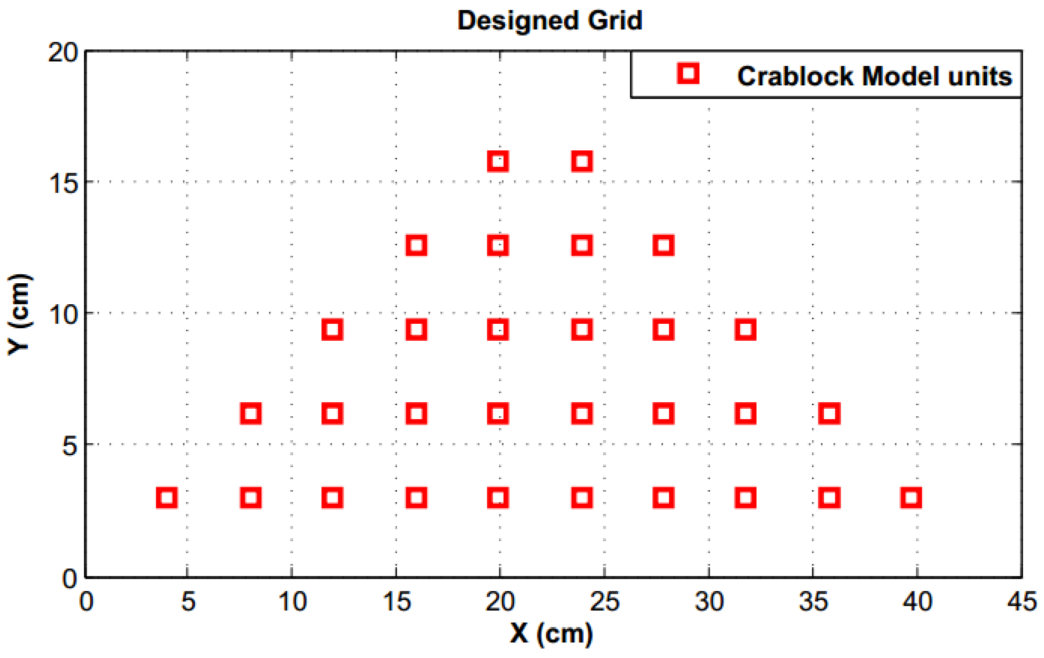


**Figure 3.22** Plan of designed rectangular grid with uniform placement ($D_x = 0.71D$, $D_y = 0.57D$ and $PD = 0.71/D_n^2$)

**Figure 3.23** Picture of placement test number one in test series twelve (Test 12.1)

### Conclusion

Overall, this placement test proved that uniform placement pattern of crablock armour units can be achieved with the use of relatively smaller under layer. As no loose units were observed at the placement test, good interlocking armour is practicable with this designed grid. Thus, it is possible to place the crablock armour units in real situations with the use of data from this test. Therefore, in order to achieve an armour layer with regularly placed crablock units this designed grid with lighter underlayer is suggested to use.

### 3.3.13. Test 13: Rectangular grid with uniform placement (Designed PD = $0.74/D_n^2$)

**Description**

The objective of the test was to investigate the crablock capability of placing as regularly oriented armour units in a smaller under layer. The rectangular grid set up was comprised of same horizontal and upslope spacing as used in the placement test series two and nine, $0.65 \times D$ and $0.60 \times D$. The resulting designed rectangular grid is printed in **Figure 3.24**.

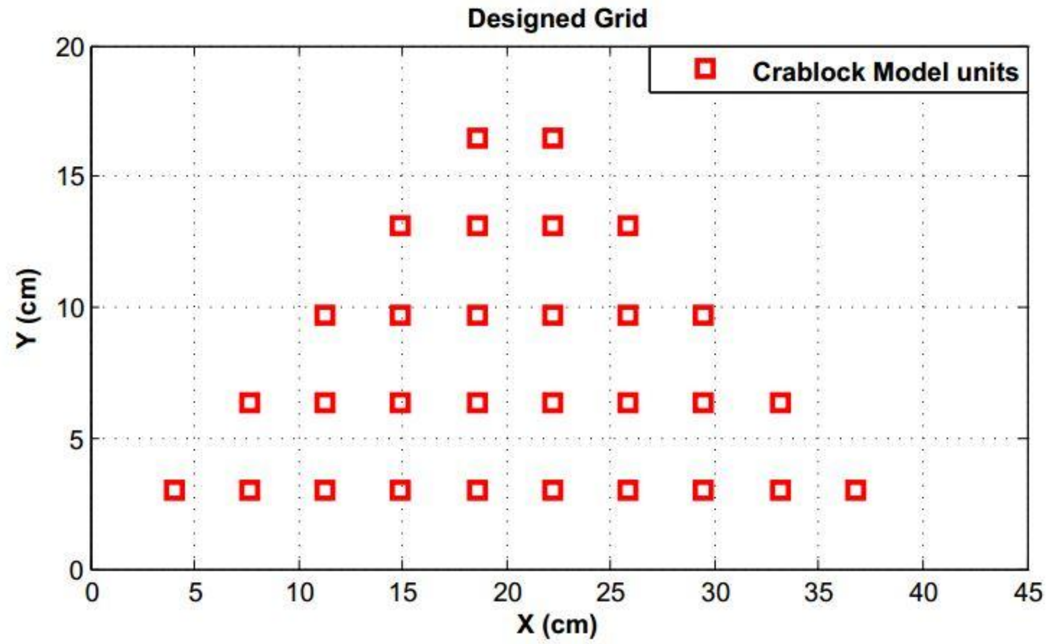


**Figure 3.24** Plan of designed rectangular grid with uniform placement ($D_x = 0.65D$, $D_y = 0.60D$ and $PD = 0.74/D_n^2$)

**Experience of placing and visual inspection**

**Figure 3.25** Picture of placement test number three in test series thirteen (Test 13.3)

The resulting armour layer of the third placement test in test series thirteen (Test 13.3) is presented in **Figure 3.25**. By the visual observation, it is seen that the placement of crablock using tiny underlayer certainly produces a proper uniform pattern. The term proper regular pattern is certainly used as no single unit observed in this test with random orientation. Moreover, it is also inspected that all the units are highly interlocked with adjoining units that means no gaps were identified in the armour layer. Indeed, this highly interlocked armour layer reduces the risk of settlement of armour layer. From the experience of placing and from **Figure 3.25**, it is believed that the accuracy of the placement in this test is quite high and reachable in the reality.

### Conclusion

In conclusion, the interlocking capacity of armour layer using this designed grid is undoubtedly better than any other considered rectangular grid. In addition, the quality of the placement in this placement test is also considerably more excellent than other placement tests. In particular, a good uniform placement pattern of crablock can be achieved with the use of smaller under layer in combination with this premeditated grid. Hence, this placement grid together with tiny underlayer is highly recommended for the placements of crablock with the intention of obtaining a proper regular pattern.

### 3.3.14. Test 14: Rectangular grid with uniform placement (Designed PD = $0.59/D_n^2$)

### Introduction

This test was performed to study the placement of crablock in a wide rectangular grid in combination with relatively smaller underlayer. The test had the similar set up of the placement test three and ten, except the model had a tiny under layer. The planned rectangular grid was comprised of horizontal spacing of 0.75 D and upslope spacing of 0.65 D is shown in **Figure 3.26**.

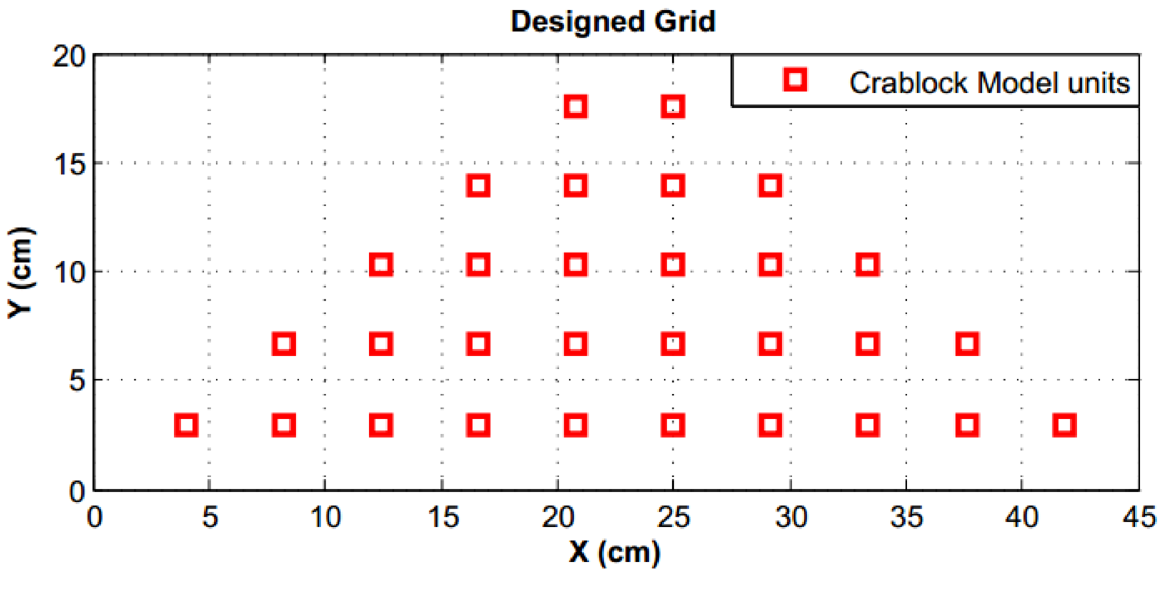


**Figure 3.26** Plan of designed rectangular grid with uniform placement ($D_x$ = 0.75D, $D_y$ = 0.65D and PD = $0.59/D_n^2$)

### Experience of placing and visual inspection

The placement pattern of crablock armour units in this planned grid can be described visually from the image presented in **Figure 3.27**. Based on the visual inspection, it is clearly monitored that this designed grid is relatively large to place the crablock units regularly. Therefore, small gaps between the armour units were observed in the armour layer; see an example in **Figure 3.27**. Due to large placement distances the armour units are not really interlocked very tightly with nearby units. However, despite of relatively wide grid the visual observation says that the uniform pattern of crablock armour layer is achievable in this designed grid.


**Figure 3.27** Picture of placement test number three in test series fourteen (Test 14.3)

**Conclusion**

In summary, as the armour units are not heavily attached with adjacent units certainly the hydraulic stability of armour layer is threatened in this grid. However, it might be applied for the application of crablock armour units in a relatively loose placement pattern. In order to ensure about the stability of armour the hydraulic tests should be carried out using this designed grid before using in reality.

## 3.4. Analysis of measurements

The analysis of each individual test has been performed based on the measured position of units for specific test. In order to avoid a bulk of analysis in the report, the analysis of only one test series (Test 13) is described in this section in details. The complete analysis of each individual test series is attached in **Appendix A** and **Appendix B**.

### 3.4.1. Measured position of units

Based on only visual observation, it is hardly possible to identify the misplaced units from the designed grid position. In order to observe the actual position of armour units in placement test number three in test series thirteen (Test 13.3), measured position and designed position of each individual unit is plotted in **Figure 3.28**. From the following graph, it is possible to compare the designed location and actual position of each armour unit easily. In particular, the graph indicates that in this designed grid it is possible to place most of the units according to their designed position. Therefore, the accuracy of the placement in this test is expected quite high and reachable in reality.

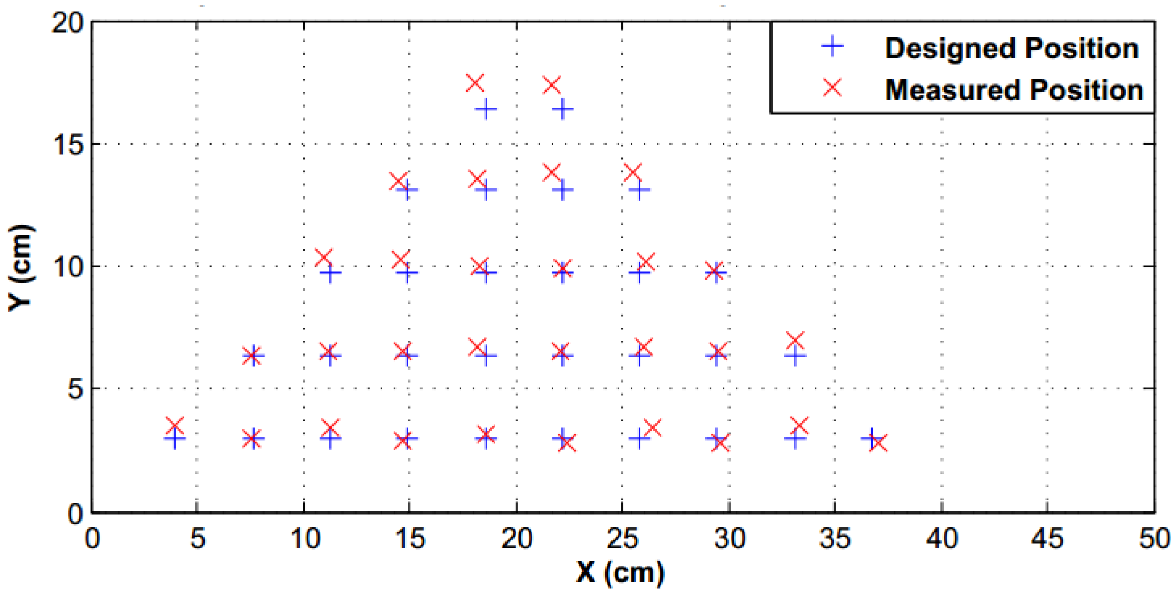


**Figure 3.28** Comparison of measured and designed position of units in Test 13.3

### 3.4.2. Deviation of units from designed position

The average horizontal deviation of units is examined $0.01D$ with a standard deviation of $0.07\,D$ and average upslope deviation of units is determined $-0.07\,D$ with a standard deviation of $0.07\,D$. The deviation of each individual unit from the designed placement grid is printed in **Figure 3.29**. In this experiment, relatively small deviation of units (see **section 3.5.2**) has been observed which indicates that this designed grid is also applicable in prototype situation.

### 3.4.3. Horizontal and upslope placement distance

The main reason for the variation of measured placement distances from the designed placement distances is the deviation of units from the designed position. As a result of the deviation of units from its intended position, the actual horizontal and upslope placement distance were also varied from the designed value. The resulting average horizontal placement distance is found $0.66 \times D$ whereas the theoretical distance was $0.65 \times D$. And the upslope placement distance is measured $0.63 \times D$, little bit higher than the designed value of $0.60 \times D$.

### 3.4.4. Packing density

The packing density of individual crablock armour units has been determined using the measured horizontal and upslope distance for each particular unit. The formula used to determine individual packing density is described in **section 2.6** (**Equation 2.13**). Since the measured spacing in horizontal and vertical direction has been varied from the theoretical value therefore calculated packing density also differed from the designed value. In this test, according to the designed grid the possible theoretical packing density is $0.74/D_n^2$ while the measured average packing density has been found $0.68/D_n^2$. Moreover, the average packing density of three repetition tests in terms of height of crablock and units per square meter are also calculated and printed in **Table 3.3**.

**Table 3.3** Packing density of crablock obtained in test series 13

| PD in $D_n$ | PD in D | PD in Units/$m^2$ |
|---|---|---|
| $0.68/D_n^2$ | $2.39/D^2$ | 756 |

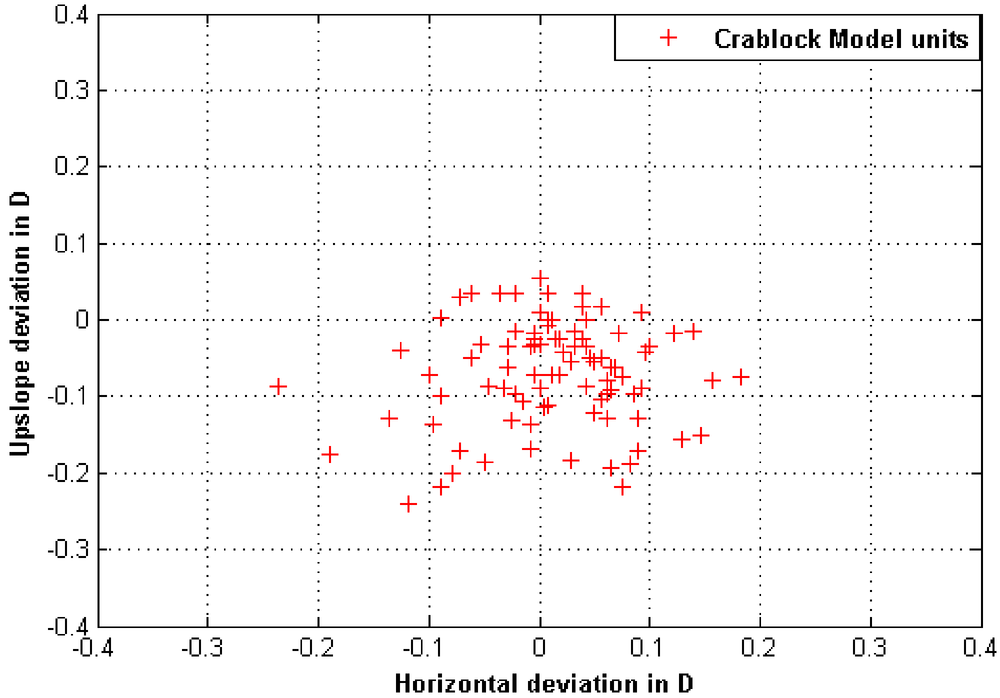


**Figure 3.29** Deviation of units from its intended position

# 3.5. Results and discussions

The outputs of each test series were determined mainly by taking an average of results obtained in three repetition tests. In this section, mainly results of placement tests are presented as a summary to avoid unwanted large report. However, the calculation and graphs for each individual test series are enclosed in **Appendix B**.

## 3.5.1. Visual observation

The placement pattern of armour layer is mainly remarked by the visual inspection of armour units. Also, the accuracy of the placement can be little bit assumed by observing the armour layer visually. For each individual dry placement test, armour layer was inspected visually to describe the placement of crablock for that specific test. The different placement patterns in a designed grid for different tests can be compared regarding to the visual inspection. For example, the following observations are made about the placement of crablock by comparing the tests regarding to visual observation.

- To scrutinize the placement pattern of crablock in a rectangular grid, **Figure 3.5**, **Figure 3.18** and **Figure 3.23** are compared based on visual inspection. All the three test series (Test1, Test8 and Tes12) were performed with the same designed horizontal and upslope placement distance. However, it was observed that small underlayer (Test 12) certainly provides better uniform placement in comparison to conventional underlayer (Test 1) in a same designed rectangular grid. Also, it was noticed from the mentioned figures that regular pattern (**Figure 3.5** & **Figure 3.23**) looks more interlocked compared to a random pattern (**Figure 3.18**).

- **Figure 3.15** (Test 6) and **Figure 3.21** (Test 11) can be compared to describe the placement pattern of crablock in a diamond-shaped grid. It is worth mentioning that both test 6 and test 11 were performed with the use of same configuration except different placement pattern. From the comparison of **Figure 3.15** and **Figure 3.21**, it was detected that more interlocking of units can be obtained with random orientation of units (Test 11) compared to uniform pattern (Test 6).

Furthermore, in order to get a complete view, visual inspection of all the tests are printed in **Table 3.4**. From the following table, it can be realized that designed uniform placement pattern could not be achieved for all cases. Also, a lot of loose units were observed for some tests which are not allowable in real situation.

**Table 3.4** Summary of visual inspection observed in all test series

| Test Series No | Placement Grid | Designed hor. dis. (D) | Designed up. dis. (D) | Designed Placement Pattern | Obtained Placement Pattern | Observation |
|---|---|---|---|---|---|---|
| 1 | Rectangular | 0.71 D | 0.57 D | Uniform | Not 100% Uniform | interlocked |
| 2 | Rectangular | 0.65 D | 0.60 D | Uniform | Not 100% Uniform | good interlocked |
| 3 | Rectangular | 0.75 D | 0.65 D | Uniform | Not 100% Uniform | loose units |
| 4 | Rectangular | 0.80 D | 0.60 D | Uniform | Not 100% Uniform | lot of loose units |
| 5 | Diamond | 0.60 D | 050 D | Uniform | Random | lot of loose units |
| 6 | Diamond | 0.70 D | 0.60 D | Uniform | Random | interlocked |
| 7 | Diamond | 0.80 D | 0.65 D | Uniform | Random | lot of loose units |
| 8 | Rectangular | 0.71 D | 0.57 D | Random | Random | interlocked |
| 9 | Rectangular | 0.65 D | 0.60 D | Random | Random | interlocked but too narrow |
| 10 | Rectangular | 0.75 D | 0.65 D | Random | Random | loose units |
| 11 | Diamond | 0.70 D | 0.60 D | Random | Random | good interlocked |
| 12 | Rectangular | 0.71 D | 0.57 D | Uniform | Uniform | interlocked |
| 13 | Rectangular | 0.65 D | 0.60 D | Uniform | Uniform | good interlocked |
| 14 | Rectangular | 0.75 D | 0.65 D | Uniform | Uniform | loose units |

### 3.5.2. Accuracy of placement

It seems very difficult to place all the armour units according to their designed position without any deviation. Due to the misplacement of units at the time of placement tests, some of the units deviated from the planned grid location. However, the accuracy of the placement is possible to predict by determining the average deviation of units from the designed grid position. Based on the measured position of units, the deviation of each individual unit can be determined. In this research, the average deviation of units in together with standard deviation has been determined for all the placement test series, see **Table 3.5**. The accuracy of the placement differed with different grids and also with different orientation of units. It should be noted that fixation of the first layer (may be by dedicated toe design) is very important for the accuracy in placement. However, in this research due to the difficulties in placement of units at toe with large underlayer and with existing model units, all the tests with conventional underlayer were performed without fixation of first row (both in rotation and location).

In order to compare the accuracy of the placement in different test series, only average total deviation of units observed in individual test series is plotted in **Figure 3.30**. Note that average total standard deviation is not provided in **Figure 3.30**, see **Table 3.5**. From **Figure 3.30**, it is inspected that in general the accuracy of placement in a rectangular grid with uniform placed crablock is larger than the rectangular grid with randomly placed crablock units. For example, the average total deviation of units in Test 2 is calculated as 0.1D which is much smaller than the average total deviation of units 0.26D found in Test 8. However, the different scenario is examined for the diamond shaped grid. For instance, the total average deviations of units monitored in Test 5, 6 & 7 with uniform placement are greater than the total average deviations of units forecasted in Test 11 with random placement, see **Figure 3.5**. Based on **Figure 3.30**, it is also remarkable that regular placement of units can be done more accurately using a relatively smaller under layer, such as deviation of units measured in Test 1 to 4 are larger than the deviation of units observed in the Test 12 to 14 using relatively smaller under layer.

**Table 3.5** Summary of deviation of units observed in all test series

| Test Series No | Avg. Dev. of X (D) | Std. Dev. of X (D) | Avg. Dev. of Y (D) | Std. Dev. of Y (D) | Total Avg. Dev. (D) | Total Std. Dev. (D) |
|---|---|---|---|---|---|---|
| 1 | 0.11 | 0.14 | -0.13 | 0.12 | 0.21 | 0.14 |
| 2 | -0.01 | 0.07 | -0.07 | 0.08 | 0.1 | 0.07 |
| 3 | -0.003 | 0.15 | -0.14 | 0.14 | 0.22 | 0.11 |
| 4 | 0.05 | 0.16 | 0.03 | 0.24 | 0.25 | 0.16 |
| 5 | -0.78 | 0.48 | -0.67 | 0.43 | 1.11 | 0.5 |
| 6 | -0.12 | 0.25 | -0.12 | 0.23 | 0.34 | 0.17 |
| 7 | 0.22 | 0.19 | -0.09 | 0.18 | 0.32 | 0.17 |
| 8 | 0.01 | 0.18 | -0.19 | 0.14 | 0.26 | 0.14 |
| 9 | -0.03 | 0.1 | -0.08 | 0.1 | 0.14 | 0.09 |
| 10 | 0.1 | 0.17 | -0.13 | 0.11 | 0.23 | 0.11 |
| 11 | -0.15 | 0.17 | -0.2 | 0.15 | 0.3 | 0.15 |
| 12 | 0.04 | 0.05 | -0.14 | 0.11 | 0.16 | 0.11 |
| 13 | 0.01 | 0.07 | -0.07 | 0.07 | 0.1 | 0.06 |
| 14 | -0.01 | 0.05 | -0.07 | 0.08 | 0.1 | 0.06 |

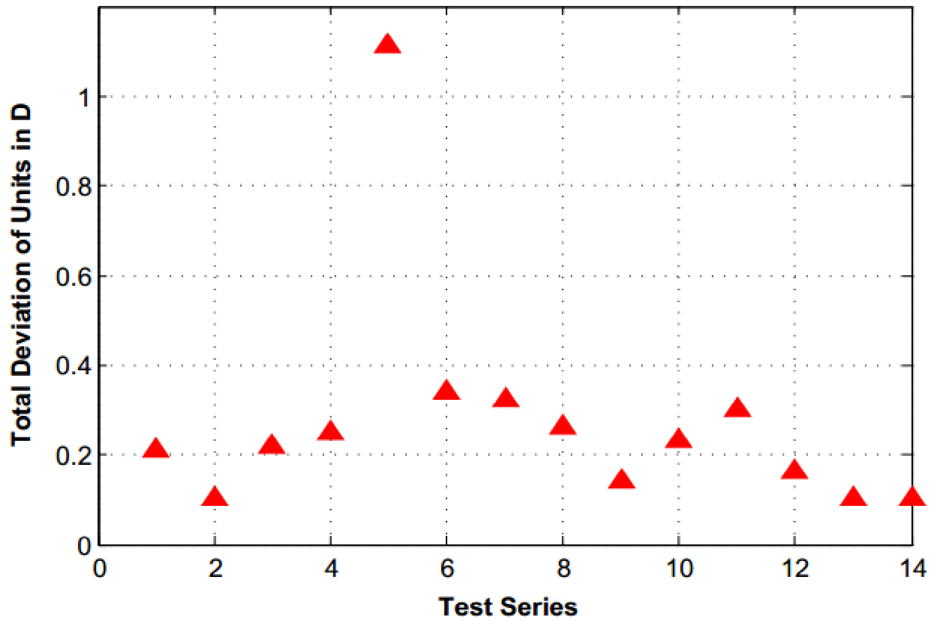


**Figure 3.30** Average total deviation of units from its intended position (without standard deviation)

### 3.5.3. Packing density

The average packing density for each particular test was determined by taking mean of local packing density of each particular unit regarding to the calculated horizontal and upslope placement distance. Because of the deviation of units the measured horizontal and upslope placement distance have been also diverged from the theoretically predicted value. As a consequence the calculated packing density also differed from the designed value.

In **Table 3.6**, packing density measured in different test series are printed alongside designed value. Also, the measured and designed placement distances are listed here. Further, **Figure 3.31** shows a comparison between the nominal packing density designed and measured in each individual test series. The test results (**Figure 3.31** and **Table 3.6**) showed that in both diamond-shaped and rectangular grid, measured packing density was lower for the randomly oriented armour in comparison to uniformly oriented crablock armour. Moreover, from the test results it is seen that lower packing density of crablock was obtained with the use of a diamond-shaped grid. It also looks that the upslope placement distance is often around 0.63D, see in **Table 3.6**.

**Table 3.6** Summary of measured packing density in all test series

| Test Series No | Designed Hor. Placement Dis. | Measured Hor. Placement Dis. | Designed Up. Placement Dis. | Measured Up. Placement Dis. | Designed Packing Density | Measured Packing Density |
|---|---|---|---|---|---|---|
| 1 | 0.71 D | 0.69 D | 0.57 D | 0.64 D | $0.71/D_n^2$ | $0.65/D_n^2$ |
| 2 | 0.65 D | 0.65 D | 0.60 D | 0.63 D | $0.74/D_n^2$ | $0.71/D_n^2$ |
| 3 | 0.75 D | 0.76 D | 0.65 D | 0.64 D | $0.59/D_n^2$ | $0.59/D_n^2$ |
| 4 | 0.80 D | 0.79 D | 0.60 D | 0.70 D | $0.60/D_n^2$ | $0.52/D_n^2$ |
| 5 | 0.60 D | 0.83 D | 0.50 D | 0.64 D | $0.96/D_n^2$ | $0.54/D_n^2$ |
| 6 | 0.70 D | 0.76 D | 0.60 D | 0.61 D | $0.68/D_n^2$ | $0.62/D_n^2$ |
| 7 | 0.80 D | 0.82 D | 0.65 D | 0.61 D | $0.55/D_n^2$ | $0.58/D_n^2$ |
| 8 | 0.71 D | 0.71 D | 0.57 D | 0.64 D | $0.71/D_n^2$ | $0.63/D_n^2$ |
| 9 | 0.65 D | 0.66 D | 0.60 D | 0.64 D | $0.74/D_n^2$ | $0.67/D_n^2$ |
| 10 | 0.75 D | 0.74 D | 0.65 D | 0.67 D | $0.59/D_n^2$ | $0.58/D_n^2$ |
| 11 | 0.70 D | 0.75 D | 0.60 D | 0.63 D | $0.68/D_n^2$ | $0.61/D_n^2$ |
| 12 | 0.71 D | 0.71 D | 0.57 D | 0.64 D | $0.71/D_n^2$ | $0.63/D_n^2$ |
| 13 | 0.65 D | 0.66 D | 0.60 D | 0.63 D | $0.74/D_n^2$ | $0.68/D_n^2$ |
| 14 | 0.75 D | 0.75 D | 0.65 D | 0.66 D | $0.59/D_n^2$ | $0.58/D_n^2$ |

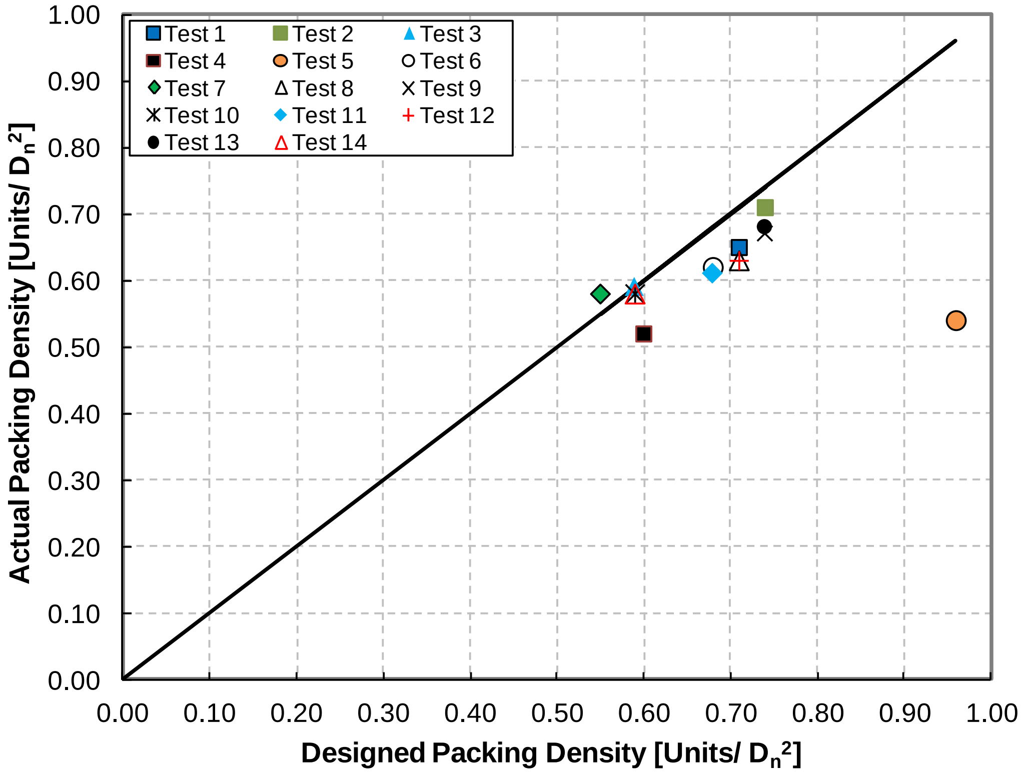


**Figure 3.31** Designed nominal packing density against measured nominal packing density

# CHAPTER 4

# Experimental 2D Flume Test Set-Up

**This chapter introduces the reader to the laboratory set up of flume tests to investigate the hydraulic stability and overtopping over crablock slopes. The first section interprets shortly the term scaling used in this experimental thesis. Section 4.2 describes the testing equipments used in this research to perform the flume tests. Section 4.3 examines the test set up of the performed 2D wave flume tests defining the cross-section of model breakwater, water depth etc. Further section 4.4 and 4.5 discuss about the materials used and wave conditions applied to perform the tests. Section 4.6 presents the test programme followed to conduct all the flume tests. In addition, the way of constructing model and way of performing all the tests are also presented in the final section.**

## 4.1. Scaling

The hydraulic tests performed in this research were not based on any prototype model that needs to be tested. Therefore, the parameters used in the experiments were not really scaled to present prototype situation in reality. The core objective of this experimental study was to observe the placement pattern and wave overtopping of crablock. The small scale tests performed in this thesis with the use of available crablock model units provided by AM Marine Works Ltd and CDR International Limited. The model crablock units were made by CSIR (2009) in a scale of 1:60 representing 15 ton prototype units. However, that does not indicate the scale of this experiment. The dimensions of the model breakwater, properties of other materials and designed wave conditions were determined with considering model crablock units.

## 4.2. Testing equipments

In this research, small scale hydraulic model tests were performed to examine the hydraulic stability of crablock armour units. All the tests were conducted at the Fluid Mechanics Laboratory of Delft University of Technology. An overview of different equipment with individual purpose used in the laboratory is listed in **Table 4.1**.

**Table 4.1** Equipments for conducting flume tests

| Equipment | Purpose |
|---|---|
| 2D Wave Flume | To do hydraulic model tests |
| Wave generator | To generate waves |
| Wave Reflection Compensator | To compensate reflected waves |
| Wave gauges | To measure wave heights |
| Cameras | To observe the damage development |
| Video Recorder | To record video during the hydraulic tests |
| Overtopping box | To measure the volume of overtopping |

### 4.2.1. Wave flume

A 2D wave flume of the Fluid Mechanics Laboratory of the Faculty of Civil Engineering and Geosciences at Delft University of Technology was used for conducting all the small scale hydraulic tests. The 2D wave flume has a length of approximately 45 m, a width of 0.90 m and a depth of 1.0 m. However, the maximum water depth was restricted to 0.90 m in order to prevent the waves overtopping over the sidewalls of the flume. The sidewalls of the flume are made of glass. **Figure 4.1** shows the image of wave flume used to perform the hydraulic tests. A wave board is attached with the wave flume to generate regular as well as random waves. Furthermore, an active reflection compensation system is equipped with the wave generator to compensate reflected waves from structure. The wave reflection compensator ensures the desired waves in the flume without the effect of reflection. Moreover, in order to dissipate wave energy a wave dissipative slope is available at the end of the flume.

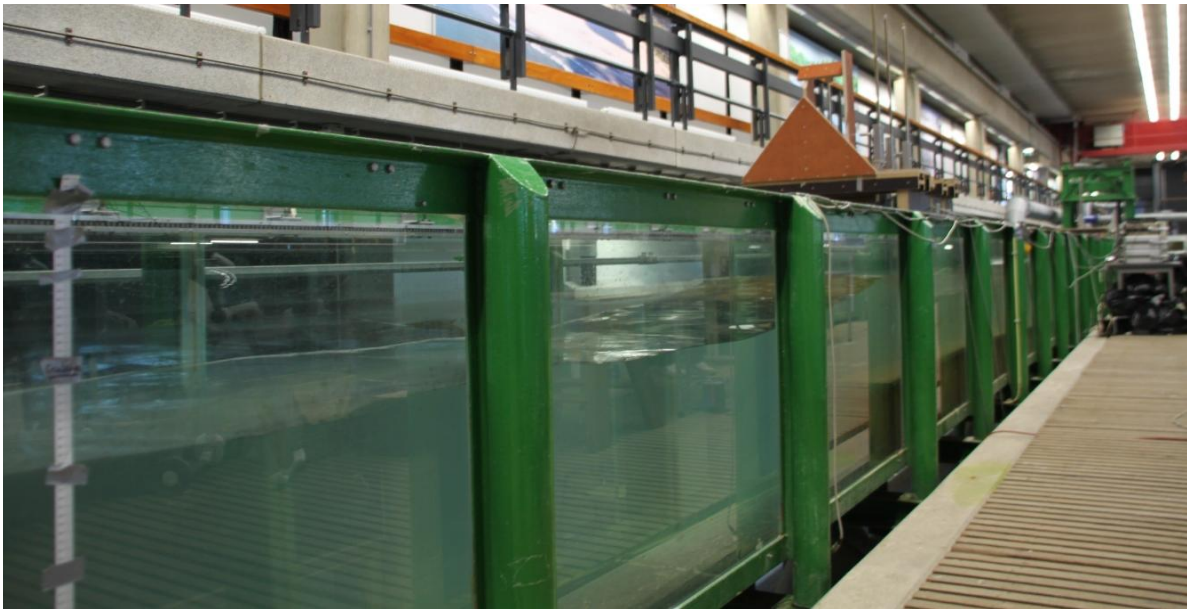

**Figure 4.1** Picture of wave flume

### 4.2.2. Wave gauges

In this experimental research, wave heights were measured with the use of wave gauges in the flume. Eight wave gauges were used in the wave flume tests. The distribution of wave gauges is presented in **Figure 4.3**. One set of wave gauges with three gauges (number 4, 5 and 6) was positioned at the horizontal length of 2m close to the structure in order to determine the wave heights at structure. The first wave gauge was set up as following the approach by Klopman and Van Der Meer (1999). They investigated that the minimum distance of placement of first wave gauge from the intersection of still water line (SWL) and breakwater should be 0.4 times of wave length in order to avoid the influence of structure on significant wave height of incident waves. Based on this knowledge the first wave gauge was placed at 1.4 m from the intersection of SWL and breakwater. Then the next two wave gauges of the group were determined regarding to the approach by Mansard and Funke (1980). This allows splitting the reflected and incoming waves with the use of least square method. The second wave gauge of the group has been set at a distance of 0.40 m from first one. And the third wave gauge at the structure was placed at 0.70 m from the first wave gauge of this series. Furthermore, in order to measure the wave heights at deep water another wave group of three wave gauges (number 1, 2 and 3) have been placed far from the structure at water depth of 0.68 m. The spacing between the wave gauges were kept as same as the group of wave gauges at the structure. The distance of the set of wave gauges at deep water from the set at structure was kept as 15 m. Also, to measure the number of overtopping waves one wave gauge was sited at the crest of the breakwater (number 7). In order to measure the water level of the overtopping box, one water level measuring instrument (number 8) was put in the overtopping box; see **Figure 4.3**.

### 4.2.3. Other equipments

In addition to wave gauges at different locations, an overtopping box was also placed on the rear side of the structure. The purpose of overtopping box was to measure the volume of overtopping water over crablock armour slope. The dimension of the overtopping box was determined based on the volume of overtopping discharge. In that case volume of mean overtopping rate has been measured by using empirical relations, see details in **section 4.3.5**. Furthermore, pictures were captured with the use of cameras at fixed position before and after each experiment. The photographs have been taken to analyze the settlement of the armour slope and damage development of armour layer. In addition to cameras, video recorder was also used for each test to record the video of the armour layer. The reason for providing video recorder was to check the progress of test later.

## 4.3. Model set-up

The set up of cross-section has been done by considering the small scale set up of accropode (Van der Meer, 1987b), set up of xbloc (DMC, 2003) and set up of CLASH by Bruce, et al. (2009) for rubble mound breakwaters with various types of armour units. Because of this, results may be compared with first results from the CLASH (2004) and xbloc concrete units.

### 4.3.1. Cross-section and slope

In this study, three cross-sections were used to perform small scale hydraulic tests in the wave flume. The rubble mound breakwater scale model consists of single layer crablock armour units, an underlayer, core, stone protection at the toe and a crest wall. The typical slope of the single layer concrete armour is 1 in 1.5 or 1 in 4/3. In this research, the slope of crablock armour has been kept as 1:4/3 similar to accropode, core-loc and xbloc in their initial model testing to define design parameters.

### 4.3.2. Crest freeboard

The crest freeboard in the design of the cross-section has been selected based on the small scale tests on other single layer units. Bruce, et al. (2009) considered a freeboard as 1.3 times the design significant wave height, considering small overtopping and 0.8 times of design significant wave height for quite some overtopping in the small scale tests using different armour units. Van der Meer (1987b) investigated that with the use of a crest freeboard of 1.33 times the significant wave height, the overtopping of waves can be restricted to only 5 to 10%. The ratio between crest freeboard and significant wave height were varied between 1.1 and 1.9 for the 2D hydraulic tests on Xbloc armour (DMC, 2003). Based on the knowledge from these three experiments, the ratio between crest freeboard and design significant wave height was fixed as 1.2 in this study allowing some waves overtopping. This design significant wave height was based on an assumed stability number around 2.8. This means that wave overtopping will be a lot more for significant wave heights higher than the design significant wave height. In this experimental research, significant wave heights higher than the design significant wave heights were tested to observe the failure of armour layer, therefore large overtopping for high wave heights can be expected.

Furthermore, in order to investigate the wave overtopping behavior with higher crest freeboard, a relative high crest height of 1.6 times the design wave height was also used in this research.

### 4.3.3. Crest wall

The crest wall has been designed to ensure the stability of the structure following the approach used by DMC (2003) and Bruce, et al. (2009). The width of the crest was considered as 3.5 times the nominal diameter of crablock model unit. A crest element of plywood was attached to the sidewalls of the wave flume in order to keep the concrete unit elements in place.

### 4.3.4. Foreshore and water depth

A sloping foreshore has been considered in front of a horizontal foreshore with a uniform slope of 1:30. The reason for using this sloping foreshore is to be able to generate depth limited wave heights. The length of sloping foreshore is 10 m starting from the bottom of the flume up to depth 0.33 m above the bottom. In addition to slopping foreshore, a horizontal length of 2 m before toe structure has been provided in order to measure wave heights accurately by a series of wave gauges.

The design stability number for crablock has been assumed initially as 2.8, equal to xbloc, core-loc and accropode II in order to define the design significant wave height

The design wave height can be estimated from the known stability number following the approach used by Bruce, et al. (2009), see **Equation 4.1**. For the crablock armour unit the design wave height is estimated as following,

$$\mathrm{H_0} = \text{Design stability no.} \times (\text{relative density} \times \text{nominal diameter}) \qquad (4.1)$$

Thus, design wave height, $\mathrm{H_0} = 2.8 \times (1.36 \times 0.03) = 0.114\ \mathrm{m}$

The ratio between water depth at the structure and significant wave height were considered from 2 to 3 for the performance of small scale hydraulic tests using accropode (Van der Meer, 1987b). In that research, only one water depth 0.40 m at the structure was used for all the tests. However, by 2003 DMC performed the small scale flume tests on xbloc armour slope with the use of water depth 0.35 m and 0.40 m at structure. Bruce, et al. (2009) defined a standard cross-section for measuring waves overtopping over rubble mound structures considering water depth at structure as 2.5 times and 3.0 times of design wave height. Nevertheless, the foreshore slope used for that research was a simple horizontal one without any slope. Based on the understanding of discussed research and available capacities of wave flume the water depth at structure has been considered as 0.35 m that means approximately 3.0 times of design wave height. In order to have water depth 0.35 m at the structure, the water depth at deep water was kept 0.68 m for all the tests. For most of the tests (test series 1 to 8), the ratio of water depth before the toe and water depth upon the toe has been fixed to 0.80, resulting in a water depth of 0.28 m upon toe of the model breakwater.

### 4.3.5. Dimension of overtopping box

The volume of overtopped waves over the crablock armour slope can be estimated using empirical equations prescribed in EurOtop (2007). The main aim of this preliminary prediction was to design the overtopping box to capture the volume of overtopped water. The wave heights used here to estimate overtopping by empirical formulas were the assumed significant wave height ($\mathrm{H_{m0}}$) at toe of the breakwater. It should be noted that in order to estimate largest overtopping volumes, a lower crest height $\mathrm{R_c} = 0.14\ \mathrm{m}$ was used in the empirical formula.

As discussed earlier, the crablock model unit has only been developed recently and no previous research has been performed on the wave overtopping over a crablock slope. As a consequence in EurOtop (2007), the influence factor ($\gamma_f$) of crablock still does not exist, see **Table 2.1**. Nevertheless, the prediction of mean wave overtopping over crablock slopes can be done by assuming the influence factor ($\gamma_f$) of xbloc, accropode or core-loc. The shape of crablock has a similarity with six legs xbloc. Therefore, in this research influence factor ($\gamma_f$) of xbloc has been used initially to estimate the average overtopping rate.

In the approximation of mean wave overtopping discharge, the probabilistic design formula with maximum value has been used, see **Equation 2.5**. The average overtopping discharge is calculated for the designed wave conditions of the flume tests to keep in line with the physical models. The mean overtopping rate (q) together with designed parameters is listed in **Table 4.2** considering the roughness of xbloc.

**Table 4.2** Mean overtopping discharge by empirical methods ($\gamma_f$ of xbloc)

| $H_{m0}$ (m) at toe | 0.06 | 0.08 | 0.1 | 0.12 | 0.14 | 0.16 | 0.18 | 0.2 |
|---|---|---|---|---|---|---|---|---|
| $R_c$ (m) | 0.14 | 0.14 | 0.14 | 0.14 | 0.14 | 0.14 | 0.14 | 0.14 |
| $\gamma_f$ | 0.45 | 0.45 | 0.45 | 0.45 | 0.45 | 0.45 | 0.45 | 0.45 |
| $\gamma_\beta$ | 1 | 1 | 1 | 1 | 1 | 1 | 1 | 1 |
| g (m/s$^2$) | 9.81 | 9.81 | 9.81 | 9.81 | 9.81 | 9.81 | 9.81 | 9.81 |
| q (m$^3$/s per m) | 1.3E-08 | 5.8E-07 | 6.1E-06 | 3.1E-05 | 1.0E-04 | 2.6E-04 | 5.3E-04 | 9.8E-04 |
| q (l/s per m) | 1.3E-05 | 0.00058 | 0.00608 | 0.030773 | 0.101578 | 0.25553 | 0.53472 | 0.98159 |
| $R_c/H_{m0}$ | 2.33 | 1.75 | 1.40 | 1.17 | 1.00 | 0.88 | 0.78 | 0.70 |

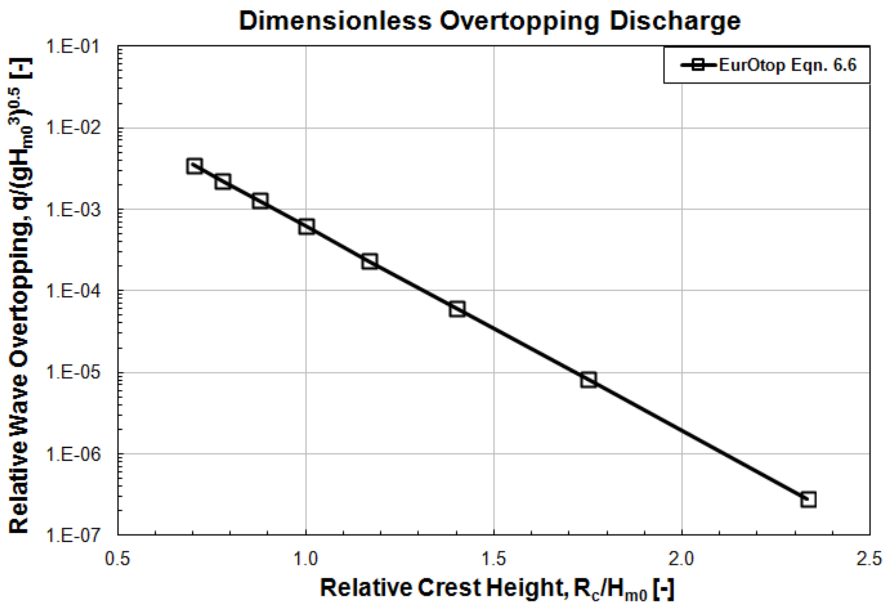


**Figure 4.2** Relation between mean overtopping discharge and relative freeboard ($\gamma_f$ of xbloc)

In **Figure 4.2**, a relation between mean overtopping discharge q (l/s per m) and relative freeboard ($R = R_c/H_{m0}$) is presented. The volume of overtopping waves can be found by using the relationship expressed in **Figure 4.2**. Furthermore, from the graph it is observed that largest mean wave overtopping rate is close to 1 l/s per m that mean 2 m$^3$ in volume for half an hour. In order to measure the volume of overtopping waves, dimension of overtopping box was determined regarding to the calculated largest mean wave overtopping discharge. Since the expected overtopping volume was quite large for highest waves, a chute (10 cm width) was provided from the crest wall to the overtopping box in order to only capture a limited amount of overtopping waves. Regarding to the estimated overtopped volume of water for highest waves, one overtopping box of 80 cm in length, 61 cm in width and 40 cm in height was designed for the flume tests. In addition to this, for the tests with smaller waves another, little overtopping box was also constructed.

**Figure 4.4**, **Figure 4.5** and **Figure 4.6** show the cross-sections of designed model breakwater for conducting flume tests.

## 4.4. Materials configuration

The armour layer of the tested cross section consisted of crablock units as one layer system. Both uniform and random orientations of units were considered for the tests. Similar to placement tests, the crablock armour unit had a mass of 0.0637 kg with a mass density of 2364 kg/m3. The resulting nominal diameter was around 0.030 m with the unit height of 0.056 m. For small scale hydraulic tests on Accropode the thickness of armour layer was used as 0.9 times of accropode model unit by (Van der Meer, 1987b). However, DMC (2003) used the thickness of armour layer on around 0.96 times of the model of Xbloc unit. In this experiment, the thickness of the crablock armour layer was primarily assumed as 0.056 m, equal to the height of the model unit. Nevertheless, this then followed from the model tests by measurements, as this is a different unit.

As under layer of armour layer, stones were provided as underlying materials. Following general rules for similar armour units, the weight of the under layer stones should be in the range of one-seventh to one-fifteenth of the weight of the armour units (Van der Meer, 1987b). Further, SPM (1984) proposed that the mass of under layer stones should be in a range of one-tenth to one-fifteenth of mass of the armour units. However, Bruce, et al. (2009) proposed the weight of the under layer stones in a range of one-fifth to one-fifteenth of weight of armour units. In this experimental research, under layer of one-tenth of crablock armour unit was considered for the model breakwater. The mass of crablock model unit was 0.0637 kg thus the mass of stone in under layer was considered around 0.00637 kg. That means the mass of rock unit in under layer with the factor of 3 grading was kept in the range of 0.003-0.009 kg Based on the placement tests also another smaller underlayer was prepared to be used in the flume tests, having a mass in the range of 0.001-0.004 kg.

A wide graded core was considered for the flume tests. The core of the breakwater comprised of stone materials of size 7 mm to 11 mm. In order to reduce scaling affects by ensuring turbulent flow, the core was dimensioned more than 6 mm in size. Failure of the toe structure might influence the stability of armour layer (DMC, 2003). Therefore, in this experiment toe was over-dimensioned to avoid this effect. The properties of various materials were used for flume tests are listed in **Table 4.3**.

**Table 4.3** Properties of various materials for flume tests

| Location | Layer thick-ness [mm] | Materials | Mass [gm] | Sizes [mm] | Mass density [kg/m$^3$] |
|---|---|---|---|---|---|
| One layer crablock armour | 56 | Concrete | 63.7 | 56 | 2364 |
| Under layer1 | 28 | Stone | 3.0-9.0 | 11-16.0 | 2650 |
| Under layer2 | 28 | Stone | 1.0-4 | 7.0-11.0 | 2650 |
| Core | - | Stone | - | 7.0-11.0 | 2650 |
| Toe protection | 70 | Stone | 40-160 | 25.0-40.0 | 2650 |

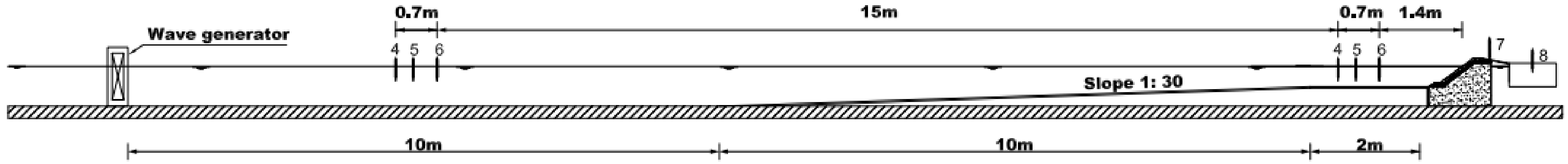


**Figure 4.3** Position of wave gauges in the flume

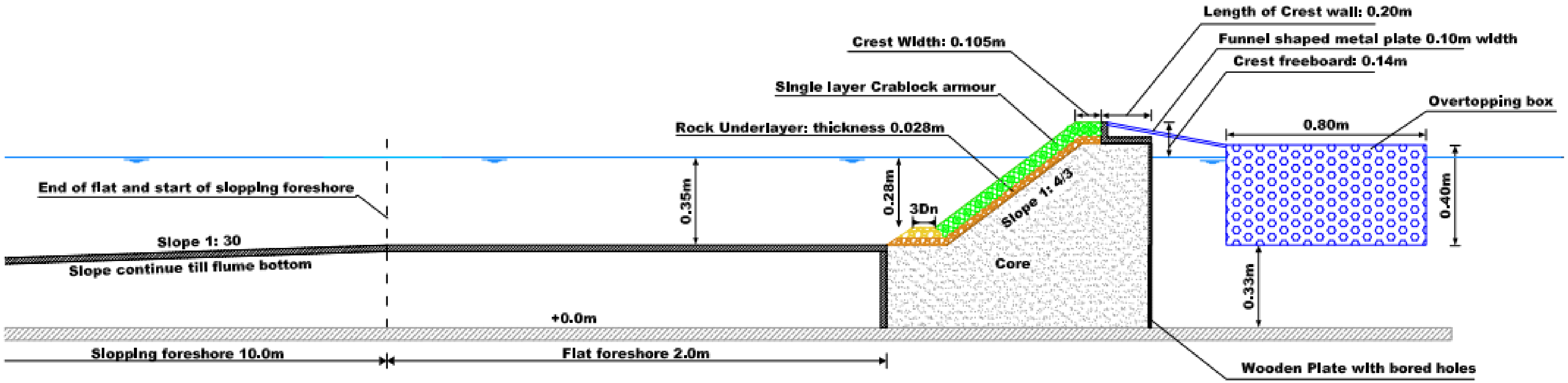


**Figure 4.4** Cross-section of model breakwater with crablock armour slope ($R_c$= 1.2 X Design wave height); tests 1-8

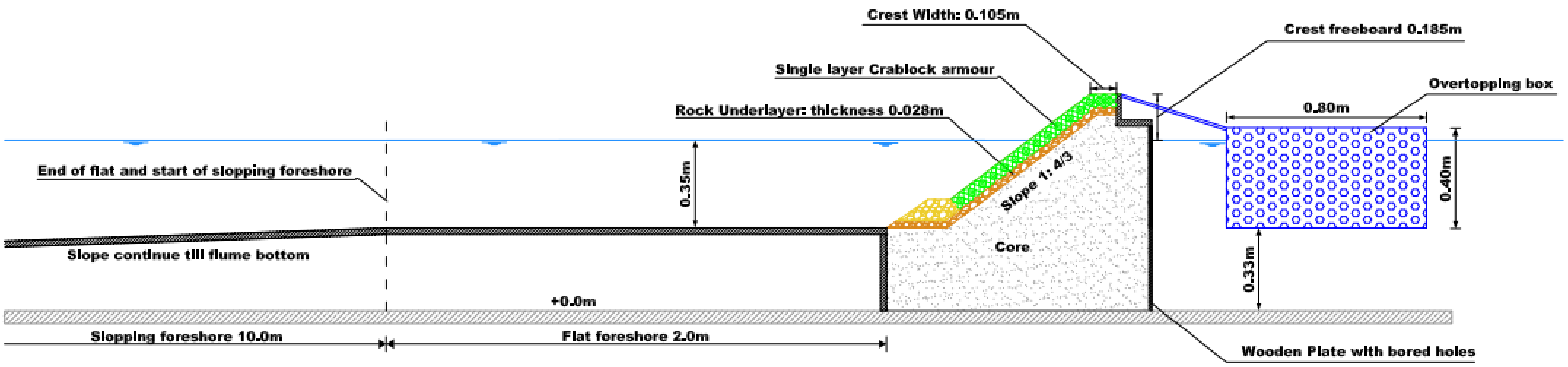


**Figure 4.5** Cross-section of model breakwater with crablock armour slope ($R_c$= 1.6 X Design wave height); tests 9-10

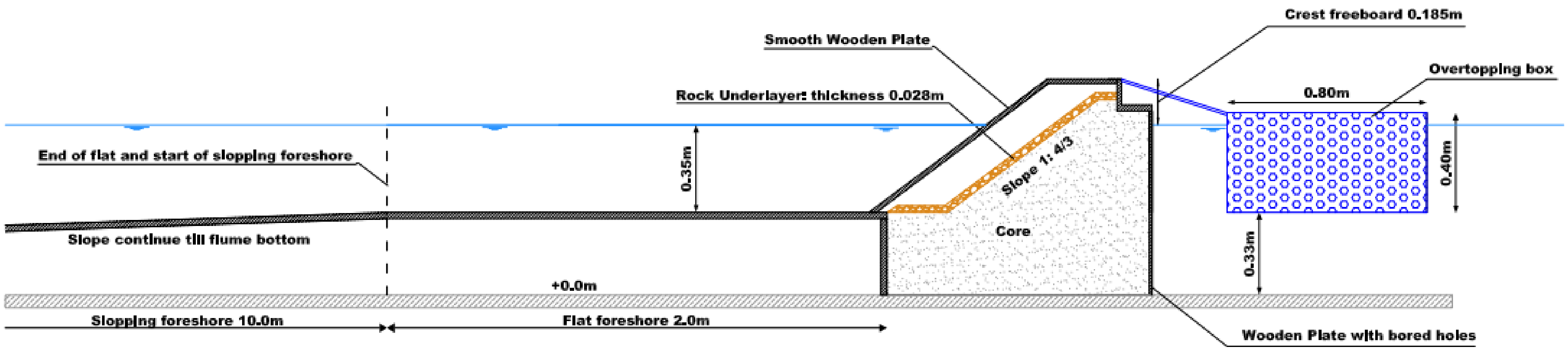


**Figure 4.6** Cross-section of model breakwater with smooth slope ($R_c$= 1.6 X Design wave height); tests11-12

## 4.5. Wave conditions

In order to perform the tests in a systematic way, testing wave conditions have been generated for all the different test series. Bruce, et al. (2009) determined the overtopping of waves over the different armour slopes of the rubble mound breakwater with the use of three wave steepnesses, $s_{op}$= 0.02; 0.035 and 0.05 in order to input in the CLASH database and to predict the wave overtopping through the application of neural network. In that research, $s_{op}$ was defined by nominal wave steepness derived from $s_{op} = (2\pi H_0/gT_p^2)$ in which $T_p$= spectral peak wave period and $H_0$= design wave height. However, in this research the wave steepness $s_{m-1,0}$ based on $T_{m-1,0}$ was used instead of $s_{op}$. In general, the spectral peak wave period ($T_p$) is 1.1 times of average wave period defined from spectral analysis ($T_{m-1,0}$). That means that wave steepness based on $T_{m-1,0}$ is 1.21 times larger than the nominal wave steepness ($s_{op}$). To cover the range of CLASH database, the following two wave steepnesses have been used: $s_{m-1,0} = 0.02$ and $0.04$ at deep water. One of the major differences of this experimental research with the set up by Bruce, et al. (2009) is, in this research sloping foreshore was used in front of structure instead of horizontal foreshore in that research. Due to the sloping foreshore and limited water depth, the spectral wave steepness $s_{m-1,0}$ higher than 0.04 could not be obtained in this experimental research since waves already break in deep water for this wave steepness. Therefore, the higher wave steepness for this small scale test has been fixed to $s_{m-1,0} = 0.04$. For different significant wave heights the $T_{m-1,0}$ has been computed from the relationship presented in **Equation 4.2**.

$$s_{m-1,0} = \frac{2\pi H_{m0}}{gT_{m-1,0}^2} \tag{4.2}$$

In which,
$H_{m0}$= significant wave height from spectral analysis
$T_{m-1,0}$ = average wave period defined from spectral analysis by $\frac{m_{-1}}{m_0}$
The maximum significant wave height assumed for this experimental investigation was 0.20 m at toe and 0.25 m at deep water; the design wave height with a stability number of 2.8 corresponds to 0.114 m. The significant wave height ($H_{m0}$) for each specific test was started with much lower than the maximum significant wave height. At the beginning of each test a significant wave height of 0.07 m was used, which continued to increase till the maximum wave height of 0.25 m. For each significant wave height also average wave period has been calculated using the **Equation 4.2**. The wave periods together with the wave heights and the wave steepness are presented in **Table 4.4**.

**Table 4.4** Input wave conditions at deep water

| $T_{m-1,0}$ [s] | | | | | | | |
|---|---|---|---|---|---|---|---|
| $s_{m-1,0}$ [-] \ $H_{m0}$ [m] | 0.07 | 0.10 | 0.13 | 0.16 | 0.19 | 0.22 | 0.25 |
| 0.02 | 1.57 | 1.88 | 2.14 | 2.38 | 2.59 | 2.79 | 2.97 |
| 0.04 | 1.13 | 1.3 | 1.45 | 1.59 | 1.72 | 1.84 | 1.95 |

## 4.6. Test programme

Based on literature the important parameters governing the geometrical design of breakwater were found as placement pattern, packing density, crest height and wave steepness in terms of wave height and wave length (Bonfantini, 2014). The placing grid, orientation of units and packing density were selected mainly based on the results of dry placement tests. With considering the important design parameters, laboratory facilities and time in total ten test series were performed for the determination of wave overtopping over crablock armour slope. Moreover, in order to investigate the accuracy of the measured wave heights and wave overtopping two test series were also executed using a smooth (wooden) slope of 1 in 4/3. Also, two test series (test 13 and 14) were done without the presence of a structure to determine the actual incident wave heights.

All tests were performed with increasing wave heights to examine the failure of armour layer as presented in **Table 4.6**. The wave period was also increased simultaneously with the increase of wave height for each test in order to keep the wave steepness constant. The number of waves was kept constant to 1000 random waves except the tests with higher wave heights. Jonswap wave spectrum was used in all the tests. **Table 4.5** shows the nominal test programme used to determine the wave overtopping over crablock armour slope. Each test was comprised of seven sub tests for different wave conditions, see **Table 4.6**. However, a test was stopped when the armour layer failed.

**Table 4.5** Test Programme for flume tests

| Test Series No. | Placement Grid | Orientation | Hor. Vs Upslope distance | Packing Density | Crest Freeboard (m) | Underlayer | Deep water Wave Steepness, $S_{m-1,0}$ | Water depth near structure (m) |
|---|---|---|---|---|---|---|---|---|
| 1 | Rectangular | Uniform | 0.65Dx0.64D | $0.69/D_n^2$ | 0.140 | 7 to 11 mm | 0.04 | 0.35 |
| 2 | Rectangular | Uniform | 0.65Dx0.64D | $0.69/D_n^2$ | 0.140 | 7 to 11 mm | 0.02 | 0.35 |
| 3 | Diamond | Random | 0.75Dx0.61D | $0.63/D_n^2$ | 0.140 | 11 to 16 mm | 0.04 | 0.35 |
| 4 | Diamond | Random | 0.75Dx0.61D | $0.63/D_n^2$ | 0.140 | 11 to 16 mm | 0.02 | 0.35 |
| 5 | Rectangular | Uniform | 0.68Dx0.64D | $0.66/D_n^2$ | 0.140 | 7 to 11 mm | 0.04 | 0.35 |
| 6 | Rectangular | Uniform | 0.68Dx0.64D | $0.66/D_n^2$ | 0.140 | 7 to 11 mm | 0.02 | 0.35 |
| 7 | Rectangular | Uniform | 0.71Dx0.64D | $0.63/D_n^2$ | 0.140 | 7 to 11 mm | 0.04 | 0.35 |
| 8 | Rectangular | Uniform | 0.71Dx0.64D | $0.63/D_n^2$ | 0.140 | 7 to 11 mm | 0.02 | 0.35 |
| 9 | Rectangular | Uniform | 0.68Dx0.64D | $0.66/D_n^2$ | 0.185 | 7 to 11 mm | 0.04 | 0.35 |
| 10 | Rectangular | Uniform | 0.68Dx0.64D | $0.66/D_n^2$ | 0.185 | 7 to 11 mm | 0.02 | 0.35 |
| 11 | Smooth 1 : 4/3 slope | | | | 0.185 | ----- | 0.04 | 0.35 |
| 12 | Smooth 1 : 4/3 slope | | | | 0.185 | ----- | 0.02 | 0.35 |
| 13 | Without structure | | | | 0.185 | ----- | 0.04 | ----- |
| 14 | Without structure | | | | 0.185 | ----- | 0.02 | ----- |

**Table 4.6** Programme for subtests

| Test No. / $H_{m0}$ (m) | 0.07 | 0.1 | 0.13 | 0.16 | 0.19 | 0.22 | 0.25 |
|---|---|---|---|---|---|---|---|
| 1 | 1a | 1b | 1c | 1d | 1e | 1f | 1g |
| 2 | 2a | 2b | 2c | 2d | 2e | 2f | 2g |
| 3 | 3a | 3b | 3c | 3d | 3e | 3f | 3g |
| 4 | 4a | 4b | 4c | 4d | 4e | 4f | 4g |
| 5 | 5a | 5b | 5c | 5d | 5e | 5f | 5g |
| 6 | 6a | 6b | 6c | 6d | 6e | 6f | 6g |
| 7 | 7a | 7b | 7c | 7d | 7e | 7f | 7g |
| 8 | 8a | 8b | 8c | 8d | 8e | 8f | 8g |
| 9 | 9a | 9b | 9c | 9d | 9e | 9f | 9g |
| 10 | 10a | 10b | 10c | 10d | 10e | 10f | 10g |
| 11 | 11a | 11b | 11c | 11d | 11e | 11f | 11g |
| 12 | 12a | 12b | 12c | 12d | 12e | 12f | 12g |
| 13 | 13a | 13b | 13c | 13d | 13e | 13f | 13g |
| 14 | 14a | 14b | 14c | 14d | 14e | 14f | 14g |

## 4.7. Construction of the model

Prior to start construction of the model, the required stones were collected by sieving the available materials. The sieving of rocks has been done to ensure the proper dimensions of the materials regarding to the design specifications. Furthermore, all the stones have been washed before use in construction in order to ensure that the water in the flume remained clear during the test. Then, a 1:30 foreshore slope of wood has been built on the bottom of flume according to the design. In order to keep the same water level on both side of the model, small pipes were provided to pump out the water from rare side to front side.

At the start of construction of breakwater, the cross-section of the model has been drawn along the side walls of the flume to guide the construction of the breakwater. Then, core was built by putting core materials as indicated by the lines on the flume. A special attention has been paid to place the core as underlayer and armour layer are constructed on top of core. After the construction of core, underlayer was erected on top of core following the specifications of the layer provided in **Table 4.3**. Afterwards, toe of the structure was put in place on top of under layer to provide support for the armour layer. Finally, the crablock armour units were placed as single layer armour system. In the placement of crablock, all the units have been positioned based on the designed horizontal and upslope placement distance to obtain the required packing density. After the construction of armour layer, the constructed packing density was checked with targeted packing density by measuring the horizontal and upslope placement distances in together with number of units in horizontal and upslope direction. A picture of constructed model is presented in **Figure 4.7**.

Construction of core and underlayer

Construction of core, underlayer and toe

Construction of uniformly placed crablock armour layer

Construction of randomly placed crablock armour layer

**Figure 4.7** Construction of the model

## 4.8. Testing procedure

Each test has been conducted following the individual test programme. At the start of each test, the wave flume was filled up to the required water level. Then before taking any reading, wave gauges have been fixed according to the designed position and calibrated to avoid error in measurements of wave heights. The calibration of the wave gauges can be simply done by moving them to higher and lower position with a certain range. In this research, the wave gauges were calibrated by moving those 9 cm up and down from their initial position. Moreover, cameras and video recorder were set up at a fixed position to capture the photographs and video. In order to capture the position of armour units in initial condition photographs were taken before starting of each test.

Afterwards, waves have been generated based on the testing wave conditions. The test was started with a lower wave height in order to protect the armour layer from sudden failure. In each test wave heights and periods were continued to measure until failure of the armour slope. Once the armour slope or under layer was damaged due to waves, the armour layer were reconstructed for the next test series. During the time of test, raw data has been collected from the signal of wave gauges and then post processed by using Matlab. After the end of every test, the water level in the overtopping box was determined to measure the volume of overtopping waves. It should be noted that number of waves overtop the structure was calculated from the signal of wave gauge placed at the crest of breakwater. Furthermore, photographs were also captured after the end of each test.

# CHAPTER 5

# Result Analysis and Discussion of Flume Tests

**In the previous chapter, the set up of flume tests, including testing procedure, testing wave conditions, test programme of flume tests etc have been described. This chapter is designed to present and to discuss the results of the 2D wave flume tests in line with wave overtopping over crablock armour slopes. First section 5.1 gives an overview of the measured wave conditions in this research. The next section describes the analysis of the hydraulic test results on wave overtopping. The resulting mean overtopping discharge, percentage of wave overtopping and influences of different parameters on overtopping are discussed in this section. Further section compares the test results on overtopping with empirical estimation and also with overtopping over other single layer units. The chapter ends with discussing the influence of Ursell parameter on wave overtopping.**

## 5.1. Measured wave conditions

### 5.1.1. Summary

In general, the wave height at the structure differs from the wave height at deep water due to complex phenomenon like shoaling and wave breaking at depth limited conditions (Van der Meer, 1987b). In this research, to determine the actual incident significant wave height at the structure, wave heights were also measured without the presence of the breakwater in the flume (test series 13 and 14). In **Table 5.1**, a comparison of measured wave conditions with and without the presence of a structure at deep water as well as at the structure is presented. Note that here only two test series (1 and 2) are compared with tests without structure (13 and 14). For each specific test series the measured wave conditions in details are presented in **Appendix C**. As shown in **Table 5.1**, it can be seen that for high wave steepness (except very high wave height) and also for lower wave heights in case of low wave steepness, the incident wave heights at the structure without the presence of breakwater were almost as same as the wave heights with breakwater. Furthermore, there is more reflection when the structure is present, see **Table 5.1** and **Appendix C**.

In order to have a better understanding about the variation in wave heights, the calculated wave heights at deep water and at structure for both with and without structure is compared in **Figure 5.1** and **Figure 5.2**. Regarding to **Figure 5.1** and **Figure 5.2**, it is visible that measured wave heights without the structure were some cases slightly higher both in case of low wave steepness and high wave steepness. This might be happening due to high reflection caused by the presence of the structure, as compared to without the structure. It may also be that the method to separate incident and reflected waves does not work properly in wave breaking conditions (no linear waves). However, to avoid possible errors in wave heights measurements in further overtopping analysis and to determine the real incident wave heights at toe with the presence of structure, for each individual tests wave heights were calibrated from the established relationship between deep water and structure; see **section 5.1.3**. It should be noted that the calibrated incident wave heights from the developed relationship of wave heights without structure were used in all the analysis.

**Table 5.1** Comparison of measured wave conditions with and without the presence of structure

| Measurement condition | Test Series | Sub-Test No. | Wave Generator | | Near Structure | | | | | Deep Water | | | | | |
|---|---|---|---|---|---|---|---|---|---|---|---|---|---|---|---|
| | | | $H_{m0}$ [m] | $T_p$ [s] | $H_{m0}$ [m] | $H_{1/3}$ [m] | $T_p$ [s] | $T_{m-1,0}$ [s] | Ref. Coff | $H_{m0}$ [m] | $H_{1/3}$ [m] | $T_p$ [s] | $T_m$ [s] | $T_{m-1,0}$ [s] | Ref. Coff |
| With Structure | 1 | 1a | 0.07 | 1.24 | 0.058 | 0.057 | 1.25 | 1.15 | 0.41 | 0.067 | 0.067 | 1.25 | 1.08 | 1.15 | 0.31 |
| | | 1b | 0.10 | 1.43 | 0.081 | 0.080 | 1.43 | 1.32 | 0.45 | 0.096 | 0.096 | 1.45 | 1.22 | 1.32 | 0.31 |
| | | 1c | 0.13 | 1.60 | 0.100 | 0.102 | 1.63 | 1.49 | 0.48 | 0.125 | 0.126 | 1.61 | 1.34 | 1.47 | 0.32 |
| | | 1d | 0.16 | 1.75 | 0.121 | 0.128 | 1.91 | 1.64 | 0.52 | 0.152 | 0.155 | 1.74 | 1.47 | 1.61 | 0.32 |
| | | 1e | 0.19 | 1.89 | 0.140 | 0.162 | 1.97 | 1.81 | 0.54 | 0.177 | 0.182 | 1.84 | 1.59 | 1.73 | 0.31 |
| | | 1f | 0.22 | 2.02 | 0.156 | 0.193 | 2.07 | 1.9 | 0.54 | 0.203 | 0.210 | 2.01 | 1.68 | 1.86 | 0.30 |
| | | 1g | 0.25 | 2.15 | 0.164 | 0.207 | 2.18 | 1.97 | 0.57 | 0.225 | 0.235 | 2.23 | 1.84 | 1.95 | 0.28 |
| | 2 | 2a | 0.07 | 1.73 | 0.058 | 0.058 | 1.71 | 1.63 | 0.50 | 0.065 | 0.068 | 1.74 | 1.45 | 1.59 | 0.35 |
| | | 2b | 0.10 | 2.07 | 0.081 | 0.093 | 2.09 | 1.97 | 0.57 | 0.098 | 0.097 | 2.01 | 1.69 | 1.90 | 0.36 |
| | | 2c | 0.13 | 2.36 | 0.093 | 0.120 | 2.33 | 2.28 | 0.65 | 0.126 | 0.126 | 2.26 | 1.90 | 2.16 | 0.35 |
| | | 2d | 0.16 | 2.61 | 0.106 | 0.136 | 2.54 | 2.44 | 0.70 | 0.156 | 0.160 | 2.56 | 2.14 | 2.37 | 0.33 |
| | | 2e | 0.19 | 2.85 | 0.143 | 0.158 | 2.39 | 2.17 | 0.60 | 0.185 | 0.191 | 2.99 | 2.30 | 2.56 | 0.32 |
| | | 2f | 0.22 | 3.06 | 0.150 | 0.167 | 2.58 | 2.14 | 0.59 | 0.203 | 0.220 | 3.02 | 2.48 | 2.70 | 0.31 |
| Without Structure | 13 | 13a | 0.07 | 1.24 | 0.058 | 0.058 | 1.25 | 1.15 | 0.12 | 0.067 | 0.067 | 1.25 | 1.06 | 1.14 | 0.10 |
| | | 13b | 0.10 | 1.43 | 0.082 | 0.082 | 1.41 | 1.30 | 0.15 | 0.096 | 0.096 | 1.42 | 1.21 | 1.31 | 0.10 |
| | | 13c | 0.13 | 1.60 | 0.102 | 0.102 | 1.58 | 1.43 | 0.16 | 0.124 | 0.125 | 1.62 | 1.34 | 1.46 | 0.11 |
| | | 13d | 0.16 | 1.75 | 0.124 | 0.126 | 1.76 | 1.55 | 0.18 | 0.153 | 0.153 | 1.74 | 1.47 | 1.60 | 0.10 |
| | | 13e | 0.19 | 1.89 | 0.143 | 0.152 | 1.91 | 1.67 | 0.19 | 0.181 | 0.183 | 1.87 | 1.58 | 1.73 | 0.09 |
| | | 13f | 0.22 | 2.02 | 0.160 | 0.177 | 2.04 | 1.76 | 0.21 | 0.206 | 0.209 | 2.04 | 1.68 | 1.84 | 0.10 |
| | | 13g | 0.25 | 2.15 | 0.180 | 0.192 | 2.17 | 2.26 | 0.30 | 0.229 | 0.235 | 2.14 | 1.80 | 1.94 | 0.10 |
| | 14 | 14a | 0.07 | 1.73 | 0.059 | 0.057 | 1.68 | 1.56 | 0.12 | 0.069 | 0.068 | 1.70 | 1.44 | 1.58 | 0.09 |
| | | 14b | 0.10 | 2.07 | 0.081 | 0.082 | 2.11 | 1.87 | 0.13 | 0.098 | 0.097 | 2.06 | 1.70 | 1.89 | 0.10 |
| | | 14c | 0.13 | 2.36 | 0.106 | 0.117 | 2.39 | 2.11 | 0.15 | 0.126 | 0.127 | 2.37 | 1.95 | 2.15 | 0.10 |
| | | 14d | 0.16 | 2.61 | 0.130 | 0.157 | 2.58 | 2.24 | 0.16 | 0.157 | 0.158 | 2.64 | 2.11 | 2.35 | 0.10 |
| | | 14e | 0.19 | 2.85 | 0.155 | 0.195 | 2.89 | 2.63 | 0.19 | 0.187 | 0.193 | 2.75 | 2.27 | 2.53 | 0.10 |
| | | 14f | 0.22 | 3.06 | 0.173 | 0.224 | 3.10 | 2.90 | 0.20 | 0.215 | 0.228 | 3.10 | 2.38 | 2.66 | 0.10 |

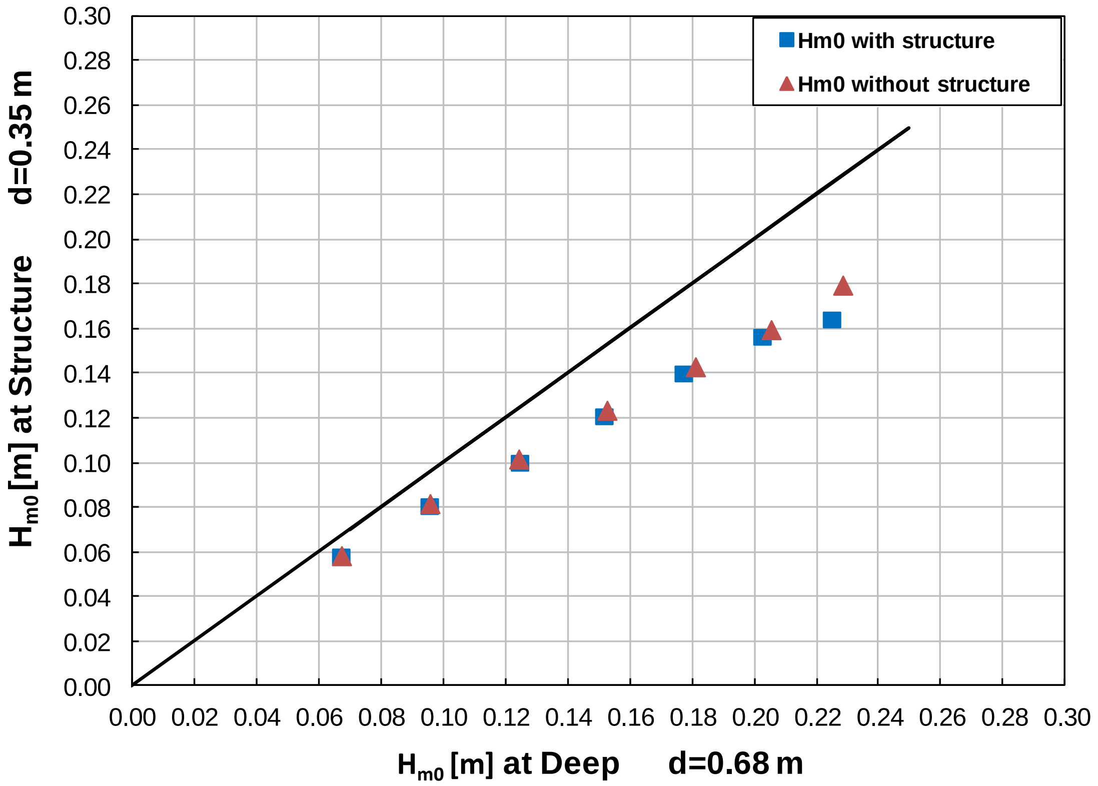


**Figure 5.1** Comparison of measured wave heights ($H_{m0}$) with and without the presence of structure (short period)

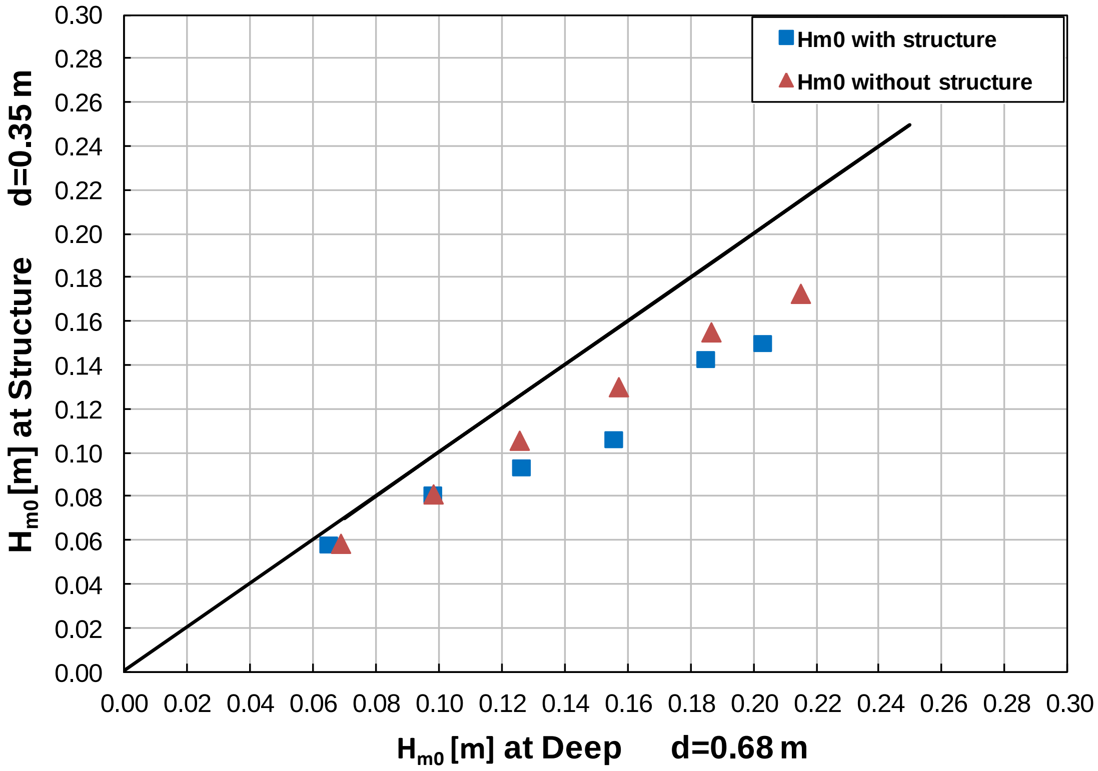


**Figure 5.2** Comparison of measured wave heights ($H_{m0}$) with and without the presence of structure (long period)

### 5.1.2. Wave height exceedance curve

In order to observe the distribution of wave height, wave height exceedance curve has been plotted for wave heights at deep water as well as at structure. Furthermore, the distribution of measured wave heights compared with the estimation of local wave height distribution described by Battjes and Groenendijk (2000) is presented. In **Figure 5.3** and **Figure 5.4**, wave height exceedance curves for the test with input of $H_{m0} = 0.16$ m at wave generator is plotted both in case of short as well as long wave period. It is noted that in the following figures X axis is Rayleigh distribution. The distributions of wave heights for all the testing wave conditions (without structure) are attached in **Appendix D**.

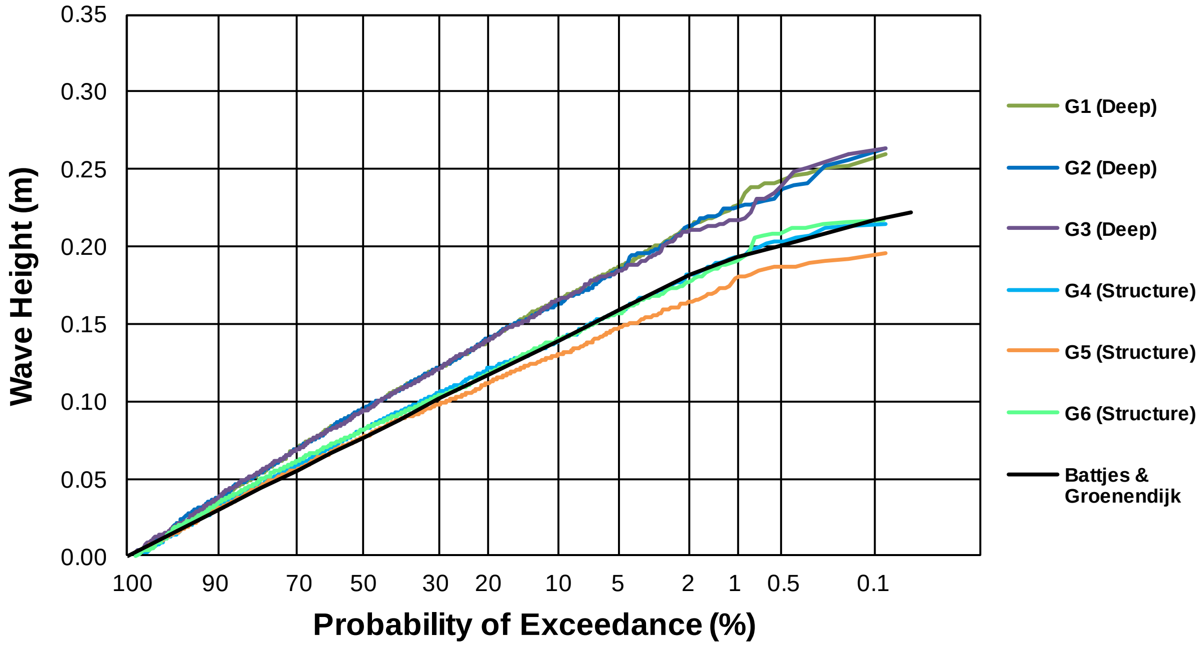


**Figure 5.3** Wave height exceedance curve for input $H_{m0}$ = 0.16 m at wave generator (short period, test 13d)

**Figure 5.3** illustrates the distribution of wave heights for one of the test performed with high wave steepness (input of $H_{m0} = 0.16$ m and $T_p = 1.75$ sec at wave generator). From **Figure 5.3**, it is remarkably inspected that near the structure waves were breaking with short period. Therefore, the resulting wave heights at structure were found lower than the wave heights at deep water.

The wave height exceedance curve for the test with relatively long wave period that means low wave steepness (input of $H_{m0} = 0.16$ m and $T_p = 2.61$ sec at wave generator) is plotted in **Figure 5.4**. The resulting graph shows that wave heights at structure are same or even larger due to shoaling with long wave period.

Furthermore, as plotted in **Figure 5.3** and **Figure 5.4**, also compare the distribution of wave heights with the prediction by Battjes and Groenendijk (2000). It is worth mentioning that in this research three wave gauges were put into deep water and also three wave gauges were set near the structure (shallow water), see **section 4.2.2**. Based on **Figure 5.3** and **Figure 5.4**, it is seen that wave height distribution at deep water (G1, G2 and G3) is pretty near Rayleigh distribution as expected. Moreover, from **Figure 5.3** it is also observed that near the structure (shallow water) the distribution is almost composite Weibull distribution similar to the prediction by Battjes and Groenendijk (2000).

However, regarding to **Figure 5.4**, it is also inspected that at the structure, the difference between measured individual wave heights and predicted wave heights by Battjes and Groenendijk (2000) is bigger in case of long wave period in comparison to short period. That may be happened due to shoaling with long wave period instead of waves breaking at shallow foreshore expected by Battjes and Groenendijk (2000); see **Figure 5.4**.

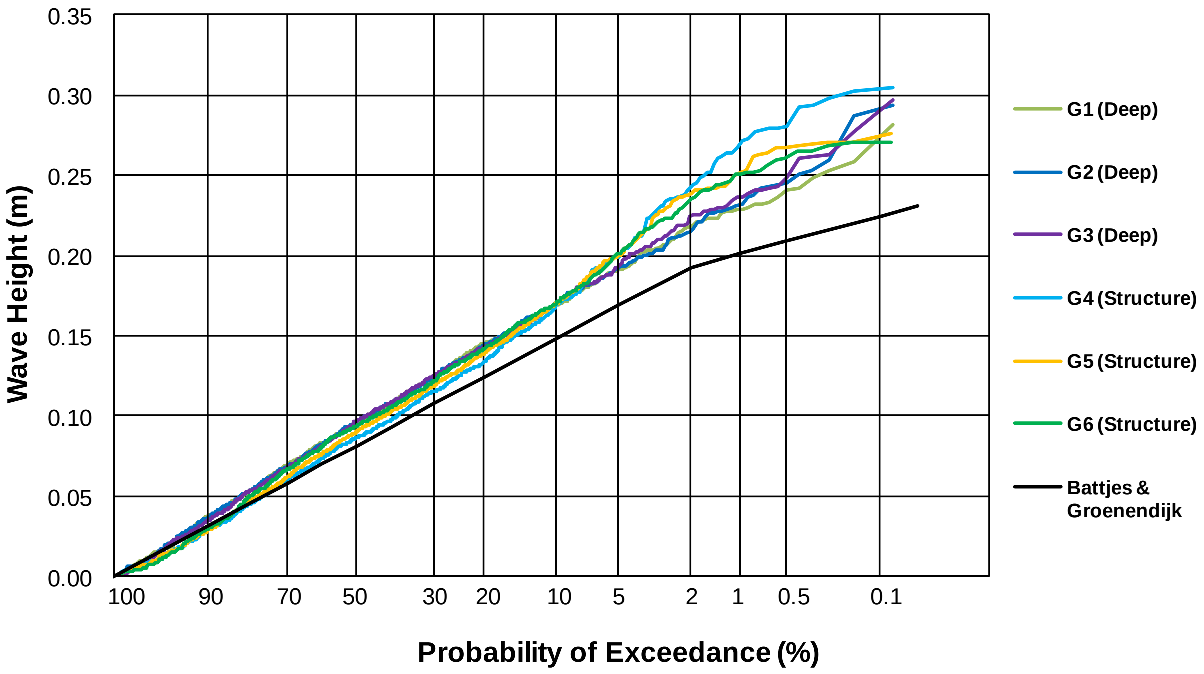


**Figure 5.4** Wave height exceedance curve for input $H_{m0}$ = 0.16 m at wave generator (long period, test 14d)

Nevertheless, it is recognised that near structure, for very high waves with long wave period this variation between measurements and prediction can be also occurred because of less wave breaking than the expectation by Battjes and Groenendijk (2000); see wave height exceedance curves for test 14e and 14f in **Appendix D**. Because of this deviation in case of highest wave heights with long periods the resulting statistical significant wave height $H_{1/3}$ at structure significantly differed from the prediction of $H_{1/3}$ by Battjes and Groenendijk (2000); see comparison of $H_{1/3}$ in **section 5.1.4**.

### 5.1.3. Relation between wave height at deep water and at structure

**Figure 5.5** presents a relation between the spectral significant wave height $H_{m0}$ at deep water and at the structure. It is worth mentioning that this relation was established without the presence of structure in the flume. During the tests the incident wave height both at deep water and at the structure was measured however the measured incident wave height near the structure might be influenced because of reflection from the model. Therefore, the incident wave height at the toe of the breakwater was determined from the relationship presented in **Figure 5.5** by using wave height at deep water.

Besides the relation between spectral significant wave height $H_{m0}$ at deep water and at structure, a similar relation was also developed for the statistical significant wave height $H_{1/3}$ calculated from time series analysis of waves, see **Figure 5.6**.

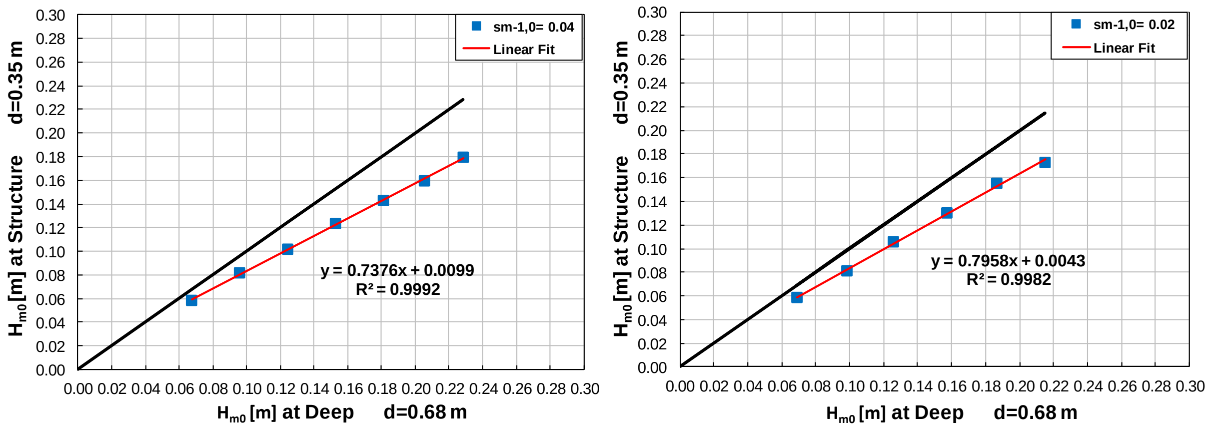


High wave steepness (short period)

Low wave steepness (long period)

**Figure 5.5** Relation between wave height ($H_{m0}$) at deep water and at structure

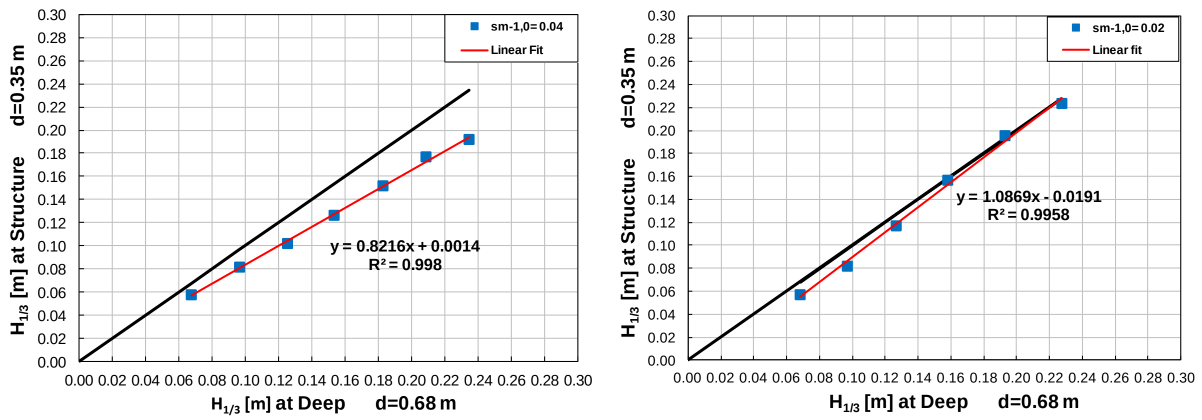


High wave steepness (short period)

Low wave steepness (long period)

**Figure 5.6** Relation between wave height ($H_{1/3}$) at deep water and at structure

### 5.1.4. Relation between $H_{m0}$ and $H_{1/3}$

Because of wave breaking process at shallow water, the spectral significant wave height $H_{m0}$ also varies from statistical significant wave height $H_{1/3}$ (EurOtop, 2007). In **Figure 5.7**, a relation between $H_{m0}$. and $H_{1/3}$ is established for both long and short wave period. As presented in **Figure 5.7**, shows that the variation of $H_{1/3}$ and $H_{m0}$ was not so considerable for the tests with short wave periods even for lower waves with long periods. However, in case of low wave steepness (long period) statistical wave height ($H_{1/3}$) was significantly differed from spectral significant wave height ($H_{m0}$) for the tests with higher waves. This substantial difference may be happened due to waves breaking in depth limited conditions.

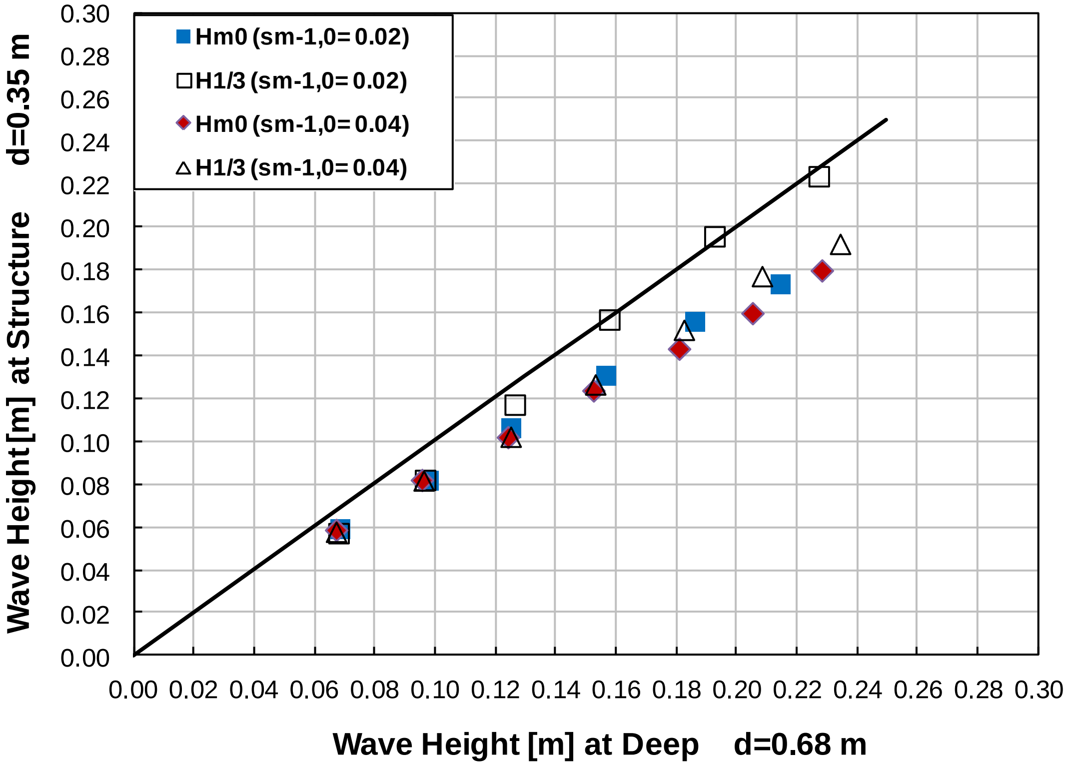


**Figure 5.7** Relation between $H_{m0}$ and $H_{1/3}$

**Figure 5.8** compares the resulting $H_{1/3}$ with the prediction by Battjes and Groenendijk (2000). The graph clearly shows that measured $H_{1/3}$ in this research is almost as same as the predicted $H_{1/3}$ by Battjes and Groenendijk (2000) except for the highest wave heights with the long wave period. Further from **Figure 5.8**, it can be concluded that in case of very high waves Battjes and Groenendijk (2000) under estimate the $H_{1/3}$ for this foreshore slope and large wave period.

However, to validate this variation of resulting $H_{1/3}$ from Battjes and Groenendijk (2000), the data of the accropode testing also has been thoroughly looked. Note that this is the actual wave data from Prof. J.W. Van der Meer, author of that research, see **Figure 5.9**. Based on **Figure 5.9**, it is seen that Van der Meer (1987b) also had found a clear deviation for highest wave heights with long periods. This undoubtedly proves that the deviation for high waves observed in this research is not a coincident, but Battjes and Groenendijk (2000) under estimate the $H_{1/3}$ for 1:30 foreshore slope and long wave period.

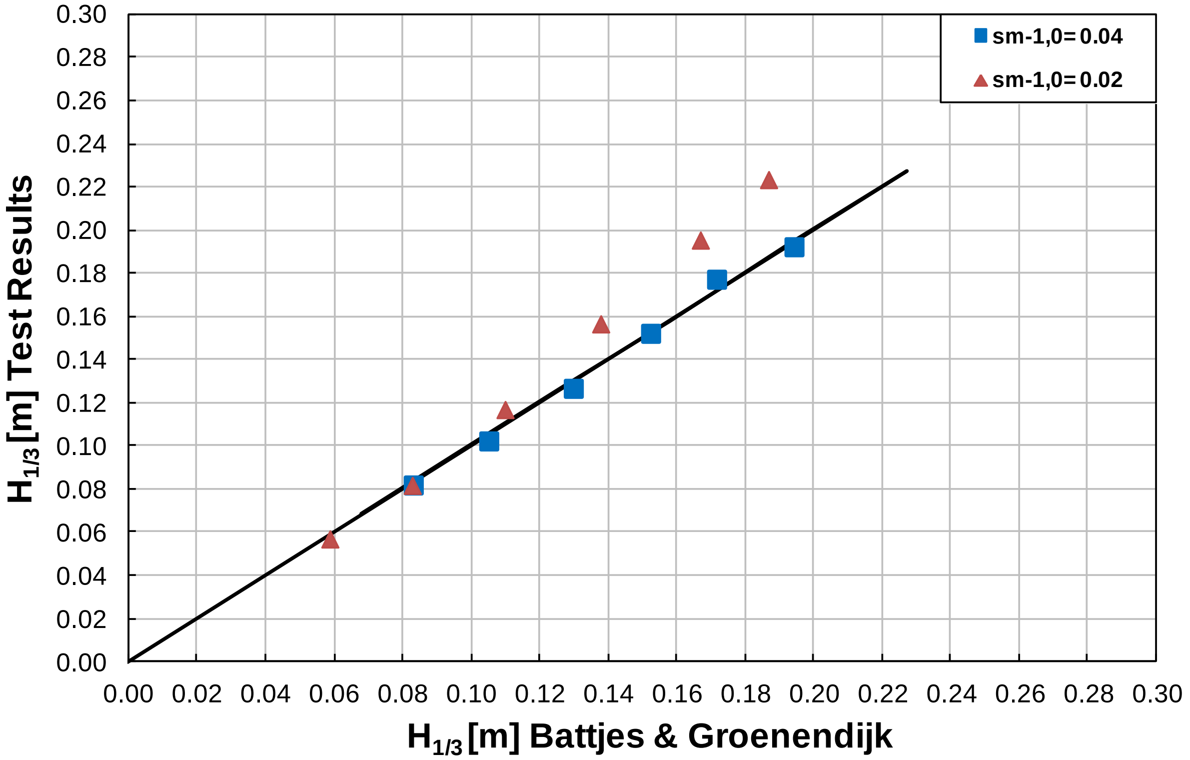


**Figure 5.8** $H_{1/3}$ of test results against $H_{1/3}$ of Battjes & Groenedijk (2000)

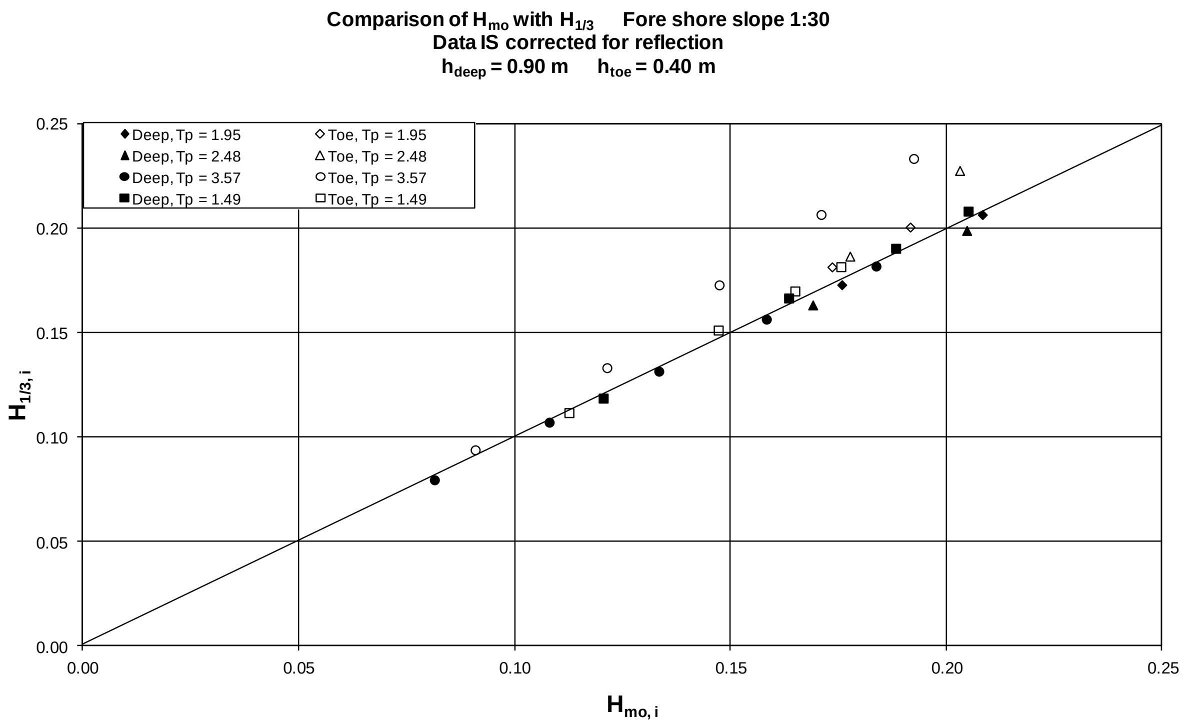


**Figure 5.9** Comparison of $H_{m0}$ with $H_{1/3}$ for foreshore slope of 1:30 [Source: (Van der Meer, 1987b)]

### 5.1.5. Wave period

In this laboratory study, wave periods have been calculated both from spectra analysis ($T_p$ and $T_{m-1,0}$) as well as from time series analysis of waves ($T_m$). **Figure 5.10** describes a relationship between the wave periods measured at deep water and at the structure (shallow water). It should be clarified that this relation was checked without the presence of structure in the flume. In **Appendix C**, the wave periods measured for each individual test series with structure is printed. Based on **Figure 5.10**, it is observed that peak wave period ($T_p$) as well as mean period ($T_m$) for almost all the cases was same both at deep and at structure (shallow water). However, average wave period ($T_{m-1,0}$) based on spectra for very high waves was found higher at shallow water than deep water in case of short as well as for long period (two tests in the figure).

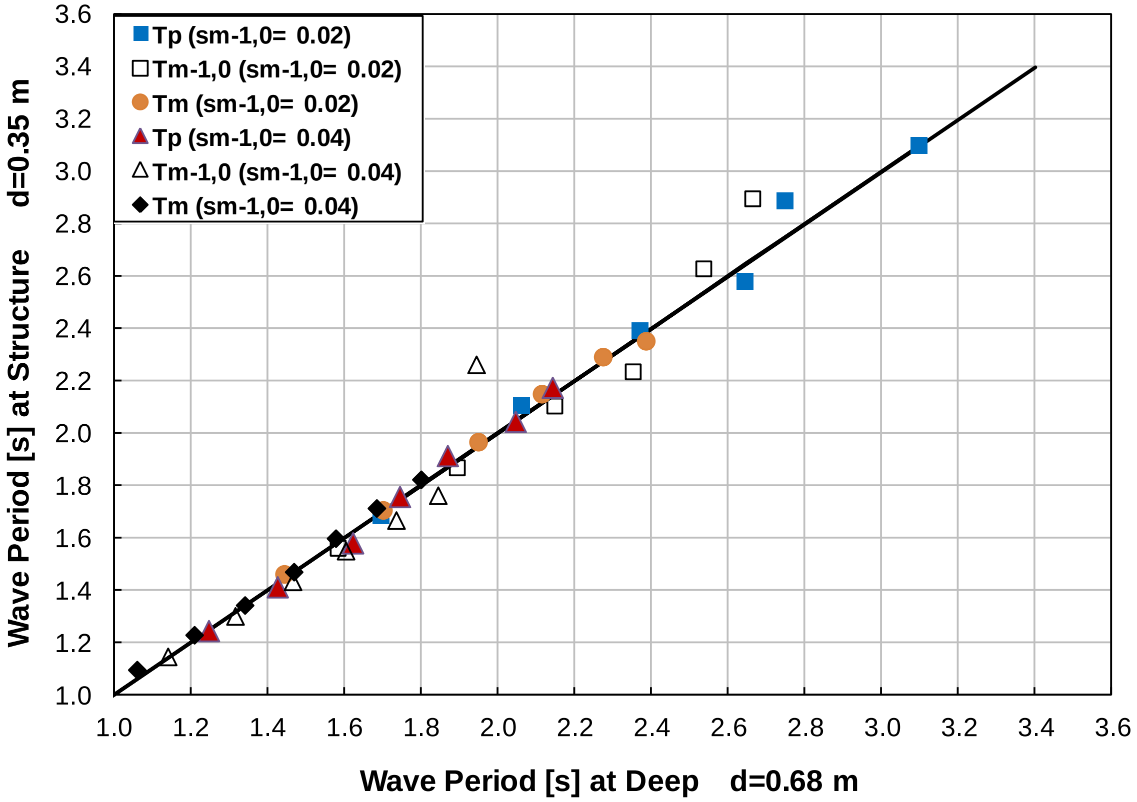


**Figure 5.10** Relation between wave period at deep water and at structure

As a general conversion rule, for a single peaked spectrum with Rayleigh distribution in deep water the ratio between the spectral peak wave period ($T_p$) is assumed 1.1 times of average wave period ($T_{m-1,0}$) defined from spectral analysis (CIRIA, et al., 2007). The test results on wave periods of this research also showed almost the same relationship in deep water as described by (CIRIA, et al., 2007, EurOtop, 2007), see **Figure 5.11**. However, in case of very shallow water this relationship is not always valid as the shape of spectrum in shallow water diverges from the shape of spectrum in deep water (Verhagen, et al., 2008). This variation of wave periods in between deep and shallow water was also found in this research; see **Figure 5.11**. For instance, as shown in **Figure 5.11**, for the test with short period (low steepness) and highest wave height ($T_p = 2.15$ s and $H_{m0} = 0.25$ m at wave paddle), $T_{m-1,0}$ was determined 2.26 s at structure while it was found 1.94 s at deep water. Nevertheless, in that case peak period $T_p$ was measured 2.14 s at deep water almost as same as shallow water (2.17 s). That clearly indicates that variation of $T_{m-1,0}$ at shallow water most likely caused the difference between $T_p$ and $T_{m-1,0}$. Mostly wave breaking at depth limiting situations changed the shape of spectrum with providing little long wave energy in the spectrum hence $T_{m-1,0}$ was shifted towards left of spectral peak, see wave spectrum in **Appendix E**.

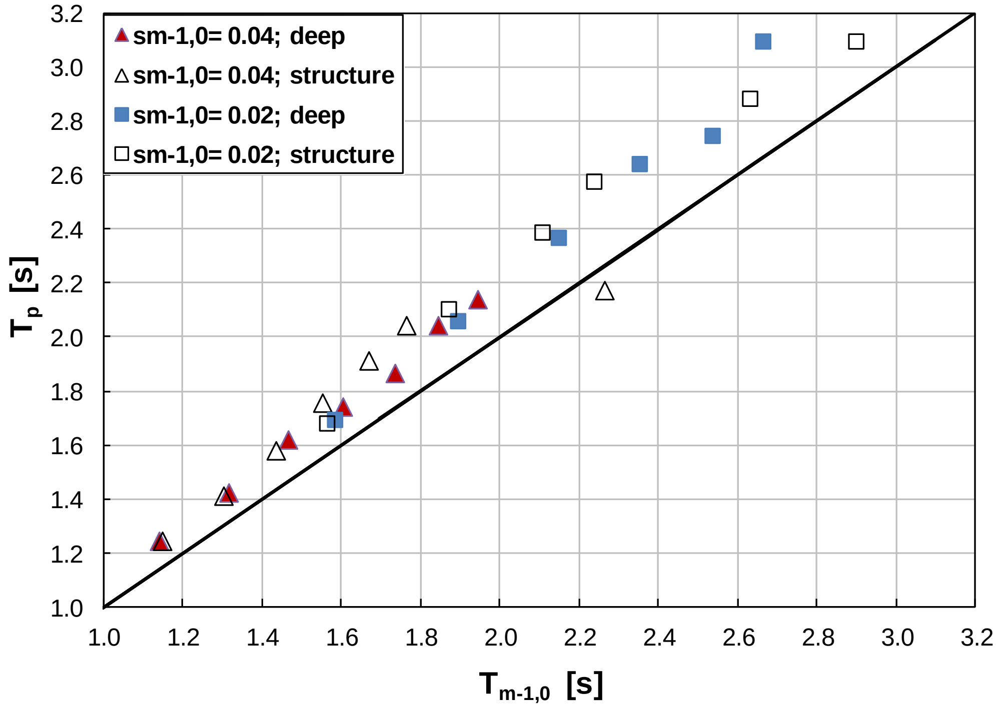


**Figure 5.11** Relation between $T_p$ and $T_{m-1,0}$

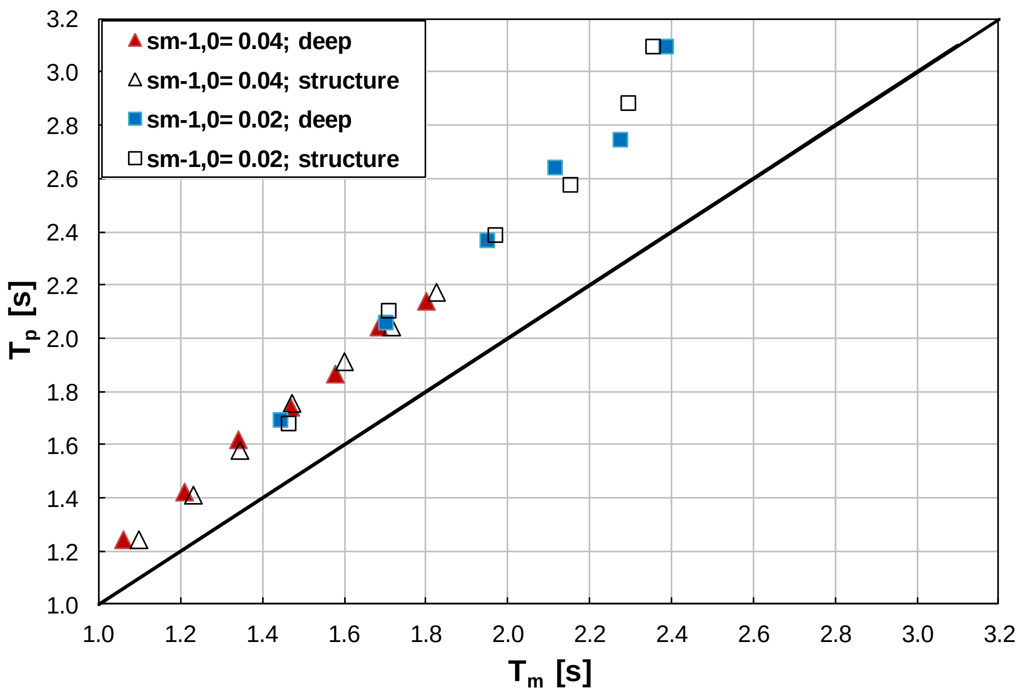


**Figure 5.12** Relation between $T_p$ and $T_m$

Furthermore, as presented in **Figure 5.10**, shows that mean wave periods from time domain analysis of waves ($T_m$) follow a linear relationship between wave period at deep and at shallow water. Also, based on the test results it can be observed that in almost all the cases (except two tests) the ratio between peak period and mean period ($T_p/T_m$) varied from 1.1 to 1.25 as same as prescribed by (CIRIA, et al., 2007, EurOtop, 2007); see **Figure 5.12**.

## 5.2. Measured wave overtopping

The mean wave overtopping rate and overtopping percentages over crablock armour slope are calculated for each specific test series and printed in details in **Appendix F**. It should be pointed that this section deals only with measured wave overtopping over crablock slope hence tests with smooth slope have not been discussed here. In all the cases the incident wave height (calibrated) at the structure is considered.

**Table 5.2** presents an overview of measured wave overtopping for test series one and two performed in this experimental research, see **Appendix F** for all test series. As printed in **Table 5.2**, test results showed that for the same wave height input (generator) with only different wave periods mean overtopping rate q (m3/s per m) as well as percentage of overtopping (%) was a little higher for test series two (long period) compared to test series one (short period).

**Table 5.2** Overview of measured wave overtopping in test series 1 and 2

| Test Series | Sub-Test No. | Crest Freeboard (m) | Wave Generator Input | | $H_{m0}$ at Deep [m] | $H_{m0}$ at Toe [m] | Mean Overtopping Rate [l/s per m] | Percentage of overtopping waves [%] |
|---|---|---|---|---|---|---|---|---|
| | | | $H_{m0}$ at Generator [m] | $T_p$ at Generator [sec] | | | | |
| 1 | 1a | 0.140 | 0.070 | 1.24 | 0.067 | 0.059 | 0 | 0 |
| | 1b | 0.140 | 0.100 | 1.43 | 0.096 | 0.080 | 0.000261053 | 0.42 |
| | 1c | 0.140 | 0.130 | 1.60 | 0.125 | 0.102 | 0.020100172 | 2.49 |
| | 1d | 0.140 | 0.160 | 1.75 | 0.152 | 0.122 | 0.165504372 | 11.22 |
| | 1e | 0.140 | 0.190 | 1.89 | 0.177 | 0.141 | 0.525394328 | 27.74 |
| | 1f | 0.140 | 0.220 | 2.02 | 0.203 | 0.159 | 1.33340678 | 45.04 |
| | 1g | 0.140 | 0.250 | 2.15 | 0.225 | 0.176 | 2.233468874 | 50.80 |
| 2 | 2a | 0.140 | 0.070 | 1.73 | 0.065 | 0.056 | 0 | 0 |
| | 2b | 0.140 | 0.100 | 2.07 | 0.098 | 0.082 | 0.005966724 | 1.06 |
| | 2c | 0.140 | 0.130 | 2.36 | 0.126 | 0.105 | 0.229268118 | 11.41 |
| | 2d | 0.140 | 0.160 | 2.61 | 0.156 | 0.128 | 0.874001901 | 28.33 |
| | 2e | 0.140 | 0.190 | 2.85 | 0.185 | 0.151 | 1.956913249 | 46.63 |
| | 2f | 0.140 | 0.220 | 3.06 | 0.203 | 0.166 | 2.853398334 | 60.23 |

### 5.2.1. Mean overtopping rate

The overtopping volume for each specific test was determined from the water level in and the dimension of the overtopping box. The overtopping volume for higher wave heights was extremely high, therefore the overtopping volume was recorded for only 500 waves for these higher wave conditions. The average overtopping rate for each tested wave heights was then calculated regarding to the volume of overtopping and duration of test. The resulting mean wave overtopping rate q (l/s per m) in line with relative crest freeboard $(\mathrm{R_c}/\mathrm{H_{m0}})$ is presented in **Figure 5.13**. As shown in **Figure 5.13**, test results showed that wave overtopping was slightly higher for tests with long wave period (low wave steepness $s_{m-1,0} = 0.02$ ) both in case of lower and higher crest level. Furthermore, based on **Figure 5.13**, it has also been observed that a different crest height gives deviation in results.

### 5.2.2. Dimensionless wave overtopping

In many cases the overtopping discharge is expressed as dimensionless overtopping rate in order to compare the wave overtopping over different armour slopes. In **Figure 5.14**, a relation between dimensionless overtopping discharge $(\mathrm{q}/\sqrt{\mathrm{gH_{m0}}^3})$ and relative freeboard $(\mathrm{R_c}/\mathrm{H_{m0}})$ is presented. Note that data points at $10^{-7}$ are the points with no overtopping. As following the approach by EurOtop (2007), an exponential distribution between the dimensionless overtopping discharge and relative crest freeboard is made in the graph. From the following graph, it is remarkably noted that relative wave overtopping was always somewhat higher for the tests with low wave steepness (Test 2, 4, 6, 8 & 10) compared to the tests with high wave steepness (Test 1, 3, 5, 7 & 9). However, **Figure 5.14** also indicates that the relative overtopping discharge for the tests with same wave steepness is quite close to each other.

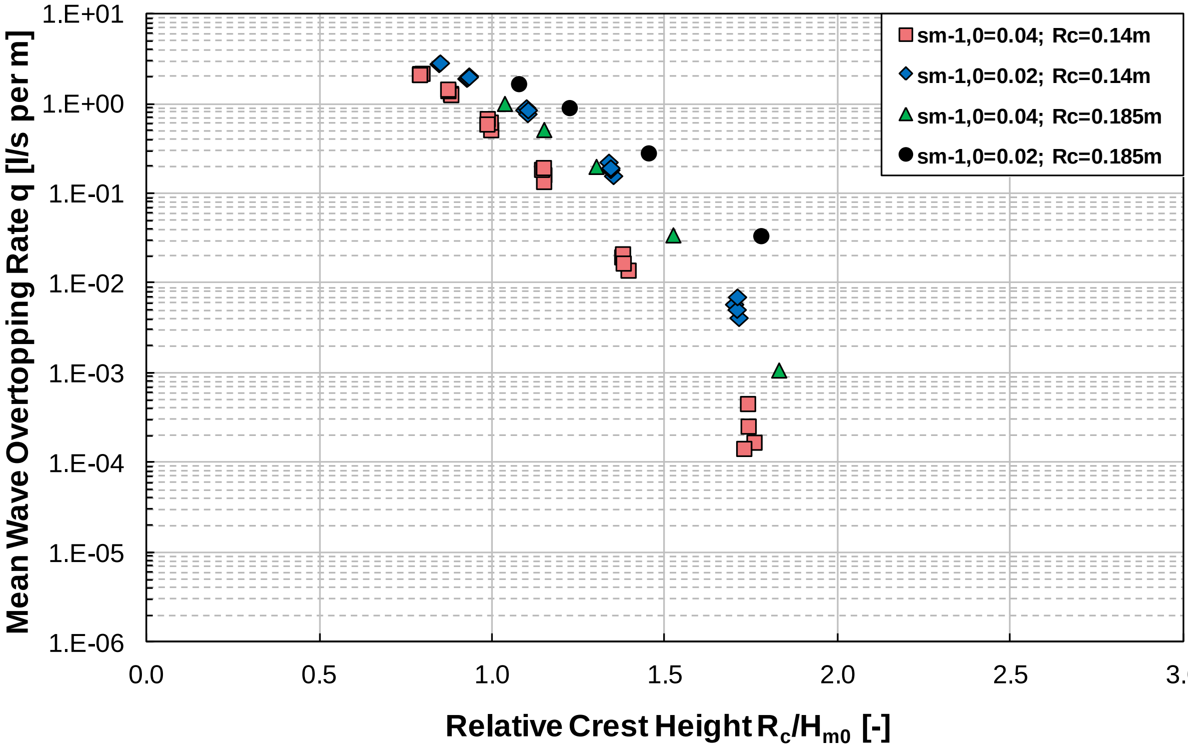


**Figure 5.13** Mean overtopping discharge as a function of relative freeboard

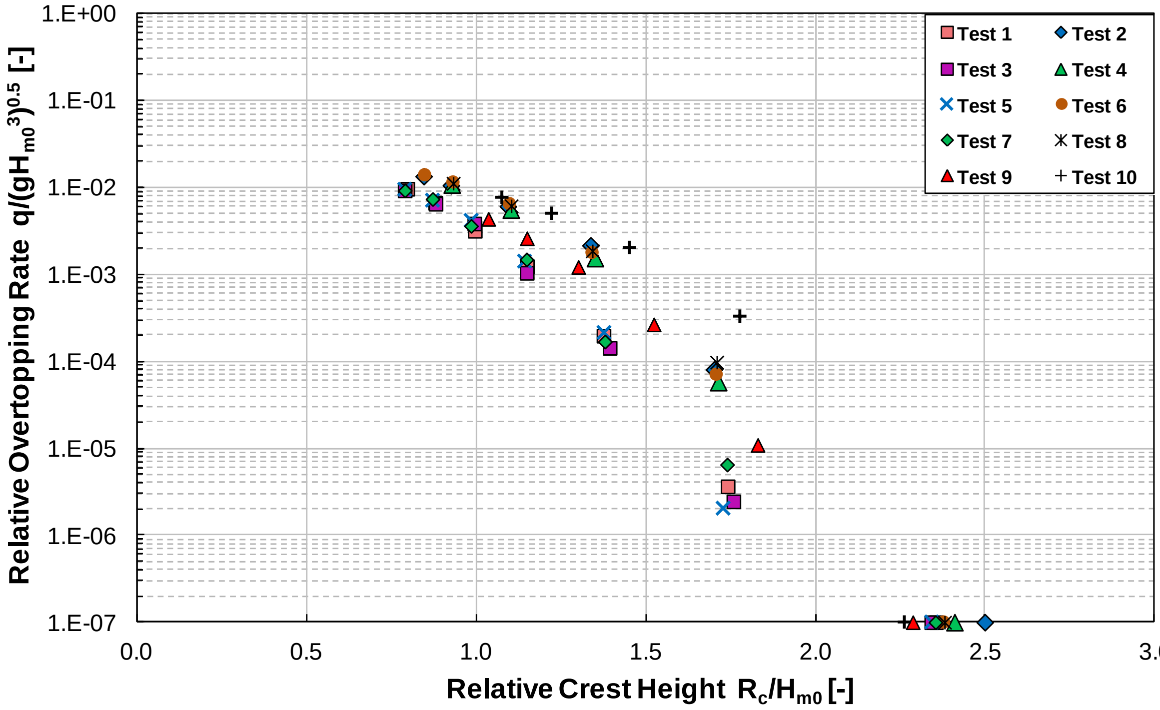


**Figure 5.14** Relative overtopping discharge as a function of relative freeboard

Furthermore, to examine the effect of packing density on wave overtopping over crablock slope, tests with randomly placed crablock (test series 3 and 4) can be discarded from the comparison as placement pattern might have also influence on overtopping. The measured dimensionless overtopping rate obtained in different test series with different packing density can be observed from **Figure 5.14**. As presented in **Figure 5.14**, for the tests with same wave steepness overtopping results did not vary much between the different test series with the change in packing density. For instance, test series 1, 5 and 7 performed with uniform placement pattern with same configuration except different packing density of armour layer. However, based on the test outputs it is remarkably inspected that the change in packing density did not really change the overtopping behaviour of these test series.

Based on the test results, it was also observed there is no difference in wave overtopping behaviour between uniform placed and randomly crablock armour. As printed in **Figure 5.14**, the dimensionless wave overtopping rate observed for different test series can be compared in order to describe the influence of placement pattern. The graphs show that test series with irregular placement of crablock result in almost same overtopping in comparison to the other test series with regular placement of crablock units for the same wave steepness. To cite an example, the comparison of measured wave overtopping in test series 1, 3, 5 and 7 (same wave period) demonstrates that regular placement (test 3) hardly have any influence on overtopping; see **Figure 5.14**.

### 5.2.3. Percentage of overtopping waves

The number of overtopping waves was determined from the signal of the wave gauge mounted at the crest of the breakwater. The total number of waves in an individual test with specific wave height and period was calculated from the time series analysis of wave. Afterwards, the percentage of waves passed the crest of the structure for a particular experiment was recorded from the measured number of overtopped and total number of waves.

In **Figure 5.15**, the measured percentage of overtopping waves with respect to dimensionless crest height is presented. In this research, nominal diameter $(\mathrm{D_n})$ of crablock was constant thus percentage of overtopping waves varied with significant wave height $(\mathrm{H_{mo}})$ at toe and armour freeboard $(\mathrm{A_c})$. The resulting graph clearly shows that percentage of wave overtopping increases with the increase of significant wave height at the toe of breakwater while it decreases with the increase of crest freeboard. Furthermore, the test results showed that in general the percentage of waves overtopped the structure were a bit higher for longer wave periods that mean for low wave steepness.

### 5.2.4. Influence of wave steepness

From the test results on wave overtopping, it is clearly noticeable that wave steepness influences the amount of wave overtopping over the crablock armour slope; see **Figure 5.14** and **Figure 5.15**. As stated earlier that in this research, only two wave steepnesses were tested. The dimensionless overtopping rate as well as percentage of overtopping discharge has found to be lower for the tests with high wave steepness, which represent short wave periods. For example, Test series 1 and Test series 2 were performed with exactly the same packing density, placement pattern and placement grid; see **Figure 5.14**. However, the wave steepness was the only difference between two test series. From **Figure 5.14**, it is observed that relative wave overtopping rate was always slightly higher for test with low wave steepness (Test 2) compared to test with high wave steepness (Test 1). Similar trend also can be remarked for percentage of wave overtopping regarding to **Figure 5.15**.

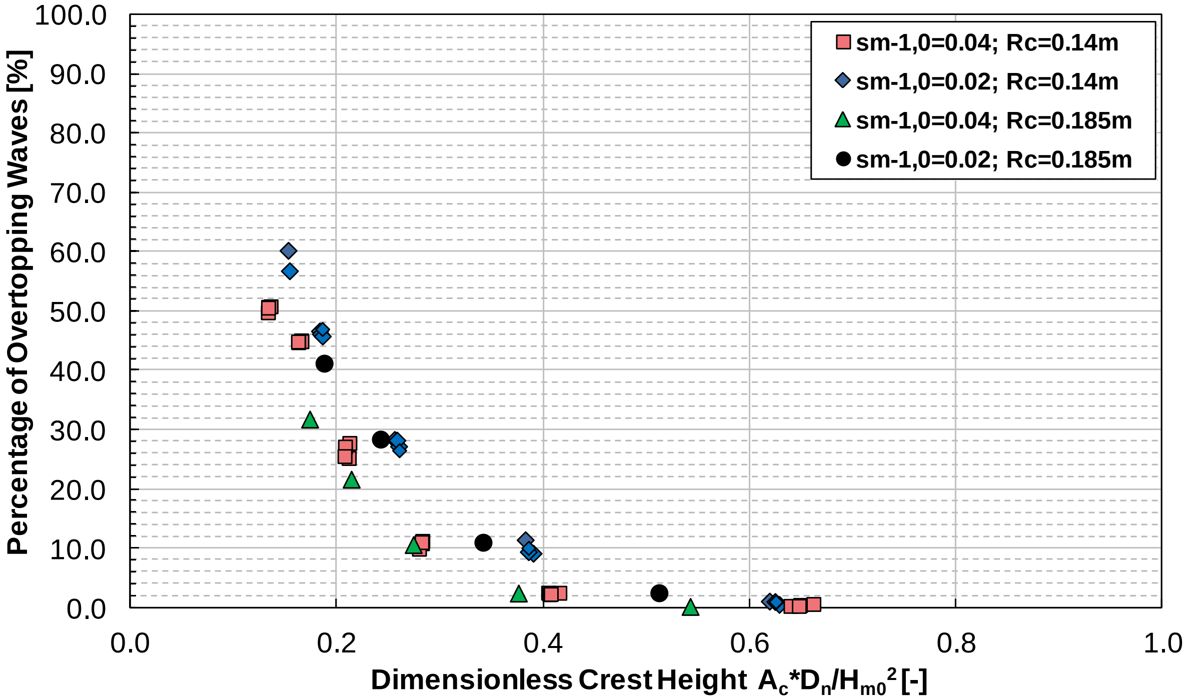


**Figure 5.15** Percentage of wave overtopping as a function of dimensionless crest freeboard

## 5.3. Comparing test results with empirical prediction and other units

This section is designed to compare the test results on wave overtopping over crablock slopes with empirical formulas and also with other existing single layer units. Also, the test results on overtopping rates over a smooth slope have also been compared with empirical prediction.

### 5.3.1. Dimensionless wave overtopping

#### Smooth slope

In **Figure 5.16**, the measured overtopping results over 1:4/3 smooth slope has been compared with the empirical prediction by Van der Meer and Bruce (2014), see **Equation 2.10**. It is worth pointing out that CLASH (2004) report provides data on overtopping over 1:1.5 smooth slopes therefore these have not been considered in this comparison. From the graph presented in **Figure 5.16**, it can be clearly seen that test results have a satisfactorily fit with the empirical line of smooth slope 1:4/3 rather than empirical line of 1:2.0.

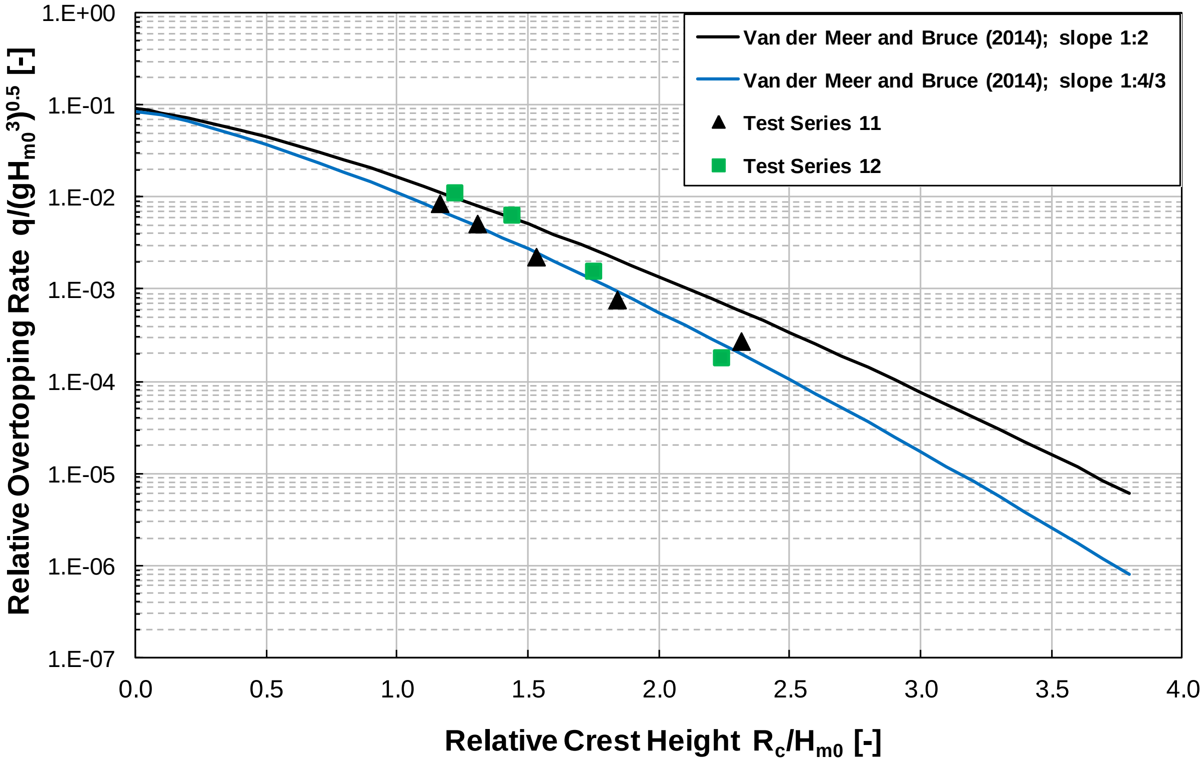


**Figure 5.16** Test results of smooth slope compare to empirical prediction by Van der Meer and Bruce (2014)

### Crablock

As shown in **Figure 5.17**, presents the comparison between the measured dimensionless overtopping discharges over crablock from flume tests verses the predictions by empirical formula (**Equation 2.9**). Besides empirical prediction with assuming roughness factor of $\gamma_f$ equal to 0.45 another empirical line has been drawn with $\gamma_f = 1.0$ to compare the test results with maximum overtopping over 1 in 2 smooth slopes. Moreover, **Figure 5.17** also compares the test results with other single layer units extracted from CLASH (2004) report and from 2D model tests by DMC (2003).

Based on **Figure 5.17**, it is observed that in almost all the cases empirical formula ($\gamma_f = 0.45$) underestimates the wave overtopping discharge over crablock slopes compared to the test measurements. Also, for high waves overtopping over crablock is somewhat larger in comparison to the overtopping over other single layer units, like accropode, core-loc and xbloc (CLASH, 2004). However, a completely different scenario is observed in case of xbloc measurements by DMC (2003). From **Figure 5.17**, it is recognised that overtopping over xbloc by DMC (2003) behaves like a smooth structure which is significantly higher compared to empirical line of rough armour, CLASH (2004) and crablock.

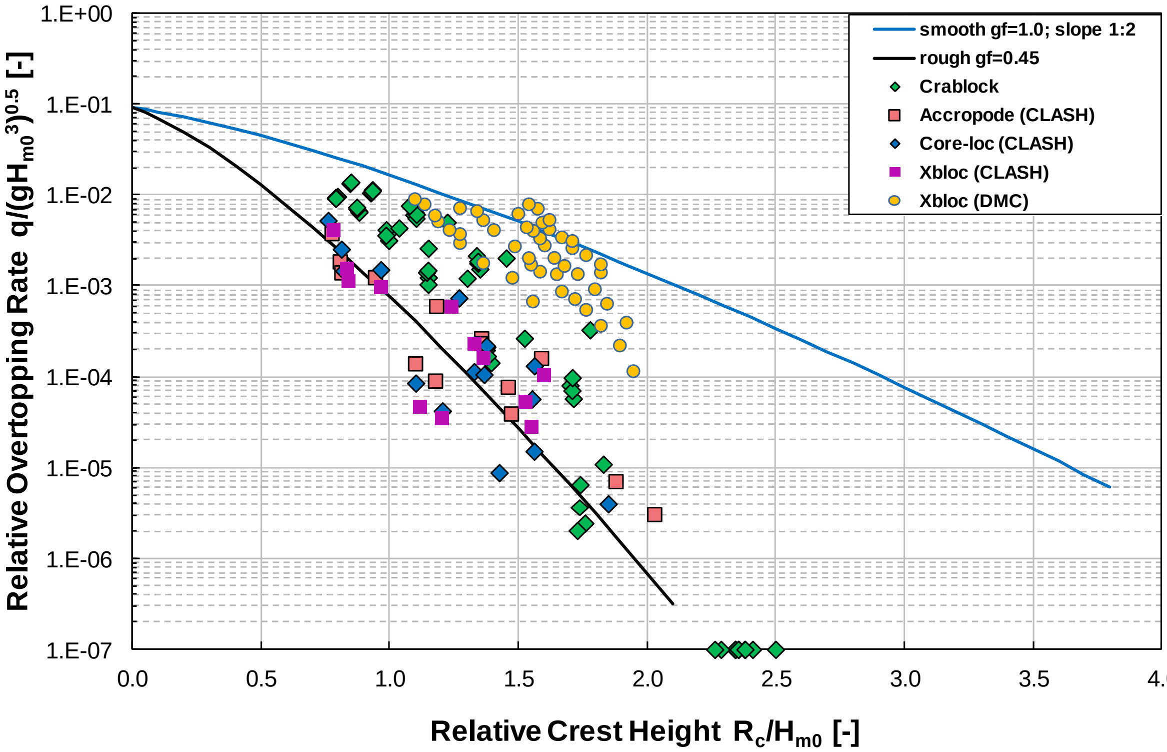


**Figure 5.17** Test results of crablock compare to empirical prediction and other monolayer units

The difference in results between the measured overtopping over crablock units, CLASH (2004) data on other concrete units and the empirical predictions might be due to the following reasons,

- CLASH (2004) data are based on 2D experiments which were performed with the use of three wave steepnesses $s_{op}$ = 0.02; 0.035 and 0.05. Nevertheless, in this study flume tests were carried out by using two constant wave steepnesses $s_{m-1,0}$ = 0.02 and 0.04 ($s_{op}$ = 0.015 and 0.035). That means all the tests with low wave steepness $s_{op}$ = 0.015 were not in the range of CLASH which mainly gave higher overtopping compared to CLASH (2004).

- All the experiments in the CLASH (2004) project were performed in a relatively simple standard cross-section without any sloping foreshore in front of the model and with relatively deep water (0.7 m). However, a sloping foreshore of 10 m in length with a uniform slope of 1:30 was used in this research. The 1:30 slope changed the shape of the waves and the waves at the structure toe showed a clear increase in velocity of the wave crest (near or at breaking).

- Wave periods ($T_p$) used in all the experiments by CLASH (2004) were in the range of $T_p$= 0.77s to 1.82 sec. However, most of the tests on crablock were executed with relatively longer wave periods in comparison to CLASH (2004). The test results of this research showed that longer wave periods also cause additional overtopping. Also, Van der Meer (1987b) found that longer wave periods give more overtopping. Therefore, wave period was one of triggering factor for large overtopping over crablock slope compared to CLASH (2004). Nevertheless, the empirical formulas recommended by EurOtop (2007) to estimate overtopping over rubble mound breakwaters indicate that there is no influence of wave period. Indeed, EurOtop (2007) provided the empirical formulas based on a lot of research and corresponding test results. The crablock has extended this area of long wave periods and there might be influence of long wave period on overtopping.

- Furthermore, instead of using conventional under layer of one tenth to one fifteenth of weight of armour, smaller underlayer of one twenty-fifth of weight of armour was used to perform the tests with uniform placement. The resulting overtopping over crablock might be also influenced by the use of less permeable underlayer.

- Also, it is worth pointing out that all the empirical formulas on overtopping are based on spectral significant wave height $H_{m0}$ at structure. As presented in **Figure 5.17**, the dimensionless wave overtopping for CLASH (2004), xbloc by DMC (2003) and test results on crablock are also based on $H_{m0}$ at structure. However, as it is already discussed and presented in **section 5.1.4** that in this research, for higher wave heights with long period $H_{m0}$ at structure considerably differed from $H_{1/3}$ at structure. Note that this was not the case for CLASH (2004) as it was performed in relatively deep water with respectively short wave periods. Therefore, the use of $H_{m0}$ instead of $H_{1/3}$ also played a role for the difference between crablock with CLASH (2004) and empirical prediction. To observe the influence of $H_{1/3}$, **Figure 5.17** is re-plotted with the use of $H_{1/3}$ instead of $H_{m0}$; see **Figure 5.18**. Based on comparison of **Figure 5.17** and **Figure 5.18**, it can be concluded that by using $H_{1/3}$ the variation between CLASH (2004) and crablock is considerably reduced. Also, the test results of crablock units performed with two different wave steepnesses has become much closer to each other. It should be noted that $H_{1/3}$ in the following graph is used only for the comparison, all other analysis of overtopping is performed with $H_{m0}$ at structure.

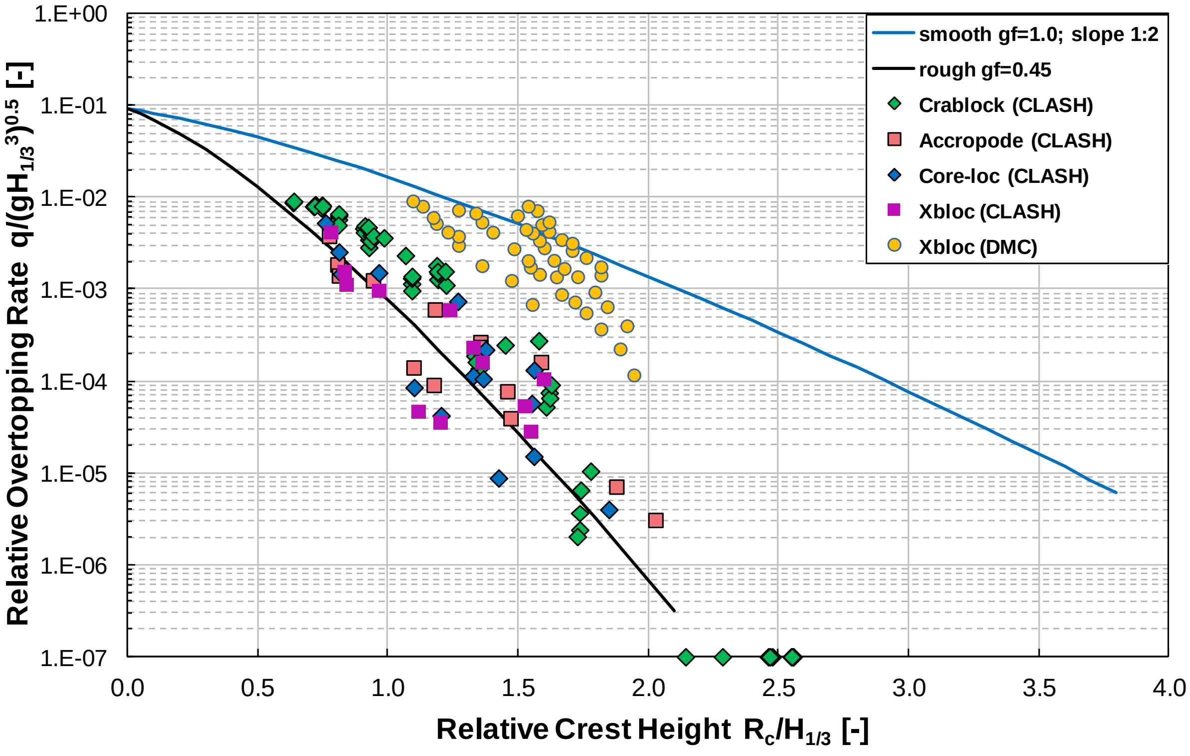


**Figure 5.18** Test results of crablock compare to empirical prediction and other monolayer units (using $H_{1/3}$)

## 5.3.2. Estimation of roughness factor ($\gamma_f$)

As already mentioned, the crablock is a new concrete armour unit and therefore the roughness factor ($\gamma_f$) is not prescribed by EurOtop (2007), yet therefore the value of $\gamma_f$ (= 0.45) was assumed in this research. It is worth mentioning that roughness factors for different armour units prescribed by EurOtop (2007) were derived from CLASH (2004). To make a comparison with CLASH (2004), the measured overtopping results of tests with low wave steepness are discarded here as it is out of CLASH (2004) range, see **section 5.3.1**. In **Figure 5.19**, only test results on overtopping with high wave steepness ($s_{m-1,0} = 0.04$ at deep water) are plotted together with estimated roughness factors. Data points at $10^{-7}$ (in the bottom of the figure) are points with no overtopping. From the graph, it can be seen that test results do not fit with the empirical line assuming roughness factor $\gamma_f$ of 0.45. However, **Figure 5.19** also shows that an estimation of $\gamma_f$ equal to 0.56 overestimates the overtopping results for small overtopping. In most of the cases small overtopping is more interesting to designers compared to very high overtopping for high waves. As presented in **Figure 5.19**, shows that estimation of $\gamma_f$ equal to 0.50 provides a relative good fit in order to compare test results with empirical prediction. Therefore regarding to **Figure 5.19**, it can be concluded that for this specific experimental research (design wave height $H_0 = 0.114$ m), a roughness factor of $\gamma_f$ = 0.50 is suited for empirical prediction of overtopping over crablock slopes for a high wave steepness only. However, it should be noted that the roughness factor of armour also depends on its porosity, which was not considered in the determination of roughness factor.

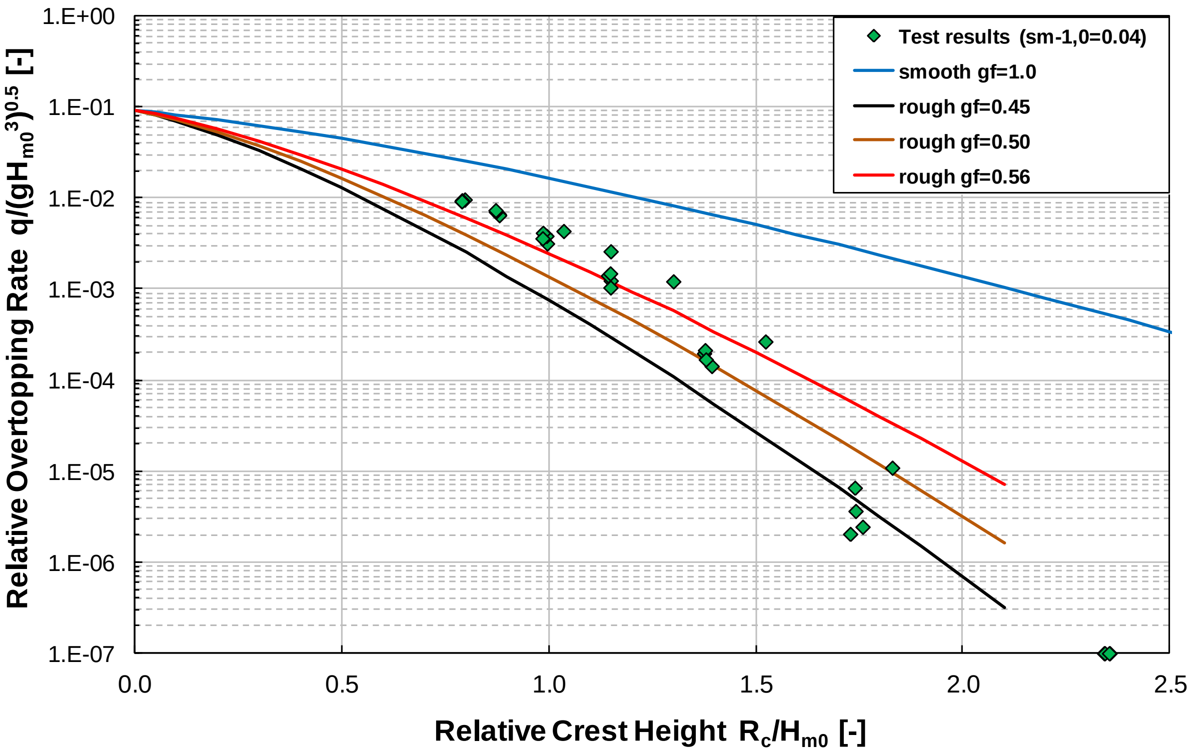


**Figure 5.19** Estimation of roughness factor for high wave steepness ($s_{m-1,0}$ = 0.04), similar to CLASH range.

Similarly, roughness factor also can be predicted for the test results with low wave steepness ($s_{m-1,0}$ = 0.02 at deep water); see **Figure 5.20**. Based on **Figure 5.20**, it is seen that in case of low wave steepness, a roughness factor of $\gamma_f = 0.70$ provides a good fit with the test results. A roughness factor of 0.70 is very high in comparison to roughness factors of other single layer units recommended by CLASH (2004). It should be however noted that this roughness factor considers only tests with low wave steepness, which is not comparable with CLASH (2004) data.

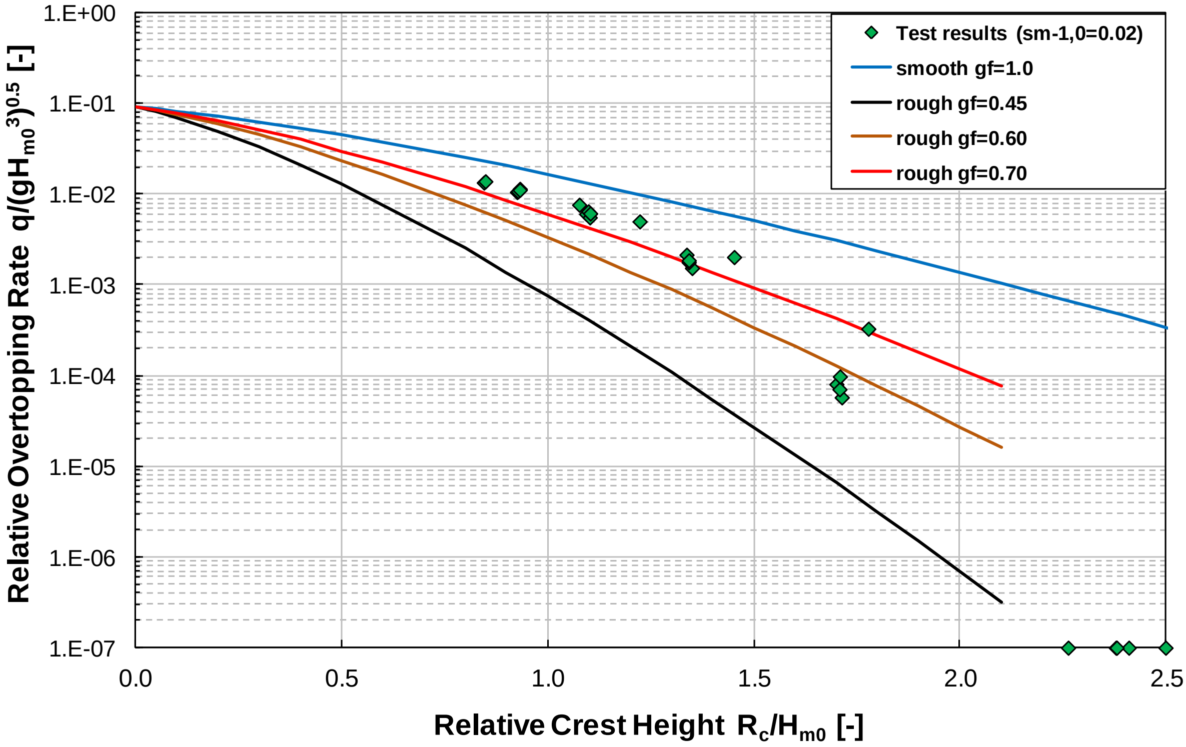


**Figure 5.20** Estimation of roughness factor for low wave steepness ($s_{m-1,0} = 0.02$)

### 5.3.3. Percentage of overtopping waves

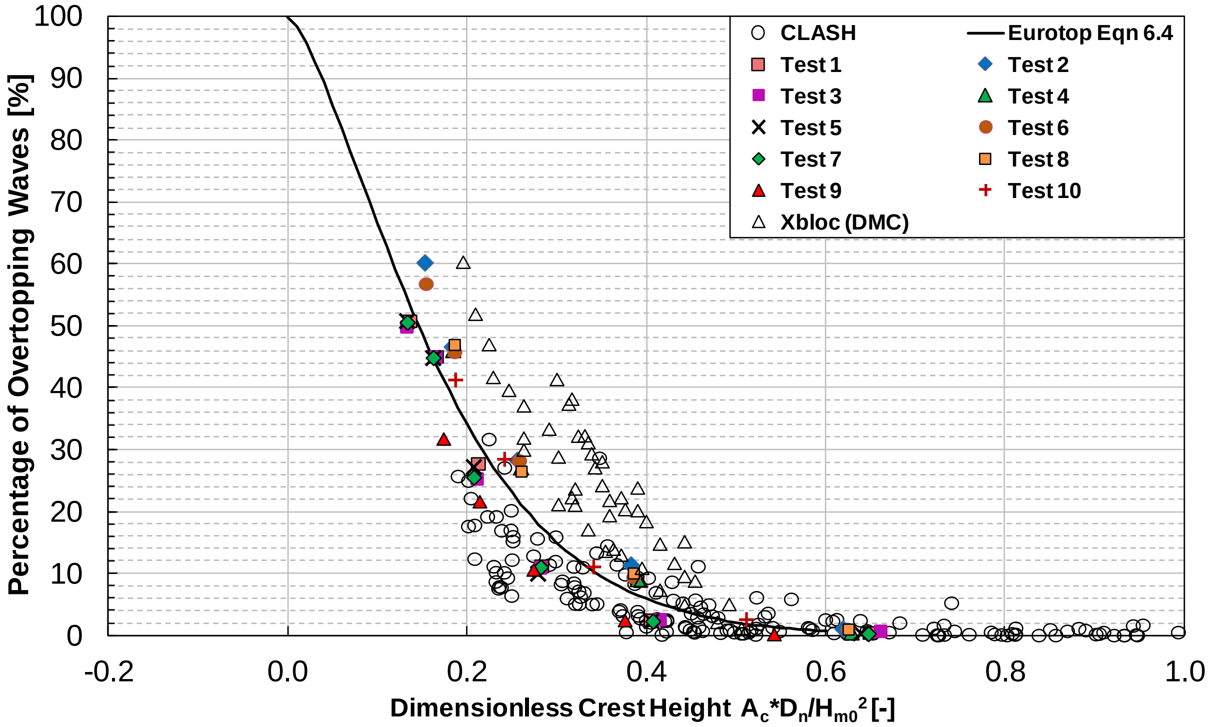


**Figure 5.21** Test results on percentage of overtopping compare to empirical prediction and other single layer units

In **Figure 5.21**, the percentage of waves overtopped over the crablock armour slope in different test series is compared with the results of CLASH (2004), xbloc (DMC, 2003) and with the prediction by the empirical formula. From the resulting graph, it can be seen that for smaller waves the test results are almost within the range of CLASH (2004). It should be noted that CLASH (2004) data contains maximum percentage of overtopping around 30% (EurOtop, 2007). Therefore, the test results on overtopping percentages for higher waves which exceeds 30% are out of CLASH (2004) range and cannot be compared with the database.

Furthermore, based on **Figure 5.21** it is also observed that in comparison to long waves EurOtop (2007) well predict the percentage of overtopping for short waves. For example, for tests 2, 4, 6 and 8 (long wave period) EurOtop (2007) underestimates the percentage of overtopping to some extent while the test results of 1, 3 and 5 (short wave period) are almost on top of EurOtop line.

However, similar to relative overtopping rate (**Figure 5.17**), **Figure 5.21** shows that the overtopping percentage over xbloc by DMC (2003) is also much higher compared to the empirical prediction by EurOtop (2007), outputs of CLASH (2004) and test results of crablock.

# 5.4. Ursell parameter

DMC (2003) introduced Ursell parameter to provide a design formula on wave overtopping over xbloc armour slope. In general, Ursell number is normally used in fluid dynamics to describe the non-linearity of waves in shallow water which can be described as following (DMC, 2003),

$$U_r = \frac{H_{m0} \times L_t^{\,2}}{d^3} \qquad (5.1)$$

In which,
$H_{m0}$ = significant wave height at structure [m]
$L_t$ = local wave length at structure derived from $T_p$ [m]
d = local water depth at structure [m]

Note that using the Ursell parameter means that one completely deviates from the assumptions in EurOtop (2007) that the wave period is more important than the local wave length (using the fictitious wave steepness), see EurOtop (2007), and that for steep slopes the influence of the wave period should be small or not existing. The Ursell parameter gives large influence to the local wave length, which is largely dependent on wave period as well as water depth. It does not say that this line of research is correct, but before the Ursell parameter becomes part of design formulae more analysis is required (and proof that the assumptions in EurOtop is some cases are not correct).

## 5.4.1. Influence of Ursell parameter on test results

As following the approach by DMC (2003), the influence of Ursell parameter on overtopping over crablock armour slope is investigated in this experimental research. In the tests the water depth did not vary. Therefore, the water depth d in the Ursell parameter was a constant and validation should be done by using also other water depths.

The dimensionless overtopping rate divided by Ursell parameter $(q/U_r\sqrt{gH_{m0}^{\,3}})$ with respect to relative crest height is printed in **Figure 5.22**. As a result of introducing Ursell parameter in the relative overtopping, only for higher wave heights the scatter of test results is reduced to some degree, see **Figure 5.22**. Surprisingly, in some cases for the tests with low wave steepness (long period) with higher wave heights the resulting overtopping is found lower than the tests with high wave steepness (short period). On the other hand, without introduction of Ursell parameter, wave overtopping was always found higher for long period, see in **Figure 5.13**. That means Ursell parameter explains wave overtopping in a different way compared to conventional representation of wave overtopping.

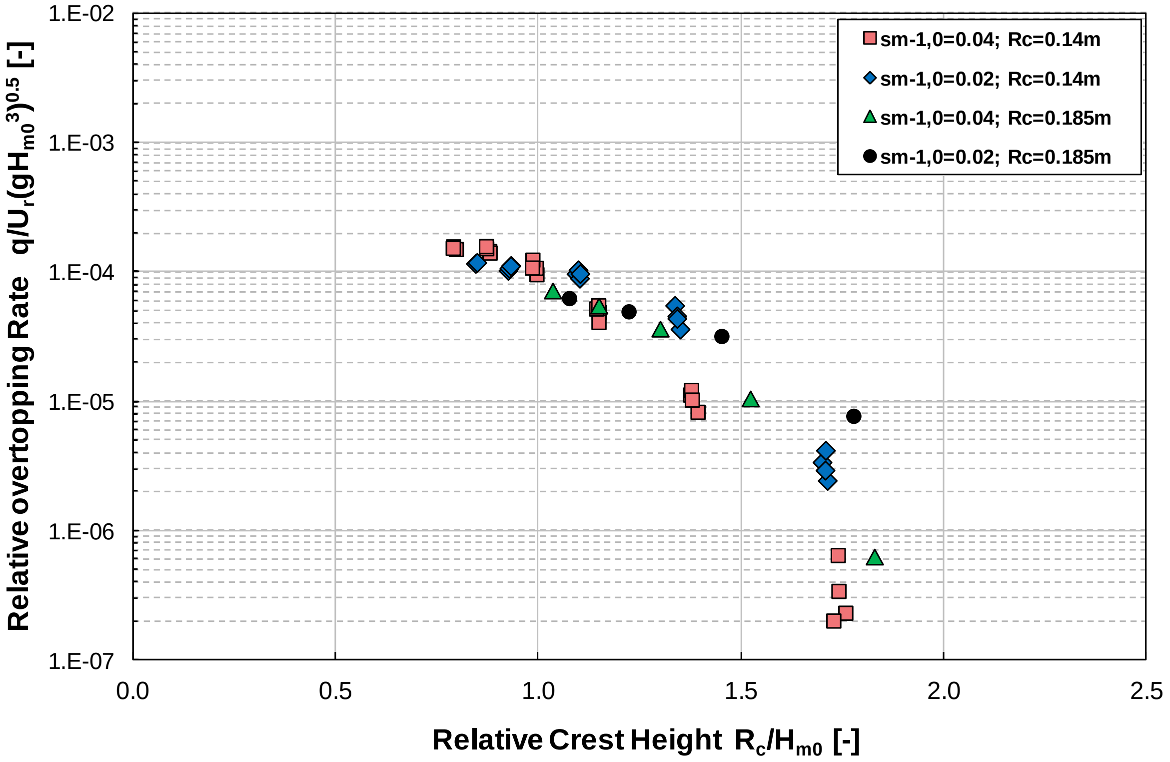


**Figure 5.22** Influence of Ursell parameter on wave overtopping discharge

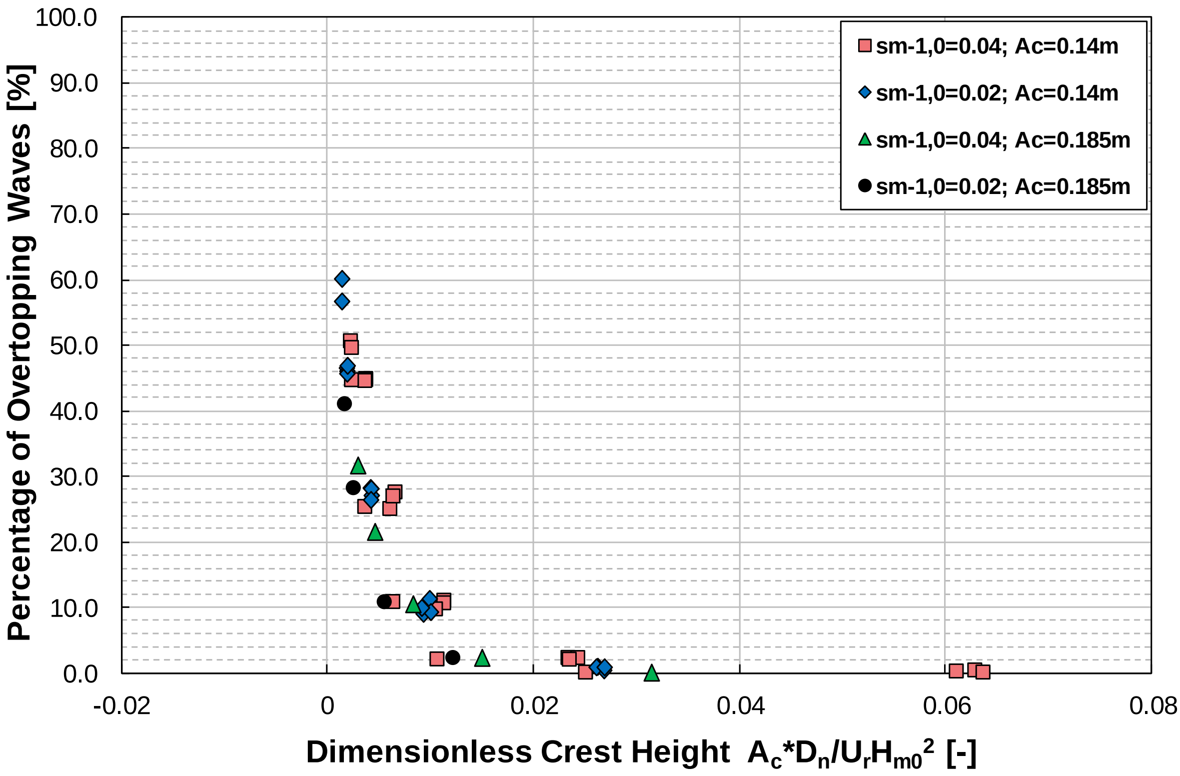


**Figure 5.23** Influence of Ursell parameter on percentage of wave overtopping

Furthermore, the effect of Ursell parameter on the percentages of overtopping over crablock is illustrated in **Figure 5.23**. Based on the comparison of **Figure 5.15** (without Ursell) and **Figure 5.23**, it is seen that in some points scattering of overtopping percentages is somewhat decreased with the introduction of Ursell parameter. Further, it is observed that in some cases tests with low steepness give lower overtopping percentages compare to tests with high steepness, see **Figure 5.23**. On the other hand, a completely different scenario has been observed for the overtopping percentages without considering Ursell parameter (conventional representation), see **Figure 5.15**. Therefore, based on comparison of **Figure 5.15** and **Figure 5.23**, it can be concluded that use of Ursell parameter in the overtopping percentages actually provides untrustworthy outputs.

### 5.4.2. Comparing test results with other units (Ursell parameter)

In **Figure 5.24**, the relative wave overtopping rate divided by Ursell parameter as calculated from CLASH (2004) report, measurements on xbloc by DMC (2003) and test results on crablock during this research is plotted against relative crest height. **Figure 5.24** explains that relative overtopping rate divided by the Ursell parameter is considerably lower for crablock units in comparison to other units.

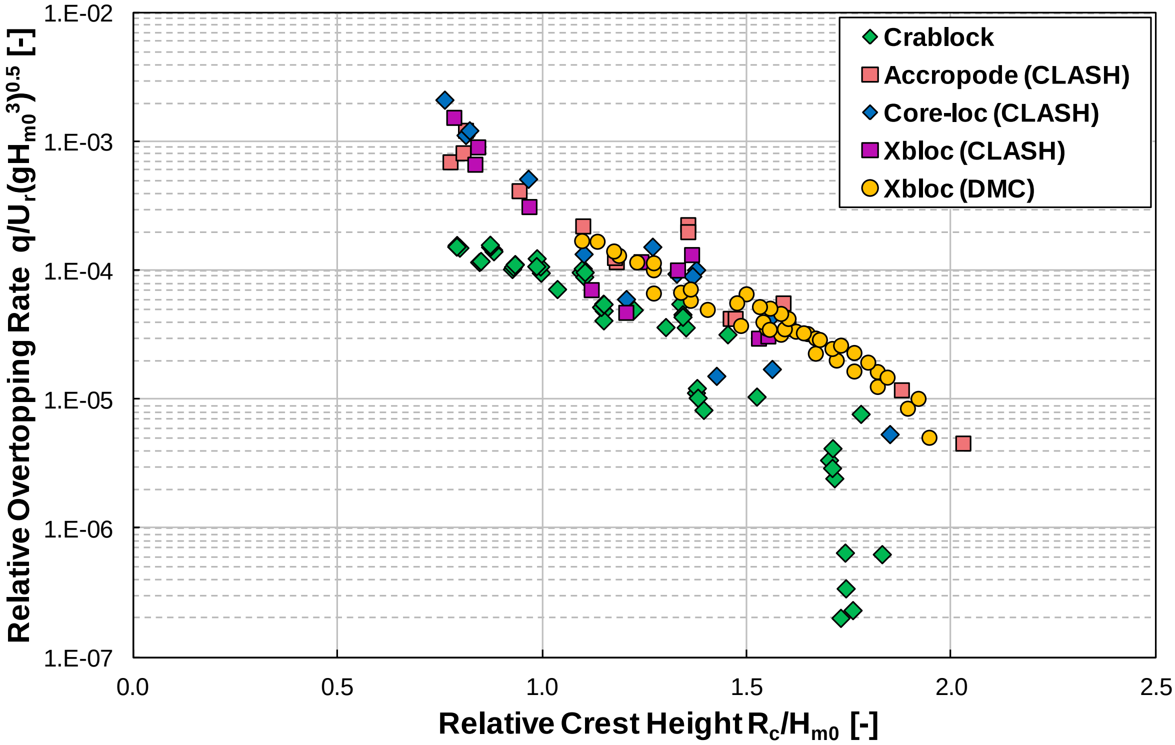


**Figure 5.24** Comparison between relative overtopping including Ursell parameter of crablock and other units

Based on **Figure 5.17** and **Figure 5.24**, it can be observed that for all the armour units presented in figure the scatter in the overtopping can be decreased by using the Ursell parameter. Furthermore, **Figure 5.24** shows that by the use of Ursell parameter the overtopping outputs of different armour units become very close to each other. It has been already mentioned in **section 5.3.1** that CLASH experiments were performed with completely different set up with a different water depth and wave periods in comparison to this experimental research and also experiments on xbloc by DMC (2003). Due to this difference in test set up (foreshore slope), local water depth and wave periods it is hardly possible to compare the overtopping results obtained from different research. However, the Ursell parameter includes the effect of local wave length and local water depth in the overtopping. Therefore, the overtopping outputs of different concrete armour units which have been derived from different experimental research may become closer to each other (**Figure 5.24**) compared to large variation without the use of Ursell parameter (**Figure 5.17**).

Note that the overtopping results for xbloc in **Figure 5.17** are very high, at least a factor of 10-100 larger. This is a very large deviation. Smaller deviations are found for the crablock. It may be coincidence that in **Figure 5.24**, xbloc and CLASH results becomes similar; the problem is now that the crablock results were found a factor of 10-100 lower than the average trend. This is too large to be accepted. It seems that use of the Ursell parameter may explain wave period differences, but introduces also unexpected differences.

## CHAPTER 6

# Conclusions and Recommendations

**The results and discussions for flume tests on wave overtopping are discussed in the previous chapter and for dry placement tests are described in chapter 3 (section 3.5). Based on these observations, the conclusions of this small scale physical tests are presented in this chapter. Furthermore, the chapter ends by giving some recommendations for future research in this area.**

## 6.1. Conclusions

Based on the results analysis and observations, the research questions are answered in this section for each specific question.

- **Which placement techniques perform better for crablock units?**
  - It was found that crablock armour units can be placed in both uniform and random pattern. Furthermore, it was observed that a rectangular grid as well as a diamond-shaped grid is applicable for the placement of crablock as single layer armour units.
  - A regular pattern of crablock was difficult to obtain properly (less uniform pattern than wanted) in a rectangular grid with conventional (large) underlayer. Nevertheless, it should be noted that tests using a conventional underlayer were performed without the fixation of the first row due to the difficulties in placement with model crablock units. If this can be fixated by designing dedicated toe units (both in rotation and location) it may perform better. Still, the large underlayer makes it difficult to place uniformly.
  - The test results and visual inspection showed that regular pattern of crablock can be achieved in a rectangular grid by using relatively small and smooth underlayer. Also, the accuracy of the placement was found slightly better compared to other tests using a large underlayer.
  - In a rectangular grid, accuracy of placement using random pattern was somewhat less compared to uniform pattern.
  - All the tests in a diamond-shaped placing grid were conducted using a conventional large underlayer. The test results showed that regular placement of crablock was hardly achievable in a diamond-shaped grid.
  - Furthermore, it was clearly noticed that in a diamond-shaped grid, random placement pattern can be achieved with higher accuracy and easily in comparison to uniform placement pattern.

❖ **What is the suitable packing density for this new single layer armour unit?**

- A best interlocked uniform pattern of crablock armour units was possible to obtain in a relatively smaller underlayer with the following measured average values:
  - Horizontal placement distance: $0.66\ D$
  - Upslope placement distance: $0.63\ D$
  - Packing density: $0.68/D_n^2$
- It was observed that in a diamond-shaped grid, the randomly oriented crablock units ensures a good interlocked armour with the following measured average values:
  - Horizontal placement distance: $0.75\ D$
  - Upslope placement distance: 0.63 D
  - Packing density: $0.61/\mathrm{D_n^2}$
- Based on the test results, it was recognized that with the use of random pattern lower packing density can be obtained compared to uniform pattern of crablock, where still on visual inspection the slope with armour units looks good.

❖ **What is the wave overtopping discharge and percentage of overtopping waves over crablock slopes?**

In total fourteen independent test series were executed to determine the overtopping rate and percentages over new armour block crablock. Based on the outputs observed in different test series (chapter 5), it was clearly seen that resulting wave overtopping is influenced by the following factors:

- Two different wave steepnesses were tested in this experimental research. Regarding to the test results, it was clear that low wave steepness (long wave period) gives higher overtopping compared to high wave steepness (short wave period).
- Both uniformly placed crablock armour and randomly placed crablock armour were tested to observe the overtopping over slope. Overtopping results showed that there is no influence of placement pattern on wave overtopping.
- The test results with same configuration except different packing density proved that overtopping behaviour does not really change with change in packing density.
- In this experimental research, most of the test series were performed with the use of crest freeboard 1.2 times the design wave height. Only two test series were conducted with very high crest freeboard, 1.6 times the design wave height. Therefore, in this research it is very difficult to conclude about the influence of different crest freeboard on wave overtopping. However, based on the test results it was monitored that different crest height gives unexpectedly deviation in results.
- For higher waves, the scattering of overtopping results can be reduced to some extent by introducing the dimensionless Ursell parameter in the overtopping analysis. However by introducing the dimensionless Ursell parameter, the crablock results were found a factor of 10-100 lower than the average trend. This is too large to accept the Ursell parameter without further research.

❖ **To what extend measured wave overtopping differ with empirical prediction and with other single layer units?**

- Regarding to the test results on overtopping over 1:4/3 smooth slope, it was clearly seen that test results fit satisfactorily with the empirical line of smooth slope 1:4/3 recommended by Van der Meer and Bruce (2014). This certainly validates the measurement of wave heights and overtopping analysis in this laboratory research.
- The relative wave overtopping over crablock obtained in different test series was compared with the empirical prediction provided by Van der Meer and Bruce (2014). It was found that empirical equation with assuming $\gamma_\mathrm{f}$ of 0.45 underestimate the measured wave overtopping over crablock slopes. Regarding to test results, it can be concluded that for this specific experimental research (design wave height $\mathrm{H_0} = 0.114\ \mathrm{m}$), a roughness factor of $\gamma_\mathrm{f} = 0.50$ in case of high wave steepness and $\gamma_\mathrm{f} = 0.70$ in case of low wave steepness provides best fit with empirical prediction.

- The test results of this research proved that longer wave periods also cause additional overtopping. However, the empirical formulas recommended by EurOtop (2007) to estimate overtopping over rubble mound breakwaters indicate that there is no influence of wave period. Indeed, EurOtop (2007) provided the empirical formulas based on a lot of research and corresponding test results. The crablock has extended this area by using large wave periods and there might be influence of large wave period on overtopping.
- The measured relative wave overtopping discharge over crablock was found slightly higher in comparison to CLASH (2004) results on accropode, core-loc and xbloc. This variation was mainly observed for the test results with low wave steepness $s_{m-1,0}$= 0.02 ($s_{op}$= 0.015) which was out of CLASH (2004) range ($s_{op}$= 0.02; 0.035 and 0.05). Besides relatively low wave steepness, most of the tests on crablock were performed with relatively long wave periods compared to CLASH (2004) which was also one of the triggering factor for higher overtopping over crablock slope compared to CLASH (2004). Moreover, the use of sloping foreshore (1:30) instead of horizontal one by CLASH (2004) might also influence the overtopping behaviour. The 1:30 slope changed the shape of the waves and the waves at the structure toe showed a clear increase in velocity of the wave crest (near or at breaking).
- The comparison between the test results on overtopping percentages and prediction by EurOtop (2007) proved that percentage of waves overtopped over crablock can be well predicted by using empirical formula.
- The percentage of overtopping obtained from the test results were also compared with CLASH (2004) outputs. Based on the comparison, it was noticed that for smaller waves the test results are within the range of CLASH outputs.
- However, it was observed that the wave overtopping over crablock is significantly lower compared to the wave overtopping over xbloc measured by DMC (2003). It is worth mentioning that here xbloc and crablock had the same foreshore (1:30) in the test, therefore the test is better comparable.
- The comparison of wave overtopping over different armour slopes with and without Ursell parameter showed completely different scenario. It is recognised that use of the Ursell parameter may explain wave period differences in some cases, but introduces also unexpected differences.

## 6.2. Recommendations

### 6.2.1. Placement of crablock

❖ The placement tests were performed only above water. However, in reality with harsh conditions in deep water the placement of armour units may be more difficult compared to dry conditions. Therefore, placement tests also need to perform under water to have a better knowledge about it.

❖ As it is already mentioned that the placement of units in first row is significantly important and dictate the accuracy of placement. However, in this research all the tests with conventional underlayer were performed without the fixation of first row due to the difficulties in placement with model crablock units. Therefore, placement tests also should be performed to fix the first row by designing the dedicated toe unit for crablock armour.

❖ In these small scale dry tests, all the units were placed only by hand which is not fully realistic. Thus, to observe the accuracy of the placement more precisely, various placement techniques should be tested in a large scale.

❖ In this experimental research, all dry placement tests were conducted in the straight section of breakwater slope. However, placement of armour units in a curved section is always challenging and different in comparison to a straight section of armour layer. Thus, the experimental study should also be performed on the placement of crablock in a curved section of breakwater slope.

❖ The hydraulic tests using designed placement grid should be carried out in order to find a stable armour layer with the correct packing density.

### 6.2.2. Wave overtopping over crablock

- ❖ All the tests were executed considering incident wave attack perpendicular to the breakwater. In future, more tests are recommended with the wave attack from different angle in order to observe the influence of oblique waves on overtopping over crablock.
- ❖ In this research, small scale tests were used to determine the wave overtopping over crablock armour. However, the outputs of small scale model tests could be perverted by scale and model effects (CIRIA, et al., 2007, Hughes, 1993, Wolters, et al., 2009). In order to minimize model effects by stopping reflection from model boundaries active wave reflection system was activated prior to test. Further, to avoid unwanted error in measurements of wave heights, wave gauges were calibrated before starting the each test. Despite all these measures, more tests are recommended to do in a larger scale in order to validate the test results and to check the scale/model effects.
- ❖ The effects of wind on overtopping did not take into account in this research. Nevertheless, in reality overtopping discharge is influenced by wind therefore the resulting overtopping by small scale tests also differs from the prototype situation, particularly for little overtopping discharges (De Rouck, et al., 2005, Lykke Andersen, et al., 2011). Therefore, it is suggested to perform more tests with considering influences of wind on overtopping.
- ❖ As stated earlier, the recommended roughness factor of different armour units for empirical prediction by EurOtop (2007) are based on the outputs of CLASH (2004) experiments. However, it is already mentioned that set up of flume tests used in this research was quite a bit different from set up of CLASH (2004). To determine the roughness factor of crablock in line with CLASH (2004), several tests should be performed as highly comparable to CLASH. For instance, additional tests may be possible to conduct with a horizontal foreshore as similar as CLASH.
- ❖ It has been observed from the test results that different crest height gives variation in relative wave overtopping outputs. In this research, two different crest freeboards were designed however most of the tests were conducted by using one fixed crest height. Therefore, to observe the influence of different crest height in relative wave overtopping, additional tests are recommended to perform for a range of crest free board.
- ❖ Only limited tests were performed with randomly placed crablock armour. However, to compare the wave overtopping over uniformly and irregularly placed crablock, further experiments should be performed with random placement.
- ❖ The water depth at structure was kept constant for all the tests therefore the water depth d in the Ursell parameter was also a constant and validation should be done by using also other water depths.

# References


Bakker P, Muttray M, Reedijk B, Van Den Berge A, Klabbers M, Rovers I (2003) Development of concrete breakwater armour units. Paper presented at the 1st Coastal, Estuary and Offshore Engineering Specially Conference of the Canadian Society for Civil Engineering, New Brunswick, Canada, 2003

Bakker P, Muttray M, Klabbers M, Berge Avd (2005) Hydraulic Performance of Xblock Armour Units. Paper presented at the 1st International Conference on Coastal Zone Management and Engineering, Middle East, Dubai, November 2005

Battjes JA, Groenendijk HW (2000) Wave height distributions on shallow foreshores. Coastal Engineering, 40: pp. 161-182, DOI 10.1016/S0378-3839(00)00007-7

Besley P, Denechere M (2010) Single layer armour systems - Toe, crest and roundhead details. Proceedings of the 9th International Conference on Coasts, Marine Structures and Breakwaters: Adapting to Change, Edinburgh, pp. 128-141

Bettington SH, Klabbers M, Carley JT (2011) Australian experience with randomly orientated single layer concrete armour for breakwaters and revetments. Paper presented at the 20th Australasian Coastal and Ocean Engineering Conference 2011, COASTS 2011 and the 13th Australasian Port and Harbour Conference 2011, PORTS 2011, Perth, WA, 2011

Bonfantini F (2014) Set-up to design guidance for the Crablock armour unit. UNESCO-IHE Institute of Water Education, Delft,Netherlands

Bruce T, van der Meer JW, Franco L, Pearson JM (2009) Overtopping performance of different armour units for rubble mound breakwaters. Coastal Engineering, 56: pp. 166-179, DOI http://dx.doi.org/10.1016/j.coastaleng.2008.03.015

CIRIA, CUR, CETMEF (2007) The Rock Manual. The use of rock in hydraulic engineering 2nd edn, C683, CIRIA, London, pp. 306-368, 486-600

CLASH (2004) Crest Level Assessment of coastal Structures by full scale monitoring, neural network prediction and Hazard analysis on permissible wave overtopping. EC-contract EVK3-CT-2001-00058, www.clash-eu.org

CLI (2011a) ACCROPODE™_Brochure. http://concretelayer.com/sites/default/files/ACCROPODE%E2%84%A2_Brochure.pdf. Cited 24th September 2014

CLI (2011b) THE ACCROPODE™ II UNIT "Technology, experience and cost-effectiveness in a single concrete unit for breakwater armouring ". http://concretelayer.com/sites/default/files/ACCROPODE_II_Doc_Incl._Refs_0.pdf. Cited 24th September 2014

CLI (2012) CORE-LOC™_Brochure. http://concretelayer.com/sites/default/files/CORE-LOC%E2%84%A2_Brochure.pdf. Cited 24th September 2014

CSIR (2009) Crablock Armour Unit 2D Physical Model Study. Built Environment, CSIR, Stellenbosch, Republic of South Africa

De Rouck J, Geeraerts J, Troch P, Kortenhaus A, Pullen T, Franco L (2005) New results on scale effects for wave overtopping at coastal structures. Proceedings of the International Conference on Coastlines, Structures and Breakwaters 2005, ICE, Thomas Telford, London, United Kingdom, pp. 29-43

DMC (2003) Hydraulic Performance of Xbloc armour units -2-D model tests at WL Delft, Delta Marine Consultants, Netherlands

DMC (nd) Overview of breakwater armour history. http://www.xbloc.com/upload/documents/downloads/Overview%20breakwater%20armour%20units.pdf. Cited 24 September 2014

EurOtop (2007) EurOtop- Wave Overtopping of Sea Defences and Related Structures: Assessment Manual In: UK: Pullen TB, T. NWH Allsop. NL: JW van der Meer. DE: H. Schüttrumpf, A. Kortenhaus. (ed), http://www.overtopping-manual.com/eurotop.pdf

Frens AB (2007) The impact of placement method on Antifer-block stability. Master of Science, Delft University of Technology

Gómez-Martín ME, Medina JR (2006) Damage progression on cube armored breakwaters. Proceedings of the 30th International Conference on Coastal Engineering 2006, World Scientific, San Diego, CA, pp. 5229-5240

Gómez-Martín ME, Medina JR (2007) Cubipod Concrete Armour Unit and Heterogeneous Packing. Proceedings of the 5th International Conference on Coastal Structures, World ScientificPublishing Co. Pte. Ltd., Venice, Italy, pp. 140-151

Hendrikse C (2014) CRABLOCK™-Concrete armour unit Originating from GCC. A M MARINE WORKS, Van Der Meer Consulting, Akkrum, NL

Hendrikse C, Heijboer D (2014) Hydraulic Design Conditions and Marine Structures design Philosophy: The UAE Case. Paper presented at the The 7th Annual Arabian World Construction Summit, Dubai, UAE, 2014

Hughes SA (1993) Physical models and laboratory techniques in coastal engineering. World Scientific, Singapore, River Edge, NJ, pp. 5-15

Jensen OJ (nd) Safety of Breakwater Armour Layers with Special Focus on Monolayer Armour Units. http://www.dansk-vandbygning.dk/sites/default/files/Safety%20of%20breakwater%20armour%20layers%20final%20update%2001%20Aug%20ojj%20final%20%202013.pdf. Cited 24th Sepetember 2014

Klopman G, Van Der Meer JW (1999) Random wave measurements in front of reflective structures. Journal of Waterway, Port, Coastal and Ocean Engineering, 125: pp. 39-45, DOI 10.1061/(ASCE)0733-950X(1999)125:1(39)

LeBaron JW (1999) Stability of A-Jacks™-Armoured Rubble-Mound Breakwaters Subjected to Breaking and Non-Breaking Waves with No Overtopping. Master of Science in Civil Engineering, Oregon State University

Lykke Andersen T, Burcharth HF, Gironella X (2011) Comparison of new large and small scale overtopping tests for rubble mound breakwaters. Coastal Engineering, 58: pp. 351-373, DOI 10.1016/j.coastaleng.2010.12.004

Mansard EPD, Funke ER (1980) The measurement of incident and reflected spectra using a least squares method. Proceedings of the 17th International Conference on Coastal Engineering, ASCE, New York, pp. 154-172

Medina JR, Gómez-Martín ME (2012) KD and safety factors of concrete armor units. Paper presented at the 33rd International Conference on Coastal Engineering, Santander, Spain, 1 July 2012 through 6 July 2012

Melby JA, ASCE AM, Turk GF (1994) The Core-loc: optimized concrete armor. Proceedings of the 24th International Conference on Coastal Engineering, ASCE, United States, pp. 1426-1438

Muttray M, Reedijk B, M. K (2003) Development of an Innovative Breakwater Armour Unit. Paper presented at the Coasts & Ports Australasian Conference, New Zealand, September 2003

Muttray M, Reedijk J, Vos-Rovers I, Bakker P (2005) Placement and structural strength of Xbloc® and other single layer armour units. Proceedings of the International Conference on Coastlines, Structures and Breakwaters 2005, ICE, Thomas Telford Ltd, London, pp. 556-567

Muttray M, Reedijk B (2009) Design of Concrete Armour Layers. Hansa International Maritime Journal, 6: pp. 111 – 118

Nik Mohd Kamel NAM (2007) Experimental Study on Xbloc® Placements for Breakwater Curvature Sections. Master of Science, Delft University of Technology

Oever ET (2006) Theoretical and experimental study on the placement of Xbloc. Master of Science, Delft University of Technology

Phelp D, Tulsi K, Abdulla Al Masaood H, Eissa C (2012) Crablock Concrete Breakwater Armour Unit Development, Modelling and Application in Oman. Proceedings of the 8th International Conference On Coastal And Port Engineering in Developing Countries, PIANC – COPEDEC VIII, IIT Madras, Chennai, INDIA, pp. 1727-1737

Reedijk B, Klabbers M, van den berge A, Hakenberg R (2003) Development Of The Xbloc Breakwater Armour Unit. Paper presented at the 2nd International conference on Port & Maritime R&D and Technology, Singapore, 2003

SPM (1984) Shore protection manual, Fourth edn, Army Coastal Engineering Research Center, Washington

Steendam GJ, Van de meer JW, Verhaeghe H, Besley P, Franco L, Van Gent MRA (2004) The international database on wave overtopping. Proceedings of the 29th International Conference on Coastal Engineering, ASCE, World Scientific, Singapore, pp. 4301-4313

TAW (2002) Technical Report on Wave Run-up and Wave Overtopping at Dikes, In: Van de meer JW (ed), Technical Advisory Committee on Flood Defence, The Netherlands

Van Buchem RV (2009) Stability of a single top layer of cubes. Master of Science, Delft University of Technology

Van der Meer JW (1987a) Stability of breakwater armour layers - design formulae. Coastal Engineering, 11: pp. 219-239

Van der Meer JW (1987b) Stability of rubble mound breakwaters. Stability formula for breakwaters armoured with ACCROPODE (R), Report on basic research H546

Van der Meer JW (1988) Stability of Cubes, Tetrapods and Accropode. Proceedings of the Breakwaters '88 Conference', Design of Breakwaters, Thomas Telford, Eastbourne

Van der Meer JW, Janssen JPFM (1995) Wave run-up and wave overtopping at dikes, In: Kobayashi N, Demirbilek Z (eds), Wave Forces on Inclined and Vertical Wall Structures, ASCE, pp. 1-27

Van der Meer JW (1999) Design of Concrete Armour layers, In: Losada IJ (ed), Proceedings of the International Conference on Coastal Structures '99, Balkema, Rotterdam, Santander, Spain, pp. 213-221

Van Der Meer JW, Van Gent MRA, Pozueta B, Verhaeghe H, Steendam GJ, Medina JR (2005) Applications of a neural network to predict wave overtopping at coastal structures. Proceedings of the International Conference on Coastlines, Structures and Breakwaters 2005, Thomas Telford, London, pp. 259-268

Van der Meer JW, Bruce T (2014) New physical insights and design formulas on wave overtopping at sloping and vertical structures. Journal of Waterway, Port, Coastal and Ocean Engineering, 140, DOI 10.1061/(ASCE)WW.1943-5460.0000221

Van Gent MRA, Spaan GBH, Plate SE, Berendsen E, Van de meer JW, d'Angremond K (1999) Single-layer rubble mound breakwaters. Proceedings of the International Conference on Coastal Structures, Balkema, Santander, Spain, pp. 231-239

Vanhoutte L (2009) Hydraulic stability of Cubipod armour units in Breaking conditions. Master of Science in Civil Engineering, Ghent University

Verhagen HJ, Van Vledder G, Arab SE (2008) A practical method for design of coastal structures in shallow water. Proceedings of the 31th International Conference on Coastal Engineering, World Scientific: Hackensack, Hamburg, Germany, pp. 2912-2922

Wolters G, Van Gent M, Allsop W, Hamm L, Mühlestein D (2009) HYDRALAB III: Guidelines for physical model testing of rubble mound breakwaters. Proceedings of the 9th International Conference on Coasts, Marine Structures and Breakwaters: Adapting to Change, Edinburgh, United Kingdom, pp. 659-670

# Appendices

## Appendix A Visual inspection of placement tests

It is worth mentioning that picture of the one sub test from each test series has been included in the description of test series **(section 3.3),** is now excluded in this section. Therefore, for each test series two pictures from two repetition tests have been attached here.

Test 1.2

Test 1.3

**Figure A.1** Photos of placement test series one

Test 2.2

Test 2.3

**Figure A.2** Photos of placement test series two

Test 3.1

Test 3.3

**Figure A.3** Photos of placement test series three

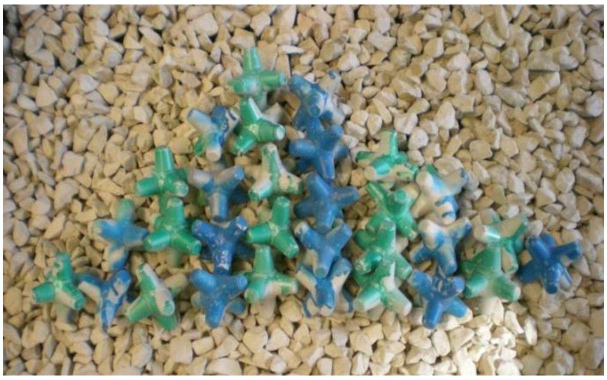

Test 4.1

Test 4.3

**Figure A.4** Photos of placement test series four

Test 5.1

Test 5.3

**Figure A.5** Photos of placement test series five

Test 6.1 | Test 6.3

**Figure A.6** Photos of placement test series six

Test 7.1 | Test 7.3

**Figure A.7** Photos of placement test series seven

Test 8.1 | Test 8.2

**Figure A.8** Photos of placement test series eight

Test 9.2

Test 9.3

**Figure A.9** Photos of placement test series nine

Test 10.1

Test 10.3

**Figure A.10** Photos of placement test series ten

Test 11.1

Test 11.2

**Figure A.11** Photos of placement test series eleven

Test 12.2

Test 12.3

**Figure A.12** Photos of placement test series twelve

Test 13.1

Test 13.2

**Figure A.13** Photos of placement test series thirteen

Test 14.1

Test 14.2

**Figure A.14** Photos of placement test series fourteen

# Appendix B Result analysis of placement tests

## 1. Deviation of units from intended position

In this part, the measured average horizontal and upslope deviation of units from its intended position are plotted for each individual dry placement test series.

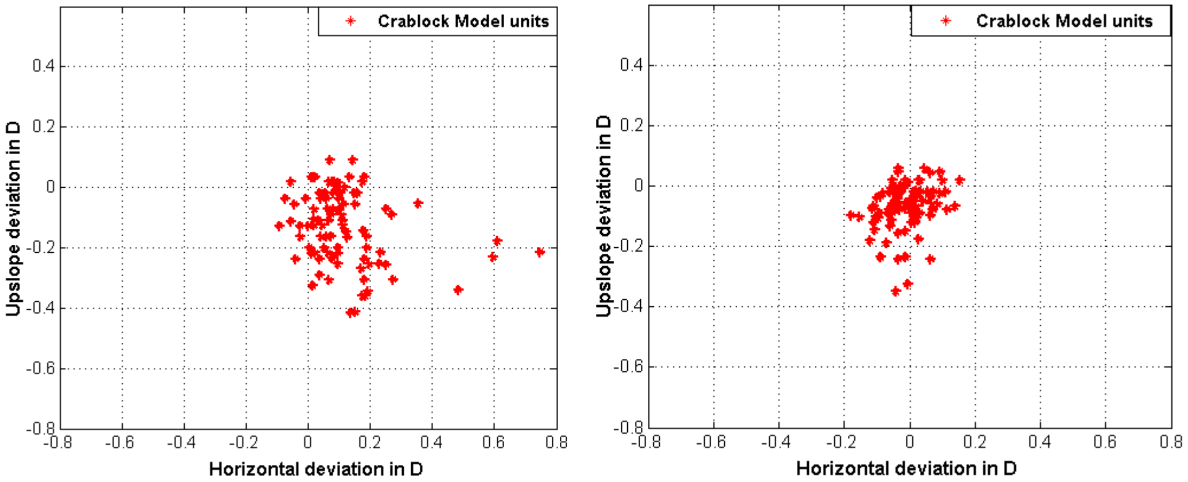


Test Series 1

Test Series 2

**Figure B.1** Deviation of units from intended position in test series 1 and 2

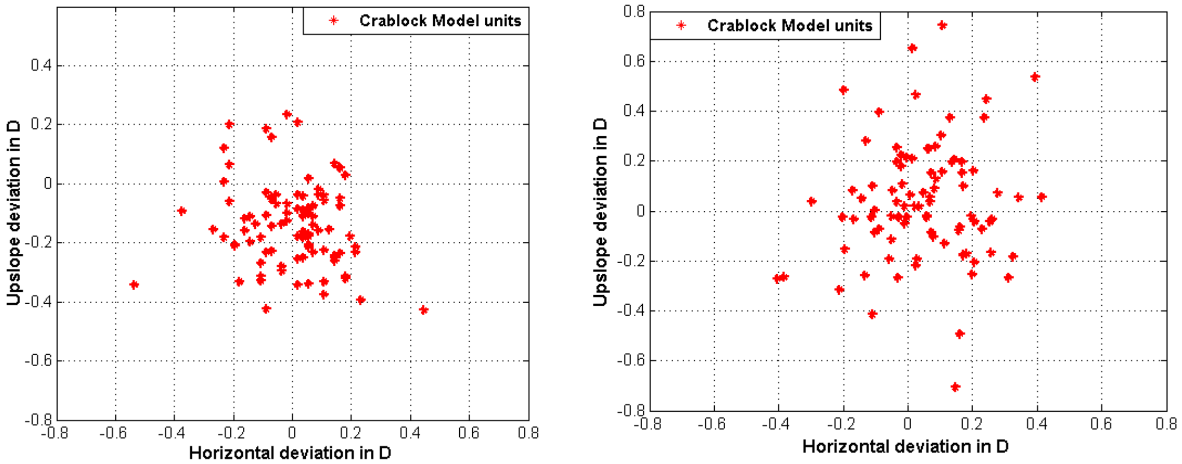


Test Series 3

Test Series 4

**Figure B.2** Deviation of units from intended position in test series 3 and 4

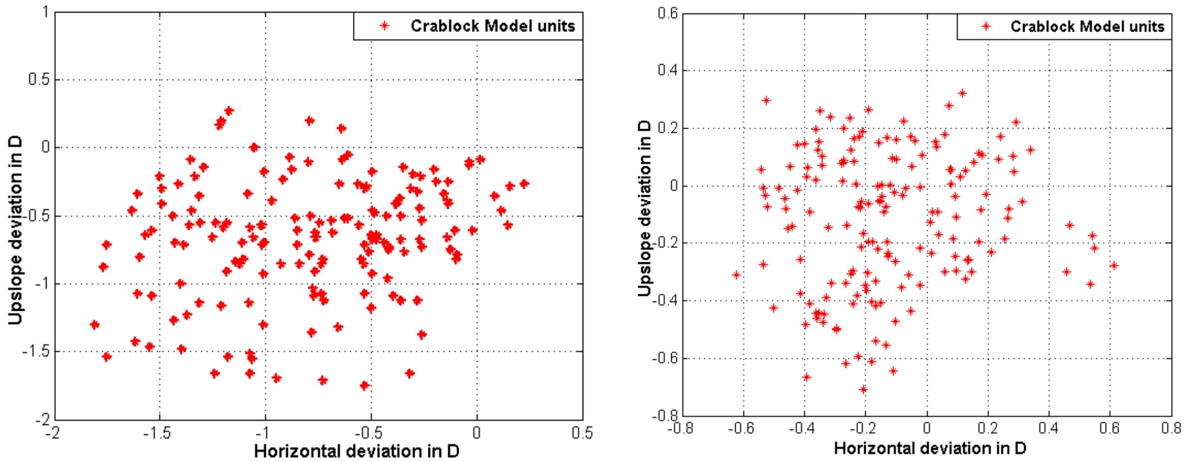


Test Series 5 Test Series 6

**Figure B.3** Deviation of units from intended position in test series 5 and 6

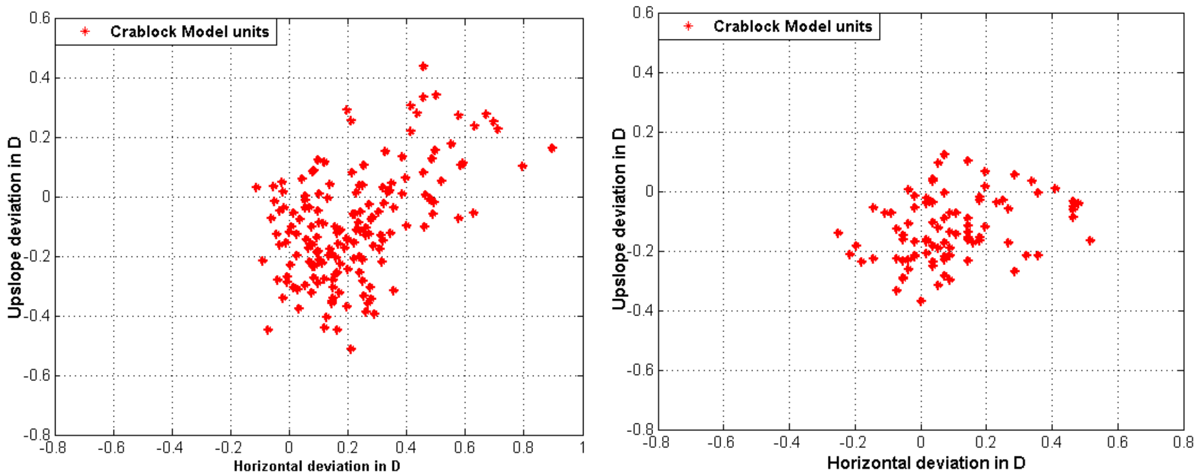


Test Series 7 Test Series 8

**Figure B.4** Deviation of units from intended position in test series 7 and 8

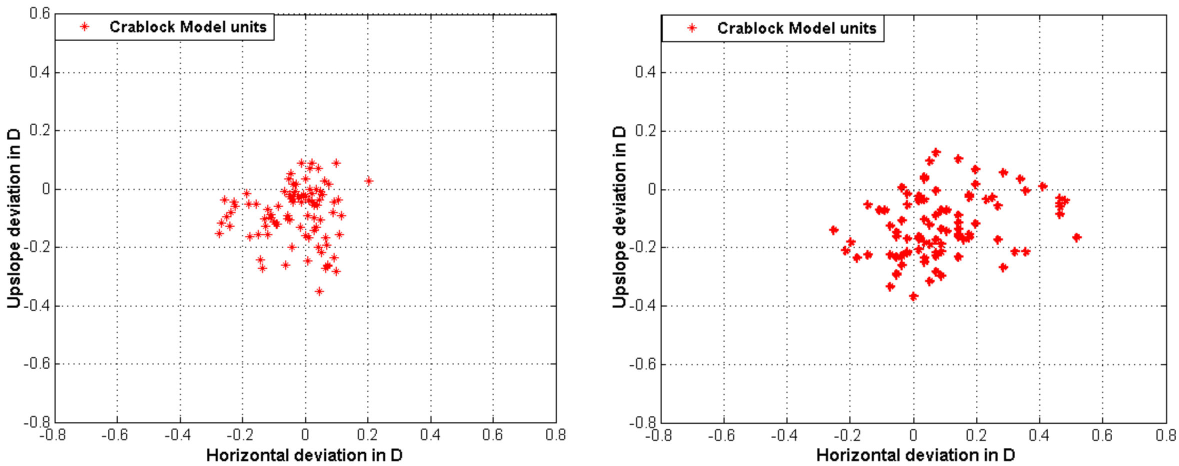


Test Series 9 Test Series 10

**Figure B.5** Deviation of units from intended position in test series 9 and 10

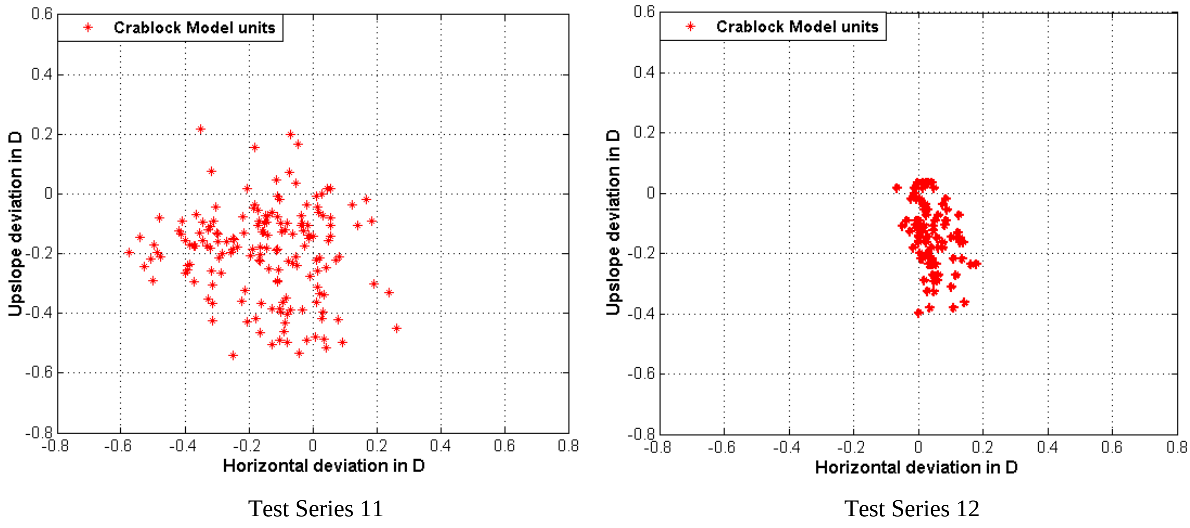


**Figure B.6** Deviation of units from intended position in test series 11 and 12

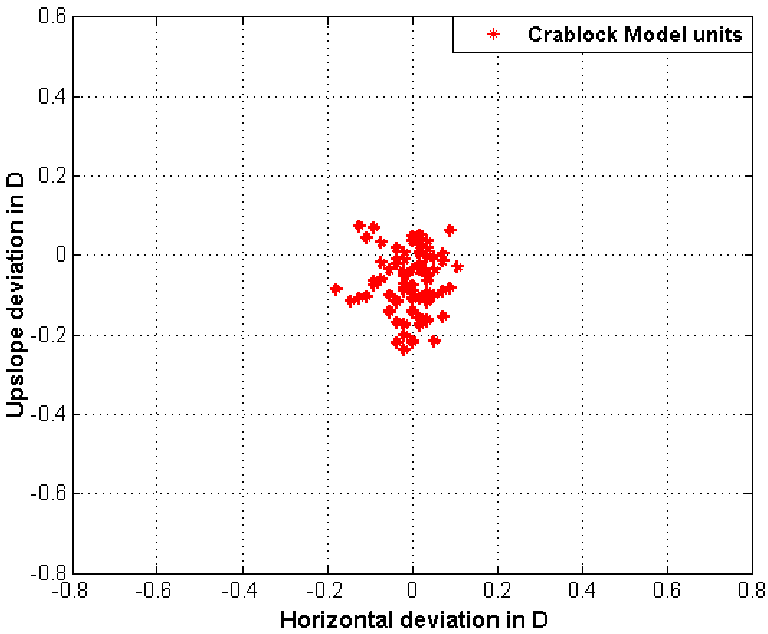


**Figure B.7** Deviation of units from intended position in test series 14

## 2. Packing density

The measured packing density in different forms with respect to designed packing density for each test series is printed in **Table B.1**.

**Table B.1** Packing density for all the test series

| Test series no | Designed packing density (per $D_n^2$) | Measured packing density | | |
|---|---|---|---|---|
| | | PD in $D_n$ | PD in D | PD in Units/$m^2$ |
| 1 | $0.71/D_n^2$ | $0.65/D_n^2$ | $2.26/D^2$ | 723 |
| 2 | $0.74/D_n^2$ | $0.71/D_n^2$ | $2.46/D^2$ | 789 |
| 3 | $0.59/D_n^2$ | $0.59/D_n^2$ | $2.06/D^2$ | 656 |
| 4 | $0.60/D_n^2$ | $0.52/D_n^2$ | $1.81/D^2$ | 578 |
| 5 | $0.96/D_n^2$ | $0.54/D_n^2$ | $1.89/D^2$ | 600 |
| 6 | $0.68/D_n^2$ | $0.62/D_n^2$ | $2.15/D^2$ | 689 |
| 7 | $0.55/D_n^2$ | $0.58/D_n^2$ | $2.02/D^2$ | 645 |
| 8 | $0.71/D_n^2$ | $0.63/D_n^2$ | $2.20/D^2$ | 700 |
| 9 | $0.74/D_n^2$ | $0.67/D_n^2$ | $2.34/D^2$ | 745 |
| 10 | $0.59/D_n^2$ | $0.58/D_n^2$ | $2.03/D^2$ | 645 |
| 11 | $0.68/D_n^2$ | $0.61/D_n^2$ | $2.11/D^2$ | 678 |
| 12 | $0.71/D_n^2$ | $0.63/D_n^2$ | $2.18/D^2$ | 700 |
| 13 | $0.74/D_n^2$ | $0.68/D_n^2$ | $2.39/D^2$ | 756 |
| 14 | $0.59/D_n^2$ | $0.58/D_n^2$ | $2.01/D^2$ | 645 |

# Appendix C Measured wave conditions

Note that test series 13 and 14 were performed without structure in the flume. Further, calibrated wave heights (test series 1-12) at structure presented in **Table C.1**, **Table C.2** and **Table C.3** are the wave heights determined from the established relationship between wave height with and without structure, see in **section 5.1**.

**Table C.1** Measured wave conditions in test series 1-3

| Test Series | Sub-Test No. | Wave Generator | | Near Structure | | | | | | | | Deep Water | | | | | | | |
|---|---|---|---|---|---|---|---|---|---|---|---|---|---|---|---|---|---|---|---|
| | | $H_{m0}$ [m] | $T_p$ [s] | $H_{m0}$ [m] | Calibrated $H_{m0}$ [m] | $H_{1/3}$ [m] | Calibrated $H_{1/3}$ [m] | $T_p$ [s] | $T_{m-1,0}$ [s] | $s_{op}$ | Ref. Coff | $H_{m0}$ [m] | $H_{1/3}$ [m] | $T_p$ [s] | $T_m$ [s] | $T_{m-1,0}$ [s] | $s_{op}$ | $s_{m-1,0}$ | Ref. Coff |
| 1 | 1a | 0.07 | 1.24 | 0.058 | 0.059 | 0.057 | 0.057 | 1.25 | 1.15 | 0.024 | 0.41 | 0.067 | 0.067 | 1.25 | 1.08 | 1.15 | 0.028 | 0.033 | 0.31 |
| | 1b | 0.10 | 1.43 | 0.081 | 0.080 | 0.080 | 0.080 | 1.43 | 1.32 | 0.025 | 0.45 | 0.096 | 0.096 | 1.45 | 1.22 | 1.32 | 0.029 | 0.04 | 0.31 |
| | 1c | 0.13 | 1.60 | 0.100 | 0.102 | 0.102 | 0.105 | 1.63 | 1.49 | 0.025 | 0.48 | 0.125 | 0.126 | 1.61 | 1.34 | 1.47 | 0.031 | 0.04 | 0.32 |
| | 1d | 0.16 | 1.75 | 0.121 | 0.122 | 0.128 | 0.128 | 1.91 | 1.64 | 0.026 | 0.52 | 0.152 | 0.155 | 1.74 | 1.47 | 1.61 | 0.032 | 0.04 | 0.32 |
| | 1e | 0.19 | 1.89 | 0.140 | 0.141 | 0.162 | 0.151 | 1.97 | 1.81 | 0.027 | 0.54 | 0.177 | 0.182 | 1.84 | 1.59 | 1.73 | 0.034 | 0.04 | 0.31 |
| | 1f | 0.22 | 2.02 | 0.156 | 0.159 | 0.193 | 0.174 | 2.07 | 1.90 | 0.025 | 0.54 | 0.203 | 0.210 | 2.01 | 1.68 | 1.86 | 0.032 | 0.04 | 0.30 |
| | 1g | 0.25 | 2.15 | 0.164 | 0.176 | 0.207 | 0.194 | 2.18 | 1.97 | 0.023 | 0.57 | 0.225 | 0.235 | 2.23 | 1.84 | 1.95 | 0.029 | 0.04 | 0.28 |
| 2 | 2a | 0.07 | 1.73 | 0.058 | 0.056 | 0.058 | 0.055 | 1.71 | 1.63 | 0.012 | 0.50 | 0.065 | 0.068 | 1.74 | 1.45 | 1.59 | 0.014 | 0.02 | 0.35 |
| | 2b | 0.10 | 2.07 | 0.081 | 0.082 | 0.093 | 0.086 | 2.09 | 1.97 | 0.013 | 0.57 | 0.098 | 0.097 | 2.01 | 1.69 | 1.90 | 0.016 | 0.02 | 0.36 |
| | 2c | 0.13 | 2.36 | 0.093 | 0.105 | 0.120 | 0.118 | 2.33 | 2.28 | 0.013 | 0.65 | 0.126 | 0.126 | 2.26 | 1.90 | 2.16 | 0.016 | 0.02 | 0.35 |
| | 2d | 0.16 | 2.61 | 0.106 | 0.128 | 0.136 | 0.154 | 2.54 | 2.44 | 0.013 | 0.70 | 0.156 | 0.160 | 2.56 | 2.14 | 2.37 | 0.015 | 0.02 | 0.33 |
| | 2e | 0.19 | 2.85 | 0.143 | 0.151 | 0.158 | 0.188 | 2.39 | 2.17 | 0.011 | 0.60 | 0.185 | 0.191 | 2.99 | 2.30 | 2.56 | 0.013 | 0.02 | 0.32 |
| | 2f | 0.22 | 3.06 | 0.150 | 0.166 | 0.167 | 0.220 | 2.58 | 2.14 | 0.012 | 0.59 | 0.203 | 0.220 | 3.02 | 2.48 | 2.70 | 0.014 | 0.02 | 0.31 |
| 3 | 3a | 0.07 | 1.24 | 0.058 | 0.060 | 0.057 | 0.057 | 1.24 | 1.16 | 0.025 | 0.34 | 0.068 | 0.067 | 1.25 | 1.05 | 1.15 | 0.028 | 0.033 | 0.26 |
| | 3b | 0.10 | 1.43 | 0.080 | 0.080 | 0.080 | 0.081 | 1.44 | 1.32 | 0.024 | 0.39 | 0.095 | 0.096 | 1.45 | 1.28 | 1.32 | 0.029 | 0.04 | 0.27 |
| | 3c | 0.13 | 1.60 | 0.100 | 0.100 | 0.101 | 0.104 | 1.52 | 1.49 | 0.025 | 0.42 | 0.123 | 0.125 | 1.61 | 1.34 | 1.47 | 0.030 | 0.04 | 0.28 |
| | 3d | 0.16 | 1.75 | 0.122 | 0.122 | 0.129 | 0.128 | 1.74 | 1.64 | 0.026 | 0.46 | 0.152 | 0.154 | 1.74 | 1.47 | 1.61 | 0.032 | 0.04 | 0.29 |
| | 3e | 0.19 | 1.89 | 0.142 | 0.141 | 0.163 | 0.151 | 1.97 | 1.79 | 0.025 | 0.49 | 0.178 | 0.182 | 1.9 | 1.58 | 1.75 | 0.032 | 0.04 | 0.29 |
| | 3f | 0.22 | 2.02 | 0.155 | 0.159 | 0.193 | 0.173 | 2.05 | 1.91 | 0.025 | 0.50 | 0.202 | 0.209 | 2.01 | 1.68 | 1.86 | 0.032 | 0.04 | 0.28 |
| | 3g | 0.25 | 2.15 | 0.166 | 0.178 | 0.209 | 0.196 | 2.16 | 1.97 | 0.024 | 0.51 | 0.227 | 0.237 | 2.16 | 1.78 | 1.96 | 0.031 | 0.04 | 0.26 |

**Table C.2** Measured wave conditions in test series 4-6

| Test Series | Sub-Test No. | Wave Generator | | Near Structure | | | | | | | | Deep Water | | | | | | | |
|---|---|---|---|---|---|---|---|---|---|---|---|---|---|---|---|---|---|---|---|
| | | $H_{m0}$ [m] | $T_p$ [s] | $H_{m0}$ [m] | Calibrated $H_{m0}$ [m] | $H_{1/3}$ [m] | Calibrated $H_{1/3}$ [m] | $T_p$ [s] | $T_{m-1,0}$ [s] | $s_{op}$ | Ref. Coff | $H_{m0}$ [m] | $H_{1/3}$ [m] | $T_p$ [s] | $T_m$ [s] | $T_{m-1,0}$ [s] | $s_{op}$ | $s_{m-1,0}$ | Ref. Coff |
| 4 | 4a | 0.07 | 1.73 | 0.058 | 0.058 | 0.059 | 0.055 | 1.72 | 1.63 | 0.013 | 0.46 | 0.068 | 0.068 | 1.70 | 1.50 | 1.59 | 0.015 | 0.02 | 0.31 |
| | 4b | 0.10 | 2.07 | 0.083 | 0.082 | 0.095 | 0.087 | 2.08 | 1.97 | 0.013 | 0.52 | 0.097 | 0.098 | 2.01 | 1.74 | 1.90 | 0.015 | 0.02 | 0.33 |
| | 4c | 0.13 | 2.36 | 0.106 | 0.104 | 0.123 | 0.118 | 2.37 | 2.13 | 0.012 | 0.56 | 0.125 | 0.126 | 2.36 | 1.92 | 2.17 | 0.014 | 0.02 | 0.32 |
| | 4d | 0.16 | 2.61 | 0.126 | 0.127 | 0.142 | 0.154 | 2.54 | 2.18 | 0.012 | 0.58 | 0.154 | 0.159 | 2.56 | 2.12 | 2.37 | 0.015 | 0.02 | 0.31 |
| | 4e | 0.19 | 2.85 | 0.145 | 0.151 | 0.158 | 0.189 | 2.38 | 2.16 | 0.011 | 0.55 | 0.184 | 0.191 | 2.96 | 2.28 | 2.57 | 0.013 | 0.02 | 0.30 |
| 5 | 5a | 0.07 | 1.24 | 0.058 | 0.060 | 0.057 | 0.057 | 1.25 | 1.14 | 0.025 | 0.38 | 0.068 | 0.068 | 1.23 | 1.07 | 1.15 | 0.029 | 0.033 | 0.29 |
| | 5b | 0.10 | 1.43 | 0.080 | 0.081 | 0.080 | 0.081 | 1.44 | 1.32 | 0.026 | 0.43 | 0.096 | 0.097 | 1.41 | 1.22 | 1.32 | 0.031 | 0.04 | 0.29 |
| | 5c | 0.13 | 1.60 | 0.099 | 0.102 | 0.101 | 0.103 | 1.68 | 1.49 | 0.025 | 0.46 | 0.124 | 0.124 | 1.61 | 1.34 | 1.47 | 0.031 | 0.04 | 0.30 |
| | 5d | 0.16 | 1.75 | 0.120 | 0.123 | 0.128 | 0.128 | 1.74 | 1.75 | 0.025 | 0.49 | 0.153 | 0.155 | 1.79 | 1.46 | 1.61 | 0.031 | 0.04 | 0.30 |
| | 5e | 0.19 | 1.89 | 0.138 | 0.142 | 0.161 | 0.150 | 1.95 | 1.80 | 0.027 | 0.51 | 0.179 | 0.181 | 1.838 | 1.56 | 1.75 | 0.034 | 0.04 | 0.30 |
| | 5f | 0.22 | 2.02 | 0.155 | 0.161 | 0.192 | 0.173 | 2.05 | 1.91 | 0.025 | 0.52 | 0.204 | 0.208 | 2.01 | 1.68 | 1.86 | 0.032 | 0.04 | 0.29 |
| | 5g | 0.25 | 2.15 | 0.165 | 0.177 | 0.207 | 0.195 | 2.16 | 1.97 | 0.024 | 0.54 | 0.227 | 0.236 | 2.16 | 1.79 | 1.96 | 0.031 | 0.04 | 0.27 |
| 6 | 6a | 0.07 | 1.73 | 0.058 | 0.059 | 0.057 | 0.055 | 1.72 | 1.63 | 0.012 | 0.50 | 0.069 | 0.068 | 1.74 | 1.44 | 1.59 | 0.015 | 0.02 | 0.34 |
| | 6b | 0.10 | 2.07 | 0.082 | 0.082 | 0.093 | 0.086 | 2.11 | 1.97 | 0.013 | 0.56 | 0.098 | 0.097 | 2.03 | 1.70 | 1.90 | 0.015 | 0.02 | 0.35 |
| | 6c | 0.13 | 2.36 | 0.093 | 0.104 | 0.120 | 0.117 | 2.33 | 2.28 | 0.013 | 0.65 | 0.126 | 0.126 | 2.26 | 1.93 | 2.16 | 0.016 | 0.02 | 0.34 |
| | 6d | 0.16 | 2.61 | 0.127 | 0.128 | 0.143 | 0.154 | 2.54 | 2.56 | 0.012 | 0.61 | 0.155 | 0.159 | 2.56 | 2.12 | 2.37 | 0.015 | 0.02 | 0.33 |
| | 6e | 0.19 | 2.85 | 0.144 | 0.150 | 0.159 | 0.188 | 2.38 | 2.17 | 0.011 | 0.59 | 0.183 | 0.190 | 2.99 | 2.29 | 2.56 | 0.013 | 0.02 | 0.32 |
| | 6f | 0.22 | 3.06 | 0.153 | 0.165 | 0.167 | 0.220 | 2.58 | 2.13 | 0.011 | 0.58 | 0.202 | 0.220 | 3.05 | 2.45 | 2.70 | 0.014 | 0.02 | 0.31 |

**Table C.3** Measured wave conditions in test series 7-9

| Test Series | Sub-Test No. | Wave Generator | | Near Structure | | | | | | | | Deep Water | | | | | | | |
|---|---|---|---|---|---|---|---|---|---|---|---|---|---|---|---|---|---|---|---|
| | | $H_{m0}$ [m] | $T_p$ [s] | $H_{m0}$ [m] | Calibrated $H_{m0}$ [m] | $H_{1/3}$ [m] | Calibrated $H_{1/3}$ [m] | $T_p$ [s] | $T_{m-1,0}$ [s] | $s_{op}$ | Ref. Coff | $H_{m0}$ [m] | $H_{1/3}$ [m] | $T_p$ [s] | $T_m$ [s] | $T_{m-1,0}$ [s] | $s_{op}$ | $s_{m-1,0}$ | Ref. Coff |
| 7 | 7a | 0.07 | 1.24 | 0.058 | 0.059 | 0.057 | 0.057 | 1.25 | 1.15 | 0.025 | 0.36 | 0.067 | 0.067 | 1.23 | 1.07 | 1.15 | 0.029 | 0.03 | 0.27 |
| | 7b | 0.10 | 1.43 | 0.080 | 0.081 | 0.080 | 0.080 | 1.42 | 1.32 | 0.026 | 0.41 | 0.096 | 0.096 | 1.41 | 1.21 | 1.32 | 0.031 | 0.04 | 0.28 |
| | 7c | 0.13 | 1.60 | 0.100 | 0.102 | 0.102 | 0.105 | 1.66 | 1.49 | 0.026 | 0.44 | 0.124 | 0.126 | 1.57 | 1.34 | 1.47 | 0.032 | 0.04 | 0.29 |
| | 7d | 0.16 | 1.75 | 0.121 | 0.122 | 0.129 | 0.128 | 1.74 | 1.65 | 0.024 | 0.47 | 0.152 | 0.154 | 1.79 | 1.47 | 1.61 | 0.030 | 0.04 | 0.29 |
| | 7e | 0.19 | 1.89 | 0.137 | 0.142 | 0.161 | 0.150 | 1.95 | 1.80 | 0.027 | 0.50 | 0.179 | 0.181 | 1.84 | 1.57 | 1.74 | 0.034 | 0.04 | 0.29 |
| | 7f | 0.22 | 2.02 | 0.156 | 0.161 | 0.193 | 0.173 | 2.06 | 1.90 | 0.026 | 0.51 | 0.205 | 0.209 | 2.01 | 1.68 | 1.86 | 0.032 | 0.04 | 0.28 |
| | 7g | 0.25 | 2.15 | 0.165 | 0.177 | 0.208 | 0.195 | 2.16 | 1.97 | 0.024 | 0.53 | 0.227 | 0.236 | 2.16 | 1.78 | 1.96 | 0.031 | 0.04 | 0.26 |
| 8 | 8a | 0.07 | 1.73 | 0.058 | 0.059 | 0.058 | 0.055 | 1.72 | 1.63 | 0.013 | 0.48 | 0.069 | 0.068 | 1.68 | 1.45 | 1.59 | 0.016 | 0.02 | 0.33 |
| | 8b | 0.10 | 2.07 | 0.081 | 0.082 | 0.093 | 0.086 | 2.08 | 1.97 | 0.013 | 0.54 | 0.098 | 0.097 | 2.00 | 1.69 | 1.9 | 0.016 | 0.02 | 0.34 |
| | 8c | 0.13 | 2.36 | 0.103 | 0.104 | 0.123 | 0.118 | 2.35 | 2.17 | 0.012 | 0.58 | 0.126 | 0.126 | 2.36 | 1.93 | 2.17 | 0.014 | 0.02 | 0.33 |
| | 8d | 0.16 | 2.61 | 0.125 | 0.127 | 0.142 | 0.152 | 2.60 | 2.22 | 0.012 | 0.60 | 0.154 | 0.157 | 2.58 | 2.11 | 2.39 | 0.015 | 0.02 | 0.32 |
| | 8e | 0.19 | 2.85 | 0.144 | 0.150 | 0.159 | 0.187 | 2.38 | 2.18 | 0.011 | 0.58 | 0.183 | 0.190 | 2.96 | 2.28 | 2.56 | 0.013 | 0.02 | 0.31 |
| 9 | 9a | 0.07 | 1.24 | 0.058 | 0.059 | 0.057 | 0.056 | 1.25 | 1.15 | 0.025 | 0.37 | 0.067 | 0.067 | 1.25 | 1.07 | 1.15 | 0.028 | 0.033 | 0.28 |
| | 9b | 0.10 | 1.43 | 0.082 | 0.081 | 0.081 | 0.081 | 1.44 | 1.32 | 0.025 | 0.42 | 0.096 | 0.097 | 1.45 | 1.22 | 1.32 | 0.029 | 0.04 | 0.29 |
| | 9c | 0.13 | 1.60 | 0.103 | 0.101 | 0.103 | 0.104 | 1.51 | 1.47 | 0.025 | 0.46 | 0.124 | 0.125 | 1.61 | 1.34 | 1.47 | 0.031 | 0.04 | 0.30 |
| | 9d | 0.16 | 1.75 | 0.122 | 0.121 | 0.131 | 0.128 | 1.74 | 1.64 | 0.026 | 0.48 | 0.151 | 0.154 | 1.74 | 1.47 | 1.61 | 0.032 | 0.04 | 0.31 |
| | 9e | 0.19 | 1.89 | 0.142 | 0.142 | 0.165 | 0.151 | 1.95 | 1.79 | 0.027 | 0.51 | 0.179 | 0.182 | 1.84 | 1.58 | 1.74 | 0.034 | 0.04 | 0.30 |
| | 9f | 0.22 | 2.02 | 0.158 | 0.161 | 0.193 | 0.173 | 2.08 | 1.89 | 0.025 | 0.53 | 0.205 | 0.209 | 2.03 | 1.69 | 1.86 | 0.032 | 0.04 | 0.30 |
| | 9g | 0.25 | 2.15 | 0.167 | 0.179 | 0.211 | 0.196 | 2.16 | 1.99 | 0.025 | 0.55 | 0.229 | 0.237 | 2.16 | 1.77 | 1.96 | 0.031 | 0.04 | 0.28 |

**Table C.4** Measured wave conditions in test series 10-12

| Test Series | Sub-Test No. | Wave Generator | | Near Structure | | | | | | | | Deep Water | | | | | | | |
|---|---|---|---|---|---|---|---|---|---|---|---|---|---|---|---|---|---|---|---|
| | | $H_{m0}$ [m] | $T_p$ [s] | $H_{m0}$ [m] | Calibrated $H_{m0}$ [m] | $H_{1/3}$ [m] | Calibrated $H_{1/3}$ [m] | $T_p$ [s] | $T_{m-1,0}$ [s] | $s_{op}$ | Ref. Coff | $H_{m0}$ [m] | $H_{1/3}$ [m] | $T_p$ [s] | $T_m$ [s] | $T_{m-1,0}$ [s] | $s_{op}$ | $s_{m-1,0}$ | Ref. Coff |
| 10 | 10a | 0.07 | 1.73 | 0.057 | 0.059 | 0.057 | 0.055 | 1.72 | 1.62 | 0.013 | 0.48 | 0.069 | 0.068 | 1.70 | 1.46 | 1.59 | 0.015 | 0.02 | 0.32 |
| | 10b | 0.10 | 2.07 | 0.081 | 0.082 | 0.092 | 0.086 | 2.08 | 1.97 | 0.013 | 0.55 | 0.097 | 0.097 | 2.03 | 1.71 | 1.90 | 0.015 | 0.02 | 0.33 |
| | 10c | 0.13 | 2.36 | 0.103 | 0.104 | 0.122 | 0.117 | 2.37 | 2.17 | 0.012 | 0.60 | 0.125 | 0.125 | 2.36 | 1.91 | 2.17 | 0.014 | 0.02 | 0.34 |
| | 10d | 0.16 | 2.61 | 0.127 | 0.127 | 0.142 | 0.152 | 2.54 | 2.21 | 0.012 | 0.62 | 0.155 | 0.157 | 2.58 | 2.10 | 2.39 | 0.015 | 0.02 | 0.33 |
| | 10e | 0.19 | 2.85 | 0.146 | 0.151 | 0.159 | 0.188 | 2.50 | 2.18 | 0.011 | 0.61 | 0.185 | 0.190 | 2.96 | 2.28 | 2.57 | 0.013 | 0.02 | 0.32 |
| | 10f | 0.22 | 3.06 | 0.157 | 0.172 | 0.171 | 0.229 | 2.53 | 2.14 | 0.012 | 0.60 | 0.211 | 0.228 | 3.05 | 2.42 | 2.71 | 0.015 | 0.02 | 0.32 |
| 11 | 11a | 0.07 | 1.24 | 0.045 | 0.059 | 0.057 | 0.057 | 1.24 | 1.26 | 0.024 | 0.89 | 0.067 | 0.067 | 1.26 | 1.04 | 1.14 | 0.027 | 0.033 | 0.67 |
| | 11b | 0.10 | 1.43 | 0.059 | 0.080 | 0.078 | 0.077 | 1.41 | 1.39 | 0.024 | 0.88 | 0.095 | 0.092 | 1.46 | 1.19 | 1.31 | 0.029 | 0.04 | 0.61 |
| | 11c | 0.13 | 1.60 | 0.083 | 0.101 | 0.100 | 0.103 | 1.65 | 1.68 | 0.025 | 0.83 | 0.123 | 0.123 | 1.62 | 1.29 | 1.46 | 0.030 | 0.04 | 0.57 |
| | 11d | 0.16 | 1.75 | 0.106 | 0.121 | 0.127 | 0.126 | 1.70 | 1.83 | 0.026 | 0.83 | 0.151 | 0.152 | 1.72 | 1.38 | 1.59 | 0.033 | 0.04 | 0.54 |
| | 11e | 0.19 | 1.89 | 0.118 | 0.142 | 0.158 | 0.149 | 1.93 | 2.01 | 0.026 | 0.82 | 0.179 | 0.180 | 1.87 | 1.47 | 1.70 | 0.033 | 0.04 | 0.51 |
| | 11f | 0.22 | 2.02 | 0.129 | 0.159 | 0.185 | 0.171 | 2.05 | 2.10 | 0.026 | 0.82 | 0.203 | 0.207 | 1.98 | 1.54 | 1.82 | 0.033 | 0.04 | 0.49 |
| 12 | 12a | 0.07 | 1.73 | 0.046 | 0.059 | 0.059 | 0.055 | 1.69 | 1.89 | 0.013 | 0.85 | 0.068 | 0.068 | 1.71 | 1.39 | 1.56 | 0.015 | 0.02 | 0.60 |
| | 12b | 0.10 | 2.07 | 0.070 | 0.083 | 0.095 | 0.085 | 2.06 | 2.11 | 0.012 | 0.84 | 0.098 | 0.096 | 2.06 | 1.56 | 1.84 | 0.015 | 0.02 | 0.56 |
| | 12c | 0.13 | 2.36 | 0.088 | 0.106 | 0.114 | 0.117 | 2.29 | 2.27 | 0.012 | 0.89 | 0.127 | 0.125 | 2.41 | 1.70 | 2.09 | 0.014 | 0.02 | 0.52 |
| | 12d | 0.16 | 2.61 | 0.107 | 0.129 | 0.124 | 0.154 | 2.39 | 2.40 | 0.013 | 0.97 | 0.156 | 0.159 | 2.54 | 1.86 | 2.35 | 0.016 | 0.02 | 0.50 |
| | 12e | 0.22 | 3.06 | 0.142 | 0.152 | 0.137 | 0.186 | 2.34 | 2.13 | 0.011 | 0.86 | 0.185 | 0.189 | 2.94 | 1.99 | 2.52 | 0.014 | 0.02 | 0.47 |

**Table C.5** Measured wave conditions in test series 13-14 (tests without structure)

| Test Series | Sub-Test No. | Wave Generator | | Near Structure | | | | | | | | Deep Water | | | | | | | |
|---|---|---|---|---|---|---|---|---|---|---|---|---|---|---|---|---|---|---|---|
| | | $H_{m0}$ [m] | $T_p$ [s] | $H_{m0}$ [m] | Calibrated $H_{m0}$ [m] | $H_{1/3}$ [m] | Calibrated $H_{1/3}$ [m] | $T_p$ [s] | $T_{m-1,0}$ [s] | $s_{op}$ | Ref. Coff | $H_{m0}$ [m] | $H_{1/3}$ [m] | $T_p$ [s] | $T_m$ [s] | $T_{m-1,0}$ [s] | $s_{op}$ | $s_{m-1,0}$ | Ref. Coff |
| 13 | 13a | 0.07 | 1.24 | 0.058 | ------- | 0.058 | ------- | 1.25 | 1.15 | 0.024 | 0.12 | 0.067 | 0.067 | 1.25 | 1.06 | 1.14 | 0.028 | 0.033 | 0.10 |
| | 13b | 0.10 | 1.43 | 0.082 | ------- | 0.082 | ------- | 1.41 | 1.30 | 0.026 | 0.15 | 0.096 | 0.096 | 1.42 | 1.21 | 1.31 | 0.030 | 0.04 | 0.10 |
| | 13c | 0.13 | 1.60 | 0.102 | ------- | 0.102 | ------- | 1.58 | 1.43 | 0.025 | 0.16 | 0.124 | 0.125 | 1.62 | 1.34 | 1.46 | 0.030 | 0.04 | 0.11 |
| | 13d | 0.16 | 1.75 | 0.124 | ------- | 0.126 | ------- | 1.76 | 1.55 | 0.026 | 0.18 | 0.153 | 0.153 | 1.74 | 1.47 | 1.60 | 0.032 | 0.04 | 0.10 |
| | 13e | 0.19 | 1.89 | 0.143 | ------- | 0.152 | ------- | 1.91 | 1.67 | 0.026 | 0.19 | 0.181 | 0.183 | 1.87 | 1.58 | 1.73 | 0.033 | 0.04 | 0.09 |
| | 13f | 0.22 | 2.02 | 0.160 | ------- | 0.177 | ------- | 2.04 | 1.76 | 0.024 | 0.21 | 0.206 | 0.209 | 2.04 | 1.68 | 1.84 | 0.031 | 0.04 | 0.10 |
| | 13g | 0.25 | 2.15 | 0.180 | ------- | 0.192 | ------- | 2.17 | 2.26 | 0.025 | 0.30 | 0.229 | 0.235 | 2.14 | 1.80 | 1.94 | 0.032 | 0.04 | 0.10 |
| 14 | 14a | 0.07 | 1.73 | 0.059 | ------- | 0.057 | ------- | 1.68 | 1.56 | 0.013 | 0.12 | 0.069 | 0.068 | 1.70 | 1.44 | 1.58 | 0.015 | 0.02 | 0.09 |
| | 14b | 0.10 | 2.07 | 0.081 | ------- | 0.082 | ------- | 2.11 | 1.87 | 0.012 | 0.13 | 0.098 | 0.097 | 2.06 | 1.70 | 1.89 | 0.015 | 0.02 | 0.10 |
| | 14c | 0.13 | 2.36 | 0.106 | ------- | 0.117 | ------- | 2.39 | 2.11 | 0.012 | 0.15 | 0.126 | 0.127 | 2.37 | 1.95 | 2.15 | 0.014 | 0.02 | 0.10 |
| | 14d | 0.16 | 2.61 | 0.130 | ------- | 0.157 | ------- | 2.58 | 2.24 | 0.012 | 0.16 | 0.157 | 0.158 | 2.64 | 2.11 | 2.35 | 0.014 | 0.02 | 0.10 |
| | 14e | 0.19 | 2.85 | 0.155 | ------- | 0.195 | ------- | 2.89 | 2.63 | 0.013 | 0.19 | 0.187 | 0.193 | 2.75 | 2.27 | 2.53 | 0.016 | 0.02 | 0.10 |
| | 14f | 0.22 | 3.06 | 0.173 | ------- | 0.224 | ------- | 3.10 | 2.90 | 0.012 | 0.20 | 0.215 | 0.228 | 3.10 | 2.38 | 2.66 | 0.014 | 0.02 | 0.10 |

# Appendix D Wave height exceedance curves

In this section, the wave height exceedance curves are plotted for all the tests performed without structure in case of both low and high wave steepness. The distribution of measured wave heights at structure is also compared with the estimation of wave height distribution described by Battjes and Groenendijk (2000).

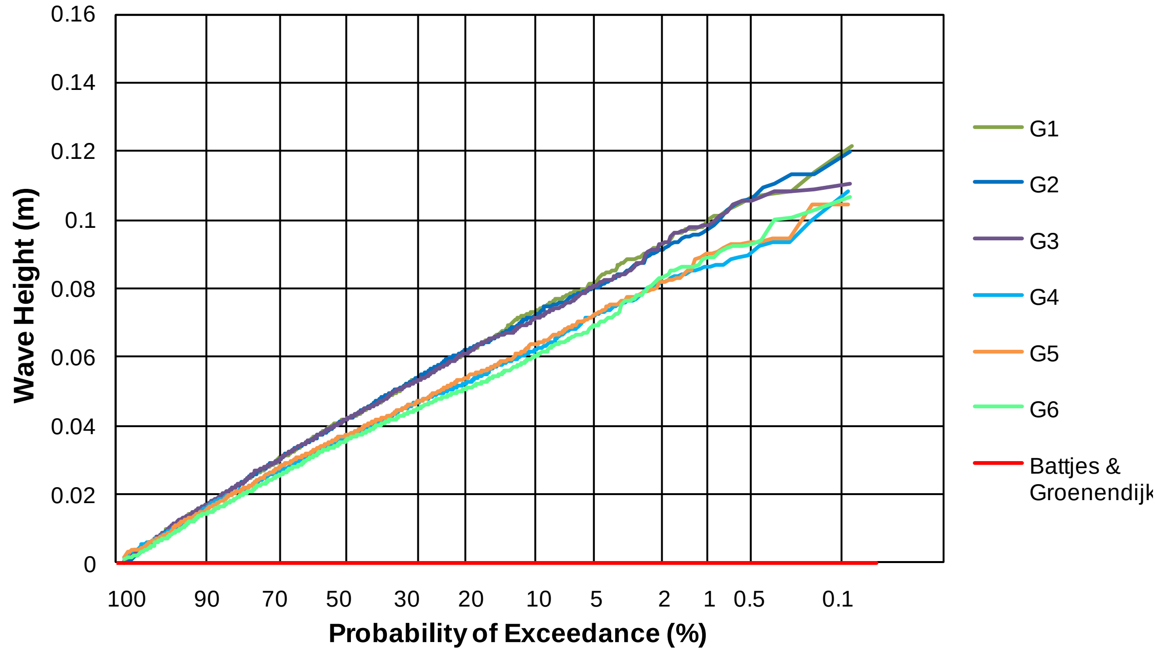


**Figure D.1** Wave height exceedance curve for test 13a

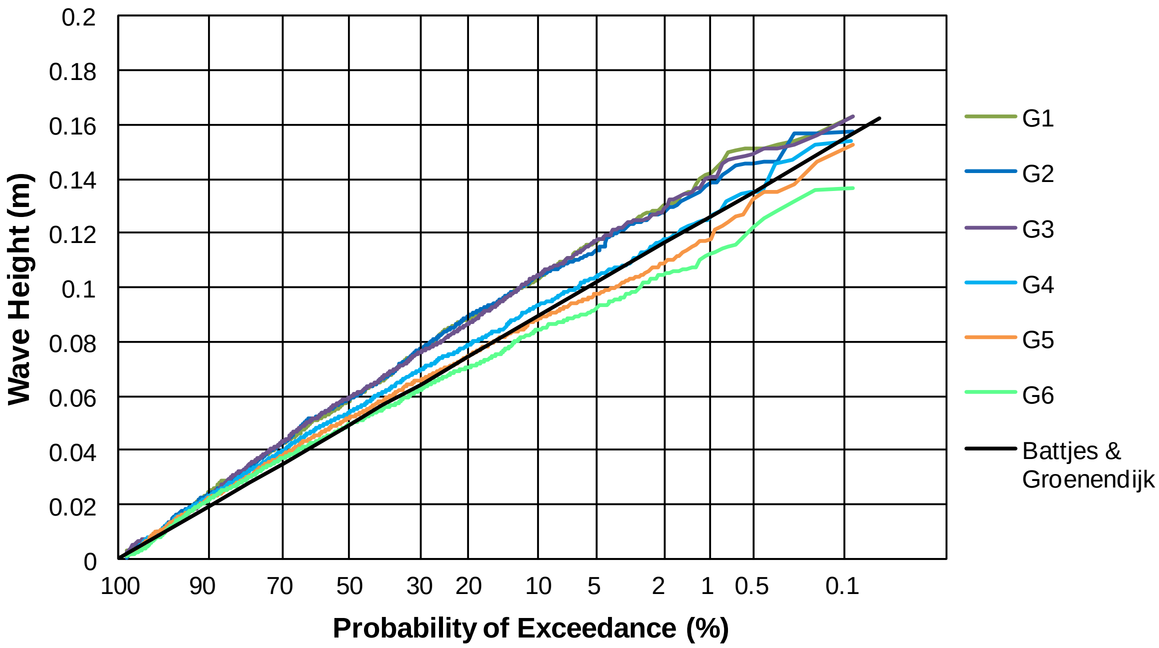


**Figure D.2** Wave height exceedance curve for test 13b

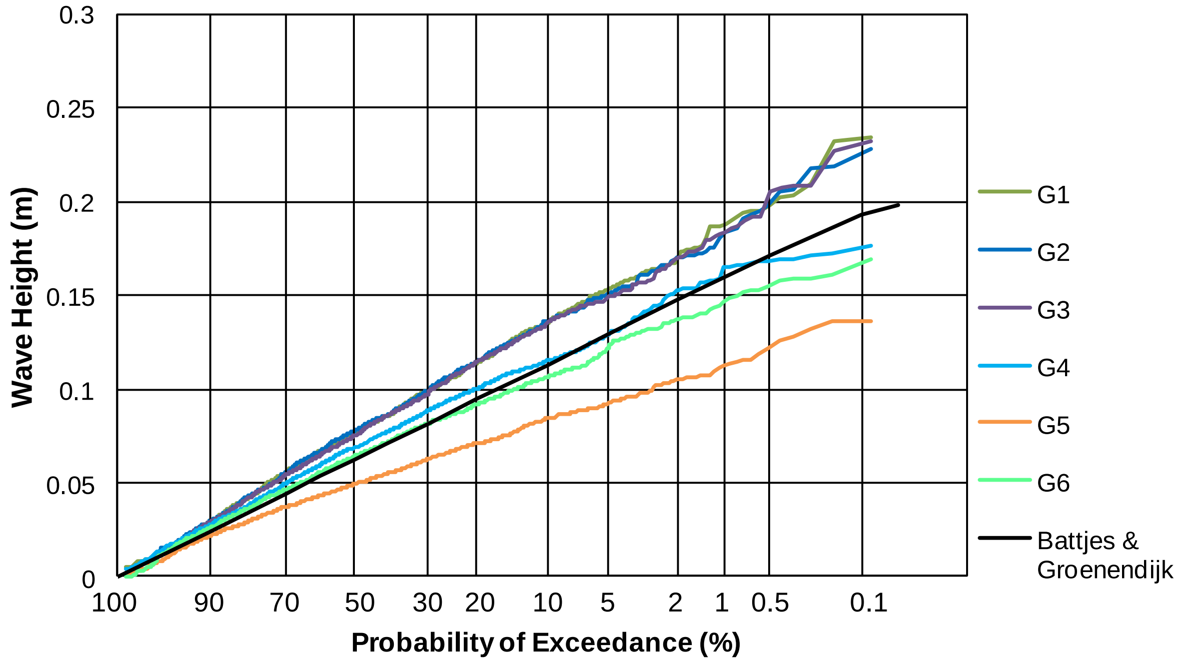


**Figure D.3** Wave height exceedance curve for test 13c

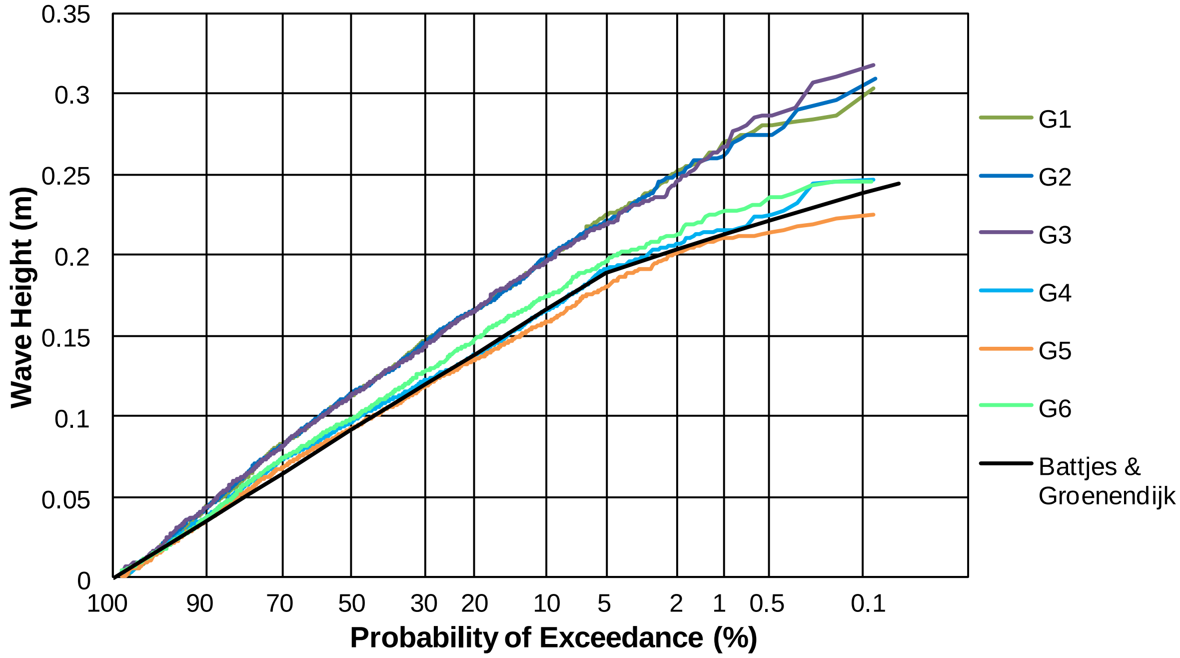


**Figure D.4** Wave height exceedance curve for test 13e

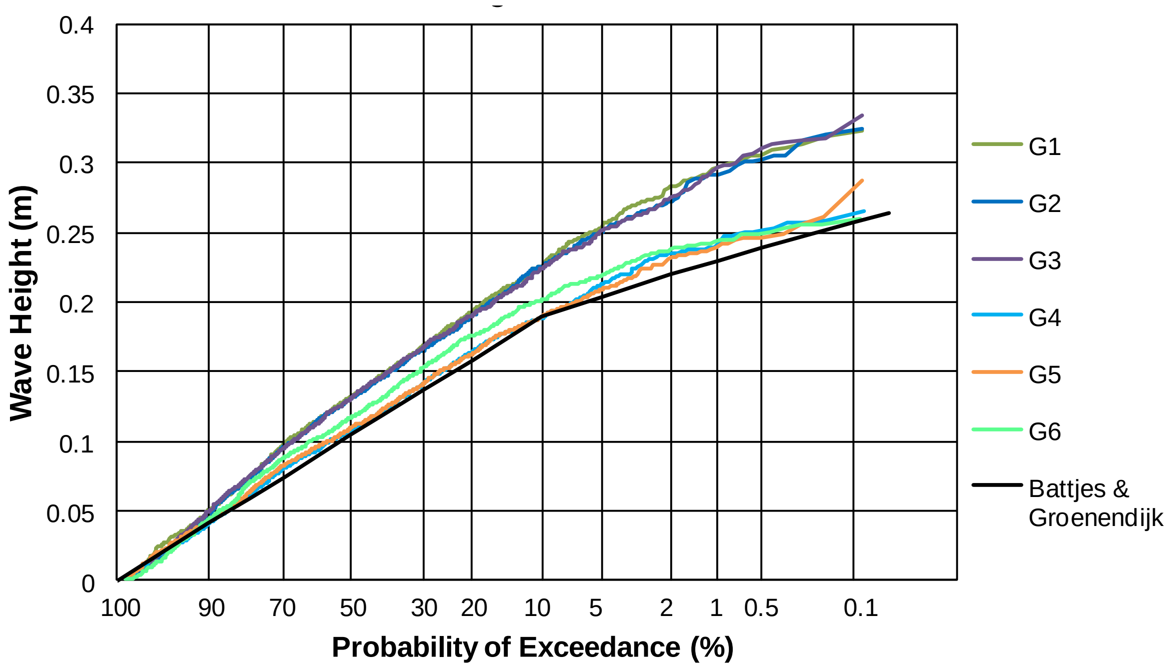


**Figure D.5** Wave height exceedance curve for test 13f

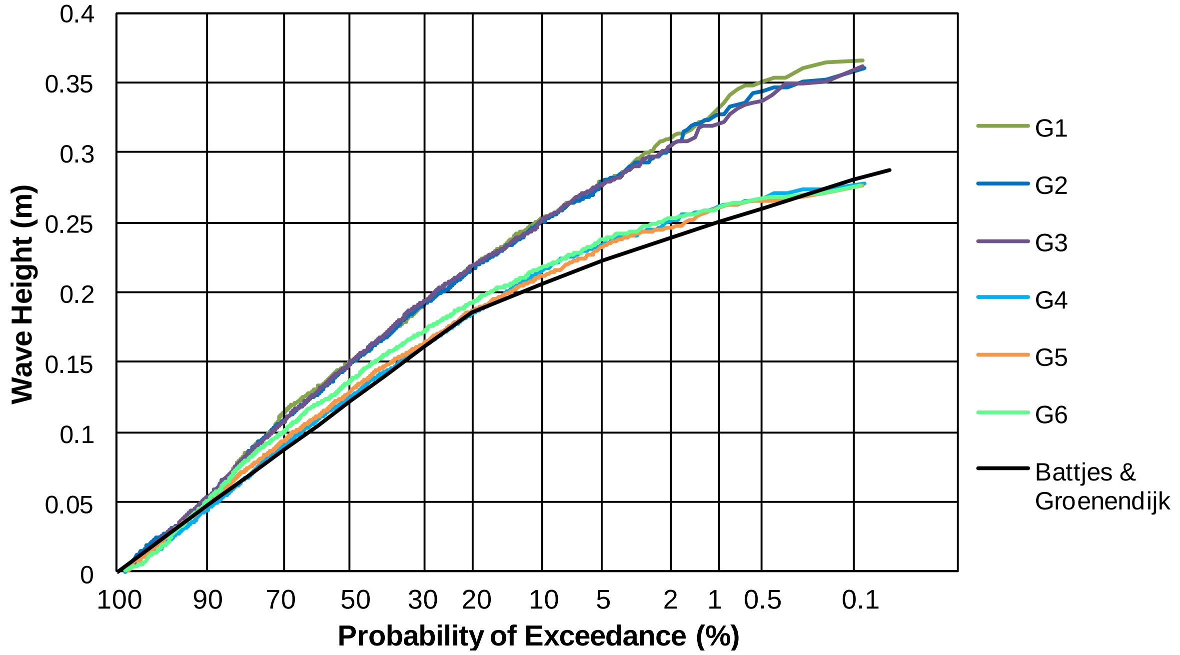


**Figure D.6** Wave height exceedance curve for test 13g

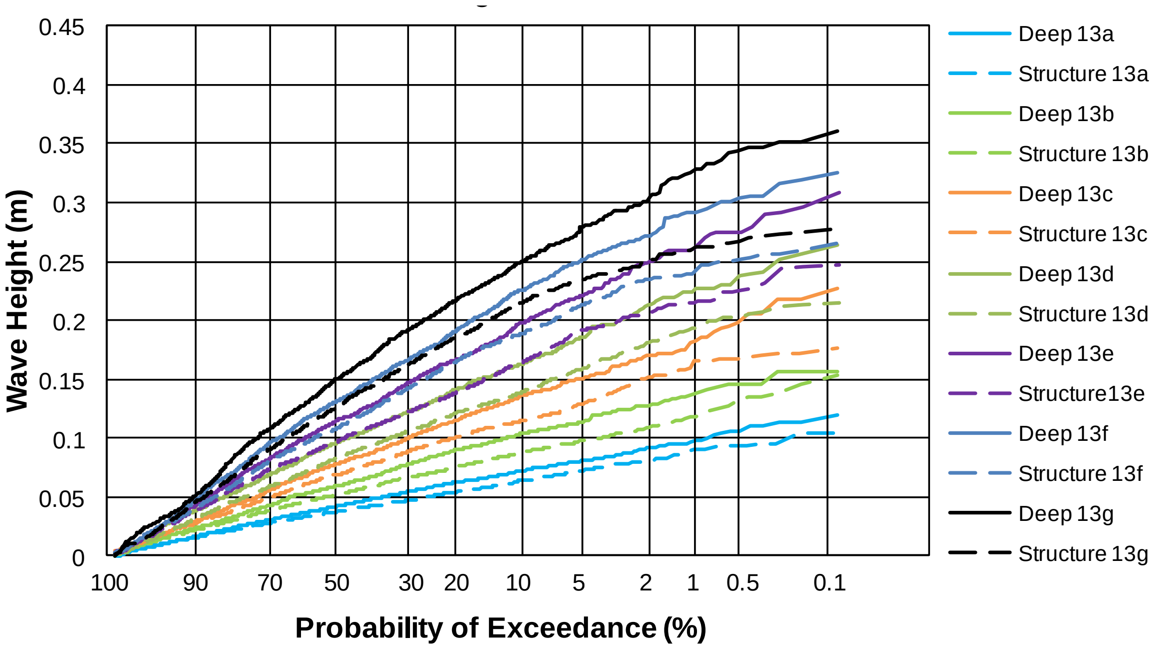


**Figure D.7** Wave height distribution at deep and shallow water for test series 13

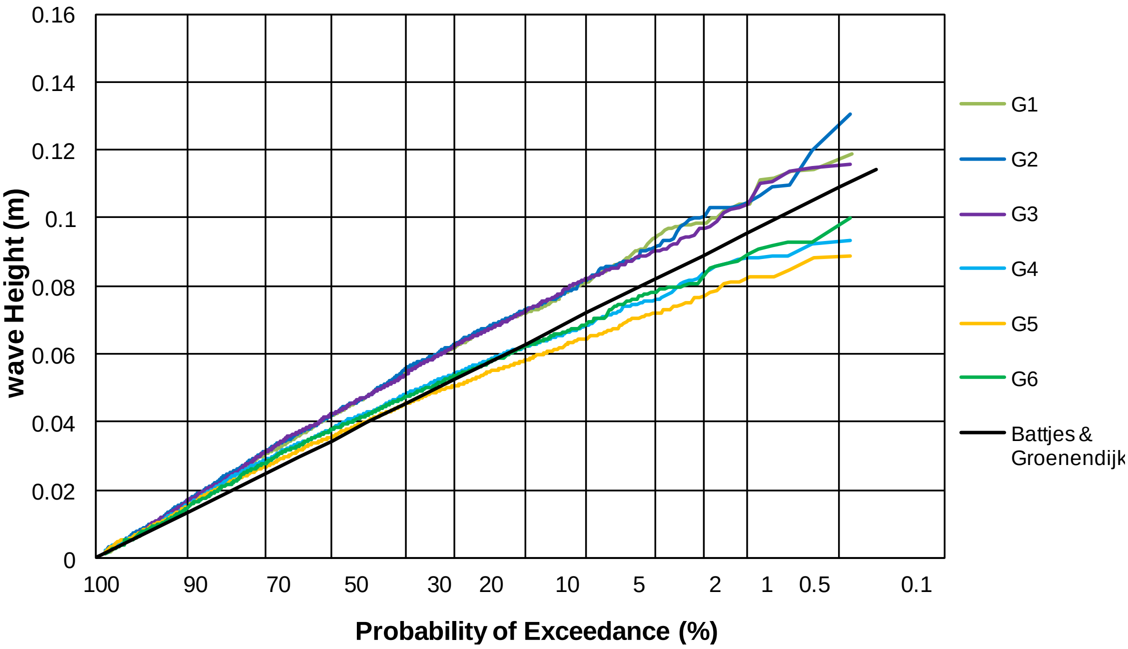


**Figure D.8** Wave height exceedance curve for test 14a

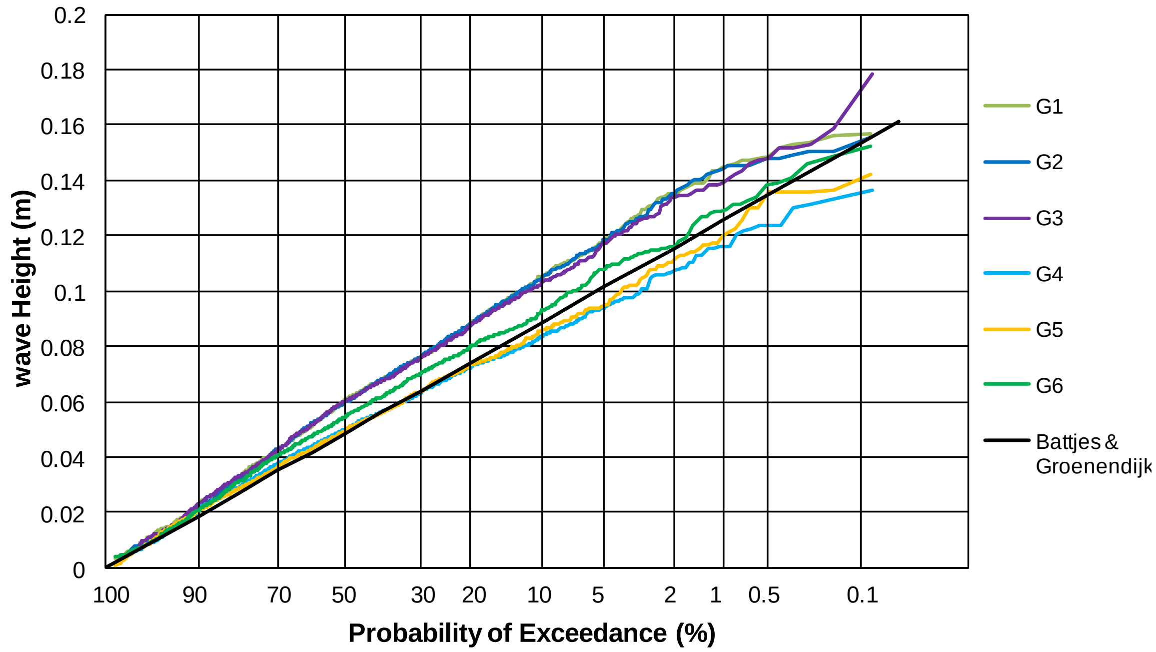


**Figure D.9** Wave height exceedance curve for test 14b

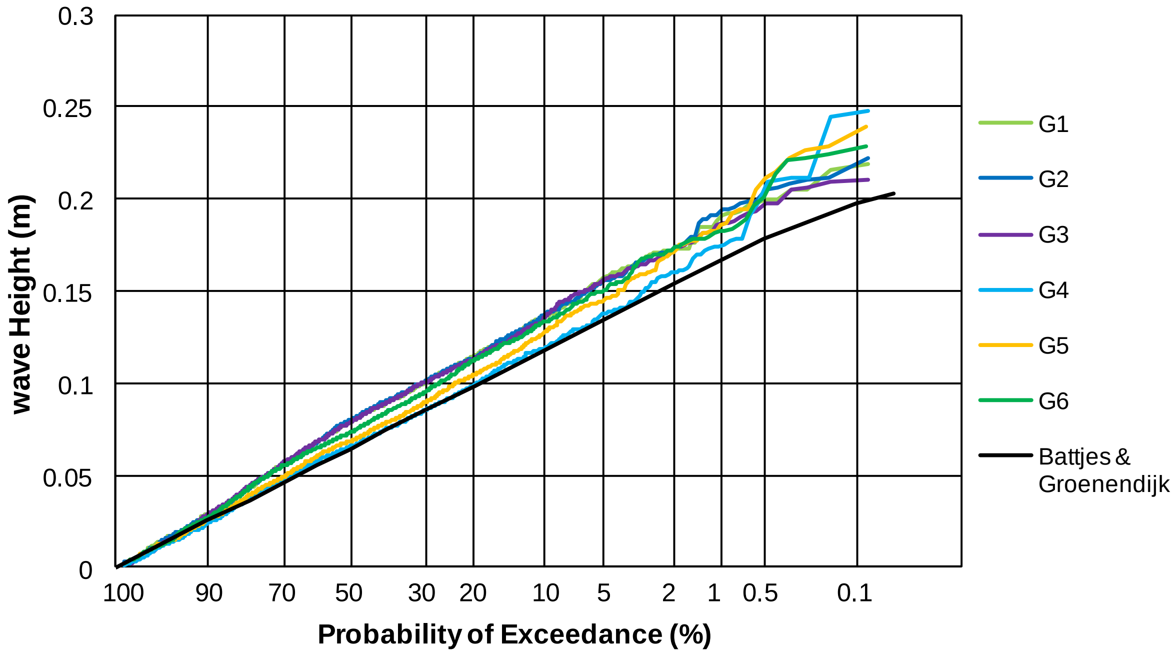


**Figure D.10** Wave height exceedance curve for test 14c

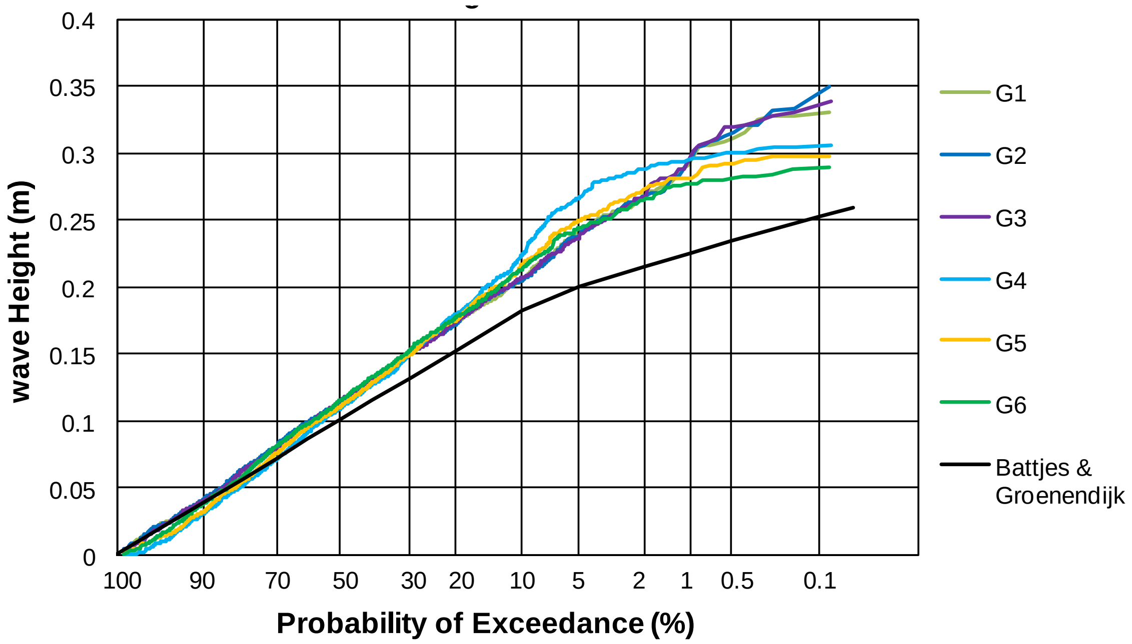


**Figure D.11** Wave height exceedance curve for test 14e

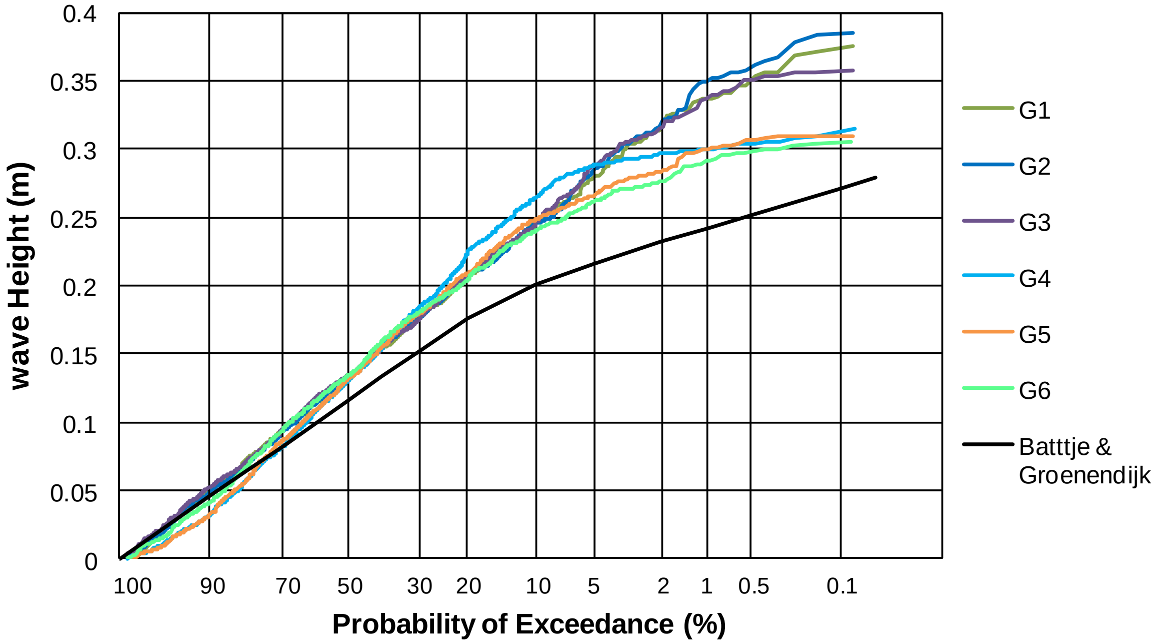


**Figure D.12** Wave height exceedance curve for test 14f

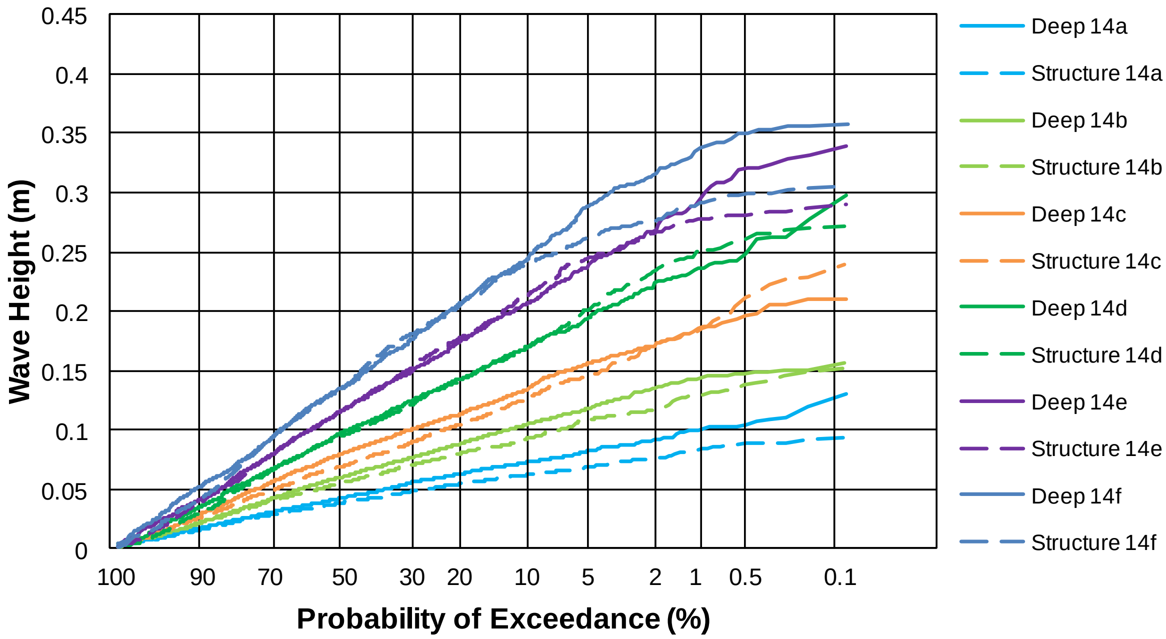


**Figure D.13** Wave height distribution at deep and shallow water for test series 14

# Appendix E Wave spectrum

The variance wave spectrum observed in different tests (without structure) is presented in this section.

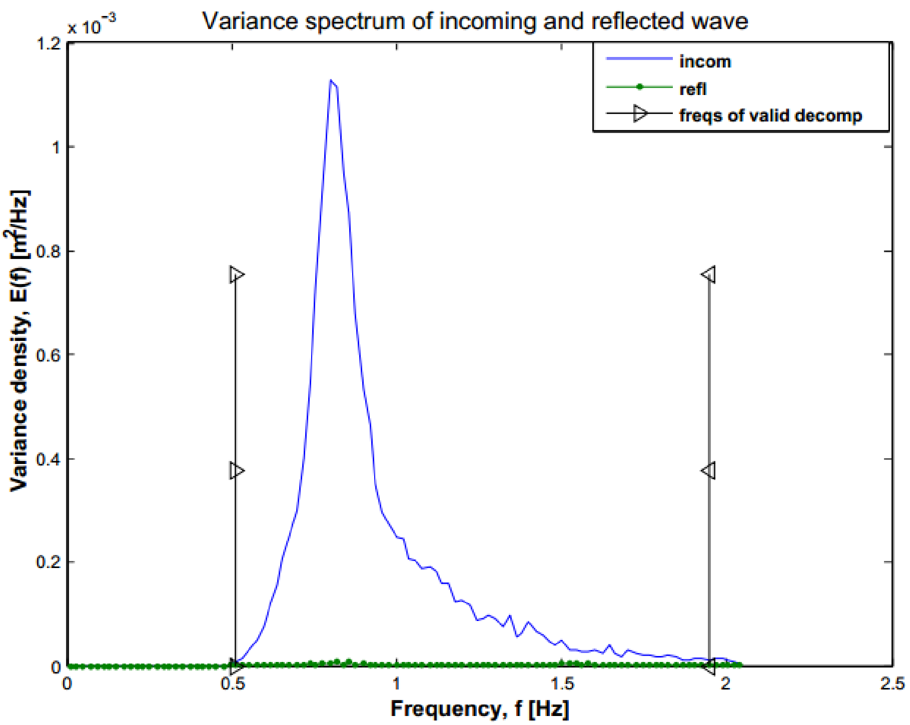


**Figure E.1** Wave spectrum at deep water for test 13a

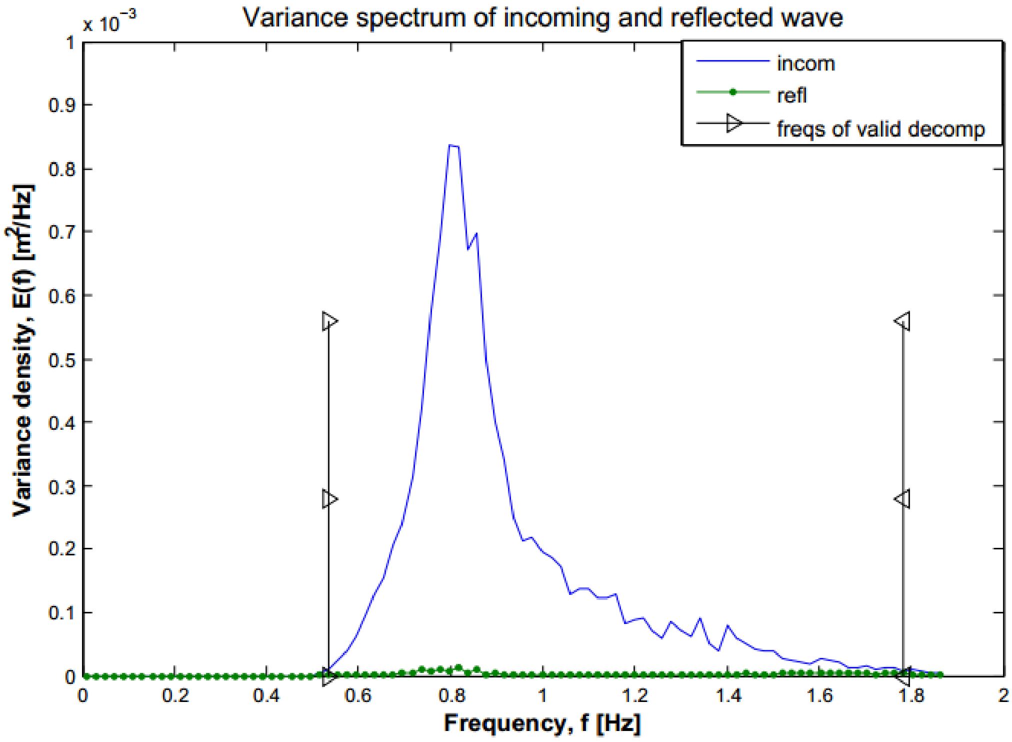


**Figure E.2** Wave spectrum at structure for test 13a

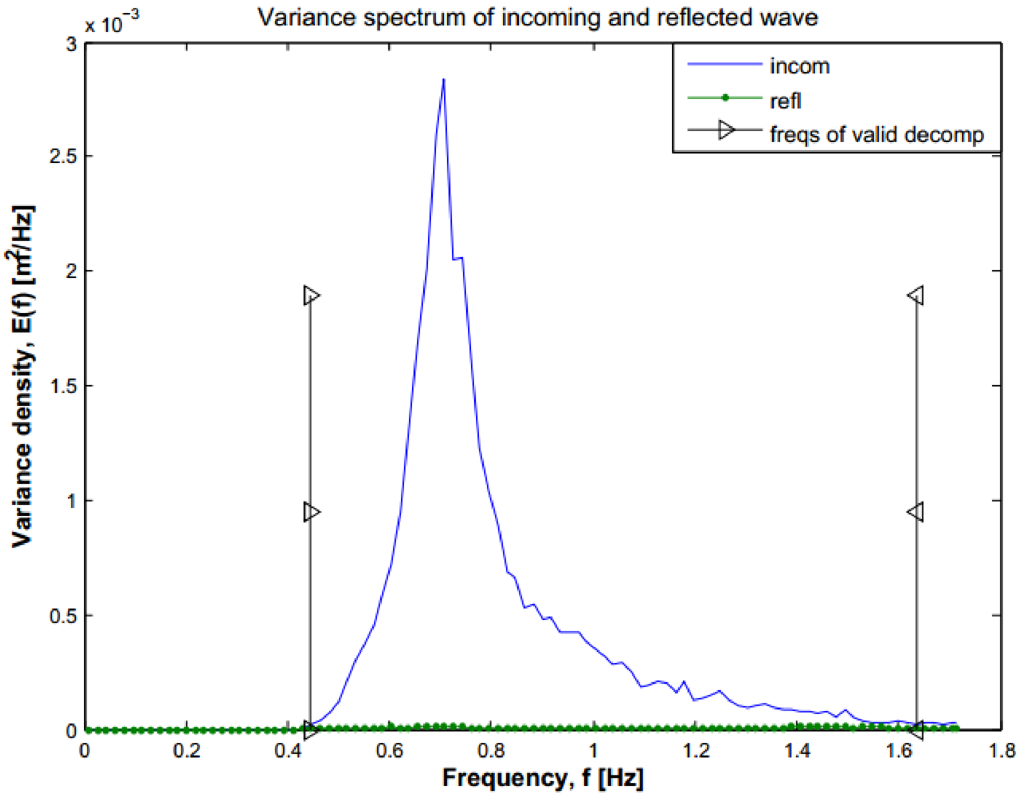


**Figure E.3** Wave spectrum at deep water for test 13b

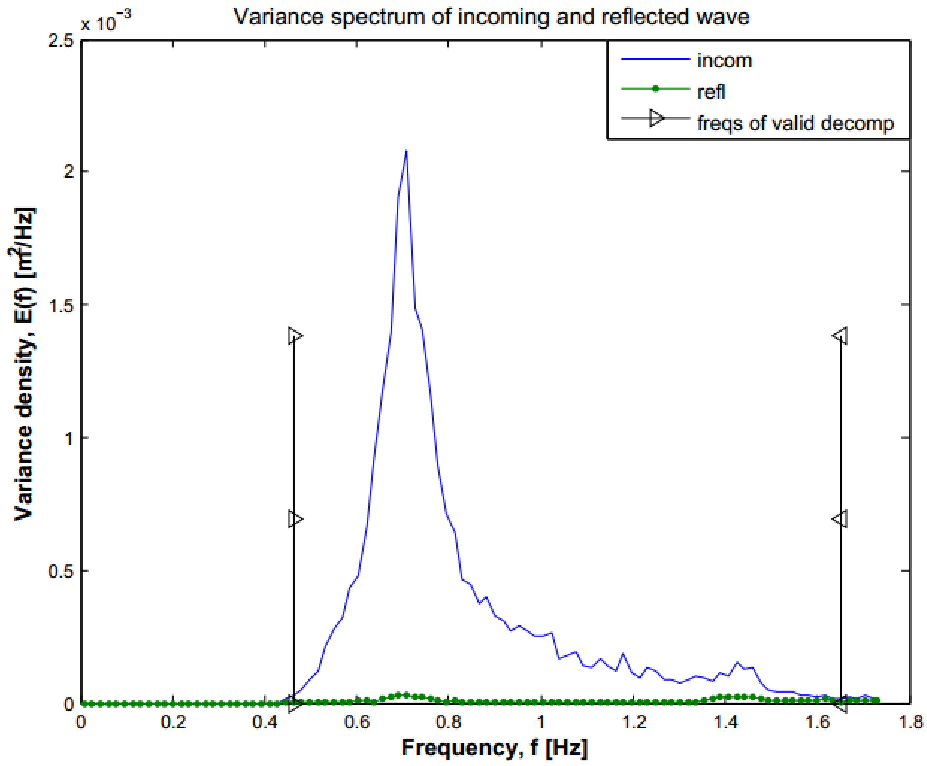


**Figure E.4** Wave spectrum at structure for test 13b

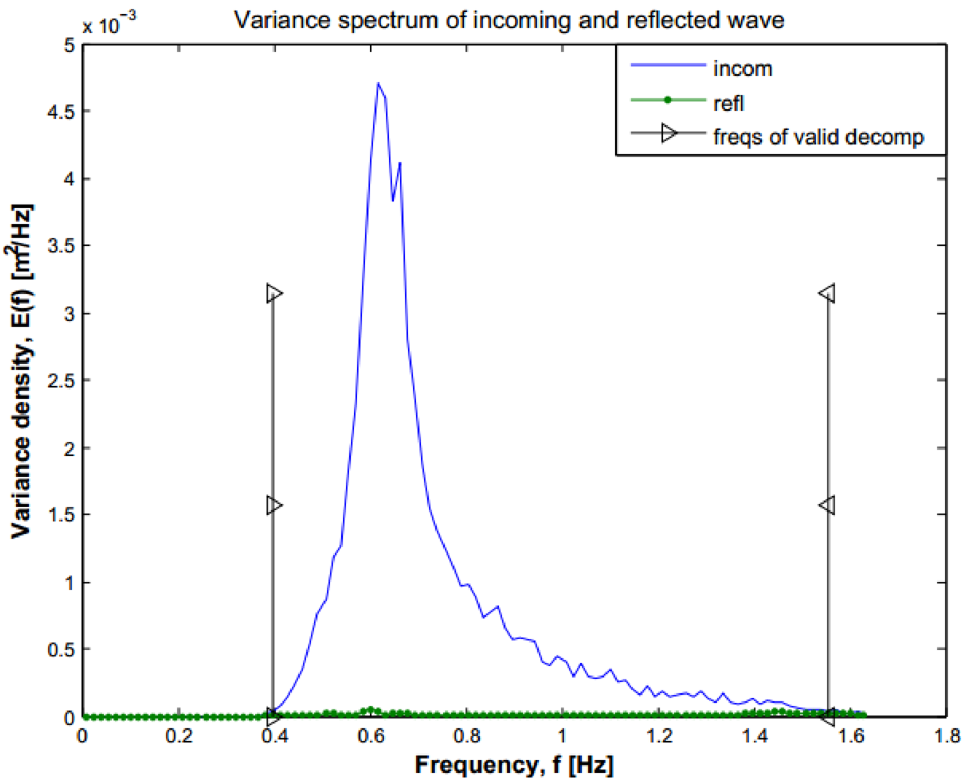


**Figure E.5** Wave spectrum at deep water for test 13c

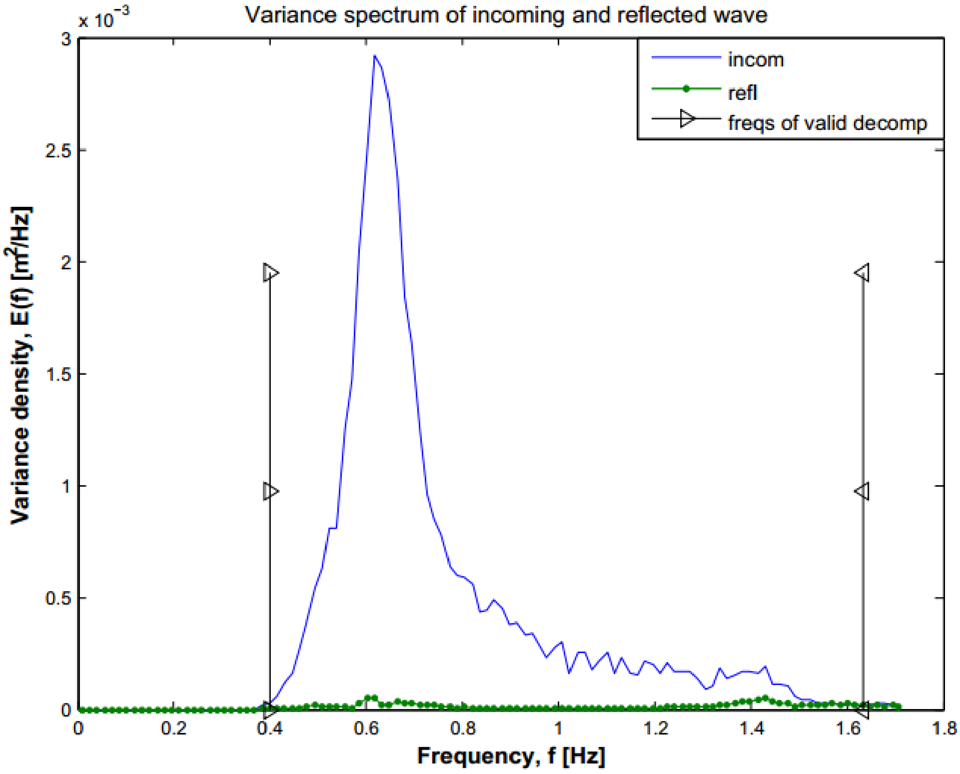


**Figure E.6** Wave spectrum at structure for test 13c

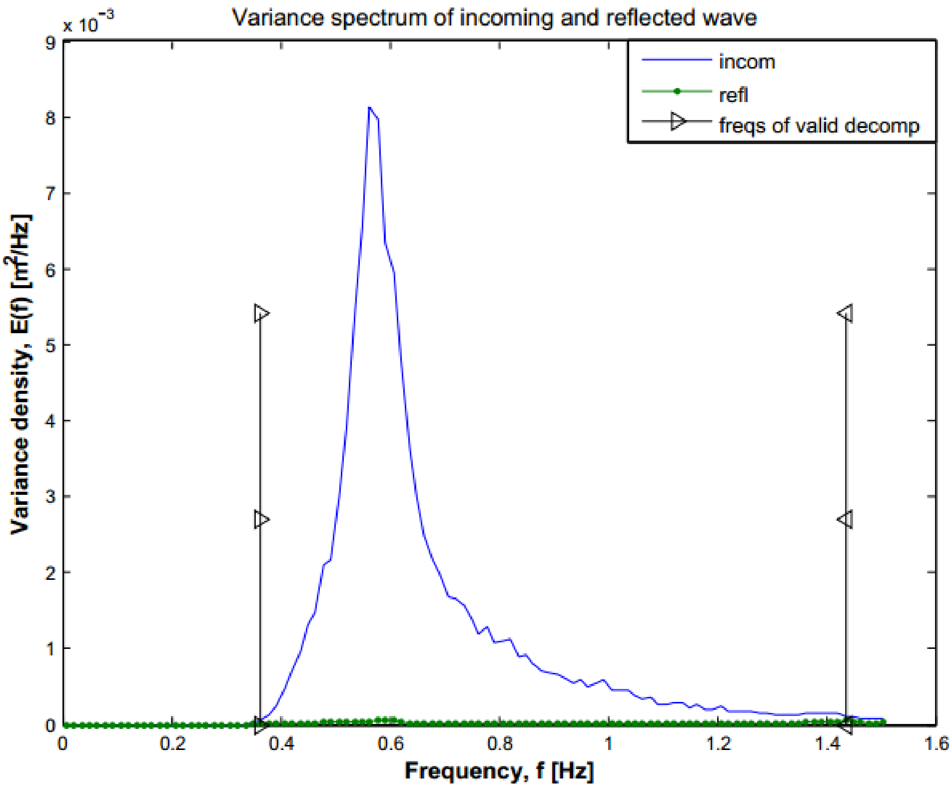


**Figure E.7** Wave spectrum at deep water for test 13d

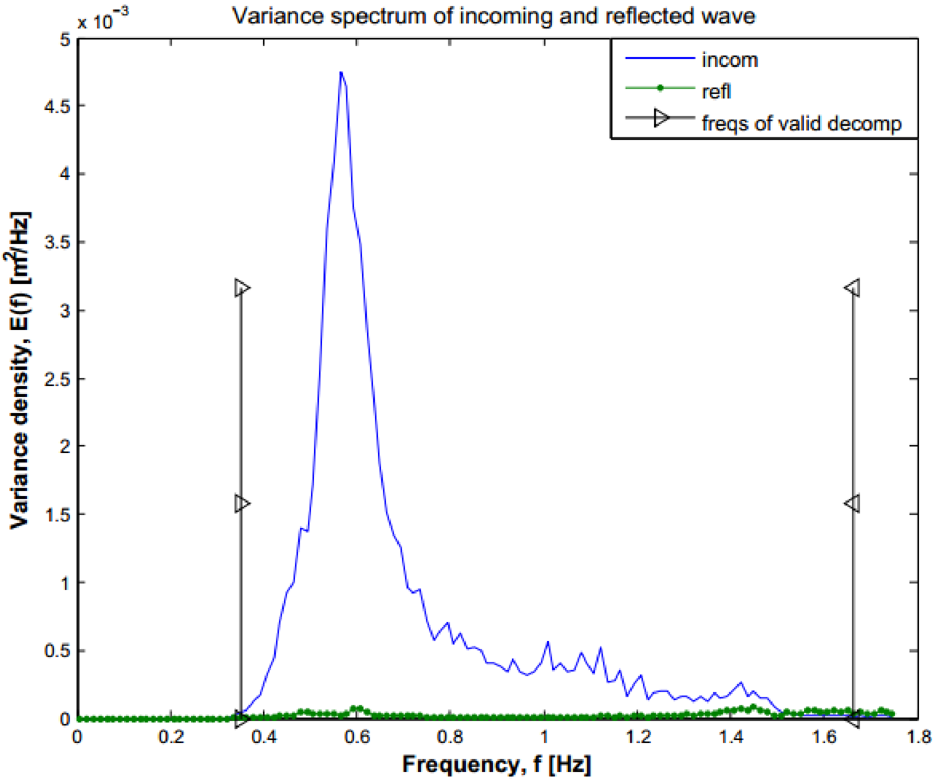


**Figure E.8** Wave spectrum at structure for test 13d

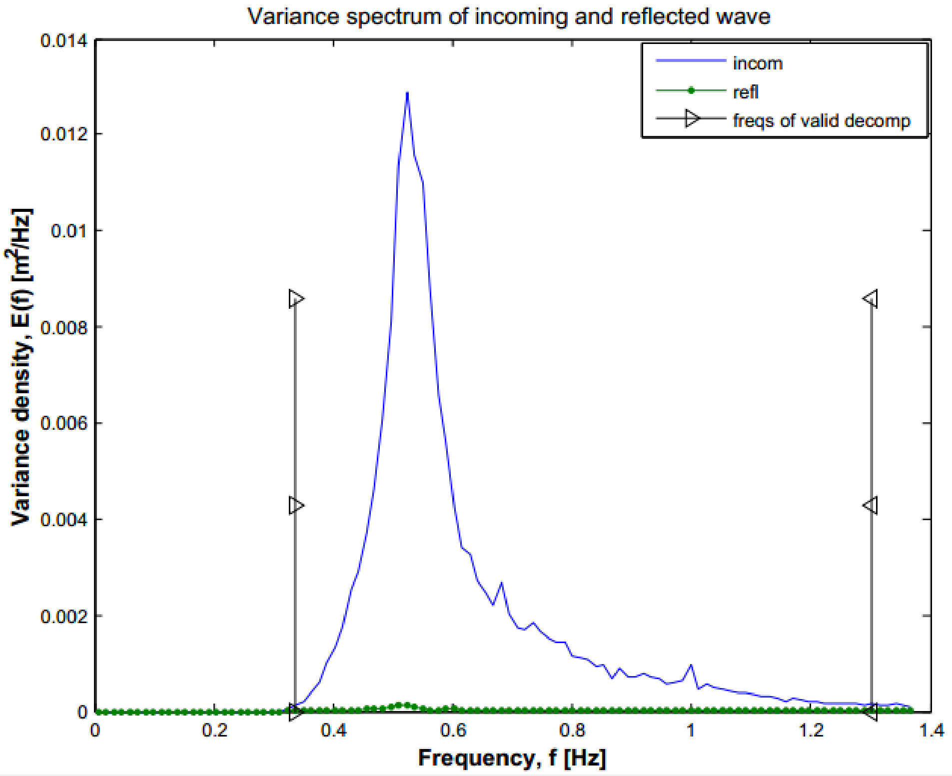


**Figure E.9** Wave spectrum at deep water for test 13e

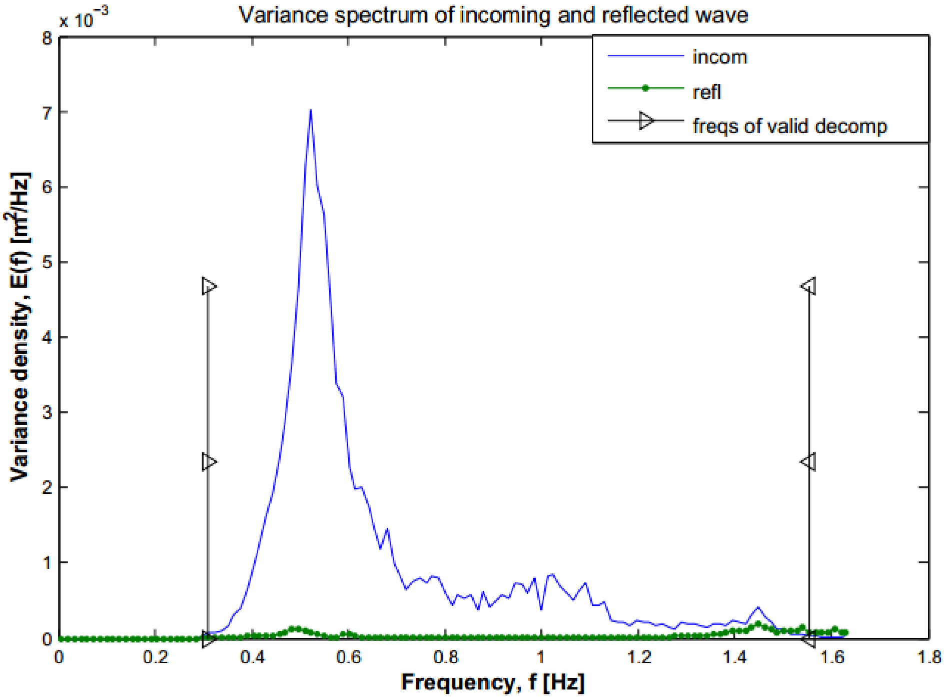


**Figure E.10** Wave spectrum at structure for test 13e

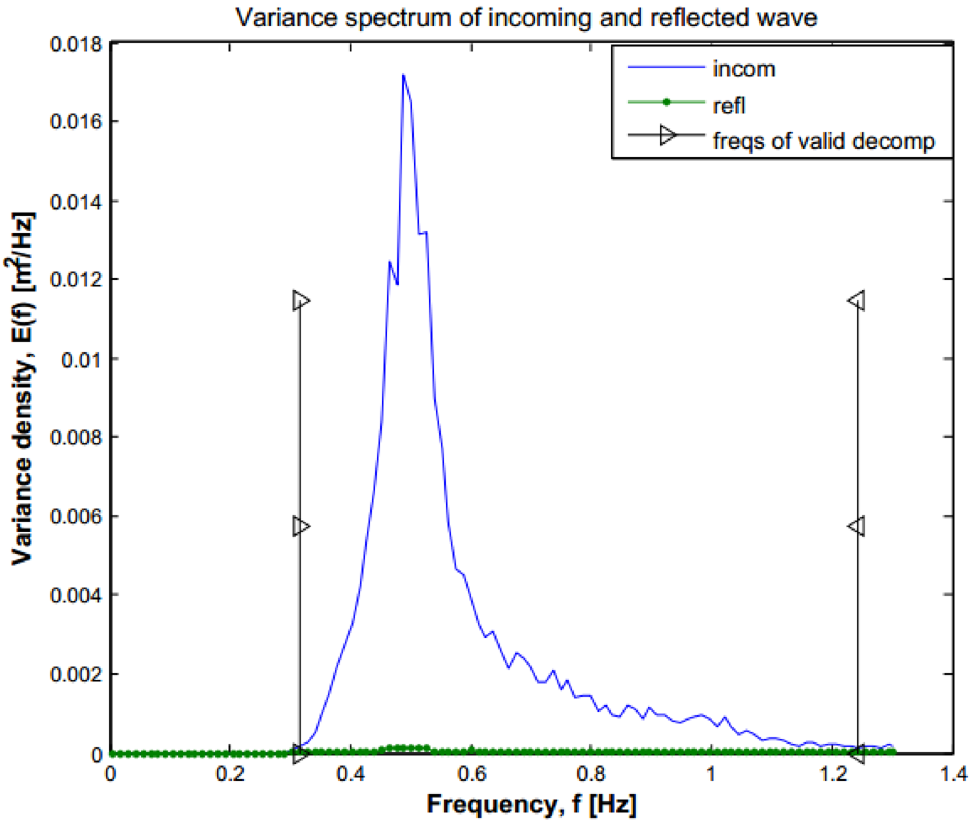


**Figure E.11** Wave spectrum at deep water for test 13f

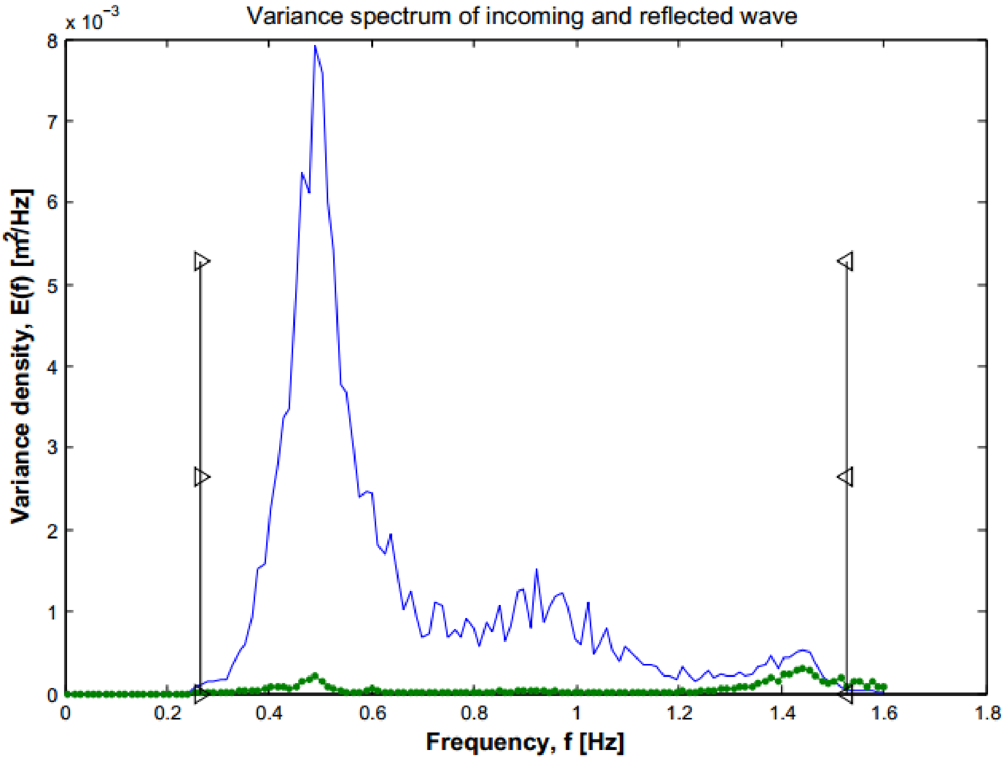


**Figure E.12** Wave spectrum at structure for test 13f

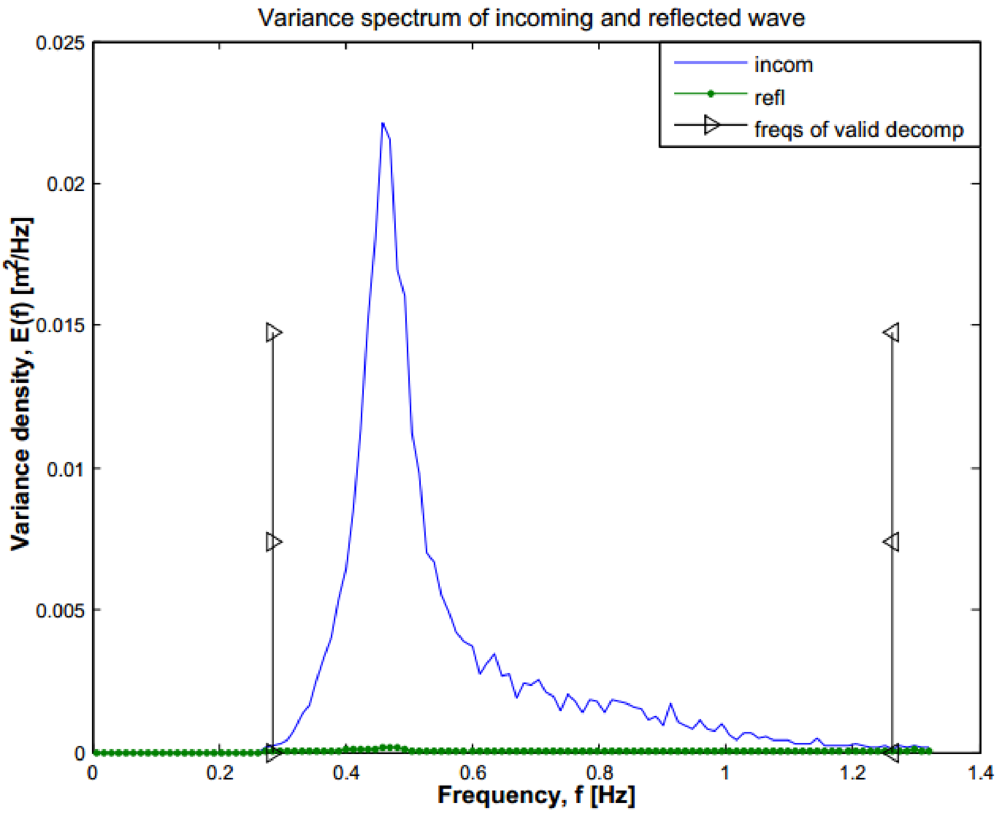


**Figure E.13** Wave spectrum at deep water for test 13g

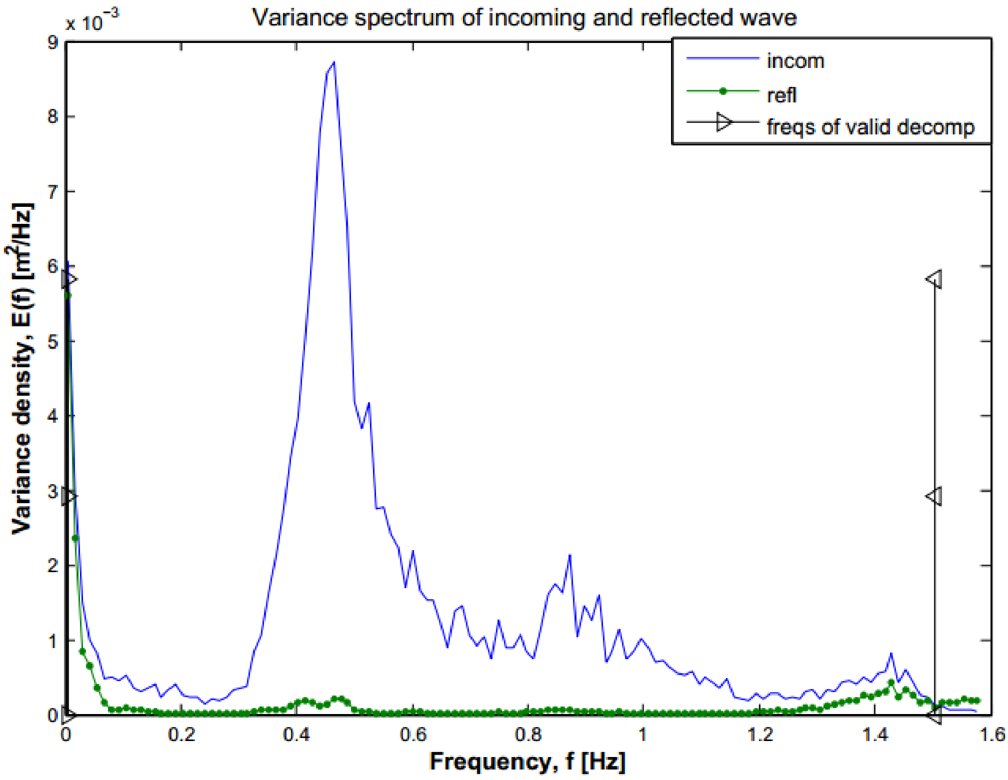


**Figure E.14** Wave spectrum at structure for test 13g

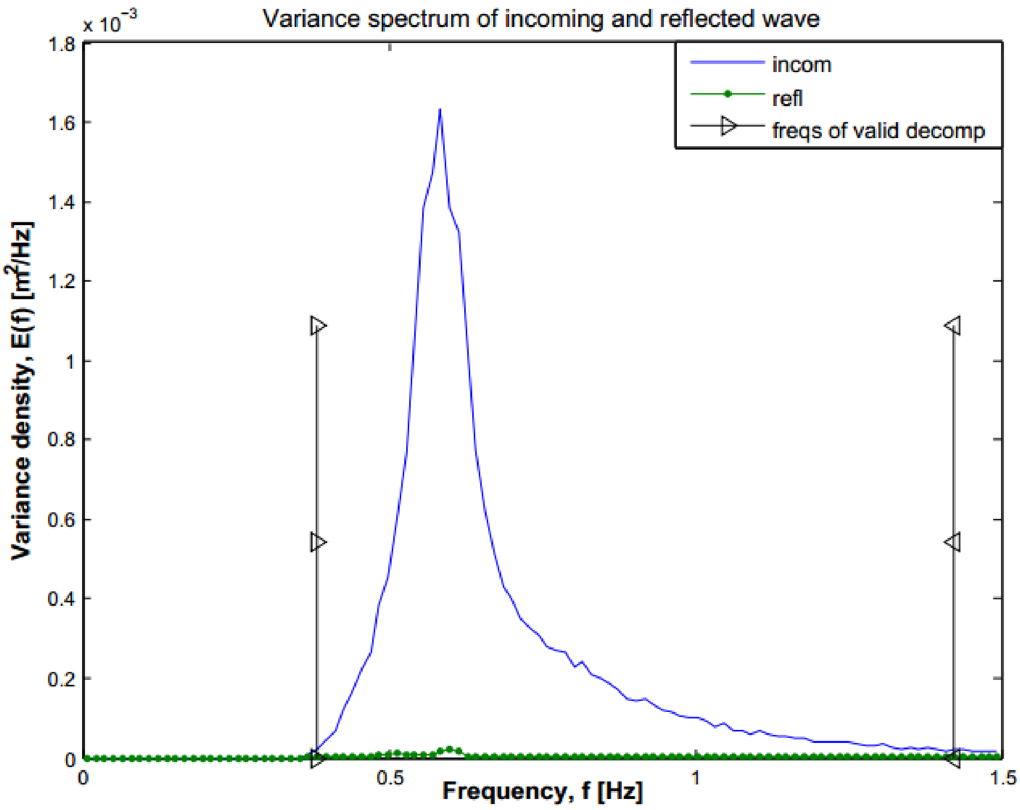


**Figure E.15** Wave spectrum at deep water for test 14a

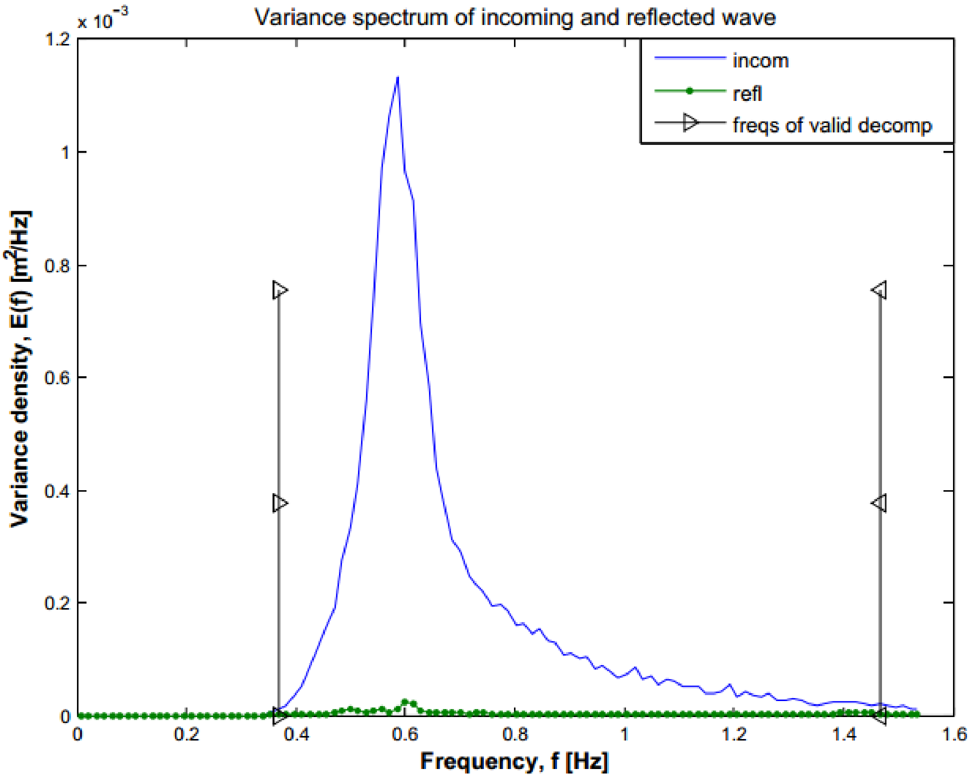


**Figure E.16** Wave spectrum at structure for test 14a

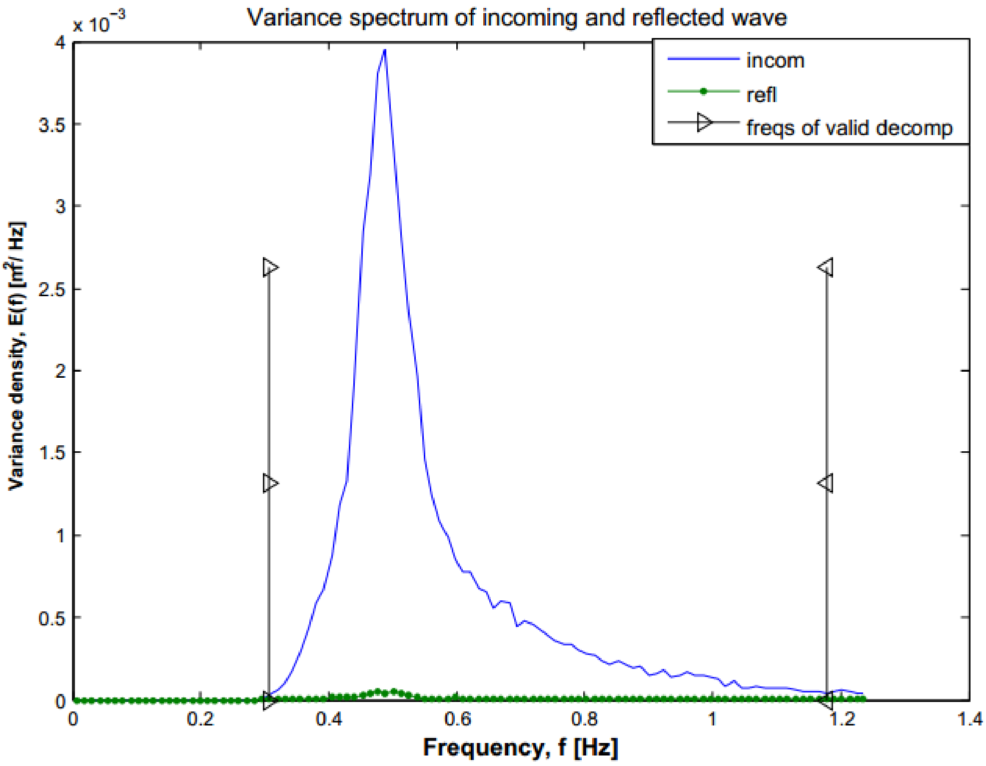


**Figure E.17** Wave spectrum at deep water for test 14b

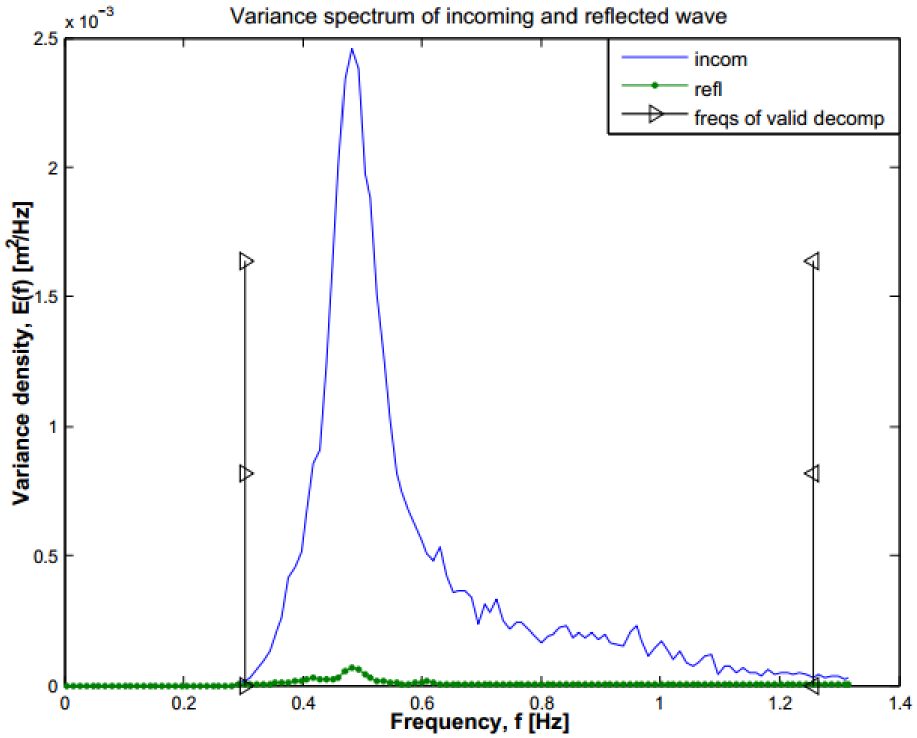


**Figure E.18** Wave spectrum at structure for test 14b

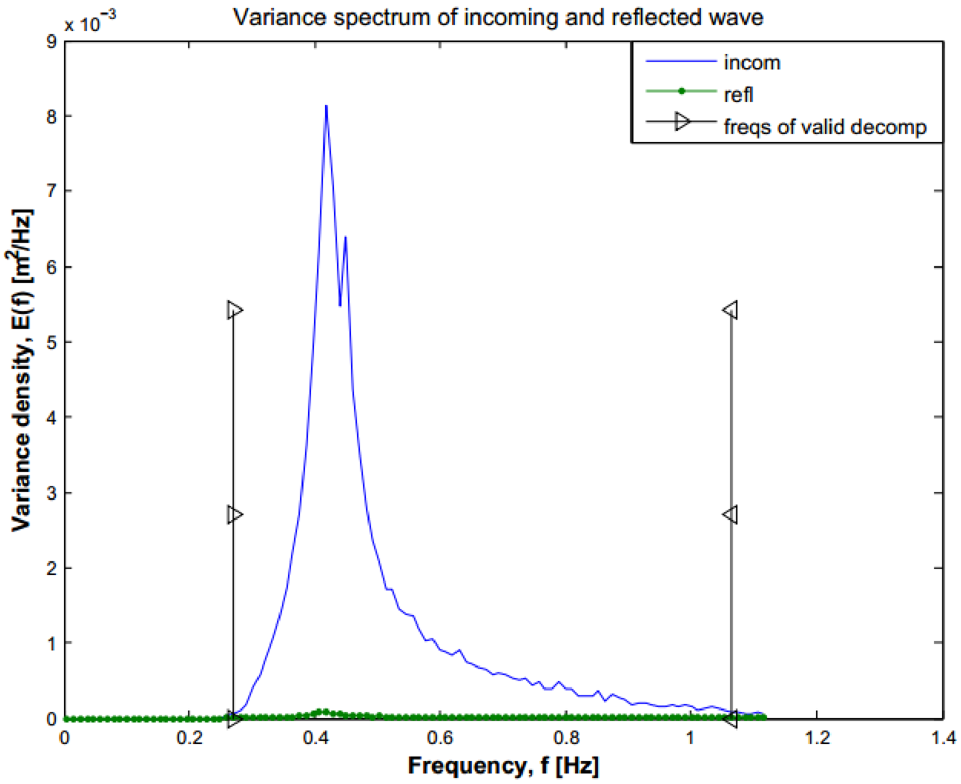


**Figure E.19** Wave spectrum at deep water for test 14c

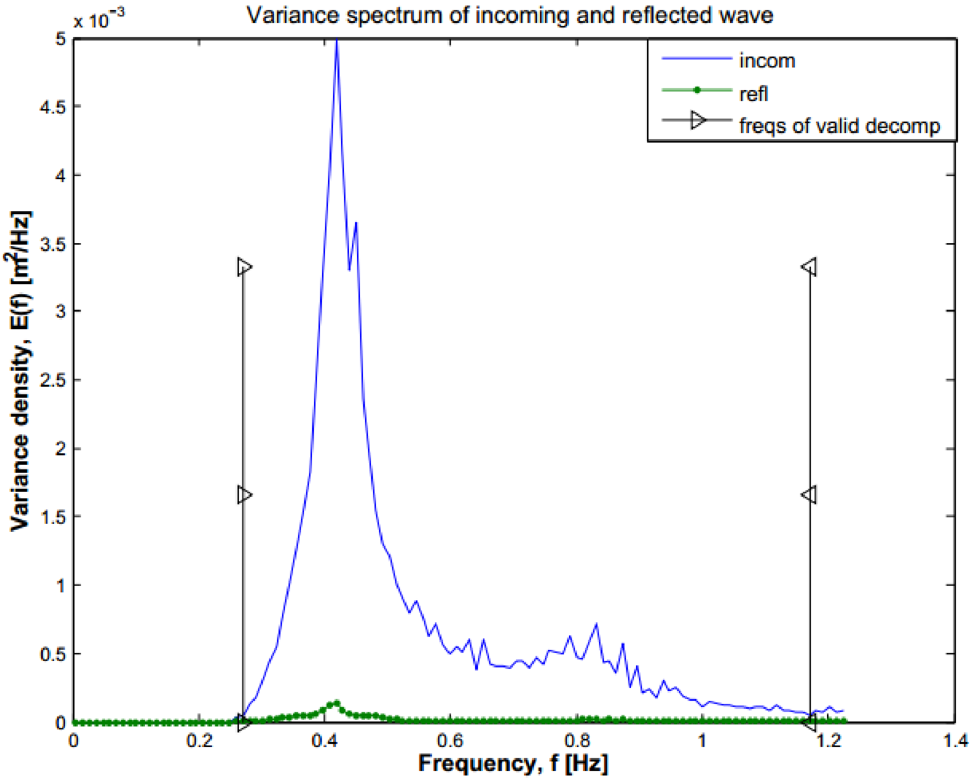


**Figure E.20** Wave spectrum at structure for test 14c

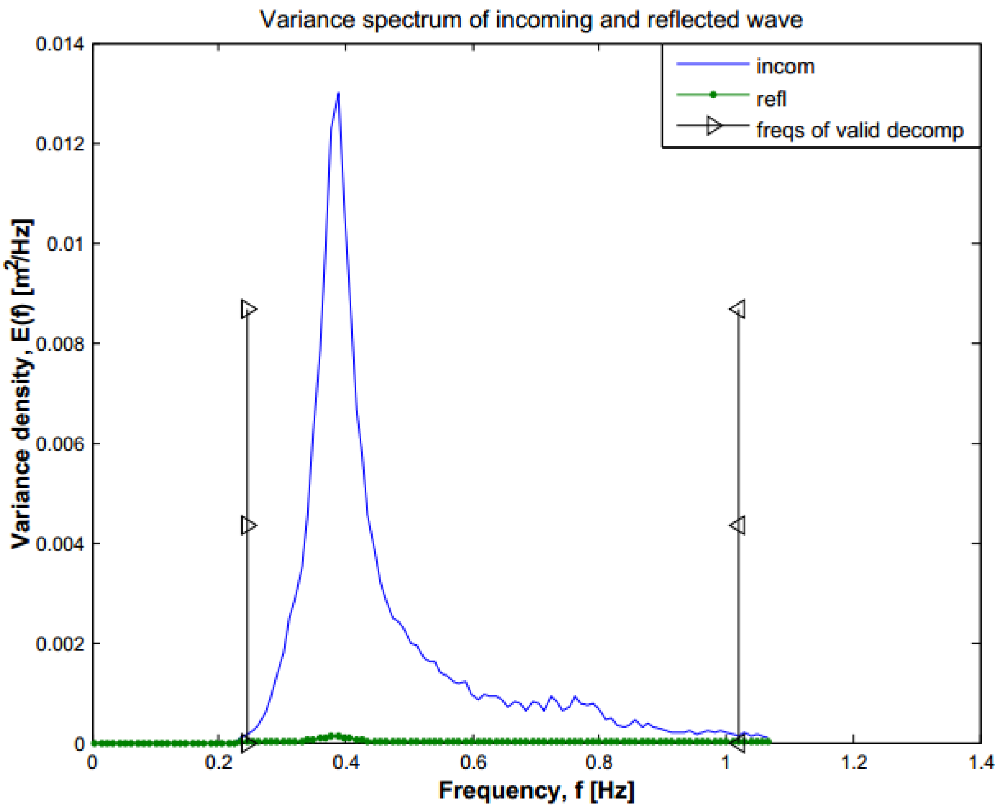


**Figure E.21** Wave spectrum at deep water for test 14d

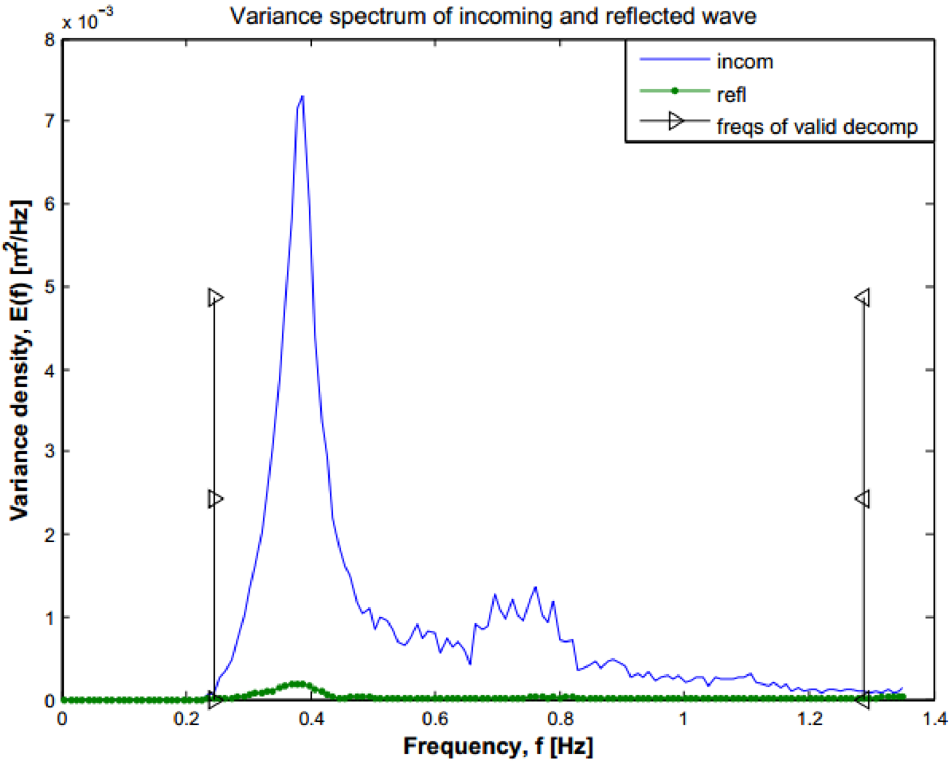


**Figure E.22** Wave spectrum at structure for test 14d

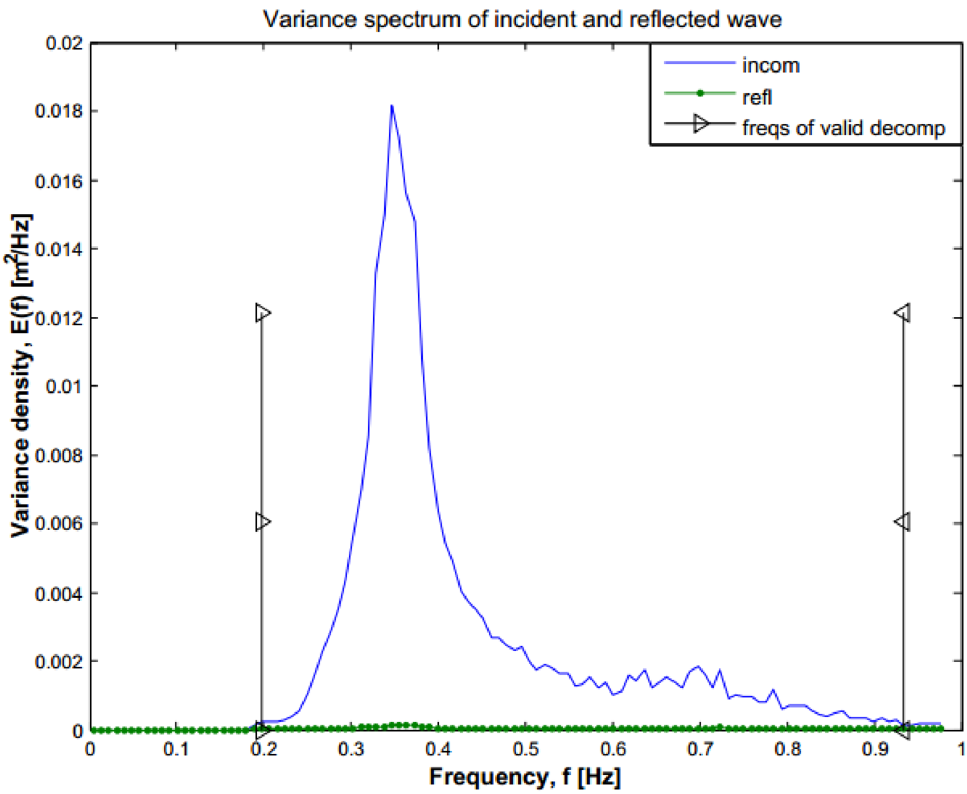


**Figure E.23** Wave spectrum at deep water for test 14e

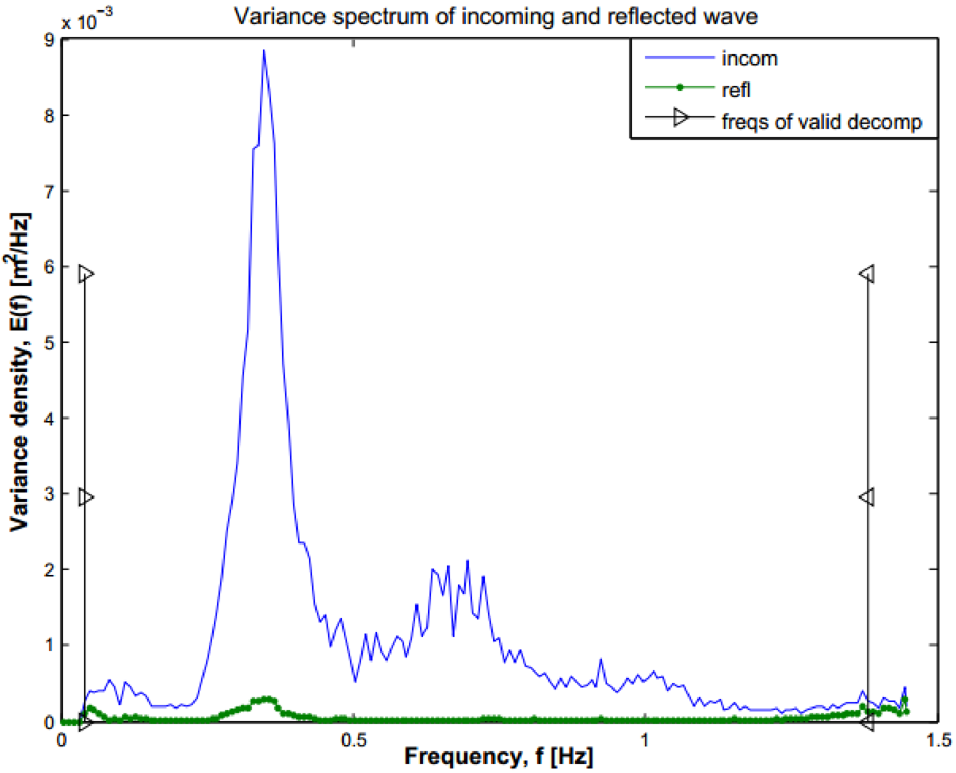


**Figure E.24** Wave spectrum at structure for test 14e

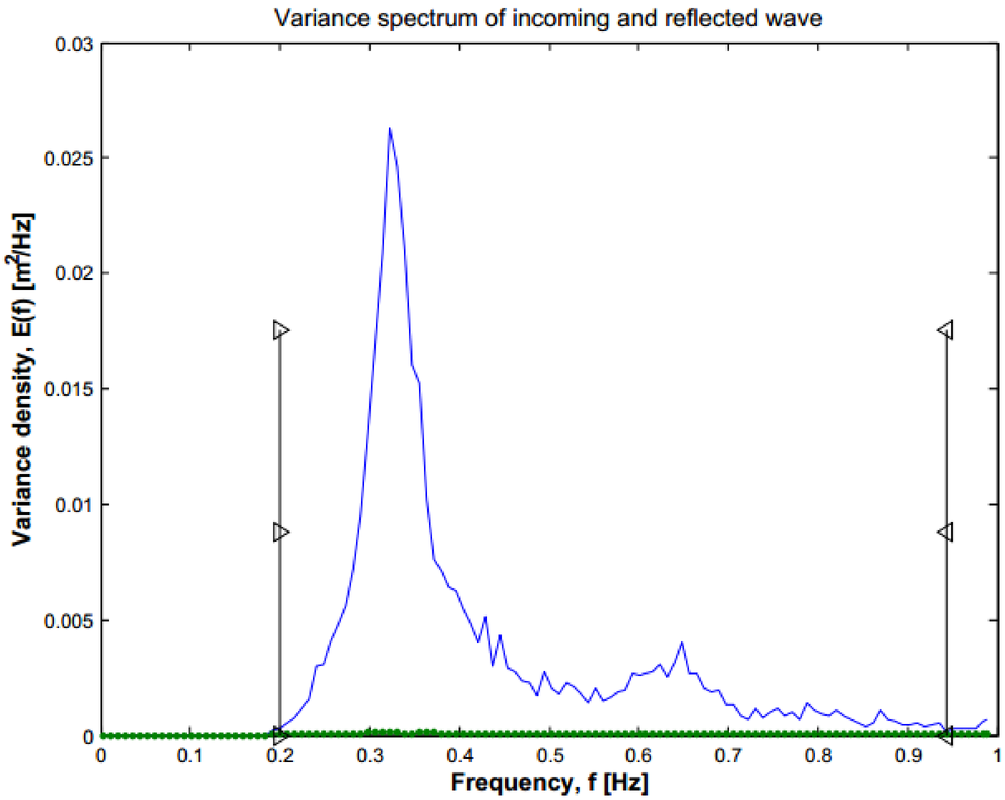


**Figure E.25** Wave spectrum at deep water for test 14f

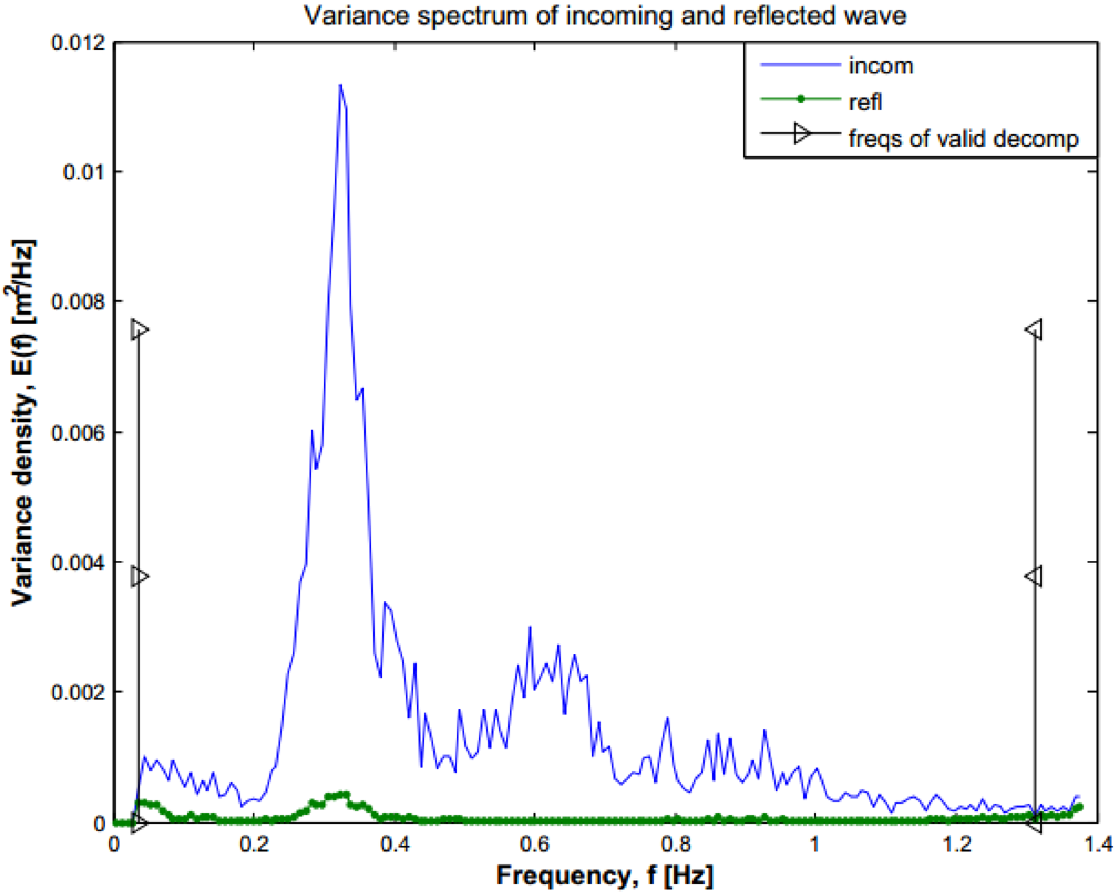


**Figure E.26** Wave spectrum at structure for test 14f

# Appendix F Measured wave overtopping

The measured wave overtopping for each individual test series is printed in details in **Appendix F**. It should be noted that in all the cases the incident wave height (calibrated) at the structure is considered.

**Table F.1** Measured wave overtopping in test series 1-3

| Test Series | Sub-Test No. | Total number of Units | Packing density (units/$D_n^2$) | Crest Height $R_c$ [m] | $H_{m0}$ [m] Toe | Rc/$H_{m0}$ [-] | Test Duration [s] | No. of Waves N [-] | No. of overtopping waves | % overtopping waves | Overtopping Vol. [litre] | Duration of overtopping measured (sec) | Funnel width (m) | overtopping discharge q [m3/s per m] | overtopping discharge q [l/s per m] | q/(gHm0^3)^0.5 |
|---|---|---|---|---|---|---|---|---|---|---|---|---|---|---|---|---|
| 1 | 1a | 484 | 0.69 | 0.14 | 0.059 | 2.355 | 1284 | 1197 | 0 | 0 | 0 | 1284 | 0.1 | 0 | 0 | 0 |
| | 1b | | | 0.14 | 0.080 | 1.741 | 1425 | 1193 | 5 | 0.42 | 0.037 | 1425 | 0.1 | 2.6E-07 | 0.00026105 | 3.7E-06 |
| | 1c | | | 0.14 | 0.102 | 1.375 | 1622 | 1207 | 30 | 2.49 | 3.391 | 1687 | 0.1 | 2.0E-05 | 0.02010017 | 2.0E-04 |
| | 1d | | | 0.14 | 0.122 | 1.149 | 1873 | 1257 | 141 | 11.22 | 30.999 | 1873 | 0.1 | 1.7E-04 | 0.16550437 | 1.2E-03 |
| | 1e | | | 0.14 | 0.141 | 0.995 | 1885 | 1182 | 328 | 27.74 | 99.037 | 1885 | 0.1 | 5.3E-04 | 0.52539433 | 3.2E-03 |
| | 1f | | | 0.14 | 0.159 | 0.879 | 2070 | 1241 | 559 | 45.04 | 276.015 | 2070 | 0.1 | 1.3E-03 | 1.33340678 | 6.7E-03 |
| | 1g | | | 0.14 | 0.176 | 0.796 | 6556 | 3559 | 1808 | 50.80 | 625.371 | 2800 | 0.1 | 2.2E-03 | 2.23346887 | 9.7E-03 |
| 2 | 2a | 484 | 0.69 | 0.14 | 0.056 | 2.499 | 1760 | 1208 | 0 | 0 | 0 | 1760 | 0.1 | 0 | 0 | 0 |
| | 2b | | | 0.14 | 0.082 | 1.700 | 2075 | 1231 | 13 | 1.06 | 1.238 | 2075 | 0.1 | 6.0E-06 | 0.00596672 | 8.1E-05 |
| | 2c | | | 0.14 | 0.105 | 1.336 | 2411 | 1271 | 145 | 11.41 | 55.277 | 2411 | 0.1 | 2.3E-04 | 0.22926812 | 2.2E-03 |
| | 2d | | | 0.14 | 0.128 | 1.093 | 2776 | 1299 | 368 | 28.33 | 121.311 | 1388 | 0.1 | 8.7E-04 | 0.8740019 | 6.1E-03 |
| | 2e | | | 0.14 | 0.151 | 0.925 | 2929 | 1267 | 591 | 46.63 | 281.013 | 1436 | 0.1 | 2.0E-03 | 1.95691325 | 1.1E-02 |
| | 2f | | | 0.14 | 0.166 | 0.845 | 6155 | 2485 | 1497 | 60.23 | 438.282 | 1536 | 0.1 | 2.9E-03 | 2.85339833 | 1.3E-02 |
| 3 | 3a | 407 | 0.63 | 0.14 | 0.060 | 2.341 | 1293 | 1225 | 0 | 0 | 0 | 1293 | 0.1 | 0 | 0 | 0 |
| | 3b | | | 0.14 | 0.080 | 1.758 | 1451 | 1035 | 6 | 0.58 | 0.025 | 1451 | 0.1 | 1.7E-07 | 0.00017271 | 2.5E-06 |
| | 3c | | | 0.14 | 0.100 | 1.393 | 1621 | 1215 | 30 | 2.47 | 2.316 | 1621 | 0.1 | 1.4E-05 | 0.01428889 | 1.4E-04 |
| | 3d | | | 0.14 | 0.122 | 1.149 | 1812 | 1229 | 133 | 10.82 | 25.215 | 1812 | 0.1 | 1.4E-04 | 0.13915714 | 1.0E-03 |
| | 3e | | | 0.14 | 0.141 | 0.994 | 1879 | 1170 | 295 | 25.21 | 119.845 | 1879 | 0.1 | 6.4E-04 | 0.63781451 | 3.9E-03 |
| | 3f | | | 0.14 | 0.159 | 0.880 | 2060 | 1207 | 542 | 44.90 | 131.919 | 1020 | 0.1 | 1.3E-03 | 1.29332522 | 6.5E-03 |
| | 3g | | | 0.14 | 0.178 | 0.789 | 3251 | 1806 | 899 | 49.78 | 234.212 | 1080 | 0.1 | 2.2E-03 | 2.16863056 | 9.3E-03 |

**Table F.2** Measured wave overtopping in test series 4-7

| Test Series | Sub-Test No. | Total number of Units | Packing density (units/$D_n^2$) | Crest Height $R_c$ [m] | $H_{m0}$ [m] Toe | $Rc/H_{m0}$ [-] | Test Duration [s] | No. of Waves N [-] | No. of overtopping waves | % overtopping waves | Overtopping Vol. [litre] | Duration of overtopping measured (sec) | Funnel width (m) | overtopping discharge q [m3/s per m] | overtopping discharge q [l/s per m] | q/(gHm0^3)^0.5 |
|---|---|---|---|---|---|---|---|---|---|---|---|---|---|---|---|---|
| 4 | 4a | 407 | 0.63 | 0.14 | 0.058 | 2.409 | 1763 | 1156 | 0 | 0 | 0 | 1763 | 0.1 | 0 | 0 | 0 |
| | 4b | | | 0.14 | 0.082 | 1.713 | 2085 | 1180 | 6 | 0.51 | 0.880 | 2085 | 0.1 | 4.2E-06 | 0.00422062 | 5.8E-05 |
| | 4c | | | 0.14 | 0.104 | 1.350 | 2396 | 1248 | 114 | 9.13 | 38.623 | 2396 | 0.1 | 1.6E-04 | 0.16119776 | 1.5E-03 |
| | 4d | | | 0.14 | 0.127 | 1.102 | 2776 | 1306 | 355 | 27.18 | 109.773 | 1388 | 0.1 | 7.9E-04 | 0.79087327 | 5.6E-03 |
| | 4e | | | 0.14 | 0.151 | 0.927 | 1433 | 622 | 287 | 46.14 | 284.715 | 1433 | 0.1 | 2.0E-03 | 1.98684849 | 1.1E-02 |
| 5 | 5a | 462 | 0.66 | 0.14 | 0.060 | 2.343 | 1280 | 1185 | 0 | 0 | 0 | 1280 | 0.1 | 0 | 0 | 0 |
| | 5b | | | 0.14 | 0.081 | 1.728 | 1440 | 1175 | 3 | 0.26 | 0.021 | 1440 | 0.1 | 1.5E-07 | 0.00014722 | 2.0E-06 |
| | 5c | | | 0.14 | 0.102 | 1.377 | 1632 | 1218 | 27 | 2.22 | 3.546 | 1632 | 0.1 | 2.2E-05 | 0.02172995 | 2.1E-04 |
| | 5d | | | 0.14 | 0.123 | 1.143 | 1794 | 1223 | 121 | 9.89 | 34.082 | 1794 | 0.1 | 1.9E-04 | 0.1899769 | 1.4E-03 |
| | 5e | | | 0.14 | 0.142 | 0.985 | 970 | 619 | 168 | 27.13 | 67.776 | 970 | 0.1 | 7.0E-04 | 0.69871837 | 4.2E-03 |
| | 5f | | | 0.14 | 0.161 | 0.871 | 2166 | 1299 | 581 | 44.74 | 154.716 | 1080 | 0.1 | 1.4E-03 | 1.43255251 | 7.1E-03 |
| | 5g | | | 0.14 | 0.177 | 0.790 | 2171 | 1227 | 622 | 50.71 | 240.196 | 1082 | 0.1 | 2.2E-03 | 2.21992789 | 9.5E-03 |
| 6 | 6a | 462 | 0.66 | 0.14 | 0.059 | 2.378 | 1761 | 1208 | 0 | 0 | 0 | 1761 | 0.1 | 0 | 0 | 0 |
| | 6b | | | 0.14 | 0.082 | 1.708 | 2072 | 1218 | 12 | 0.99 | 1.079 | 2072 | 0.1 | 5.2E-06 | 0.00520757 | 7.1E-05 |
| | 6c | | | 0.14 | 0.104 | 1.342 | 2400 | 1245 | 117 | 9.40 | 45.170 | 2400 | 0.1 | 1.9E-04 | 0.18820937 | 1.8E-03 |
| | 6d | | | 0.14 | 0.128 | 1.098 | 2781 | 1312 | 370 | 28.21 | 128.628 | 1390 | 0.1 | 9.3E-04 | 0.92537884 | 6.5E-03 |
| | 6e | | | 0.14 | 0.150 | 0.932 | 2889 | 1265 | 579 | 45.77 | 301.986 | 1440 | 0.1 | 2.1E-03 | 2.09712733 | 1.1E-02 |
| | 6f | | | 0.14 | 0.165 | 0.848 | 3072 | 1252 | 711 | 56.79 | 448.681 | 1534 | 0.1 | 2.9E-03 | 2.9249069 | 1.4E-02 |
| 7 | 7a | 440 | 0.63 | 0.14 | 0.059 | 2.353 | 1294 | 1208 | 0 | 0 | 0 | 1294 | 0.1 | 0 | 0 | 0 |
| | 7b | | | 0.14 | 0.081 | 1.739 | 1451 | 1203 | 3 | 0.25 | 0.068 | 1451 | 0.1 | 4.7E-07 | 0.0004658 | 6.5E-06 |
| | 7c | | | 0.14 | 0.102 | 1.379 | 1626 | 1239 | 28 | 2.26 | 2.787 | 1626 | 0.1 | 1.7E-05 | 0.01714003 | 1.7E-04 |
| | 7d | | | 0.14 | 0.122 | 1.148 | 1823 | 1253 | 138 | 11.01 | 36.259 | 1823 | 0.1 | 2.0E-04 | 0.19889812 | 1.5E-03 |
| | 7e | | | 0.14 | 0.142 | 0.984 | 1959 | 1250 | 319 | 25.52 | 119.146 | 1959 | 0.1 | 6.1E-04 | 0.60819996 | 3.6E-03 |
| | 7f | | | 0.14 | 0.161 | 0.871 | 1062 | 1295 | 581 | 44.85 | 158.035 | 1062 | 0.1 | 1.5E-03 | 1.48809296 | 7.4E-03 |
| | 7g | | | 0.14 | 0.177 | 0.789 | 2175 | 1230 | 622 | 50.57 | 231.686 | 1070 | 0.1 | 2.2E-03 | 2.1652932 | 9.3E-03 |

**Table F.3** Measured wave overtopping in test series 8-10

| Test Series | Sub-Test No. | Total number of Units | Packing density (units/$D_n^2$) | Crest Height $R_c$ [m] | $H_{m0}$ [m] Toe | Rc/$H_{m0}$ [-] | Test Duration [s] | No. of Waves N [-] | No. of overtopping waves | % overtopping waves | Overtopping Vol. [litre] | Duration of overtopping measured (sec) | Funnel width (m) | overtopping discharge q [m3/s per m] | overtopping discharge q [l/s per m] | q/(gHm0^3)^0.5 |
|---|---|---|---|---|---|---|---|---|---|---|---|---|---|---|---|---|
| 8 | 8a | 440 | 0.63 | 0.14 | 0.059 | 2.380 | 1770 | 1234 | 0 | 0 | 0 | 1770 | 0.1 | 0 | 0 | 0 |
| | 8b | | | 0.14 | 0.082 | 1.709 | 2075 | 1230 | 12 | 0.98 | 1.493 | 2075 | 0.1 | 7.2E-06 | 0.00719623 | 9.8E-05 |
| | 8c | | | 0.14 | 0.104 | 1.342 | 2402 | 1255 | 126 | 10.04 | 47.460 | 2402 | 0.1 | 2.0E-04 | 0.1975837 | 1.9E-03 |
| | 8d | | | 0.14 | 0.127 | 1.103 | 2685 | 1283 | 340 | 26.51 | 234.322 | 2685 | 0.1 | 8.7E-04 | 0.87270736 | 6.2E-03 |
| | 8e | | | 0.14 | 0.150 | 0.932 | 1440 | 639 | 300 | 46.97 | 293.884 | 1440 | 0.1 | 2.0E-03 | 2.04086359 | 1.1E-02 |
| 9 | 9a | 462 | 0.66 | 0.185 | 0.059 | 3.119 | 1295 | 1226 | 0 | 0 | 0 | 1295 | 0.1 | 0 | 0 | 0 |
| | 9b | | | 0.185 | 0.081 | 2.287 | 1470 | 1206 | 0 | 0 | 0 | 1470 | 0.1 | 0 | 0 | 0 |
| | 9c | | | 0.185 | 0.101 | 1.829 | 1630 | 1226 | 2 | 0.16 | 0.179 | 1630 | 0.1 | 1.1E-06 | 0.00110104 | 1.1E-05 |
| | 9d | | | 0.185 | 0.121 | 1.523 | 1810 | 1241 | 30 | 2.42 | 6.392 | 1810 | 0.1 | 3.5E-05 | 0.03531529 | 2.7E-04 |
| | 9e | | | 0.185 | 0.142 | 1.300 | 2044 | 1283 | 136 | 10.60 | 41.882 | 2044 | 0.1 | 2.0E-04 | 0.20490389 | 1.2E-03 |
| | 9f | | | 0.185 | 0.161 | 1.149 | 2157 | 1285 | 278 | 21.63 | 113.855 | 2157 | 0.1 | 5.3E-04 | 0.52784021 | 2.6E-03 |
| | 9g | | | 0.185 | 0.179 | 1.035 | 2171 | 1221 | 388 | 31.77 | 111.565 | 1082 | 0.1 | 1.0E-03 | 1.03110386 | 4.4E-03 |
| 10 | 10a | 462 | 0.66 | 0.185 | 0.059 | 3.141 | 1761 | 1193 | 0 | 0 | 0 | 1761 | 0.1 | 0 | 0 | 0 |
| | 10b | | | 0.185 | 0.082 | 2.262 | 2074 | 1227 | 0 | 0 | 0 | 2074 | 0.1 | 0 | 0 | 0 |
| | 10c | | | 0.185 | 0.104 | 1.778 | 2387 | 1255 | 31 | 2.47 | 8.270 | 2387 | 0.1 | 3.5E-05 | 0.03464453 | 3.3E-04 |
| | 10d | | | 0.185 | 0.127 | 1.452 | 2685 | 1283 | 141 | 10.99 | 77.792 | 2685 | 0.1 | 2.9E-04 | 0.28972969 | 2.0E-03 |
| | 10e | | | 0.185 | 0.151 | 1.223 | 2914 | 1272 | 361 | 28.39 | 135.073 | 1457 | 0.1 | 9.3E-04 | 0.92706234 | 5.0E-03 |
| | 10f | | | 0.185 | 0.172 | 1.076 | 3060 | 1274 | 525 | 41.20 | 262.234 | 1530 | 0.1 | 1.7E-03 | 1.71394639 | 7.7E-03 |

**Table F.4** Measured wave overtopping in test series 11-12

| Test Series | Sub-Test No. | Total number of Units | Packing density (units/$D_n^2$) | Crest Height $R_c$ [m] | $H_{m0}$ [m] Toe | Rc/$H_{m0}$ [-] | Test Duration [s] | No. of Waves N [-] | No. of overtopping waves | % overtopping waves | Overtopping Vol. [litre] | Duration of overtopping measured (sec) | Funnel width (m) | overtopping discharge q [m3/s per m] | overtopping discharge q [l/s per m] | q/(gHm0^3)^0.5 |
|---|---|---|---|---|---|---|---|---|---|---|---|---|---|---|---|---|
| 11 | 11a | smooth slope | | 0.185 | 0.059 | 3.113 | 670 | 664 | 0 | 0 | 0 | 670 | 0.1 | 0 | 0 | 0 |
| | 11b | | | 0.185 | 0.080 | 2.314 | 721 | 623 | 18 | 2.89 | 1.407 | 721 | 0.1 | 2.0E-05 | 0.01951027 | 2.8E-04 |
| | 11c | | | 0.185 | 0.101 | 1.840 | 734 | 660 | 42 | 6.36 | 5.692 | 734 | 0.1 | 7.8E-05 | 0.0775434 | 7.8E-04 |
| | 11d | | | 0.185 | 0.121 | 1.530 | 910 | 669 | 116 | 17.34 | 27.203 | 910 | 0.1 | 3.0E-04 | 0.29893657 | 2.3E-03 |
| | 11e | | | 0.185 | 0.142 | 1.305 | 969 | 669 | 203 | 30.34 | 84.120 | 969 | 0.1 | 8.7E-04 | 0.86811234 | 5.2E-03 |
| | 11f | | | 0.185 | 0.159 | 1.161 | 1091 | 724 | 315 | 43.51 | 187.419 | 1091 | 0.1 | 1.7E-03 | 1.71786686 | 8.6E-03 |
| 12 | 12a | smooth slope | | 0.185 | 0.059 | 3.153 | 901 | 650 | 0 | 0 | 0 | 901 | 0.1 | 0 | 0 | 0 |
| | 12b | | | 0.185 | 0.083 | 2.240 | 1083 | 683 | 15 | 2.20 | 1.450 | 1083 | 0.1 | 1.3E-05 | 0.01338849 | 1.8E-04 |
| | 12c | | | 0.185 | 0.106 | 1.751 | 1230 | 724 | 82 | 11.33 | 20.754 | 1230 | 0.1 | 1.7E-04 | 0.16873247 | 1.6E-03 |
| | 12d | | | 0.185 | 0.129 | 1.439 | 1412 | 760 | 215 | 28.29 | 129.957 | 1412 | 0.1 | 9.2E-04 | 0.92037217 | 6.4E-03 |
| | 12f | | | 0.185 | 0.152 | 1.220 | 1462 | 733 | 309 | 42.16 | 300.758 | 1462 | 0.1 | 2.1E-03 | 2.05717049 | 1.1E-02 |